

POLITECNICO DI TORINO

Master's Degree in Mechanical Engineering

Master's Degree Thesis

Simulation of an Excavator Hydraulic Circuit



Academic supervisor:

Prof. Massimo Rundo

Candidate:

Vincenzo Maria Briganti

Academic Year 2021/2022

ABSTRACT

The aim of this thesis is the study of a midi Excavator Hydraulic Circuit through the new 3D mechanical library in Simcenter Amesim®. First, a description of the excavator classifications, as well as the load sensing working principle will be illustrated, with the explanation of the hydraulic components used on these types of hydraulic circuits. After that, it has been modelled the real excavator created in SolidWorks® given by the FPRL into Amesim® with two element types of this mechanical library: Rigid body and Recursive joints, this latter is able to take into account the inertia transfers from one body to another, useful because the inertia depends on the positions of each element that compose the excavator arm, but also from the load that the bucket has when it is full after dig. Then, it has been implemented the hydraulic circuit in two configurations, pre-compensated and post-compensated, and given the input of the normal duty cycle, verifying that the system works correctly. Moreover, it has been carried out the studies of two critical conditions for both the hydraulic circuits, pressure-saturation, and flow-saturation, analysing the results, describing how the system behaves, and make sure that the system works as expected. In conclusion, some considerations about the models' limitations and the future challenges in the operating machines construction will be discussed.

Contents

CHAPTER 1: INTRODUCTION	4
1.1) Excavator classifications	4
1.2) Excavator description	7
1.3) Load Sensing Systems (LS)	9
1.3.1) The problem	9
1.3.2) LS implementations	12
1.3.3) LS system with variable displacement pump	13
1.3.4) Speed control of more users	16
CHAPTER 2: HYDRAULIC COMPONENTS WORKING PRINCIPLE	20
2.1) Variable displacement pump	20
2.2) Displacement variation systems	21
2.2.1) Absolute pressure limiter	21
2.2.2) Differential pressure limiter	23
2.3) Gear pump	26
2.3.1) External gear machines	26
2.4) Distributors with local compensators	28
2.4.1) LS Proportional distributor	28
2.4.2) The local pre-compensators	29
2.4.3) The local post-compensators (anti-saturation compensator)	35
2.5) Hydraulic actuators	41
2.5.1) Hydraulic actuators with flow regeneration	48
CHAPTER 3: SIMCENTRE AMESIM EXCAVATOR MODEL	53
3.1) 3D CAD model	53
3.2) 2D Simcentre Amesim model	54
3.3) 3D Simcentre Amesim models	64
3.3.1) 3D model with rigid body	64
3.3.2) 3D model with recursive joints	77
3.4.1) LS pre-compensated hydraulic circuit	83
3.4.2) LS post-compensated hydraulic circuit	85
3.4.3) Hydraulic circuit for the turret rotation	86
3.5) Complete hydraulic circuits	88
CHAPTER 4: RESULT ANALISYS	93
4.1) Normal duty cycle	93

4.1.1) 3D system with pre-compensated hydraulic circuit and rigid bodies.....	93
4.1.2) 3D system with post-compensated hydraulic circuit and rigid bodies.....	104
4.1.3) 3D systems with recursive joints.....	110
4.2) Saturation conditions.....	115
4.2.1) Pressure saturation in pre-compensated hydraulic circuit.....	115
4.2.2) Flow saturation in pre-compensated hydraulic circuit.....	119
4.2.3) Pressure saturation in post-compensated hydraulic circuit.....	122
4.2.4) Flow saturation in post-compensated hydraulic circuit.....	125
CONCLUSIONS	132
APPENDIX A: Computation of the Resistive Forces	133
A1: Description and usage	133
A2: Parameter settings	134
A3: Theory and equations	140
BIBLIOGRAPHY	144

CHAPTER 1: INTRODUCTION

1.1) Excavator classifications

Each Original Equipment Manufacturers (OEMs) have different way to classify their equipment, for example classification based on carriers or classification based on the working mechanism. Usually, the excavators are classified in three size classes, according to the weight of the machine.

Mini excavators (figure 1.1) are any excavators that weigh less than 7 metric tons [9]. These small excavators are sometimes called compact excavators and are perfect for tight job sites.



Figure 1.1: Mini excavator [7]

Mini excavators can manoeuvre in small spaces for landscaping tasks such as digging holes for trees or trenches for pipes. Mini excavators often have zero or near-zero tail swing, so operators can use them comfortably around buildings and other structures. For job sites with many pipes or gas lines underground, mini excavators offer greater precision than larger digging equipment. Another benefit of mini excavators is that they are easy to transport on a truck or trailer and require less fuel than larger excavators. Because they are lighter, mini excavators can operate on soft terrain without tearing up the ground, or on finished sites without damaging the sidewalks or pavement. However, mini excavators are not as powerful as larger excavators and may not be able to provide the necessary dig depth or lift capacity for every job.

Standard-sized excavators (figure 1.2) weigh between 7 and 45 metric tons [9]. These versatile excavators are the most common size for commercial construction projects and offer enough power and hauling capacity to handle a variety of tough jobs.



Figure 1.2: Standard excavator [7]

Many hydraulic standard excavators can also support a variety of work tools, so contractors can customize their excavator to suit their project needs. Standard excavators are still easy to manoeuvre and can significantly increase productivity on a job site. However, these more massive excavators may cause damage to finished sites or soft soil. Depending on their size, reach and tail swing, a standard excavator may also be challenging to operate in tighter spaces. Conventional excavators that fall on the heavier end of this excavator weight class could also pose transportation and storage challenges.

It is possible sometimes that standard excavators are broken into two excavator weight classes: small (figure 1.3) and medium (figure 1.4) excavators. Small excavators are those at the bottom of this size class that weigh between 7 and 10 metric tons, instead the medium excavator weight goes from 10 to 45 metric tons. These two excavator types are a compromise between the mini and standard excavators, because they have smaller size and lower tail swing with respect to standard excavators useful for many of the same tasks as mini excavators, but offer more power reach, and dig depth than mini excavators.



Figure 1.3: small excavator [7]



Figure 1.4: medium excavator [7]

These hefty excavators (figure 1.5) weigh more than 45 metric tons and are suited for heavy-duty jobs [9]. Large excavators provide serious power for major commercial construction projects or large-scale demolition.



Figure 1.5: Large excavator [7]

Large excavators can be valuable for digging foundations for shopping centres or apartment complexes or moving large volumes of soil for civil engineering tasks. Although transportation and storage of large excavators can be challenging, a large excavator may be worth the investment if you need to tackle serious excavation projects with ease.

1.2) Excavator description

The excavator under study is a small excavator shown in figure 1.6, it has been designed to create a compact machine useful in particular situations [3]. Thanks, the boom rotation, it can move easily in narrow spaces, at the same time it has high digging force and an excellent stability due to the frontal blade. This excavator has a weight of 7.4 t, a digging depth of 4.21 m, a bucket capacity of 0.25 m³, a diesel engine of 51kW that generate the useful power for the hydraulic control group, made of two different pumps to power the hydraulic users. The axial piston pump with variable displacement powers the users with load sensing (LS) architecture, while the gear pump with fixed displacement is used for user without load sensing. The hydraulic circuit has load sensing distributors with the neutral position in closed centre configuration. The pumps are placed near the engine on the motor hood and direct connected on it, sucking the oil from a reservoir of 70 litre placed in the lateral hood. The piston pump being for the LS users supplies the following users:

- Translational motors;
- Boom actuator;
- Dipper actuator;

- Bucket actuator;
- Swing arm actuator.

Instead, the gear pump is used for:

- Blade actuator;
- Turret swing motor.

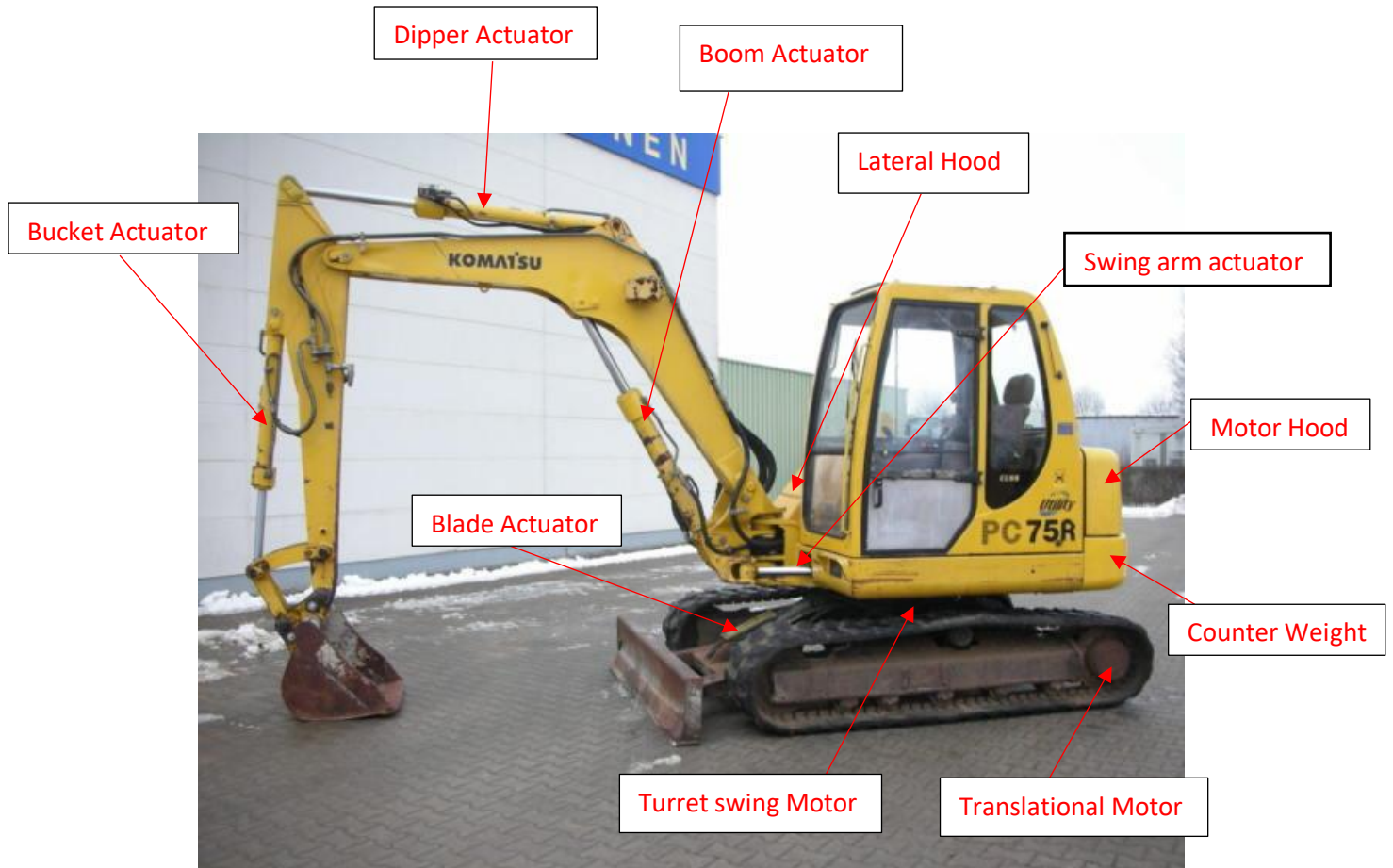


Figure 1.6: Excavator Komatsu PC75R [7]

All the actuators are double effect, while the hydrostatic transmissions for the tracks (in steel or rubber) movement are open circuit. Inside the lateral hood there are the distributors, that are activated from the servo controls, that power the users. Servo controls are leverage that are activated directly from the operator, they are powered from the flow generation unit suitable to generate the flow rate at reduced pressure, necessary for its proper operation. Such flow rate is generated and delivered from the axial piston pump.

1.3) Load Sensing Systems (LS)

1.3.1) The problem

The load sensing systems have been developed with the scope to overcome two problems of some hydraulic circuits [1]:

- Maintain under control more actuators that manage different loads and seen in parallel from the hydraulic power unit.
- The energy saving.

To understand how this system works, a simple circuit made of a flow generation unit (GA) with variable displacement pump and an absolute pressure limiter tuned at p^* , that powers a generic user group (GU) through a proportional valve that is commanded by a controller C, is illustrated in figure 1.7.

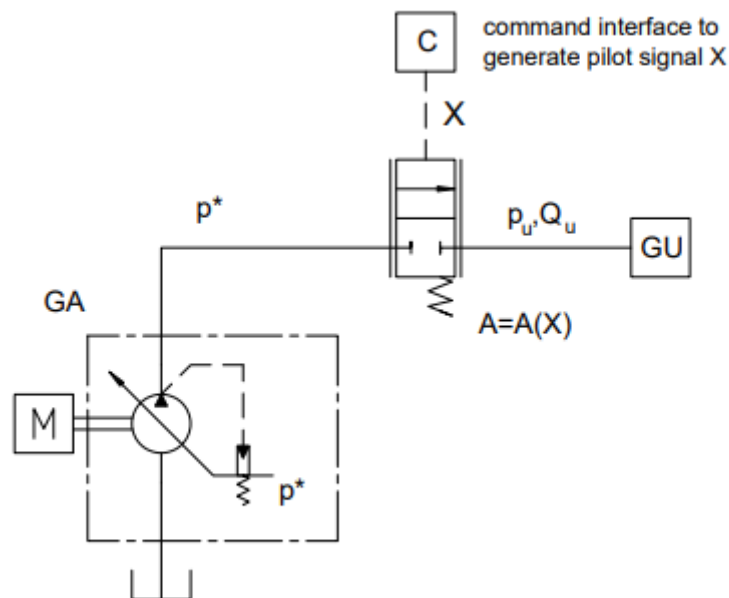


Figure 1.7: GU Velocity dependent on the load pressure [1]

The controller C generates a pilot signal X, that can be hydraulic, electric, or mechanical, that regulates the spool position of the proportional valve: from the position $X = 0$ due to the spring, that correspond to an infinite resistance when there is flow rate, where the valve is fully closed, to the position $X = 1$ where the valve is fully open, if supposed a normalized signal. Since the scope is to realise the actuator speed control (for example), it is worth to analyse the system behaviour on the power plane (Q_u, P_u) and on the controllability plane (Q_u, X).

On the power plane in figure 1.8, the point U represents the conditions where the general user works, this value must be inside the region defined between two limit values:

- The horizontal line, that is the maximum flow rate of the pump and is equal to $Q_{tot} = \omega * V_{max}$, where ω is the angular velocity at which the pump is running, and V_{max} is its maximum displacement.
- The vertical line, that is the maximum pressure p^* of the absolute pressure limiter.

The point U is identified by Q_u that is the flow rate asked by the user and the pressure P_u imposed by the user. Instead, the pump works at point P characterized by coordinates p^* , Q_u .

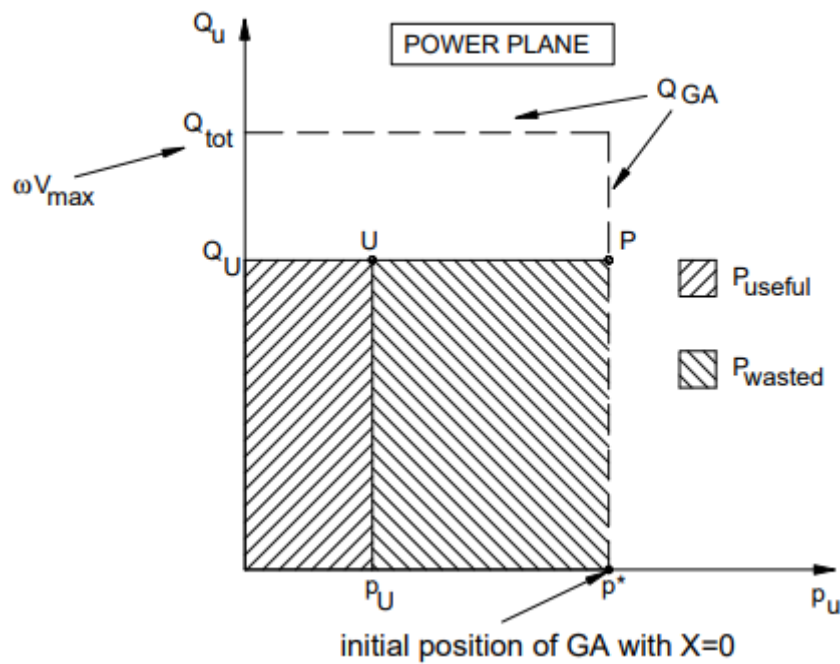


Figure 1.8: Power plane [1]

The useful power is:

$$P_U = Q_U * p_U \tag{1.1}$$

While the expended power is:

$$P_S = Q_U * p^* \tag{1.2}$$

So, the lost power P_p is the difference between the power expended P_s and the useful power P_u :

$$P_P = P_S - P_U = Q_U * (p^* - p_U) \tag{1.3}$$

These calculations and the power plane show that, the lost power is high if P_u is low, imposed by the load, and/or Q_u is high that is directly correlated to actuator velocity. With these

considerations, it is important that the system works with high pressure and low flow rate as much as possible but trying to satisfy the user velocity needs.

For what concerning the controllability point of view, the flow rate that the user needs, is:

$$Q_U = C_e * A(X) * \sqrt{\frac{2 * (p^* - p_U)}{\rho}} = k(X) * \sqrt{p^* - p_U}$$

(1.4)

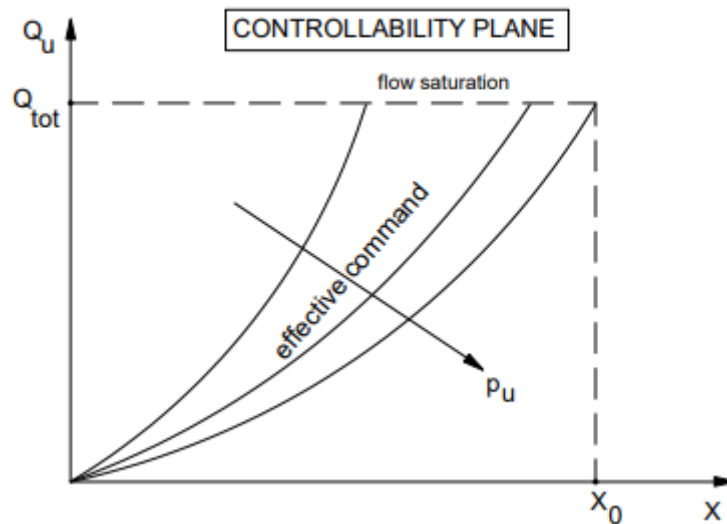


Figure 1.9: Controllability plane [1]

It is a function of the command X that can be modified from the operator to regulate the actuator velocity, but also from the pressure p_U that depends on the load history, as show the figure 1.9, that cannot be controlled. On the controllability plane are reported how the flow rate changes, in function of X at given pressure p_U , and how the characteristic changes if the pressure p_U increases. When $X = 0$ and the valve is closed, the system is described at point $(0,0)$. Increasing the command, if the pressure p_U is roughly constant, the flow rate behaviour can be parabolic or linear, so the valve behaves like a variable restrictor until the flow saturation is reached, where the pump is at its maximum displacement, delivers its maximum flow rate, hence even if the valve opens more, the pump does not satisfy the user needs and consequently the pressure decreases. Actually, it is needed to take into account that the load is variable during normal duty cycles like in an excavator. if a constant command X is imposed, moving horizontally on the controllability plane, and the load is variable in time, there is a flow rate variation, that means a velocity variation, so the user is not controlled. On the other hand, the operator could adjust the command X to take under control the user velocity, but this task could be heavy and not easy.

1.3.2) LS implementations

Mobile hydraulic machines operate under conditions extremely mutable, hard to predict, and usually involving simultaneous functions, which means that their controllability and their performance are key aspects to consider during the design of a system [6]. The machine size and the specific application field set different requirements for the working hydraulics. Typically, the target of the hydraulic systems dedicated to compact machinery with a curb weight below ten metric tons such as small excavators, is to guarantee the independent velocity control of each actuator during contemporaneous movements. In medium/large size applications such as large excavators, perceiving the load is preferable instead of accurately controlling the actuator velocity. Moreover, the system's overall energy efficiency is becoming a more significant parameter; in a multi-actuator hydraulic layout characterized by a single pump that supplies actuators at different pressure levels, the throttling losses in the control valves represent a major contribution to the fuel consumption (e.g., a third of the energy supplied by the prime mover of state-of-the-art excavators is lost through throttling in the hydraulic system). Therefore, some applications are conceived with multiple pumps dedicated to distinct parts of the hydraulic circuit in addition to the heavy use of electronic control strategies. Furthermore, the trend for mobile hydraulics from the industry perspective showing the clear tendency toward electronic controls, higher automation, and more efficient circuits. Other factors that steer the system design are cost effectiveness, robustness, minimum downtime, and reduced control complexity. Multiple system architectures were therefore developed in the past, divide the non-hybrid valve-controlled systems into two major categories, namely, the mechanical–hydraulic and the electrohydraulic solutions. Further classifications are then proposed depending on the different control concepts.

The mechanical hydraulic systems rely on pure mechanical–hydraulic regulations, which means electronics is not involved in the control of the system. Examples of the devices used to control these applications are manually operated control valves of an agricultural tractor, or mechanical–hydraulic joysticks of an excavator. Some of these primal hydraulic architectures developed throughout many decades are still commonplace since they typically guarantee robustness, reduced initial investment and simplified maintenance (often accessible to non-specialist workers). More in general, these systems are traditionally divided into open-centre and closed-centre type depending on the design of the proportional directional control valves (PDCVs), where the definition refers to the nature of the connection established between pump and reservoir when the valves are centred.

Mainly due to the increased reliability and to the more affordable cost of electronic sensors and components, mobile hydraulics based on electrohydraulic solutions started to gain ground in the last decades. In fact, advanced control strategies unfeasible in the past allow more flexible machine setups and/or increased energy efficiency. Some electrohydraulic architectures are the developments of the mechanical–hydraulic counterparts so that electronics can be involved at different levels (e.g., electronic joysticks actuate the PDCVs to manipulate the control inputs accordingly, or a more massive usage of electrohydraulic components can be explored). In parallel, new layouts based on different concepts were also studied.

These are the most important system architectures used to control the working hydraulics of non-hybrid, valve-controlled mobile machines. It emerged that relevant efforts were devoted to design and improve, over several decades, mechanical–hydraulic solutions suitable for different machines. The well-established, cost effective, open-centre systems with fixed-displacement pumps characterized by very good inherent damping and fast response time are affected by poor energy efficiency. New implementations dominated by variable-displacement pumps were proposed to reduce the energy losses while maintaining good system damping. Significant improvements in terms of energy efficiency were then achieved by combining closed-centre PDCVs with variable displacement pumps at the expense of system damping, response time, and cost. The main features of the predominant mechanical–hydraulic solutions are summarized in Table 1.1.

Criteria	Open-center fixed pump	Open-center variable pump	Closed-center fixed pressure	Closed-center variable pressure
Inherent damping	Good	Good	Good	Poor
Response time	Good	Good	Good	Acceptable
Cost-effectiveness	Good	Acceptable	Acceptable	Poor
Energy efficiency	Poor	Acceptable	Poor	Good

Table 1.1 [6]

1.3.3) LS system with variable displacement pump

On the sketch in figure 1.10 is shown instead of a system with an absolute pressure limiter, a system with a differential pressure limiter that compares the pressure from the load p_U (load sensing), through a pilot line, plus a constant term s due to the spring, with the delivery pump pressure [1].

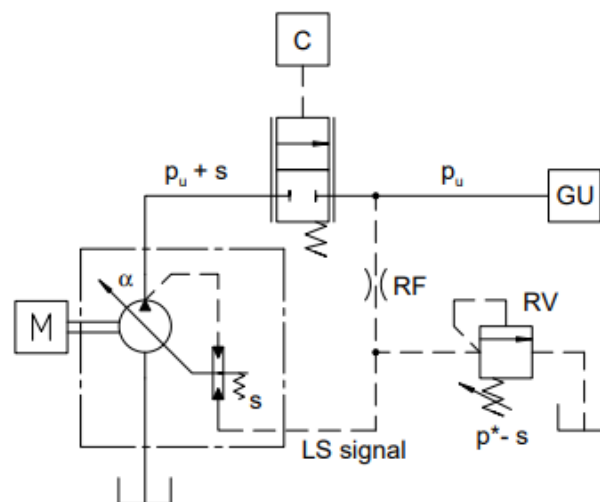


Figure 1.10: load sensing principle [1]

In this way both the pressure difference between upstream and downstream on the proportional valve is constant and the controllability in every load condition. The differential pressure limiter tunes the pump displacement to guarantee that the pressure at the pump delivery is $p_p = p_U + s$, that is also the pressure upstream of the proportional valve, downstream instead there is the pressure p_U , and so the pressure difference on the proportional valve is equal to s :

$$\Delta p = p_p - p_U = (p_U + s) - p_U = s$$

(1.5)

This pressure difference keeps constant the flow rate if the command X is fixed.

On the energy point of view (figure 1.11), the user works on the point U (p_U, Q_U), while the pump works on the point P ($p_U + s, Q_U$) supplying the flow rate needed to the user, with a pressure higher than the load pressure that is imposed from the differential pressure limiter spring setting.

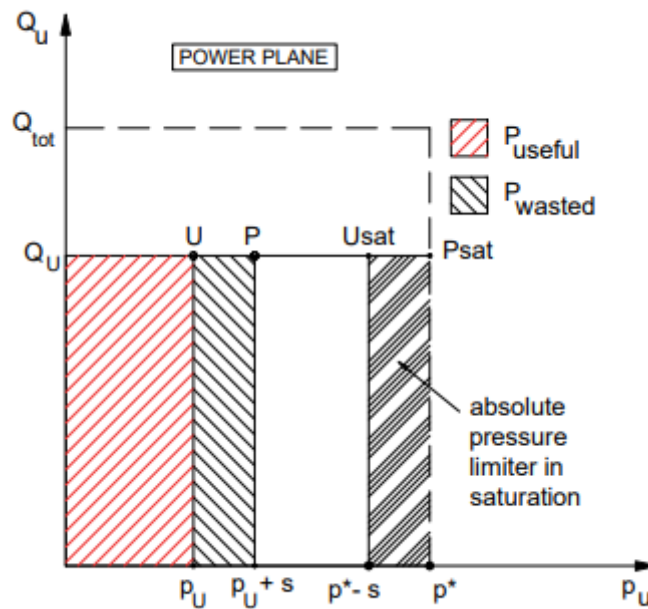


Figure 1.11: working points in regulation and in saturation on the power plane [1]

The useful power is the same of the previous one, instead the expended power is:

$$P_s = Q_U * (p_U + s)$$

(1.6)

So, the lost power is equal to:

$$P_P = P_s - P_U = Q_U * (p_U + s) - (Q_U * p_U) = Q_U * s$$

(1.7)

It is less than the previous one, and mainly it is load independent, so it is preferred maintain s as low as possible in order to limit the power loss (s is about 20 bar). If the load increases and the pressure $p_U = p^* - s$, the relief valve regulates, tuned at pressure $p^* - s$. The system is not able to guarantee the controllability, in fact the pressure upstream to the proportional valve is equal to p^* instead the user pressure can continue to increase. In this case there is pressure saturation due to the pressure limiter that maintains the pressure fixed at p^* and does not follow the load history. It is worth to notice that the functional restrictor RF does not work when the relief valve does not regulate, that means no flow rate. So, the pressure information pass through the functional restrictor. When the relief valve regulates, there is flow rate that passes through it, therefore there is a pressure drop that allow the relief valve regulation without interference of the pressure fluctuations due to the user, so the functional restrictor allows to decouple the pressures when the relief valve regulates. Concerning the controllability, there is only one curve that is load independent, that allows a full velocity control, changing the command X , represented in figure 1.12.

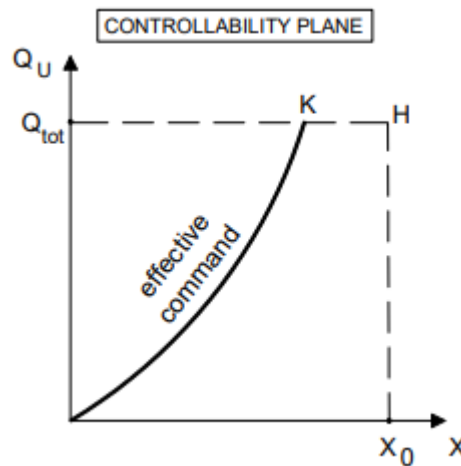


Figure 1.12: controllability plane [1]

Could happen also the flow saturation if with an increase of the command X , the flow rate does not increase. This phenomenon could happen if there is a wrong pump dimensioning, such that it is not able to satisfy speed increments needed by the user, or if it is used a small and more compact pump, because there is not the need to go beyond a certain actuator velocity.

1.3.4) Speed control of more users

When there is the need to control more than one user, the system is equipped by one or more shuttle valves to take the biggest load signal and send it to the pump differential pressure limiter, like in figure 1.13, and in this way, it is possible to move the user with higher load and also the others [1].

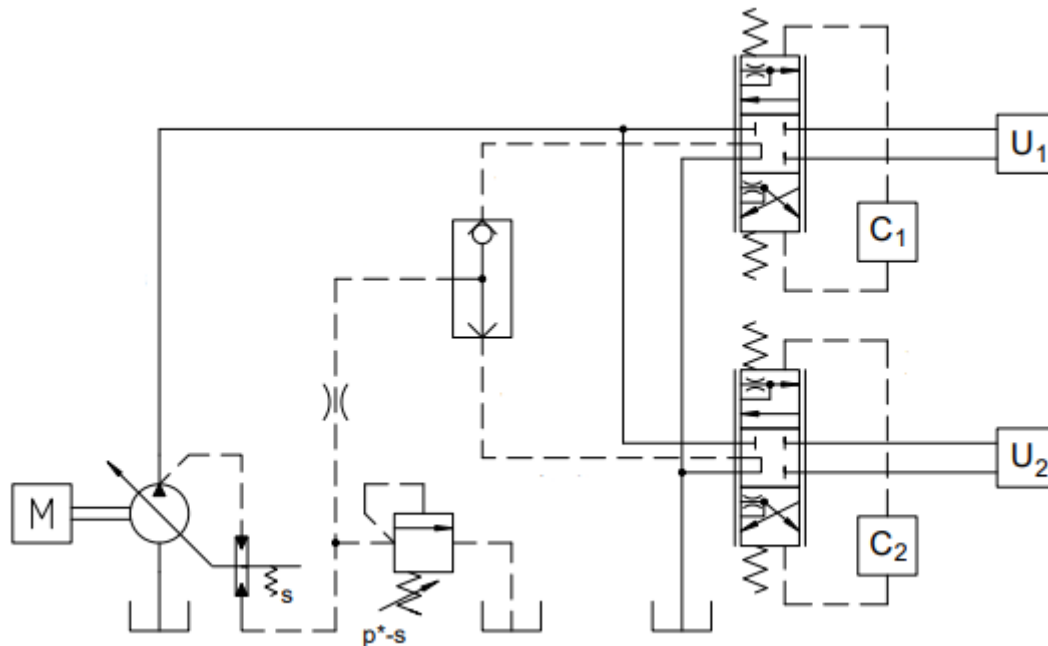


Figure 1.13: LS circuit with two general users [1]

Furthermore, in hydraulic circuits with more users, it is necessary to distinguish the type of load sensing signal:

- When there is a load sensing signal that is the biggest than the others, so it is the global load sensing (LSG), because it comes from the shuttle valve and goes to the flow generation unit;
- When the load sensing signals are limited to the users because they are lower, so they are called local load sensing (LSL).

If there are two users with equal loads, and they impose the same pressure $p_i = p_j$. The delivery pressure is:

$$p_p = p_i + s = P_j + s$$

(1.8)

On the power plane (figure 1.14), the two working points U_i and U_j have the same pressure p_u but different flow rates, so different velocities.

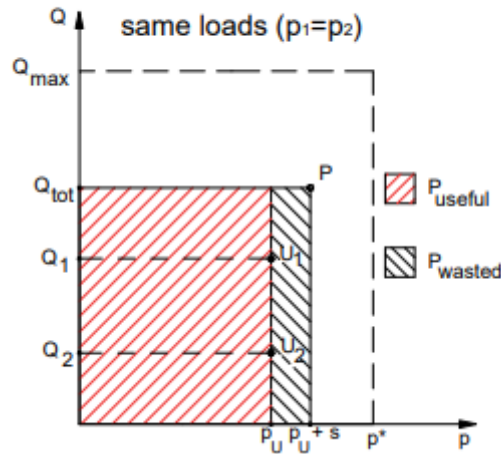


Figure 1.14: Power plane of two users equally loaded [1]

The pump flow rate is the sum of the two user flow rates, and its pressure is the users' pressure plus s , so the lost power is:

$$P_P = Q_{tot} * s = (Q_i + Q_j) * s$$

(1.9)

The speed control is guaranteed, because there is the same pressure drop across the distributors, for each command in each distributor correspond a defined user velocity.

In reality, what happens is described in the figure 1.15:

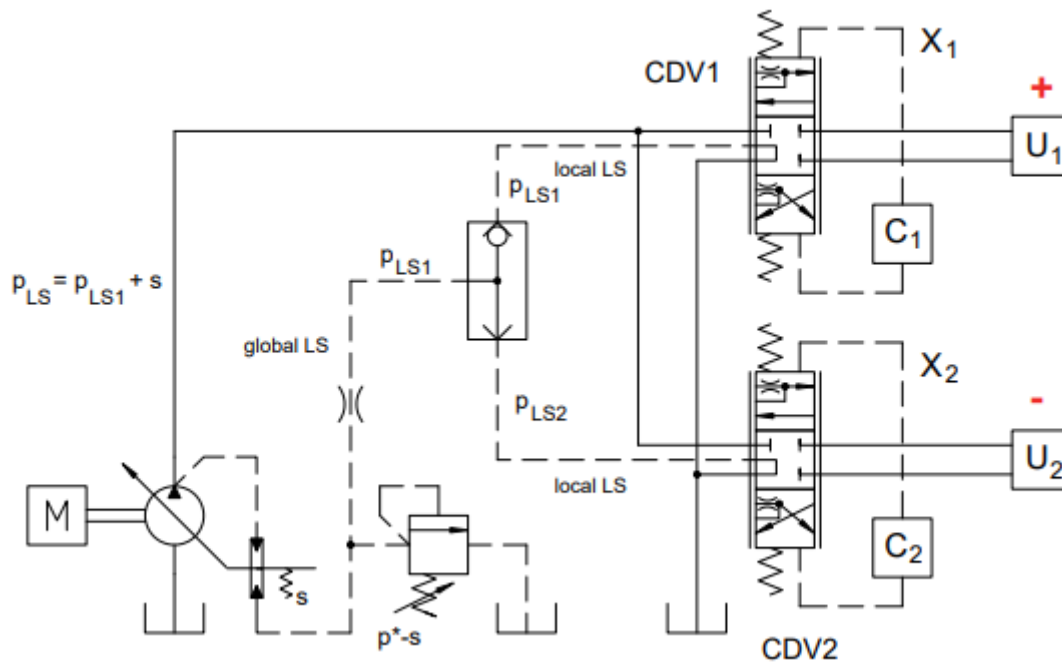


Figure 1.15: LS circuit with a user more loaded than other [1]

The users impose different loads, $p_i > p_j$. On the differential pressure limiter arrives the highest pressure, and so the delivery pressure is:

$$p_p = p_i + s$$

(1.10)

While downstream of the distributors there are pressures related to loads. In this condition it is important notice that:

- On the power plane (figure 1.16), the working point U_i is the same as before, while the working point U_j is lower, therefore this latter receives more flow rate, because the pressure drop on its distributor is higher than s . The new working point $U_j (p_j, Q'_j)$ has a higher flow rate with respect to the user needs, and also the lost power increases because, both for the flow rate increasing and for the higher distributor pressure drop $(p_i + s - p_j)$. In particular:

$$\begin{cases} P_U = Q'_j * p_j + Q_i * p_i \\ P_S = Q'_{tot} * (p_i + s) = (Q_i + Q'_j) * (p_i + s) \\ P_P = P_S - P_U = Q_i * s + Q'_j * (p_i + s - p_j) \end{cases}$$

(1.11)

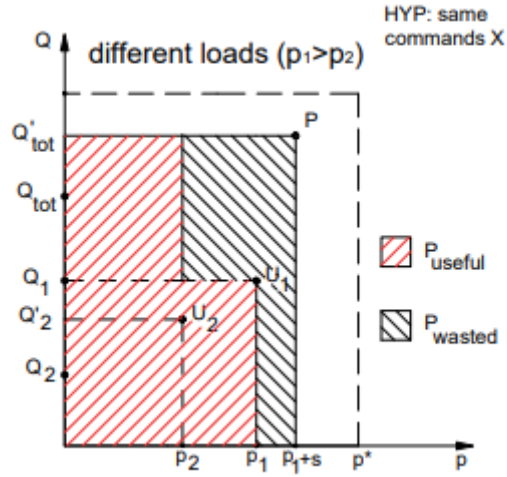


Figure 1.16: Power plane with two users differently loaded [1]

- On the controllability plane, also in this case, the user with the highest load has only one curve, instead the other will be powered with a flow rate that depends on the load history, therefore it loses the controllability:

$$\left\{ \begin{array}{l} Q_i = C_e * A_{v1} * \sqrt{\frac{2 * (p_{LS1} + s - p_{LS1})}{\rho}} = K_1 * \sqrt{s} \\ Q'_j = C_e * A_{v2} * \sqrt{\frac{2 * (p_{LS1} + s - p_{LS2})}{\rho}} = K_2 * \sqrt{p_{LS1} + s - p_{LS2}} \end{array} \right. \quad (1.12)$$

Where A_{v1} and A_{v2} are the areas created by the proportional valves from the commands, and K_1, K_2 are constant values.

CHAPTER 2: HYDRAULIC COMPONENTS

WORKING PRINCIPLE

2.1) Variable displacement pump

This pump type, where the cross section is illustrated in figure 2.1, has certain number of pistons located in parallel and equidistant with respect to a unique body axis that contains all pistons, that is called the barrel, in which there are the same number of cylinder holes respectively, that work in a specific tolerance with pistons [1].

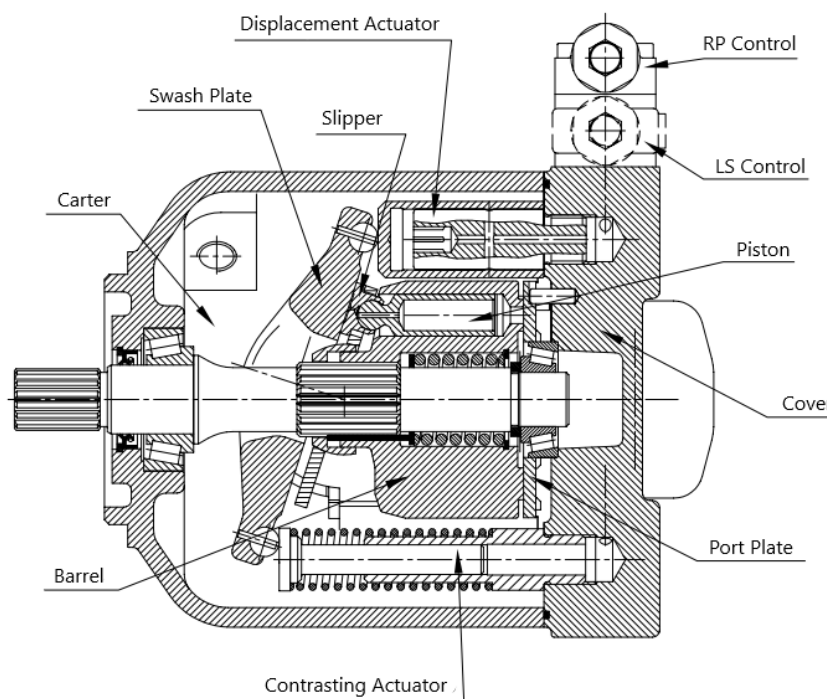


Figure 2.1: Variable displacement piston pump cross section [1]

The alternated movement that produces the pump effect is transmitted to the pistons by a particular kinematic solution. The barrel axis is equal to the input shaft axis. The input shaft exchange torque and angular speed by means of a spline shaft. The piston external ends are spherical heads, they are located on hydrostatic slippers, that are constrained by the retainer plate, to travel in a planar track made on the swash plate. By varying the swash plate inclination, with respect to its axis of rotation, it is possible to determine the piston stroke, and so the pump displacement. The oil distribution is obtained as follows: during half revolution in which each piston moves outwards, the chambers are connected through a fixed hole with the suction ports, to fill the cylinders with the oil. In the next half revolution, the cylinder meets another hole connected with the delivery port, so the piston when move inwards discharges the oil. When the swash plate is at zero degree, the piston alternate movement is null, and consequently also the flow rate. This pump can be equipped with three control systems to regulate its

displacement. In particular, a system with an absolute pressure limiter (RP control), that when regulates, adjusts the swash plate inclination, in order to impose a constant pressure value equal to the limiter pressure setting, on the pump delivery line. The second one, that together with the absolute pressure limiter, constitutes a differential pressure limiter (LS control), used to change the pump displacement, to manage load sensing logic. The third one is a torque limiter (not present on the sketch), that limits the torque needed by the pump to a fixed value. To change the pump displacement, the swash plate is subjected to forces generated by actuators that act on different surfaces. The contrasting actuator, that has lower section area, is subjected continuously both to the actual delivery pressure and the elastic force due to non-adjustable spring. The displacement actuator (actuator with higher section area), receives pressure information, properly regulated, from a continuous position spool valve with three ports. In neutral position, without pressure signals, the swash plate assumes a configuration that corresponds to the maximum pump displacement.

2.2) Displacement variation systems

2.2.1) Absolute pressure limiter

This device (figure 2.2) can create a power group with true pressure, therefore guarantee on the pump delivery line a constant pressure, independent of the user flow rate needs [1].

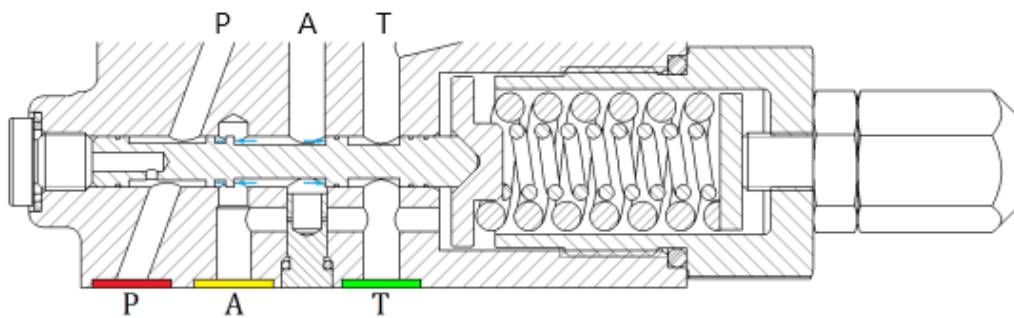


Figure 2.2: Absolute pressure limiter cross section [4]

The pressure can be decided through an elastic element regulation. This device is a three port, continuous position distributor: the port P is connected to the pump delivery port, the port A is connected to the actuator that perform the displacement variation, and the port T to the reservoir. The P and T channels continuum after the spool because, it is possible to connect a load sensing control, moreover there is a connection between the port T and the spring chamber to drain the spring environment. The elastic element regulation is performed by a screw on the right. The spool has near the port A, a double shoulder that meet the port A, the unique port that is longer with a blind drill due to a project choice that lead to have a flow rate gain. It is important notice that, there is a restrictor from port A to port T on the absolute

limiter body. The restrictor geometry is characterized by a hole near the port A, followed by a cylinder hole, in which it ends on a different diameter due to a hexagonal wrench seat. The restrictor produces a stable connection from the A environment, in which the aim is send a modulated pressure signal, to the pump carter environment. Its function, optimise the actuator dynamics deciding the pump displacement during the regulation phase, that means during transient. In neutral conditions the port A is connected to T, while the connection between P and A is completely closed. The spool central shoulder has an axial length lower than the diameter of the blind hole that increase the port A length, so is possible an intermediated configuration in which the porta A is connected both T and P, with the two metering edges that generate a restrictor in both connections.

From the figure 2.3, it can be explained the absolute pressure limiter (LPA) working principle.

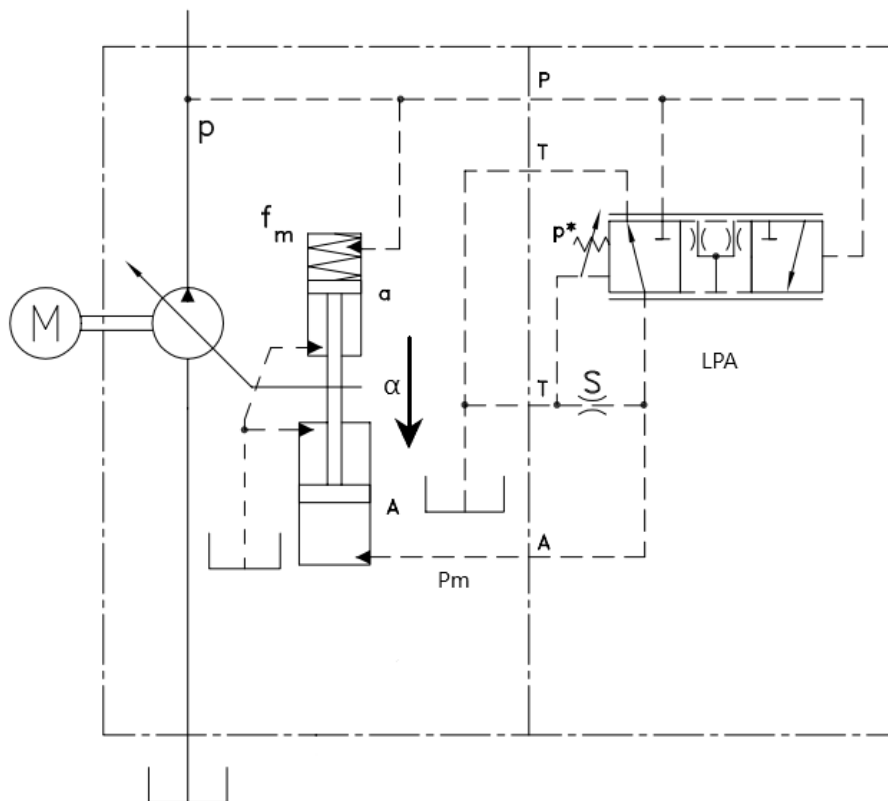


Figure 2.3: Displacement control with an Absolute pressure limiter [1]

Considered a load that increase in time, in which the delivery pressure increase, from a lower value of the setting pressure imposed through the spring pre-load p^* . in this condition, the delivery pressure and the spring of the contrasting actuator win the force produced by the carter pressure that exert on the displacement actuator, keeping the pump at maximum displacement. When the delivery pressure reaches the value p^* , the absolute pressure limiter

spool starts to move, if it allows a flow rate from the port P to A, increasing in this way the modulated pressure p_m . Since there are different acting surfaces on the two actuators, the variable displacement actuator action is higher than the contrasting one, so the pump displacement decrease that means the delivery flow rate decrease. Such action continuum till the delivery pressure is stabilized at the limiter pressure setting when the spool is in equilibrium.

In order that, also the swash plate is in equilibrium, as well as the pump gives the needed flow rate to the load at given fixed pressure at the delivery, must be equal both actuator forces:

$$p_m * A = f_m + p * a \tag{2.1}$$

Since, in the spool equilibrium conditions the delivery pressure p is equal to the limiter pressure setting p^* , the pressure that this one must keep on the variable displacement actuator is:

$$p_m = p^* * \frac{a}{A} + \frac{f_m}{A} \tag{2.2}$$

2.2.2) Differential pressure limiter

The second variable displacement control, realise a differential pressure limiter (LPD), illustrated in figure 2.4.

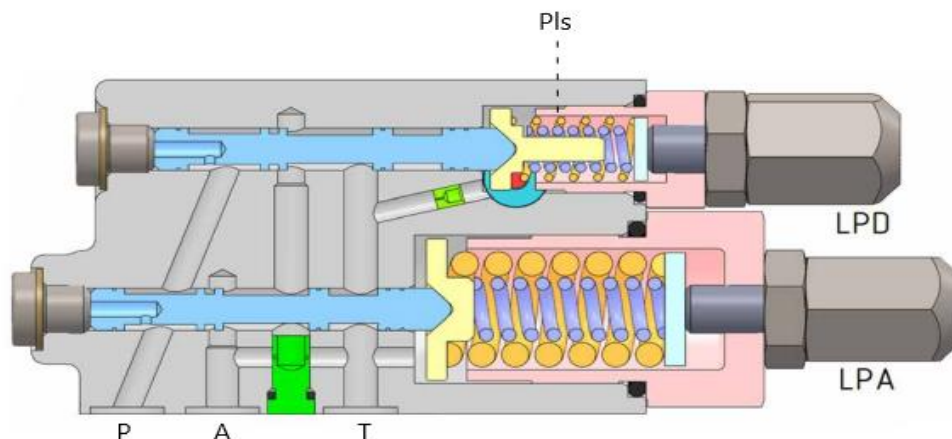


Figure 2.4: Differential pressure limiter together with an Absolute pressure limiter [4]

This principle allows the load sensing logic, as explained in the previous chapter. It is needed change the pump displacement to guarantee a constant pressure drop across the continuous position distributor (DPCV), located on the user line, equal to a spring pressure setting [1]. This means, send a flow rate to the load dependent only of the DPCV opened section area. Such component must be valid independently of the pressure level imposed by the load. For these reasons are collected two piloted signals, upstream and downstream of the distributor, and are brought on a spool continuum position active surfaces with three ports. With the scope of manage the pressure saturation, that means the load pressure increased beyond an acceptable limit, this device must limit the pump delivery pressure. So, to overcome this problem, an absolute pressure limiter is adopted, already discussed in the previous paragraph, together with the LPD. The external connections are the port P that receives the pump delivery pressure, the port T connected to the pump carter, and the port A that is connected to the variable displacement actuator. Very important for the control is the LS signal, that is brought on the spring environment of the LPD. It is important underline that, there are are two coaxial springs, where the internal one has a free length lower than the external one. The total elastic characteristic has a discontinuity, with a slope increasing when both the springs are working. Analysing the LPD structure, it is again a continuous position valve with three ports: the port P connected to the pump delivery, port T to the pump carter, and the third port, in central position, is connected at the port T of the LPA. The three ports are internal channels directly connected to the LPA. The pilot signal with the load pressure information, reach the springs environment. On the limiter spool, act the delivery pressure (such pressure tends to close the connection between the ports T and A and open the connection A and P), on the other end act the springs and the load sensing signal. The active surfaces are the same on the two ends. In neutral condition, the two shoulders on the left divide P from A, with a positive cover, while the port A and T are in connection, also the LS signal is discharged (when the pump is at standstill) due to a restrictor (S2) placed between the springs chamber and the port T, but during the normal function the restrictor uncoupled the LS pressure from the carter pressure. The two coaxial springs are packed from to plates and are regulating through a screw on the right.

On this scheme in figure 2.5, is possible to understand how the limiter works:

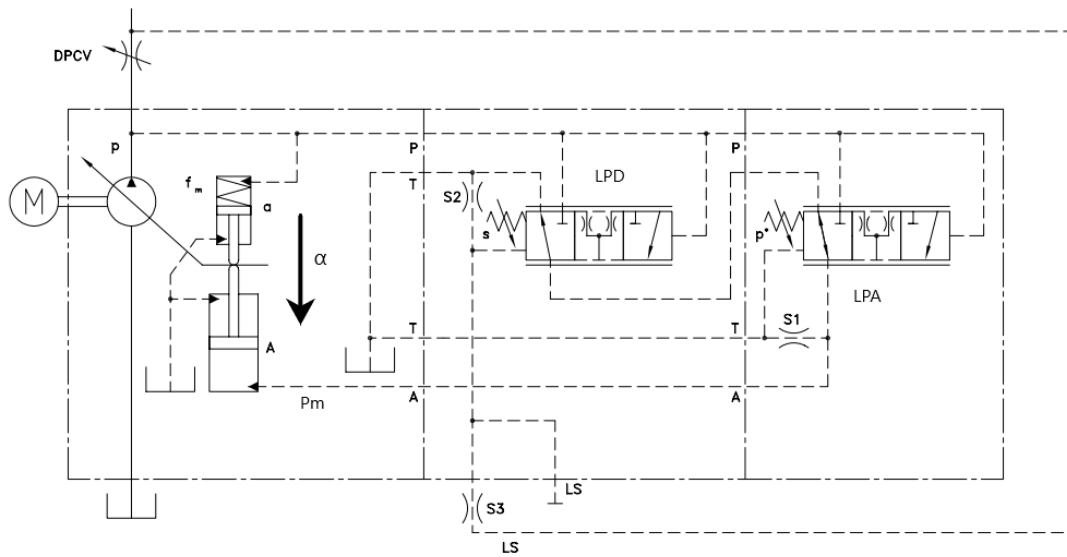


Figure 2.5: Pump with load sensing control [1]

Starting from a condition in which the DPCV is completely open, so the pressure information upstream (p) and downstream (p_{LS}) of the distributor are the same, the differential pressure limiter spool is in the neutral position due to coaxial springs. The modulated pressure p_m on the variable displacement actuator is equal to the pressure on the pump carter and so the pump is at its maximum displacement. Considering a reduction of the user flow rate, the DPCV will regulate. Since there is a pressure drop on the delivery line, the pressure signal p increase, as long as there is an equilibrium on the spool with the load sensing signal LS and the springs. The spool passes from a neutral position to a condition where P and A are in communication. In this way p_m acts on the variable displacement actuator, reducing the pump displacement. This action keeps going until an equilibrium position, given by:

$$p = p_{LS} + s \tag{2.3}$$

Being s the LPD pressure setting (due to the tuning of coaxial springs pre-load). The last equation shows that the control acts in order to fix the pressure drop on the distributor. This guarantee that the flow rate that pass through the distributor is directly proportional to the opened area of the distributor itself, like the load sensing principle works. It happens, independently from the load, that means of the p_{LS} value. So that the swash plate is in equilibrium, and so the pump supplies the required user flow rate, must be valid the equation 2.1, but in this case when the spool is in equilibrium the p pressure value is given by the equation 2.3. The pressure inside the variable displacement actuator is:

$$p_m = (p_{LS} + s) * \frac{a}{A} + \frac{f_m}{A} \tag{2.4}$$

It is important remember that, when the pressure imposed by the load on the delivery pump line exceed the safety pressure setting, the absolute pressure limiter intervene. The pressure signal generated on the port A of the LPD, must passes into the LPA metering edge, so this component is a priority to manage the pressure p_m .

2.3) Gear pump

The gear hydraulic machines are the most used and cheapest because they have constructive simplicity [1]. They are classified in external gears and internal ones (crescent). The first typology are constitute by a carcass where are located gears with straight teeth and unitary transmission ratio. The two gears are supported by shafts, and one of them allows the prime mover connection. On the carcass are obtained the delivery ports and the suction ports. There are usually present sealing plates that can, regarding the constructive solutions, have different geometry, in terms of axial thickness and machining (milling) done on it. Generally, these plates are loaded with the delivery pressure for the axial play compensation. The gear pump working principle is the typical of the rotary volumetric machines. For the suction phase, the working fluid is taken from an external environment to the pump and isolated on the spaces in between the teeth and the carcass. In this way, it is realised a fluid transportation from the low-pressure side to the delivery side. Where the gears have contact, there is not a completely null transportation volume, but there is a trapped fluid volume that is connected through channel on the plates, that communicates either with the delivery environment or with the suction one. On the crescent machines, the driven gear has internal teeth, and it is placed directly on the machine body without shaft. An element integral with the carcass, called crescent, allows to separate the environments with high and low pressure. The advantages of internal gear machines are the lower flow rate irregularity and the lower size with the same displacement. The disadvantage is the higher construction complexity to reach high working pressure.

2.3.1) External gear machines

In an external gear machine, each volume that transport fluid, is identify by a space between two rotor teeth [1]. If Z is the number of rotor teeth, the number of chambers is $N = 2Z$. In this type of machines, the volume chamber is at maximum value for the cycle majority, varying only when the teeth are in contact. The number of cycles per round is equal to one. Regarding the unitary displacement, can be seen that, the maximum volume V_{max} is clearly identified, the minimum volume is shared between two chambers, one belongs to a drive gear, and the other belong to a driven gear. In particular, can be observable that, for certain rotor positions exist a trapped volume V_t , as shown in figure 2.6.

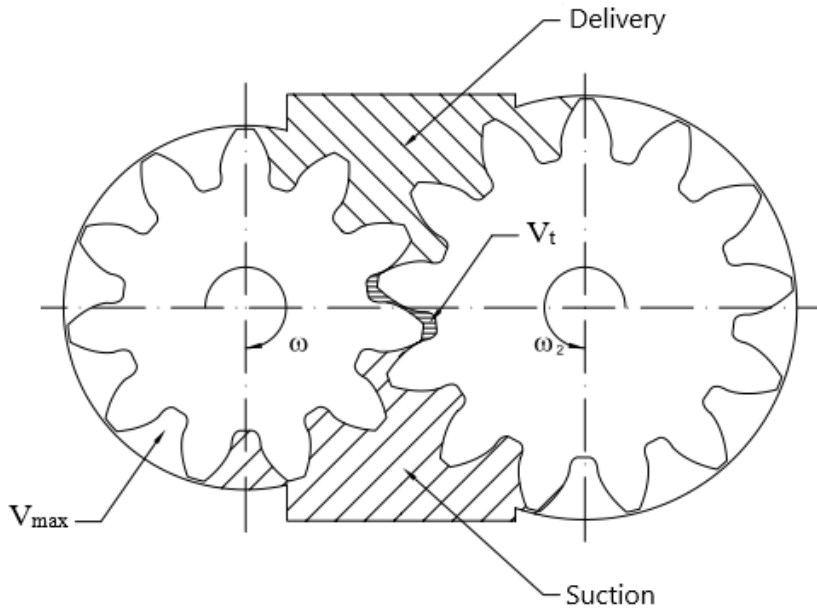


Figure 2.6: External gear pump [1]

When the two gear teeth have only one point of contact, all volume that is above the teeth belongs to the delivery side and the volume below belongs to the suction side. To ensure motion continuity, it must be guaranteed that there are two points of contact before the upper point of contact disappears. When the volume is closed between teeth, it has a proper independent evolution. In particular, at the beginning it is reduced, reaching the minimum volume, when the distance from the points to the axis that connects the rotor centers is the same. It is possible to exploit this volume reduction to transfer the fluid opening a connection from the plate to the delivery volume. Continuously with the rotation, the trapped volume increases until the contact point above the teeth disappears. The fluid volume that ideally comes back to the suction is the minimum of the trapped volume: such volume is half for the drive gear and half for the driven gear. The unitary displacement is:

$$V_0 = V_{max} - \frac{V_{min}}{2} \quad (2.5)$$

So, the pump displacement is:

$$V = 2ZV_0 = Z(2V_{max} - V_{min}) \quad (2.6)$$

2.4) Distributors with local compensators

2.4.1) LS Proportional distributor

The distributor is a continuous position bidirectional valve with five ports and three positions. When is given a command X, the pilot signal LS is taken from the actuator direct line that is powered through the pump. In neutral position the LS signal is discharged, in order that the pressure on the distributor upstream line is keeping at minimum pressure value equal to s , imposed by the pump differential pressure limiter.

The spool positions represented with dashed line on figure 2.7 (intermediate positions) highlights that, before the user is powered, the load sensing signal is pressurized to the load pressure.

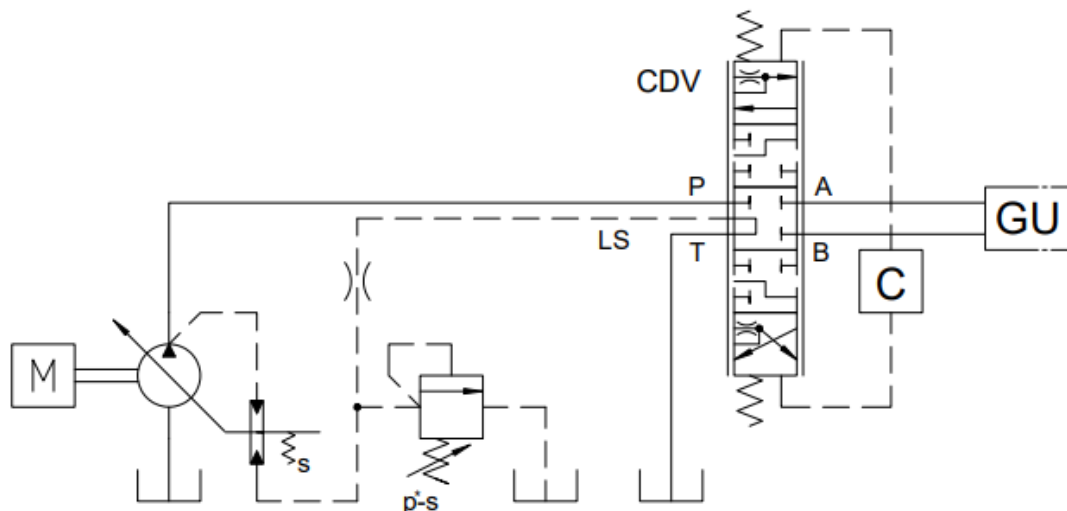


Figure 2.7: velocity control bidirectional [1]

In order to have on the distributor upstream a well-timed pressure equal to p_U plus the differential pressure limiter pressure setting, in this way it is guarantee a fast system response and avoid possible flow rate reflux.

2.4.2) The local pre-compensators

Introducing the local compensators on the system, it can re-establish the controllability in any load condition [1]. Each of them, is placed upstream of its distributor respectively, like in figure 2.8.

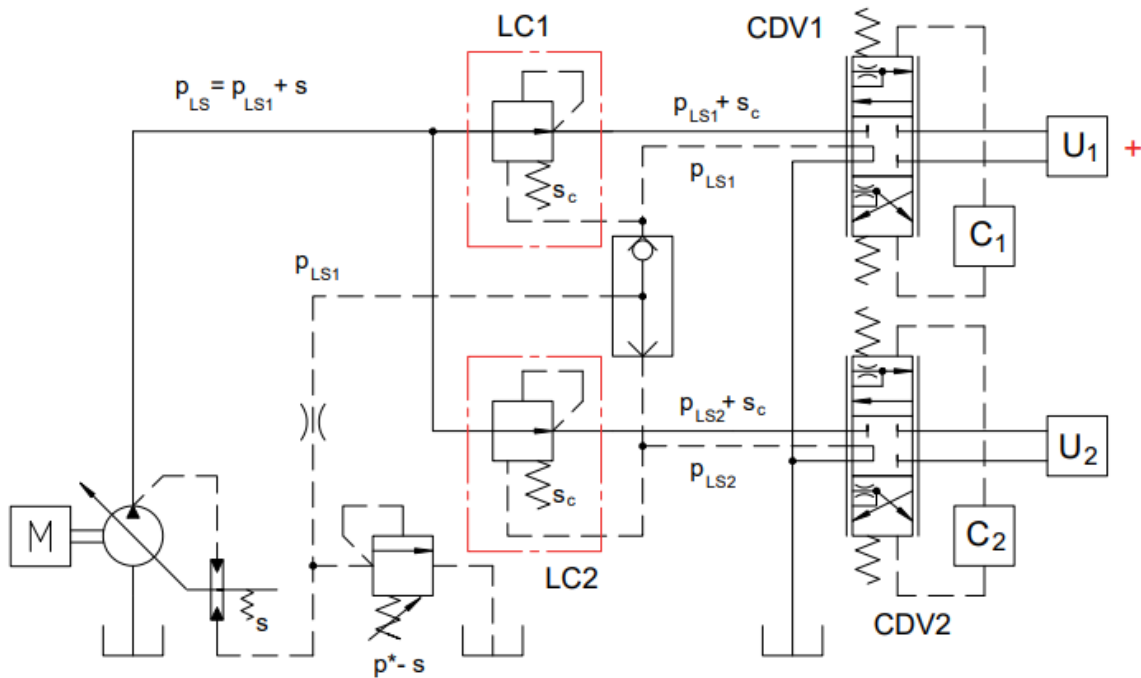


Figure 2.8: LS circuit with local pressure pre-compensated [1]

When a user is less loaded, the local compensator generates a pressure drop in order to recreate a constant pressure drop equal to s on the distributor, that is the condition that guarantee the user controllability. Ideally, on the most loaded user, the local compensator behaves as a valve normally open that does not regulate, and its cracking pressure is equal to the limiter pressure setting. Each user is given the required flow rate independently of the pressure condition that it imposes.

On the energetic point of view, with these load conditions and distributor positions, the useful power is:

$$P_U = Q_i * p_i + Q_j * p_j \quad (2.7)$$

The expended power to generate it is:

$$P_S = Q_{tot} * (p_i + s) = (Q_i + Q_j) * (p_j + s) \quad (2.8)$$

The power loss:

$$P_P = Q_{tot} * s + Q_j * (p_i - p_j) \tag{2.9}$$

the power loss, is constitutes from two contribute, that can be visualized in the power plane of the figure 2.9:

- The total flow rate times the pressure limiter settings;
- The flow rate sends to the user with lower load, multiplied for the pressure drop introduced by the local compensator.

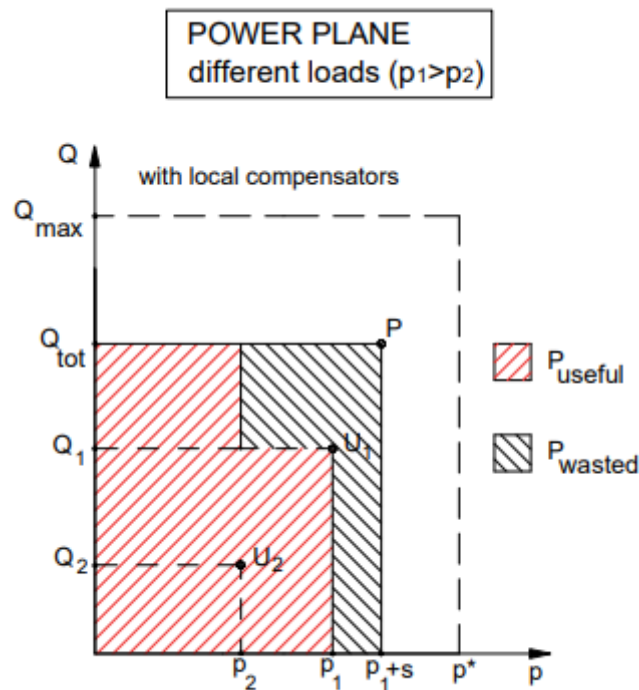


Figure 2.9: Power plane [1]

This means that, higher pressure difference between relative LS pressure signals, higher the power loss. This is a compromise that can be accepted to keep the user velocity control, without the present of pressure and flow saturation phenomena.

In the figure 2.10, it is resuming the pressure distribution on different part of the most loaded user and on all the other users, when the compensator regulates.

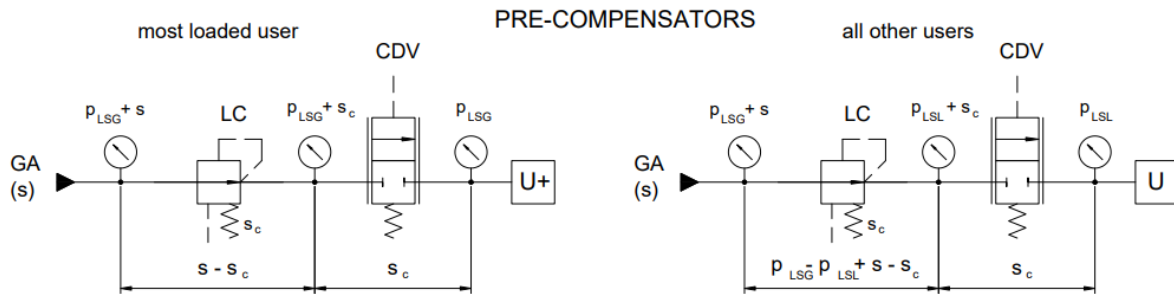


Figure 2.10: Pressure scheme in a pre-compensated plant [1]

LSG and LSL are referred to the global and local load sensing signal respectively. It is evident that, the pressure drop across the distributor is equal to the compensator cracking pressure s_c . from the theoretical point of view, that means without losses on connection lines, s_c should be equal to the differential pressure limiter settings s . the global setting pressure s is chosen consider at least equal to the pressure drop generate when on the distributor pass the maximum flow rate at minimum temperature (s is about 15-25 bar). if is impose $s_c = s$, means that the compensator does not introduce losses, so it is positive because it is the maximum load, and the compensator is completely open. The imposition of a pressure drop across the compensator does not make sense both functionally, because the desired pressure is already imposed by the hydraulic power unit, and energetically. Furthermore, it is important consider that the flow rate decides by the distributor is function of its throttle area, that is limited, on the compensator cracking pressure s_c , that on the formula is on the square root. So, the discharged flow rate can be heavy limited if s_c is not sufficiently high. However, it must be taken into account the pressure drops due to distribution losses on the hydraulic lines (figure 2.11), evaluated at maximum flow rate and so the actual local compensator cracking pressure is lower than the global by a quantity equal to the maximum pressure drop due to the hydraulic lines:

$$s_c = s - \Delta p_{Q_{max}} \tag{2.10}$$

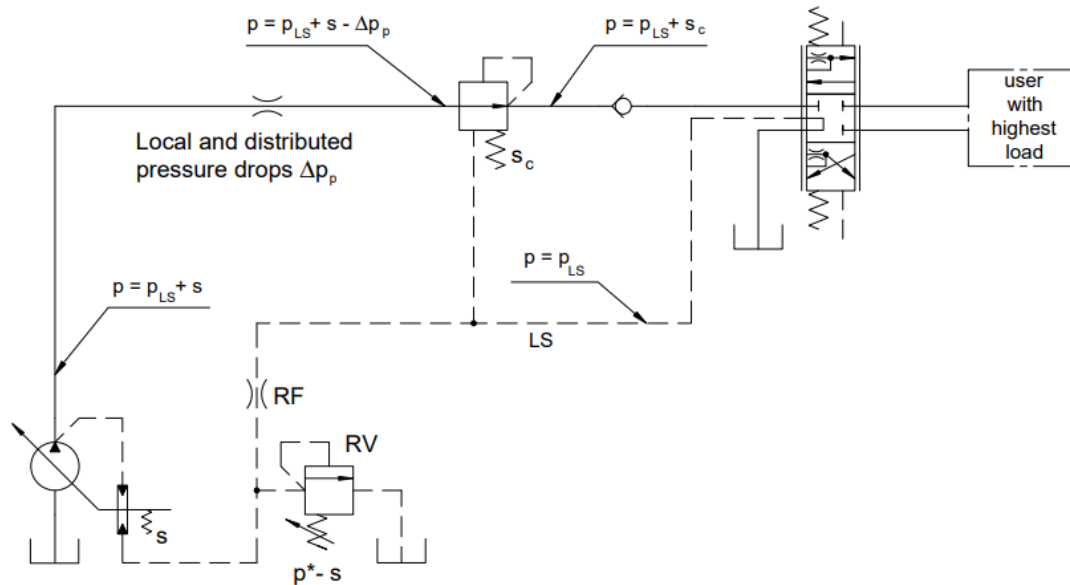


Figure 2.11: Resume scheme for the choice of the local pre-compensator cracking pressure [1]

The actual local cracking pressure is lower than the global, of a quantity at least equal to the losses at maximum flow rate, because being impossible to realise perfect tuning, this difference should be for safety reasons more pronounced. If this rule is not respected, it implies the loose controllability of the load, in the sense that the pressure drops on the local compensator of the most loaded user depend on the distributed losses that are variable and not only from constant variables. For example, if s is equal to 15 bar and the hydraulic losses from the pump delivery to the compensator at maximum flow rate are 5 bar, the suggested local compensator cracking pressure is 10 bar. If the flow rate delivered by the pump is lower than the maximum flow rate, also the distributed losses are lower. This means that also the local compensator of the highest load must regulate.

One of the first compensators that appear on the market was the PVB60, illustrated in figure 2.12.

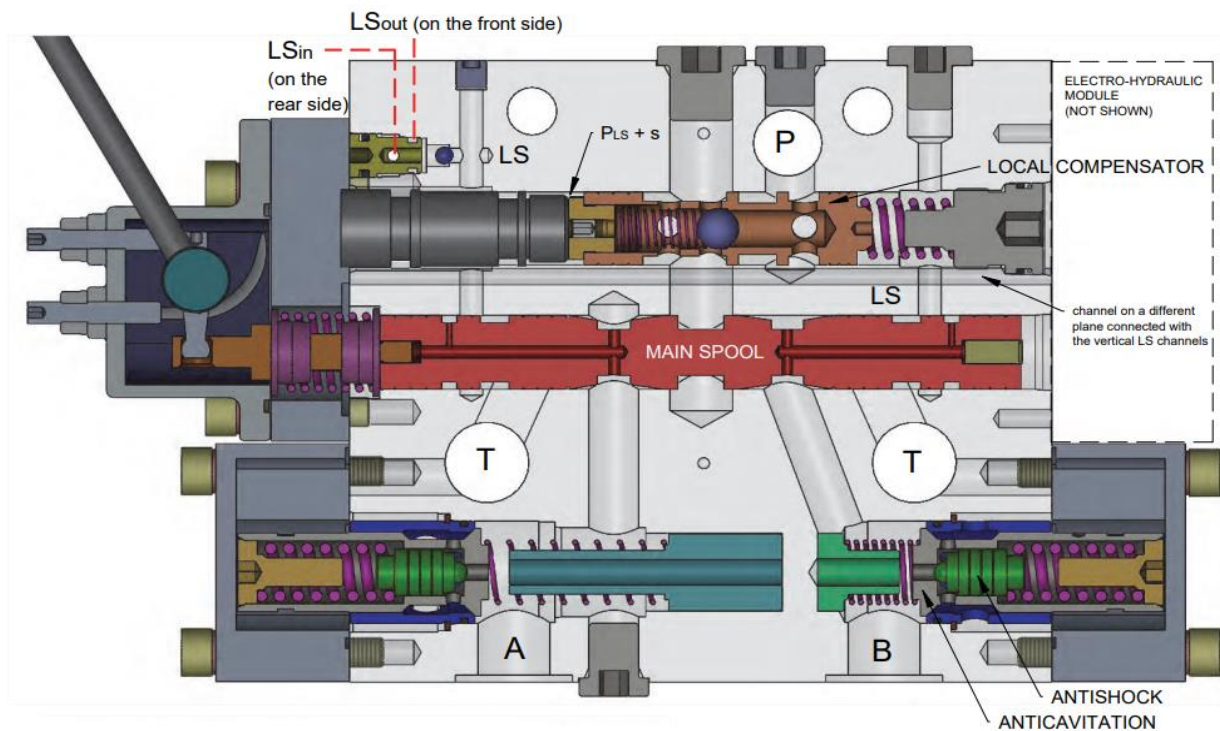


Figure 2.12: Cross section PVB60 [1]

In the upper part, can be notice the local compensator that has inside a unidirectional valve, in the centre position the main spool, that determine the throttling area, and on the lower part, there are valves that limits local pressure signals, anti-shock and anti-cavitation [1]. on the right is indicated the position of the electric hydraulic module PVE, while on the left is visible part of the leverage for the emergency mechanical activation. The pump delivery port is located on the upper part, while the user ports A and B are on the lower part. In addition, LS indicate the regions where there is the pressure of the load sensing, instead T indicate the regions where there is the tank pressure. With the main spool in neutral position, the distributor is in the closed centre configuration the compensator is normally open and the LS signal is discharged. For instance, the main spool moves to the right, it put in connection the delivery port with the port A, such movement put in connection also the load sensing line with the port A, slightly in advance with respect to the connection with the port T. in detail, the load signal is taken thanks to the internal path on the main spool, passing through shuttle valves with the aim of select the major one, and send to the pump. The port B in discharged, and the opposite spool movement create obviously the opposite connection, P with B and A with T.

The pressure given by the pump (port P) does not influence the spool equilibrium, because the surfaces where the pressure acts are the same. In regulating position, through the spool

metering edge will be a pressure drop. On the local compensator spool acts the following pressures (figure 2.13):

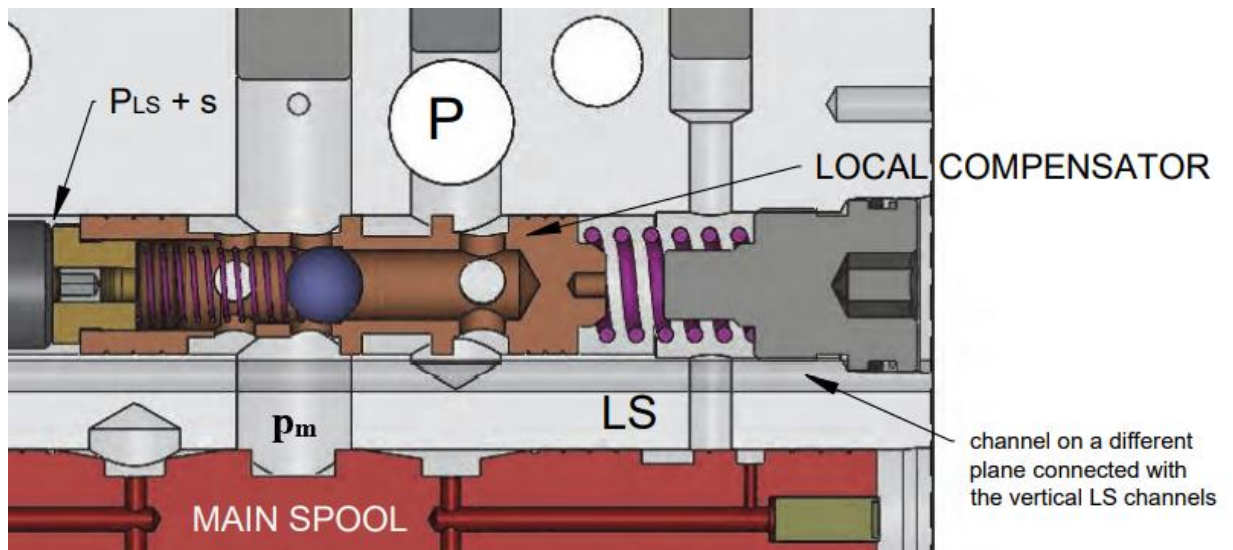


Figure 2.13: Detail pressure compensator PVB60 [1]

- To the right, the pressure information provided by the load p_{LS} (given by A or B) and transmitted through one of two twin channel presents on the principal spool body, that open.
- To the left, the pressure $p_m = p_{LS} + s_c$, thanks to the spool equilibrium, that close.

The p_{LS} , with a horizontal channel in a different plane that intercept a vertical channel, has a comparison through the shuttle valve with the higher-pressure information, that is the result of others comparison done by other shuttle valves between load connected with other PVB module. From the comparison in the shuttle valve will come out the highest pressure that will be send to the line LS_{out} outside of the module itself. It is important notice that, the two pressures that are present are the pressures present immediately upstream and downstream on the main spool. The local compensator, maintain constant and equal to the equivalent spring pressure, the pressure different on the metering edge of the main spool. This is obtained paralysing more or less its throttling area in order to change, in the right way, the pressure p_m as a function of p_{LS} . The local compensator, saw together with the variable restrictor determined by the main spool metering edge, realise a flow control valve with two ports on the user point of view that desire to regulate in speed.

2.4.3) The local post-compensators (anti-saturation compensator)

Considering a situation when the flow rate delivered to the pump does not satisfy the flow rate required by all the users:

$$\sum Q_i > Q_{max}$$

(2.11)

So, the pump works at maximum displacement. If the throttling area of the most loaded distributor increase, for instance U1 in figure 2.14, the pressure p_c decrease, its local compensator is not in equilibrium anymore and so the compensator opens completely.

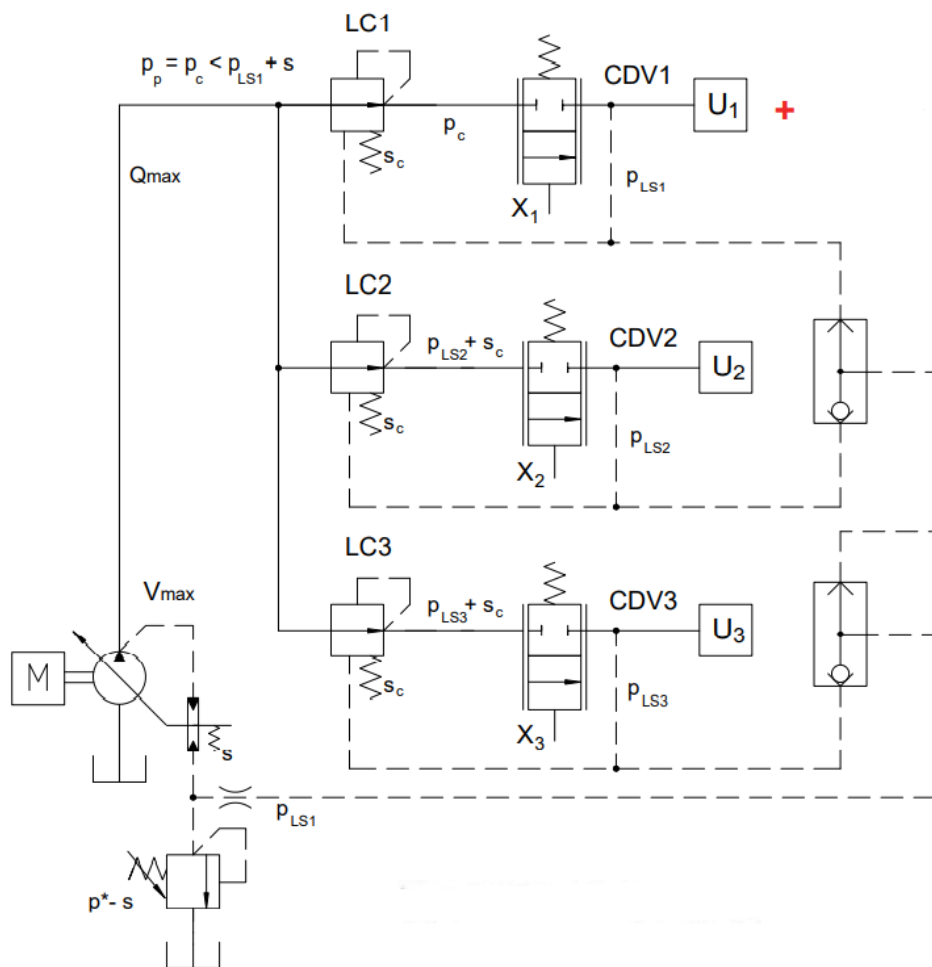


Figure 2.14: Pre-compensated plant in flow saturation [1]

Since the pump displacement control does not regulate:

$$p_p = p_{LS1} + \Delta p'$$

(2.12)

Where $\Delta p'$ is lower than s , this implies that the pressure drop on the lower user compensators are:

$$\Delta p_i = p_{LS1} + \Delta p' - (p_{LSi} + s_c) \approx p_{LS1} - p_{LSi} > 0 \quad (2.13)$$

Instead, the pressure drop that corresponds to the distributors are both equal to s_c . Since there is not a pressure drop on the most loaded user local compensator, the pressure drop on its distributor is equal to $\Delta p'$, but this one depends also on the command of other user, therefore the most loaded user receive the remaining flow rate.

$$Q_1 = Q_{max} - Q_2(X_2) - Q_3(X_3) \quad (2.14)$$

To overcome this problem, it is implemented a post compensator strategy (figure 2.15), called also anti-saturation, where the local compensators are normally closed and placed downstream of the metering edge of the main spool.

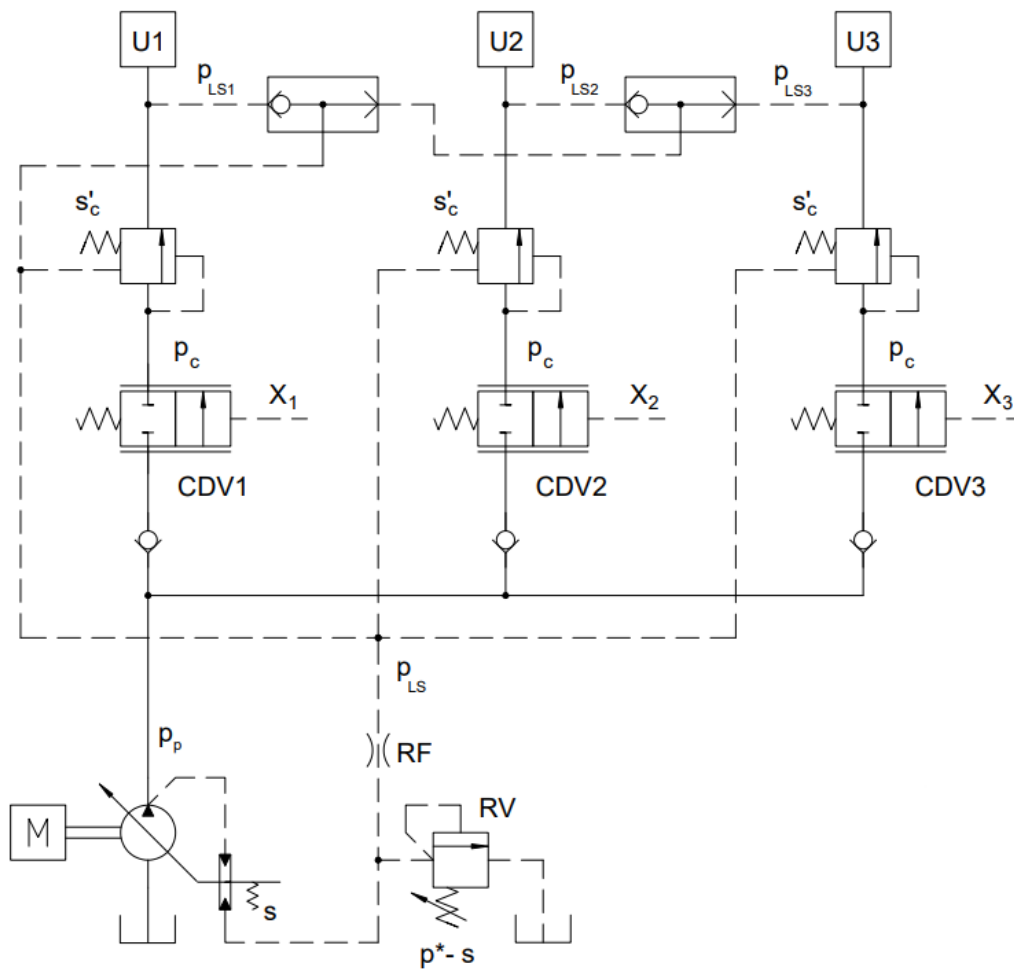


Figure 2.15: Post-compensated plant [1]

When it regulates, obey at this relation:

$$p_c = p_{LS} + s'_c \quad (2.15)$$

Where p_{LS} is the maximum value of the load sensing signals, furthermore, the pressure drop on all distributor is constant:

$$p_c = p_p - p_c = p_{LS} + s - p_{LS} - s'_c = s - s'_c \quad (2.16)$$

Therefore, the flow rate is:

$$Q_i = C_d A_i(X_i) \sqrt{\frac{2(s - s'_c)}{\rho}} \quad (2.17)$$

In condition of flow saturation, the pump delivery pressure is lower than the highest load sensing signal plus the differential pressure limiter setting, so the pressure drop across the distributors are lower but the same for all.

$$\Delta p_{sat} = p_p - p_{LS} - s'_c < s - s'_c \quad (2.18)$$

Therefore, the flow rate now is:

$$Q_{i,sat} = C_d A_i(X_i) \sqrt{\frac{2\Delta p_{sat}}{\rho}} = k Q_i \quad (2.19)$$

Where k is lower than 1, so the summation of all flow rate is equal to the maximum flow rate, and the flow rate through all CDV depends only on the command X_i .

In this case, the situation is like the pre-compensate plant, but it is evident that, on the most loaded the pressure the drop that there is across the compensators, is equal to its cracking pressure s'_c (figure 2.16).

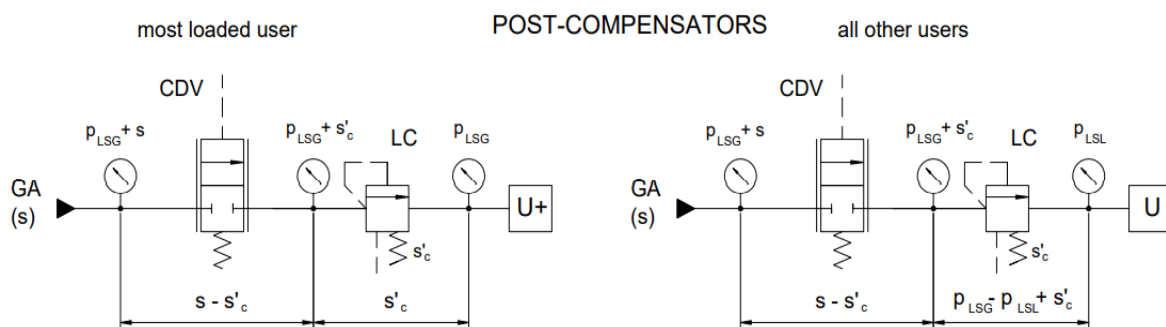


Figure 2.16: pressures scheme in a post-compensated plant [1]

As already know, the compensator is normally closed, so, in order that there is a flow rate passing through, it must regulate, is easy to understand the interest is to minimize s_c' . moreover, it can worth notice that the pressure drop on the CDV is the difference between the global pressure setting and the local pressure setting is $(s - s_c')$ like in figure 2.16. if the local pressure setting would be too much higher, the Δp value on the metering edge of the main spool would have a high decreasing, producing a heavy reduction of the discharged flow rate. To overtake this limit of the pressure drop, it could increase the global pressure setting, but a useless power loss will generate. Finally, the local pressure setting s_c' is completely different from the pre-compensated case and definitely lower, in general in the order of 1 or 2 bar.

The PVB100 (figure 2.17) is a post-compensated distributor, based on the concepts illustrated up to now [5].

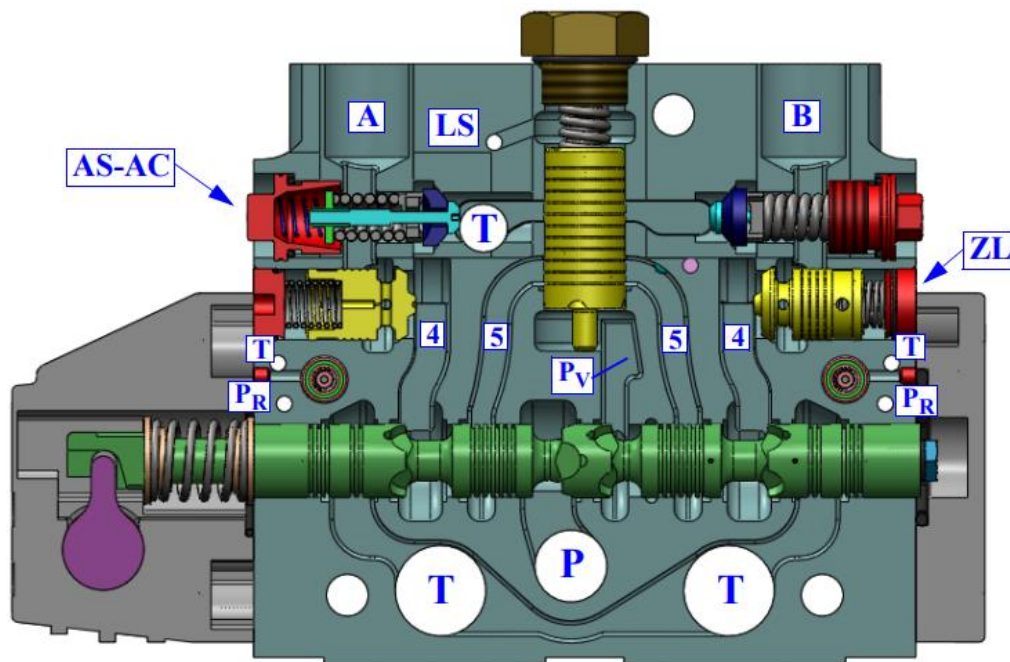


Figure 2.17: PVB100 distributor cross section [5]

On the upper part, in central position, can be notice the pressure compensator, the anti-shock AS and anti-cavitation AC valves, the two zero leakage ZL, that guarantee perfect sealing when there is not action on the distributor, main spool. The connection ports are with the pump P and the reservoir T on the lower part, with the users A and B on the upper part and the global load sensing signal. There are other connections dedicated to the activation of the ZL valves, while behind the compensator, there are channels that collect eventually bleeds.

If for instance, the main spool moves to the left, the oil that arrive from the port P pass the metering edge and so to the local compensator, at this point, exploiting the channel on the right, will be powered the user B. At the same time, the return oil that arrive from the port A pass through the main spool metering edge and arrive on T. Can be notice that, to make these phenomena, the block valve of the port B opens naturally, instead the block valve of the port A will be open thanks on the pilot stage delivery pressure, such action is generated at the same time with the movement of the main spool toward the left.

In figure 2.18, ZL indicate the blocked valve seen by the spring side, the brown element (A) is a piston that allows the stage movement, and the green one (B) is a poppet. Furthermore, on 3 acts the load pressure, maintaining the pilot stage as in the figure and ZL closed, because the main spool position put in connection the environment 2 with the tank and isolate 1, these connections are holes on the carcass visible behind the pilot stage elements.

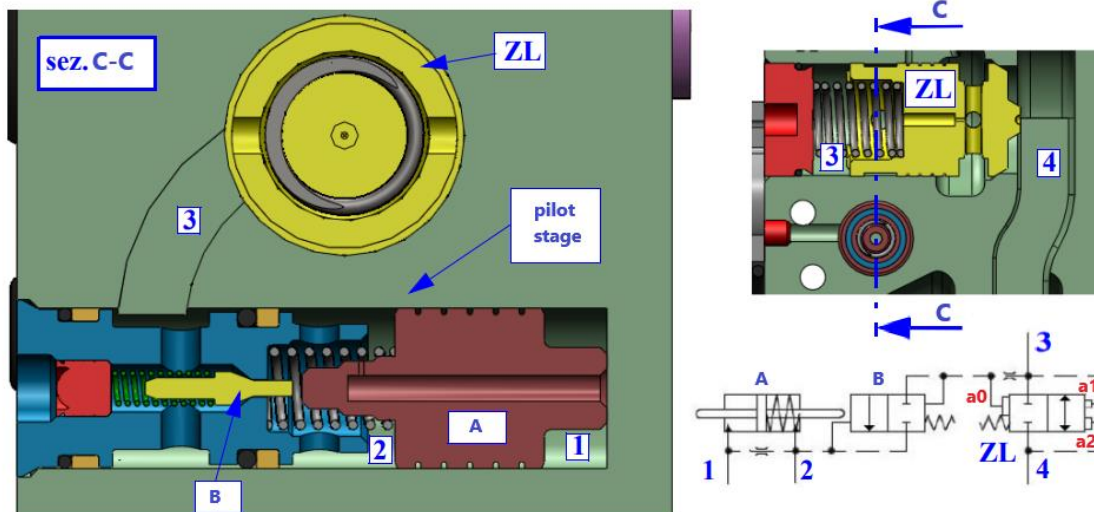


Figure 2.18: Pilot stage for the ZL valve [5]

Along the powered line, 2 remain connected to T and 1 is not powered, so the poppet (B) remains at standstill. The main valve poppet moves, allowing the fluid to go toward the user, being that the open action is prevalent, because the pressure that acts on a2 is higher than the load pressure. Instead, on the discharged line, 2 seen again the tank, while 1 is powered from the reduced delivery pressure generated in an inlet module that powered also the electro-hydraulic module for the main spool. This produces the piston (A) movements and consequently the poppet (B) movement. Therefore, the a0 surface will be discharged thanks the throttling area opened by the poppet (B), and the ZL opens due to the pressure in 3 on surface a1, this area is given by the crown on the ZL poppet, and even if it is small, it is sufficient to win the spring preload that give a small contribution.

Looking more in detail the compensator in figure 2.19, it is normally closed. The load sensing pressure and the spring tend to close the compensator, while the pressure downstream of the main spool tends to open it.

$$p_v = p_{LSG} + \frac{f_m}{S} = p_{LSG} + s_c$$

(2.20)

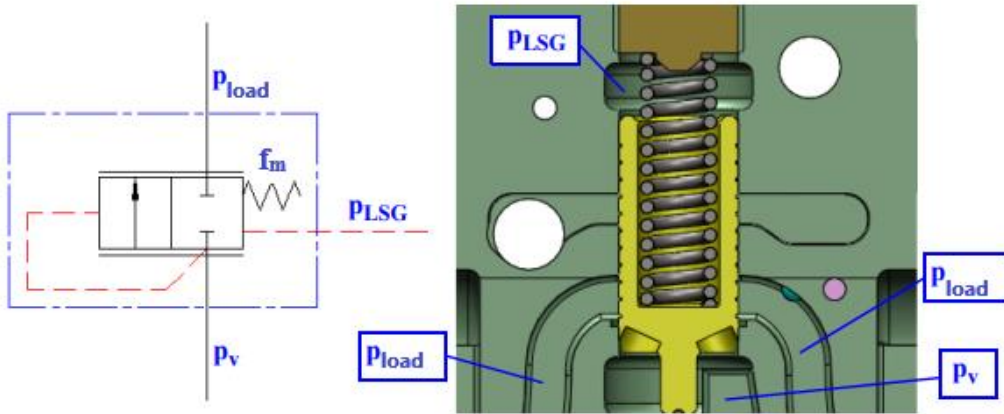


Figure 2.19: Pressure compensator detail and its ISO scheme [5]

Both the pressures are acting on the same surface S . Moreover, since the pressure upstream of the main spool is decided by VDL (figure 2.20), the pressure drop on the metering edge is:

$$\Delta p_{main\ spool} = (p_{LSG} + s_p) - (p_{LSG} + s_c) = s_p - s_c$$

(2.21)

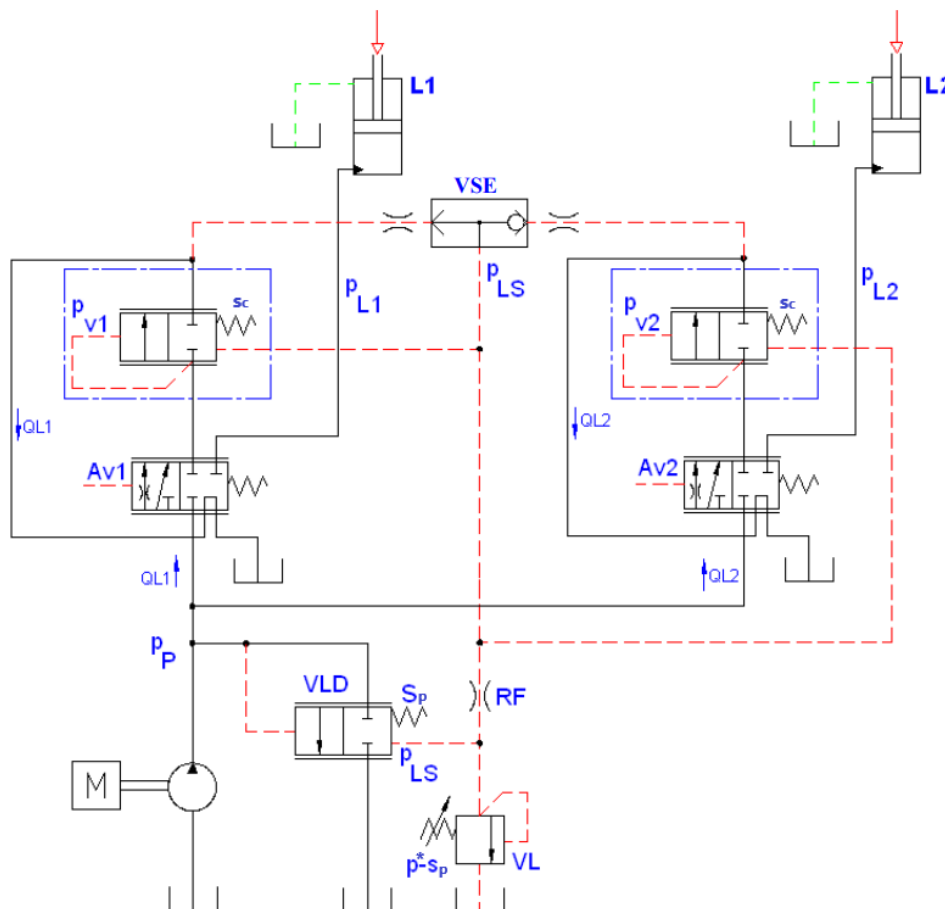


Figure 2.20: simplified scheme with the distributor PVB100 [5]

Constant pressure drop that, allows the load controllability, also when it change. In case of flow saturation, the VDL is saturated and closing stop to impose the delivery pressure. So, the new delivery pressure will be lower and equal to:

$$p_p = p_{L1} + s' < p_{L1} + s_p \quad (2.22)$$

where s' is lower than s_p and $L1$ is the most loaded user. Consequently, the pressure drops on the two spools are:

$$\Delta p_{main\ spool} = p_p - p_v = (p_{LS1} + s') - (p_{L1} + s_c) = constant < s_p - s_c \quad (2.23)$$

These, even if are reduced, they are again constants, allowing the load controllability with proportionally low speed. The load stops only when there is a pressure saturation and the load pressure become $p_{L1} > p^*$.

2.5) Hydraulic actuators

The hydraulic actuators (figure 2.21), called also linear motors or jacks, like all the user groups, converts the hydraulic power, from the power group, in mechanical power [1].

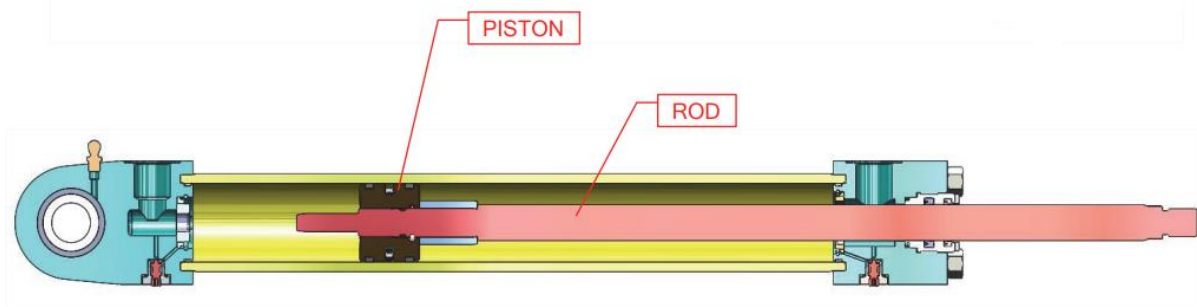


Figure 2.21: Hydraulic actuator cross section [1]

They are study plotting the pressure-flowrate characteristic (Q_u, p_u), so is known the situation on the inlet line of them. At this point, there is the need to build the actuator mechanical characteristic, that give the linear velocity (v) as a function of the force (F). The linear actuators are device with three ports and so are described from three equations, in which two of them have extensive quantities (flowrate, speed) and one have intensive quantities (force, pressure). A linear actuator can work with a flowrate imposed on one of the two ports (inlet, outlet), or a pressure impose. Moreover, depending on the circuit used, it can work in condition of resistant load or an overrunning load.

A load is defined resistant if its velocity is in opposite direction with respect the force direction that it applies, as represented in figure 2.22 and figure 2.23. Considering the case, in

which is imposed a flowrate on the inlet port and writing the translation equilibrium, the flowrate (velocity) conservation equations and the rod speed expressions, are obtained:

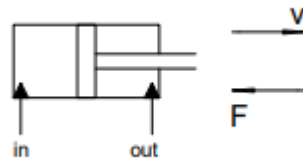


Figure 2.22: Case rod come out resistant load [1]

$$p_{in} * A = p_{out} * a + F \tag{2.24}$$

$$\frac{Q_{out}}{a} = \frac{Q_{in}}{A} \tag{2.25}$$

$$v = \frac{Q_{in}}{A} \tag{2.25}$$

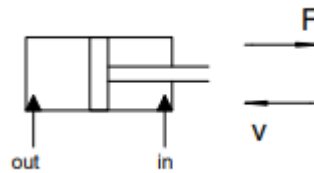


Figure 2.23: Case rod return resistant load [1]

$$p_{in} * a = p_{out} * A + F \tag{2.26}$$

$$\frac{Q_{out}}{A} = \frac{Q_{in}}{a} \tag{2.27}$$

$$v = \frac{Q_{in}}{a} \tag{2.28}$$

When the velocity and force are with the same direction, the load is called overrunning (figure 2.24 and 2.25):

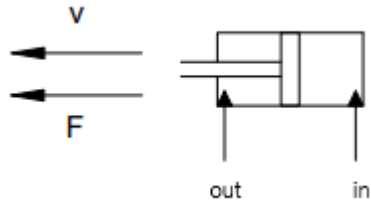


Figure 2.24: Case rod come out overrunning load [1]

$$p_{out} * a = p_{in} * A + F \tag{2.29}$$

$$-\frac{Q_{in}}{A} = -\frac{Q_{out}}{a} \tag{2.30}$$

$$-v = -\frac{Q_{out}}{a} \tag{2.31}$$

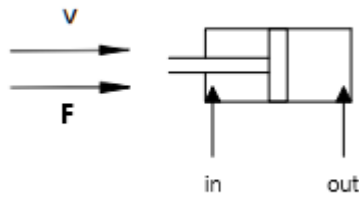


Figure 2.25: Case rod return overrunning load [1]

$$p_{out} * A = p_{in} * a + F \tag{2.32}$$

$$-\frac{Q_{in}}{a} = -\frac{Q_{out}}{A} \tag{2.33}$$

$$-v = -\frac{Q_{out}}{A} \tag{2.34}$$

On the scheme in figure 2.26, there is a hydraulic power unit with constant flowrate that powers, through a 4/3 distributor spring centred and solenoidal activated, a double effect linear actuator, where on its rod there is always a resistant load.

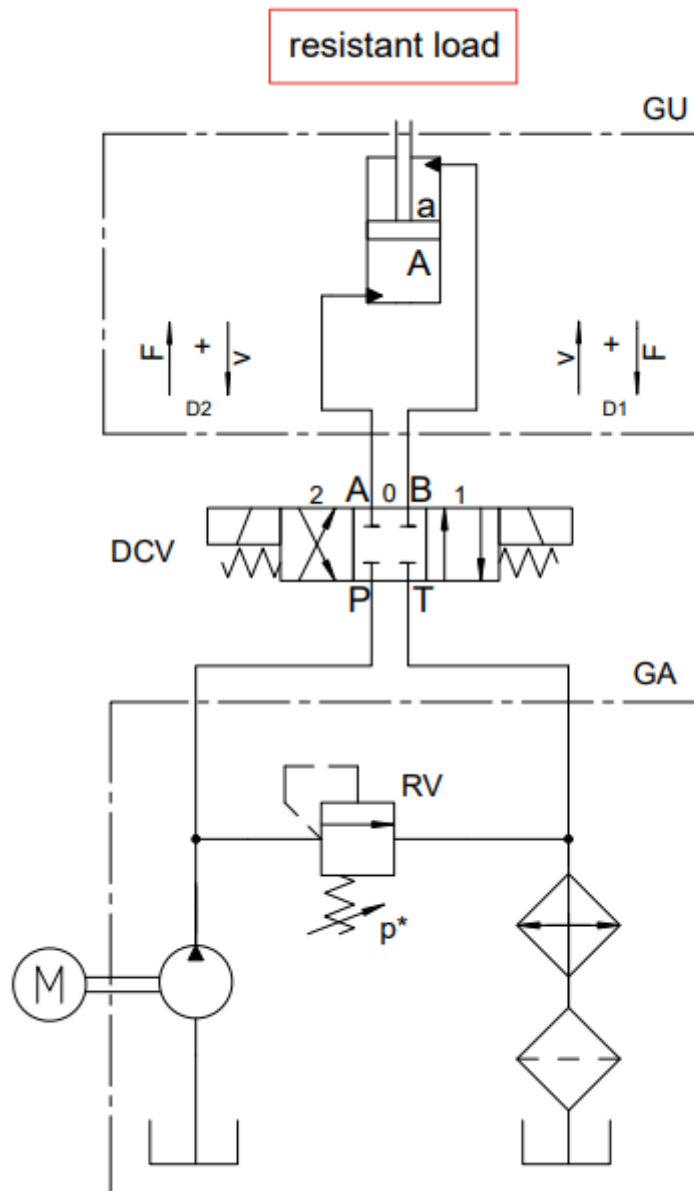


Figure 2.26: Reference power unit for linear actuator [1]

For example, if it is choice the position 1 of the distributor, the rod come and so lift the load. This is clearly a load resistance condition. Instead, if it choice the position 2, the rod return, but being for hypothesis always resistance load, it will be again that the velocity and the load are opposite. Now, it is clear that with this scheme is not possible to manage overrunning load, because there is not a back pressure on the outlet port of the actuator and is not possible identify equilibrium situations. This means that, is not possible to consider that the load is

invertible, at the same speed, or speed inversion at the same load (no characteristics in the 2nd and 4th quadrant in figure 2.27).

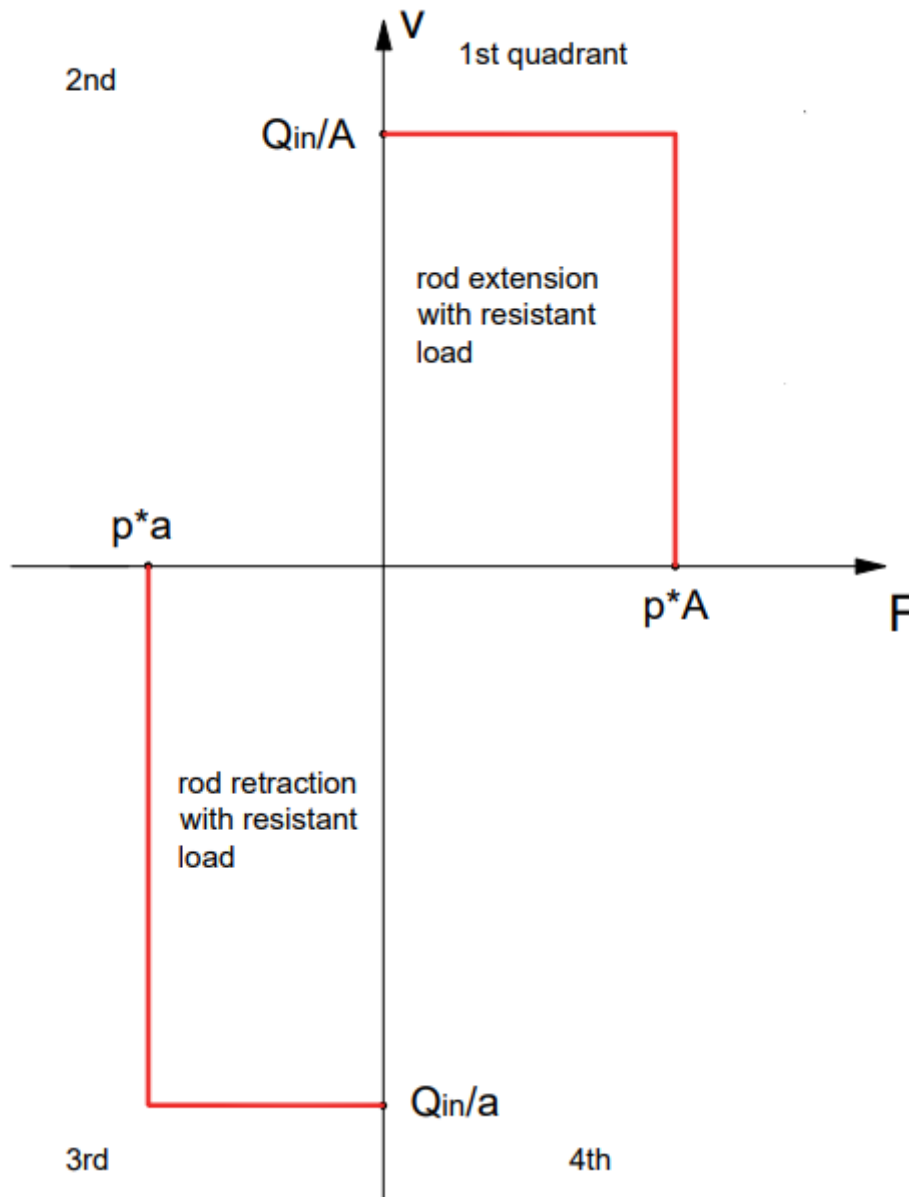


Figure 2.27: Mechanical characteristic [1]

This observation, notice that there are some problems on the distributor configurations (parallel or cross arrows). Also, on the central position there are some inconvenient. First, the idea that the closed centre can hold a load in an actuator intermediate position is wrong, because there are some bleeds on the distributor that does not guarantee this aspect. Second, the lines that connect the distributor to the actuator do not are protected from possible overpressure or depression due to impulsive load, and there is not a limit value for the maximum pressure on the lines. Finally, the third critical aspect is related to the closed centre on the distributor central position toward the power group. In this way, the entire flow rate

generated by the pump is throttle toward the tank, with the maximum pressure p^* due to the pressure relief valve, that means a high energy dissipation. Anyway, in figure 2.28 there are all possible configuration that the valve can has, but nothing of them in the distributor centre position only, is appropriate to solve the problems listed before, so there is the need to use other valves to achieve the goal.

issues with DCV in 0	load hold condition*	limit positive and negative pressure peaks	energy saving
Closed centre 	YES	NO	NO
Open centre 	YES	NO	YES
Float centre 	NO	YES	NO
By-pass centre 	NO	YES	YES

* however if there is the need to maintain the actuator perfectly blocked under load, a poppet valve must be used

Figure 2.28: possible configuration in the distributor centre position [1]

The mechanical characteristic of this user group (figure 2.27), highlight that is not possible handle overrunning load. On the first quadrant there is the characteristic when the rod come out with resistant load, while in the third quadrant the rod returns with resistant load. The mechanical characteristic is asymmetrical due to the different actuator active surfaces. When the relief valve regulates, the actuator works with an imposed pressure and consequently impose the force. On the other hand, in this situation, the velocity cannot be imposed from the actuator, because the relief valve, discharge a variable flowrate.

An example of the float distributor centre is illustrated in figure 2.29. The float function is mainly used in applications with excavating activities [8].

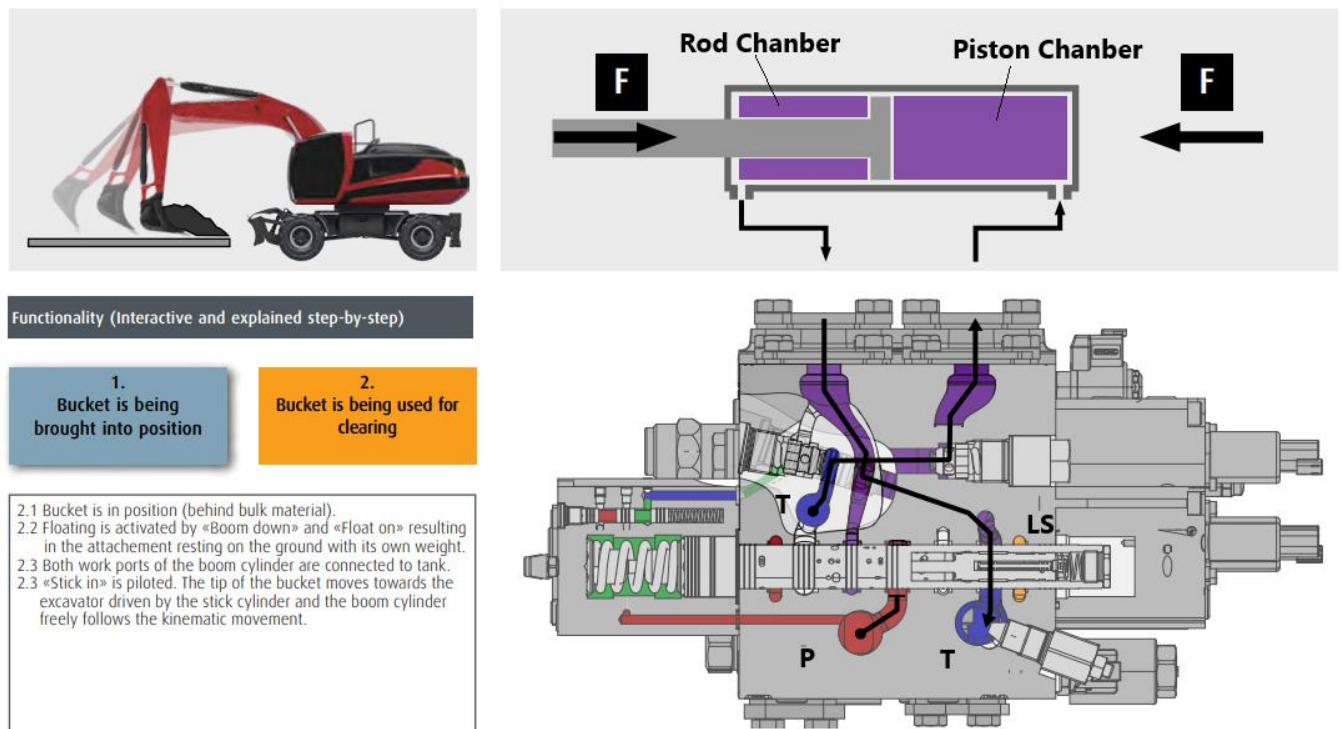


Figure 2.29: Boom distributor and actuator in floating condition [8]

Common examples are the actuators lift and the bucket of a wheeled loader or the boom of an excavator. In conventional control valves, an actuator is continuously clamped in position. In this way, the function always counteracts external forces. In certain application it is desired, that a cylinder yields to external forces by enabling to be pulled out or pushed in. This is particularly important when either increased wear of the attachment on a hard surface or the damage of a sensitive surface by the attachment is to be avoided. A typical example is the unloading of bulk cargo on a ship where you would like to avoid damage to the deck. In the context of control valves, the term «float» refers to the floating cylinder of a function that can be moved without resistance. This is achieved by connecting the piston chamber of the linear actuator to tank via the spool. The lowering characteristics remains unchanged. The rod chamber is connected to the tank by unlocking the regeneration check valve via an external signal on the float pilot. Following this procedure, the rod can be moved without significant resistance on the cylinder to ensure a smooth workflow, less wear of the material and less pump flow is required.

2.5.1) Hydraulic actuators with flow regeneration

The aim of this principle is to allow a discrete speed variation when the road come out when the jack is powered by the pump [1]. It is important notice that:

- The jack has a ratio $A: a = 2:1$;
- The distributor 4/4 has also a position 3.

The distributor has a mechanical brake that allows to maintain a defined position through the possible positions. When it is selected the position 3, the two chamber are connected and both to the pump delivery, so they are at the same pressure. This principle consists of to send the flowrate discharged from the rod side together with the pump flow rate to the piston side (figure 2.30).

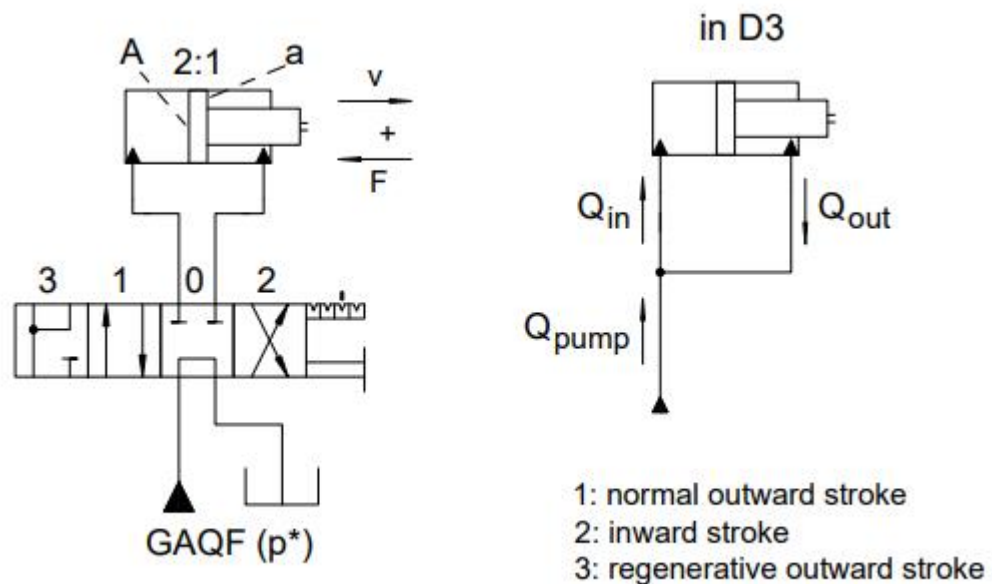


Figure 2.30: Circuit with distributor able to fulfil the flow regeneration [1]

$$Q_{in} = Q_{out} + Q_p \quad (2.35)$$

$$v_{reg} = \frac{Q_{in}}{A} = \frac{Q_{out}}{a} \quad (2.36)$$

$$Q_{in} = v_{reg} * A; Q_{out} = v_{reg} * a \tag{2.37}$$

$$v_{reg} * A = v_{reg} * a + Q_p \tag{2.38}$$

$$v_{reg} = \frac{Q_p}{A - a} \tag{2.39}$$

It is obtained an outward velocity amplified with respect to the case without regeneration. This situation is true until the pump delivery pressure reaches the p^* value, with such pressure value the relief valve of the power and control group starts to regulates, so:

$$F = p^* * (A - a) \tag{2.40}$$

This latter equation is the limit force for the regeneration, that is lower than the no-regenerative force ($F = p^* A$). In this application is possible to choose two possible outward rod velocity and one inward velocity, as the figure 2.31 shows, regarding the distributor position, in particular:

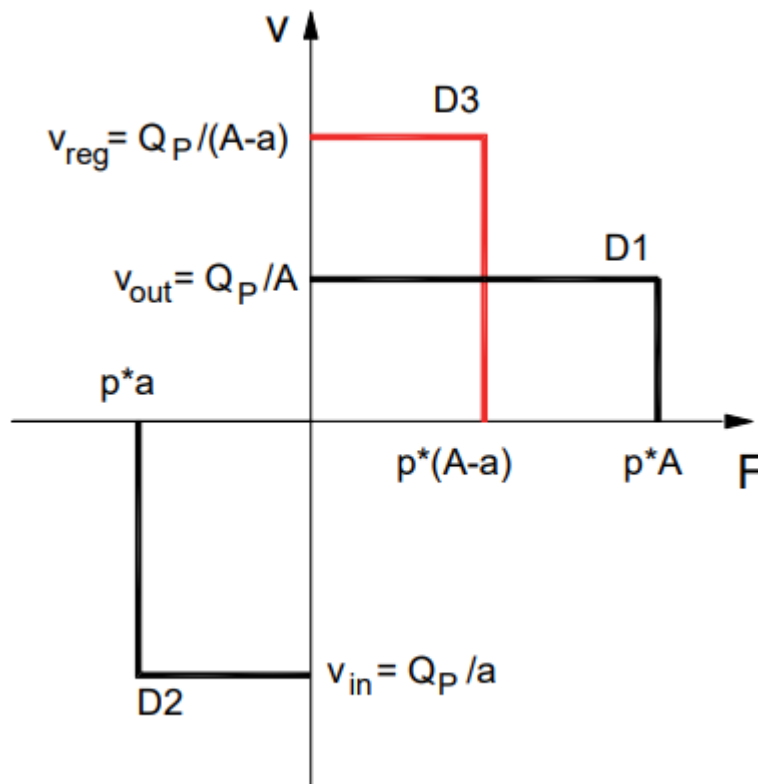


Figure 2.31: Hydraulic actuator mechanical characteristic for the three different configurations [1]

- No-regenerative rod outward, the speed is low and equal to Q_p/A , but it possible to handle higher load until $p^* A$;
- Rod inward with Q_p/a and maximum force $p^* a$;
- Regenerative rod outward, with higher speed $Q_p/(A-a)$ but equilibrate lower load $F = p^* (A-a)$, with a power conservation.

It is worth notice that, for the power conservation, the three different areas are the same. To understand the reason to choose the ratio $A : a = 2 : 1$ is consider a situation where, it is needed that the inward rod velocity is the same to the outward regenerative velocity so:

$$\frac{Q_p}{A - a} = \frac{Q_p}{a} \tag{2.41}$$

That lead to:

$$A = 2a \tag{2.42}$$

If now is considered the ratio chosen, the maximum outward force became $F = p^* a$, and it is evident that such force is coincident with the force exceed by the inward rod in configuration 2. In conclusion, this ratio allows to have the same speed and the same force obtained during the regenerative rod outward (characteristics 2 and 3 are symmetric).

Some useful regeneration applications are shown in figure 2.32 and 2.33. The boom/lift-regeneration is employed for lifting functions, such as the boom of the excavator or lift of the wheeled loader [8].

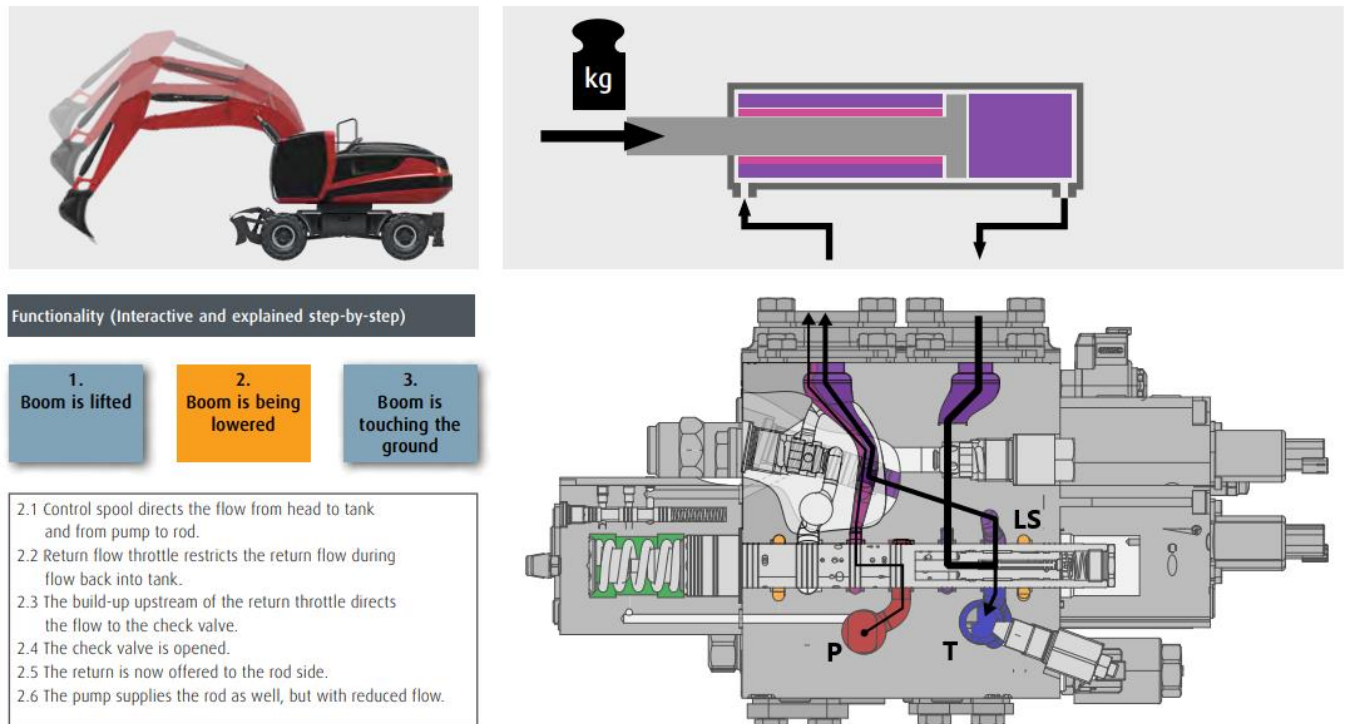


Figure 2.32: Boom distributor and actuator with flow regeneration [8]

When the boom is elevated, the weight force of the whole attachment (e.g., boom, stick and bucket in context of an excavator) continuously acts on the lifting cylinder of the boom. This force would compress the cylinder even without the help of the pump. However, to enable a fast-lowering process, a high flow is required on the rod's side. If the flow is too low, on the cylinder the cavitation phenomena take place. The boom/lift-regeneration utilizes the weight force during lowering and partially redirects the oil flow from the return flow of the lift cylinder to the opposite side. In this way, the flow required here is already provided to a large degree without any pump effort, so there is an energy saving. In addition, the tendency to cavitation is eliminated. The flow saved in this process is thus directly available for other functions and there is higher dynamics of the whole application.

Another regeneration application is, the Rod-to-Piston-regeneration is used for cylinder functions with high flow and high actuator speed at a simultaneously low-pressure level, such as the excavator's dipper (figure 2.33).

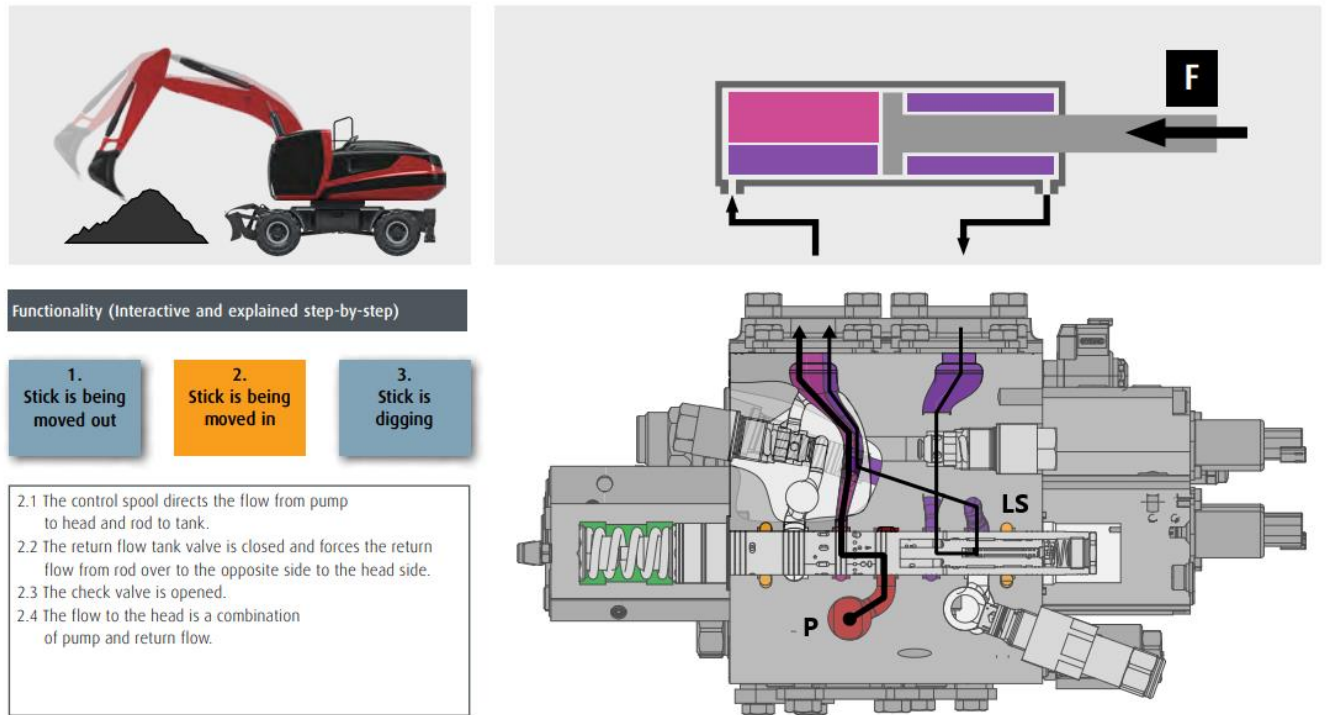


Figure 2.33: Dipper distributor and actuator in rod to piston regeneration [8]

If, for instance, in the case of an excavator the operator uses the dipper for fast and light motions, the full pump flow would be required in conventional systems [8]. If additional functions were also in use, they would inevitably be slowed down. The rod-to-piston regeneration avoids exactly this effect and eliminates the need for a high pump flow. In the example of the dipper function, the return flow of the rod side gets redirected to the piston side when the cylinder is being extended. Thus, the pump now only must provide the differential flow between the rod and the piston. Any additional pump flow that exceeds this quantity now has a positive effect on the moving speed of the cylinder. That way, substantially more dynamic movements are possible with simultaneously less pump effort and imbalances within the system. Once the load on the stick increases, the regeneration is switched off automatically.

CHAPTER 3: SIMCENTRE AMESIM EXCAVATOR MODEL

3.1) 3D CAD model

As a starting point, for the studying of the excavator hydraulic circuit, it has been supplying the CAD model, by the FPRL, reproduced in Solidworks® of the real excavator (figure 3.1).



Figure 3.1: CAD Excavator model

This model is fundamental, because since it has the real dimensions, it was possible to directly take the dimensions of the parts interested in. The excavator parts that have a motion are:

- The Arm, composed by the bucket, two leverages: bar A connected to the dipper and bar B connected to the bucket, dipper, and boom. They have a rotation around the pin that connect each other, thanks own linear actuator respectively.
- The Turret, composed by the operator cabin, the support where is connected the arm and the linear actuator for the small arm rotation, attached to the cabin.

They rotate with respect to the lower frame.

The lower frame is composed by the frame itself, the trucks, and the blade with its actuator, that are at standstill, because when the excavator performs a normal duty cycle of digging activity they do not move.

3.2) 2D Simcentre Amesim model

Another useful tool, available from the FPRL, was the complete 2D Simcentre Amesim® arm model (figure 3.2). this model represents the real excavator, composed by both mechanical and hydraulic parts, where each element of the system, has the real parameters and dimensions set up, coming from the 3D Solidworks® model.

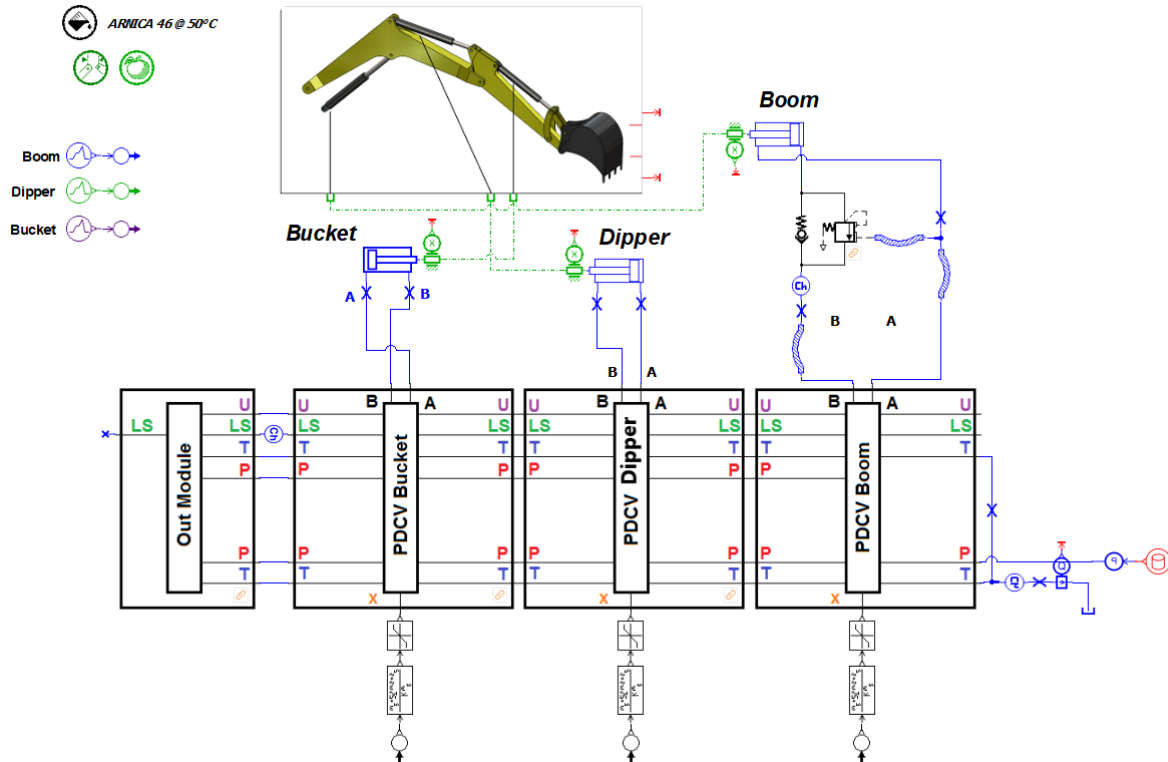


Figure 3.2: 2D Hydraulic circuit and arm in Amesim project environment

Inside the icon that represents the excavator arm, there is the arm mechanical model, shown in figure 3.3, modelled with the 2D mechanical library of Amesim.

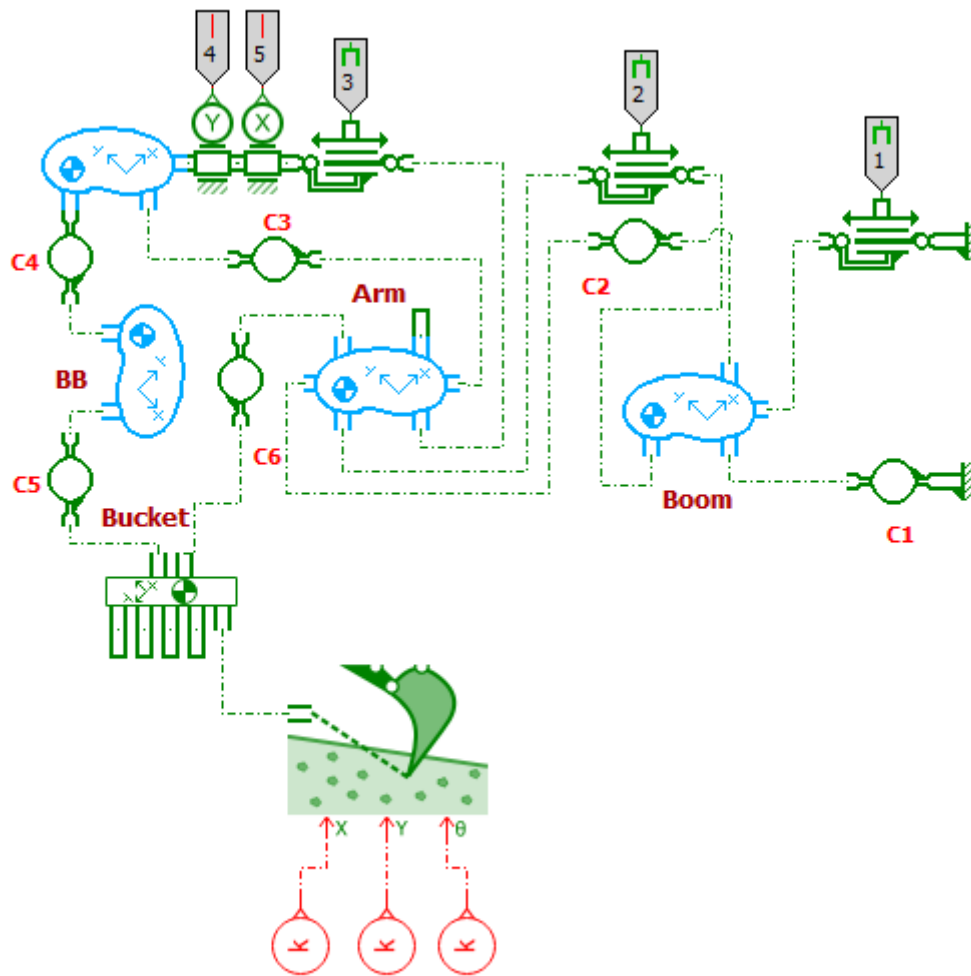


Figure 3.3: 2D Amesim arm mechanical model

Since the arm is composed by five rigid bodies, and on the plane, there are three degrees of freedom, so there are fifteen degrees of freedom in total, but on the system, there are six hinges that block two DOFs each. In this way, the whole system has three degrees of freedom that are the rotation of the boom, the dipper, and the bucket respectively.

On the table 3.1, are reported the names and functions of each single element that compose the arm of the 2D model.

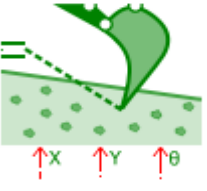
N°	Element	Name	Function
1		plmrefwall	Schematize the non-moving parts
2		plmjack	Represent the actuators' mechanical part
3		plmpivot	Hinge that connects the rigid bodies
4		plmbody	Rigid body that reproduces the moving parts except the bucket
5		dynamic_plmbody	Rigid body that represents the bucket
6		digging_force	Compute the digging force during the excavation activity
7		constant	Set the ground position and the slope

Table 3.1: Description of the elements belonging to the arm

The plmbody (element 4) and the dynamic_plmbody (element 5) are the same, but plmbody is considered obsolete with the new versions of Amesim, so they could be replaced with the dynamic_plmbodies.

This model simulates the real kinematic movements, only on the X, Y plane, moreover it is possible to compute the soil resistance forces when digging, that in the new 3D mechanical model it is not possible, imposing the soil characteristics, the bucket geometry and friction parameters between bucket and soil on the digging_force sub model (figure 3.4), and connect on the ports 1,2 and 3 of it the constant terms that represents the soil position along x and y and the soil inclination.

Submodel

digging_force [PLMDIGF00] External variables

computes the digging force on earthy ground Image >>

Parameters

Title	Value	Unit	Tags
# volume in tool	0	m**3	
digging way	positive along x axis		
submodel icon	excavator		
soil density	2192	kg/m**3	
repose angle	30	degree	
soil failure angle	45	degree	
emptying time constant	1	s	
tool dimensions			
tool maximum capacity	0.265	m**3	
tool blade length	0.6	m	
tool top corner x position	0.325	m	
tool back plate length	0.77	m	
tool width	0.8	m	
soil in tool center of gravity relative x ...	0.45	m	
soil in tool center of gravity relative y ...	0.3	m	
friction parameters			

Save Load Default value Max. value Reset title Min. value Help Close Options >>

Figure 3.4: digging_force parameters

The arm model of figure 3.3 is connected to the linear actuators belonging to the hydraulic circuit through the port 1,2 and 3, as shown in figure 3.2.

Concerning the hydraulic part, the hydraulic linear actuators are governed by means of three directional control valves, one for each actuator. These valves are made in a detailed way, using the hydraulic component design library, and located inside the PDCV blocks, that show only the external connections in figure 3.2. As input into this 2D system, it has been given the main spool displacements (figures 3.5,3.6 and 3.7) connected on the x port of each PDCV block. On the boom PDCV, a positive main spool displacement produces an outward stroke, instead a negative main spool displacement produces an inward stroke of the boom actuator, this because the port A of the valve is connected to the actuator rod side and the port B is connected to the actuator piston side (figure 3.2).

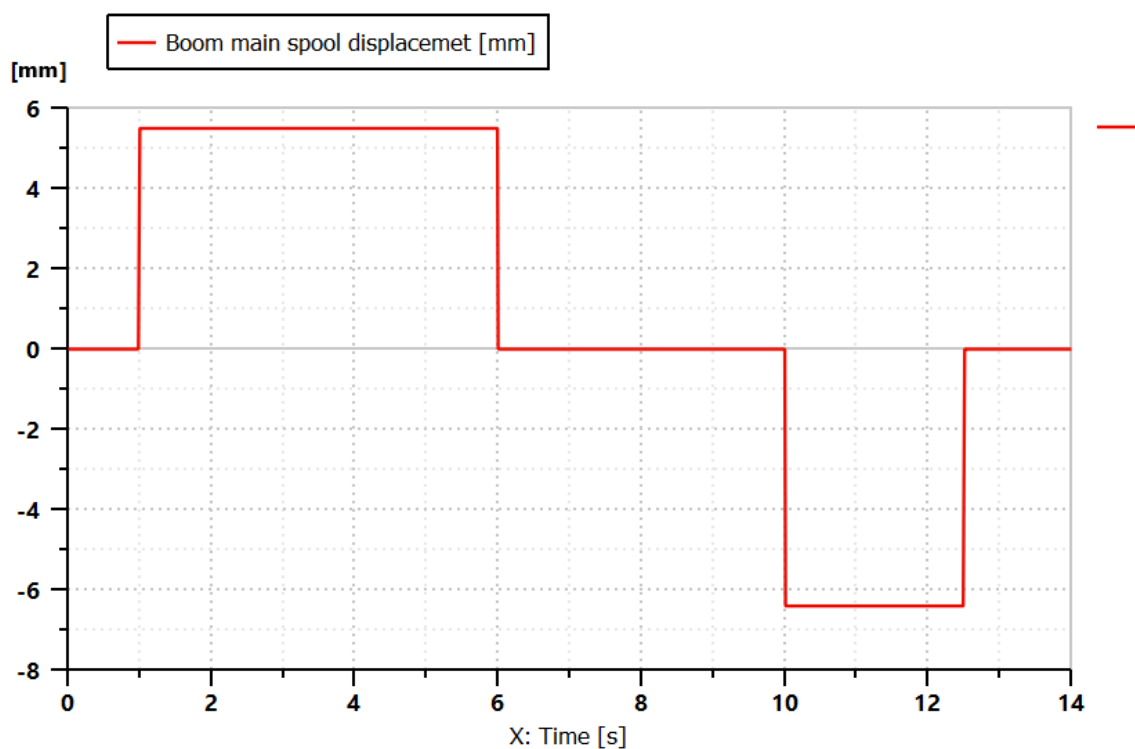


Figure 3.5: Boom main spool displacement

On the contrary, since the ports A and B of the bucket and dipper valves are connected in opposite way to the actuators with respect to the boom (figure 3.2), a negative main spool displacement produces the outward stroke, and the positive main spool displacement produces the inward strokes.

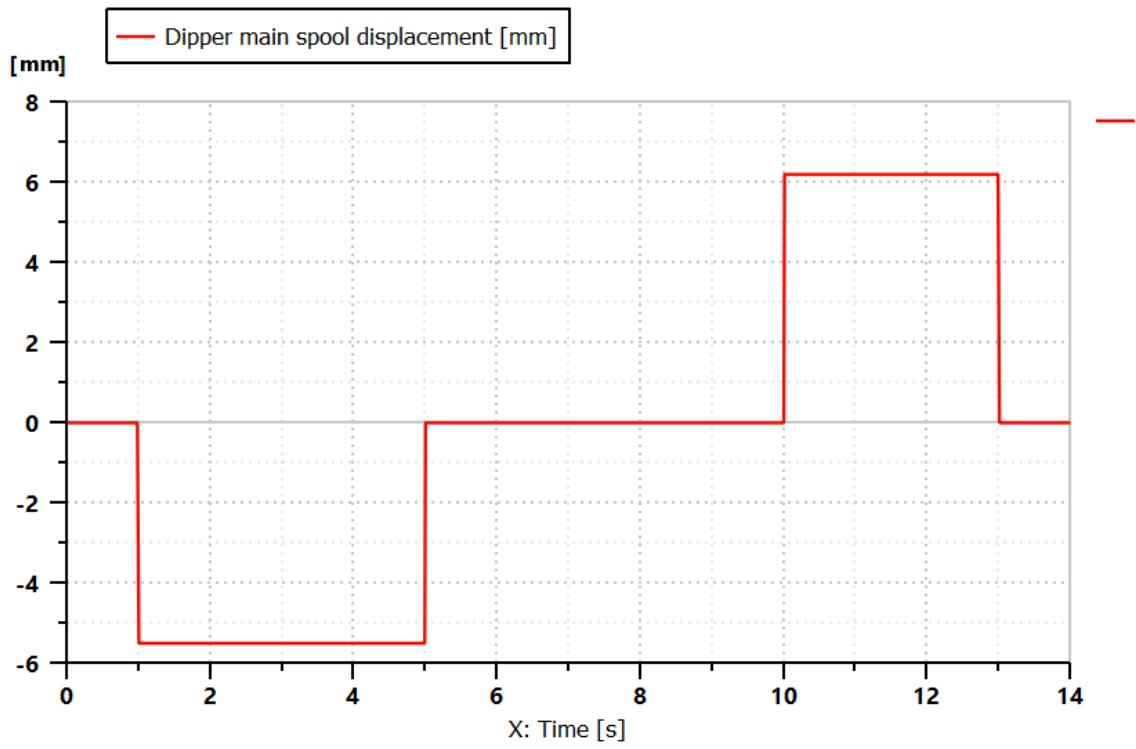


Figure 3.6: Dipper main spool displacement

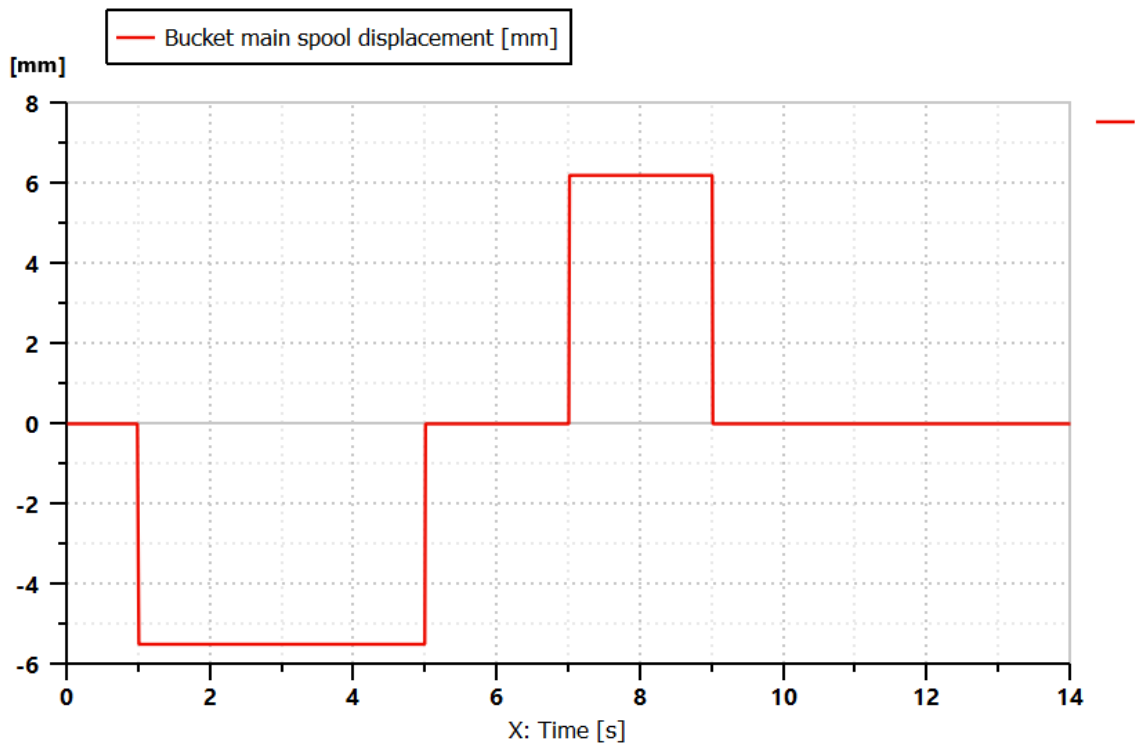


Figure 3.7: Bucket main spool displacement

After run the simulation, have been obtained some variables, but for thesis aim, the interest is focused on the actuator displacements shown in the figures 3.8, 3.9 and 3.10, where on the boom piston displacement can be notice a change of slope at about 5 s, this because on the original system there was another gear pump that was activated as soon as the material inside the bucket was lifted, to increase the flow rate and so the boom actuator outward velocity,

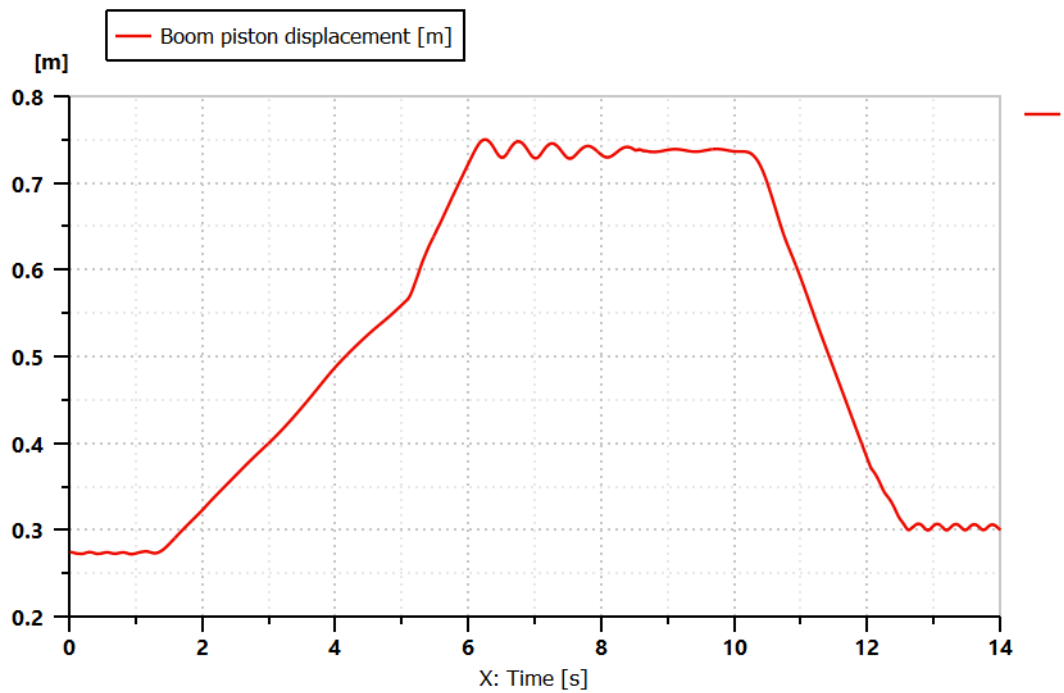


Figure 3.8: Boom piston displacement

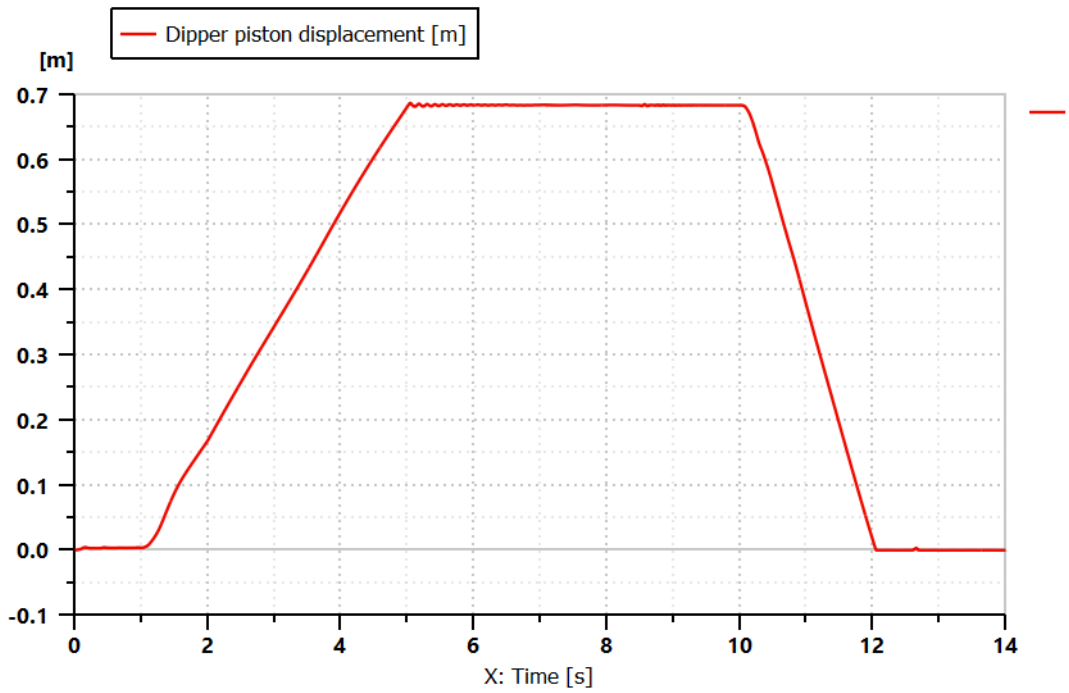


Figure 3.9: Dipper piston displacement

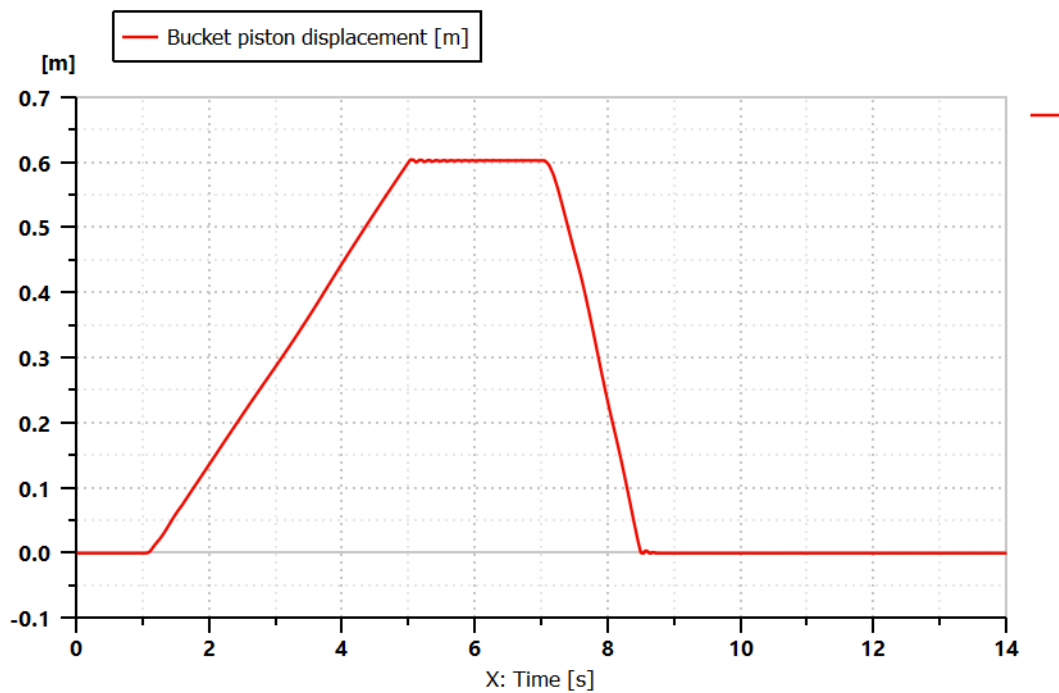


Figure 3.10: Bucket piston displacement

the forces exchanged between the ground and the bucket along X (figure 3.11) and Y (figure 3.12) direction

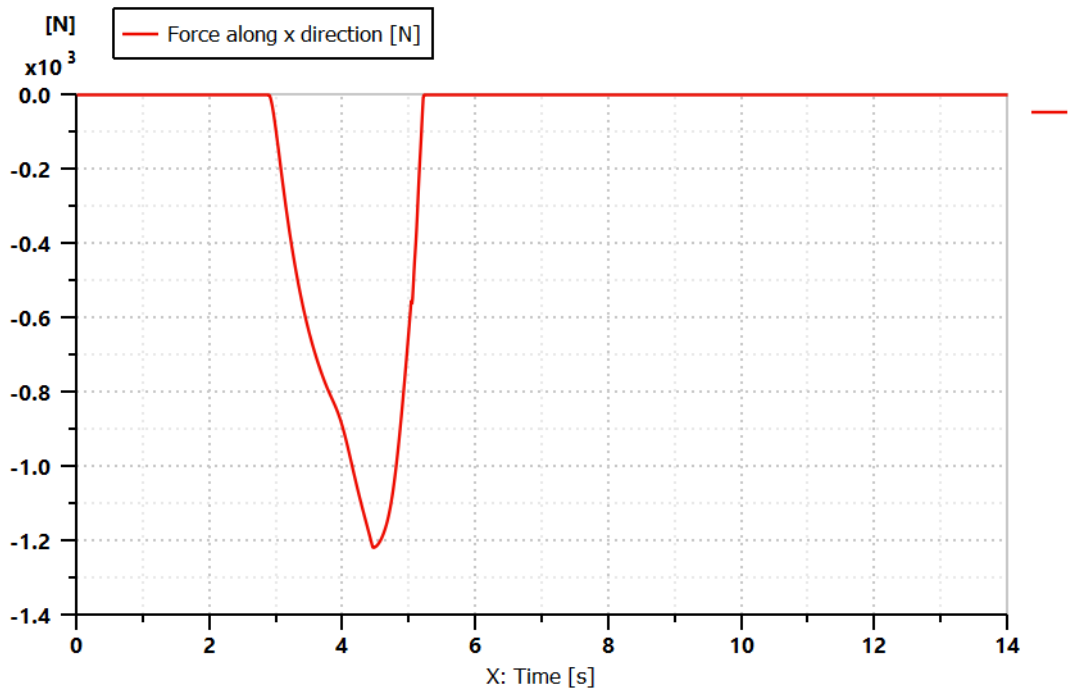


Figure 3.11: Force along x direction

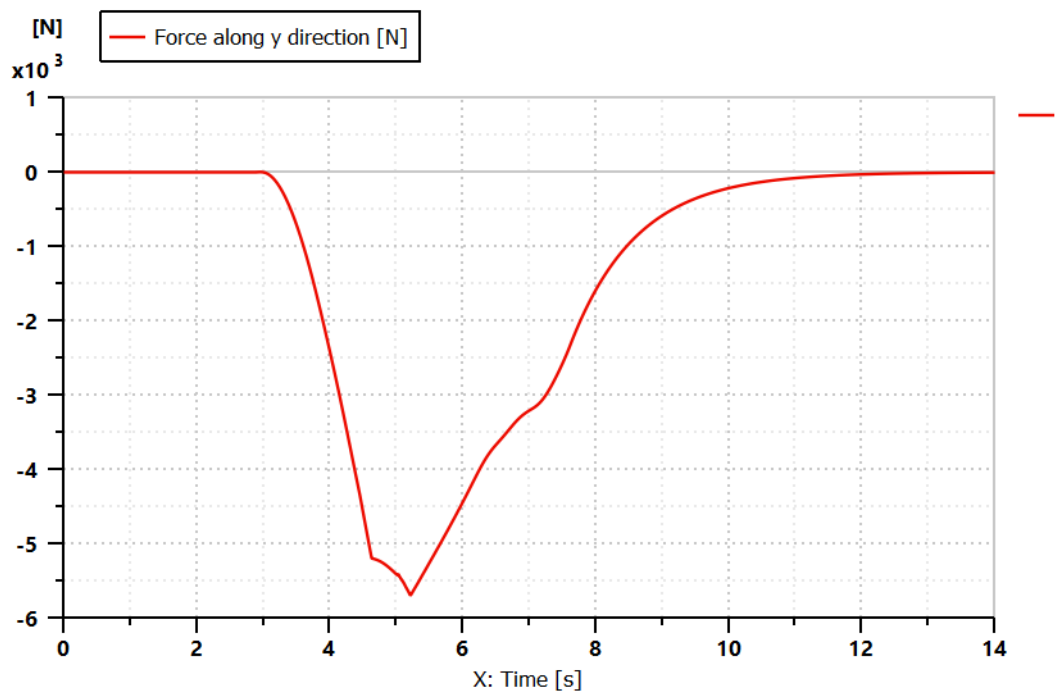


Figure 3.12: Force along y direction

both forces are negative defined because their vectors have opposite direction with respect the reference frame, as the figure 3.13 shows,

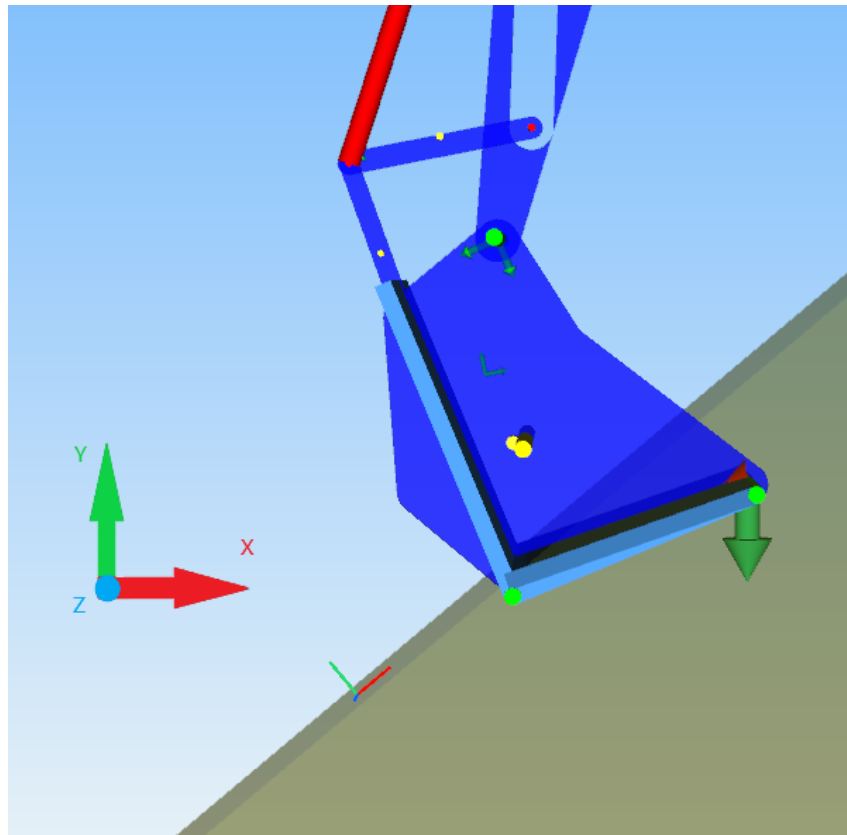


Figure 3.13: Directions of the force vectors

as well as the torque (figure 3.14), positive when the torque vector has the same direction of the Z axis and negative in opposite direction.

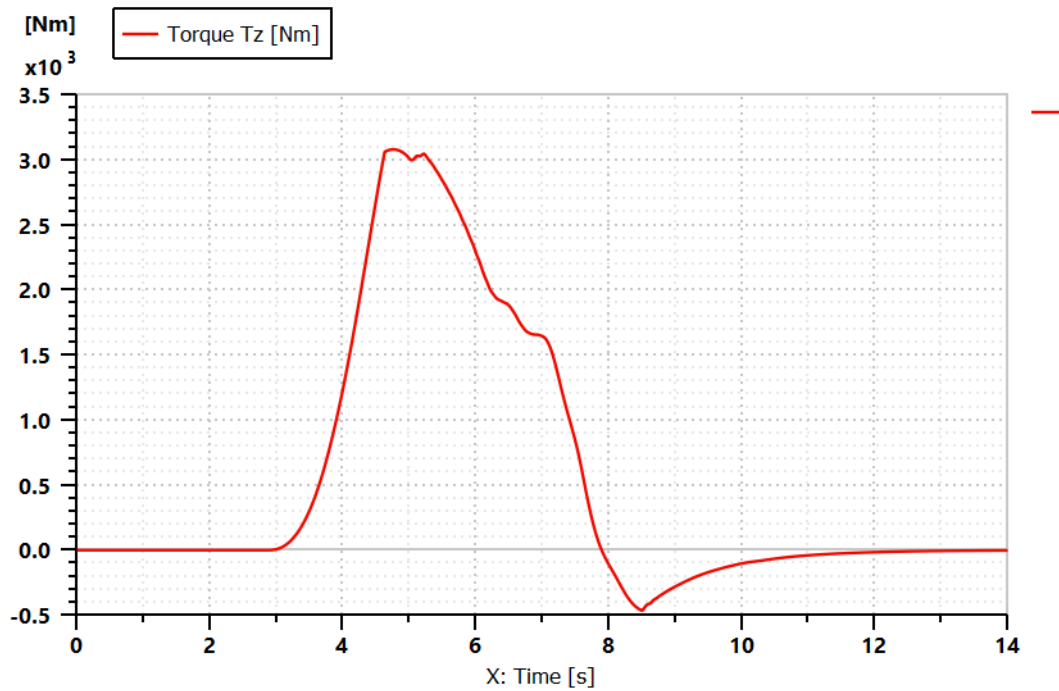


Figure 3.14: Torque obtained

The variables obtained by the simulation of the 2D model constitutes the inputs for the 3D model.

3.3) 3D Simcentre Amesim models

3.3.1) 3D model with rigid body

At this point, to create the 3D model, it has been considered a similar approach like the 2D. The 3D model works on the space, so there are for each excavator rigid body that has motion, six degrees of freedom. Since, there are six elements in this model (boom, bucket, dipper, bar A, bar B and turret), there are thirty-six degrees of freedom in total, so in this case will be blocked thirty-two DOFs, so that, are allowed only the four motions that the excavator must do.

The table 3.2, summarizes the constraints of the 3D mechanical library used for this purpose:

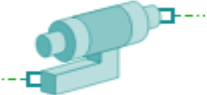
N°	Element	DOF	Constrain
1		Rotation about y axis	Translation along x, y, z and rotation about x, z axis
2		Rotation about z axis	Translation along x, y, z and rotation about x, y axis
3		Translation along x, and rotation about x, y, z axis	Translation along y, z axis
4		No degree of freedom	Translation along x, y, z and rotation about x, y, z axis

Table 3.2: Constrain in the 3D model

The zerospeedsource (4), is a sub model of a fixed body used to represents all the mechanical parts that do not have motion, that means all the parts under the turret that belongs to the lower frame. This sub model can be considered as a zero acceleration and velocity source, (figure 3.15), and its position and its frame orientation remain constant throughout the simulation.

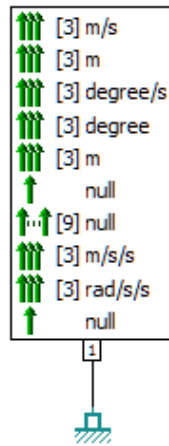


Figure 3.15: zero speed source outputs [11]

The parameters that can be imposed in this sub model are the position and the orientation on the 3D space (figure 3.16).

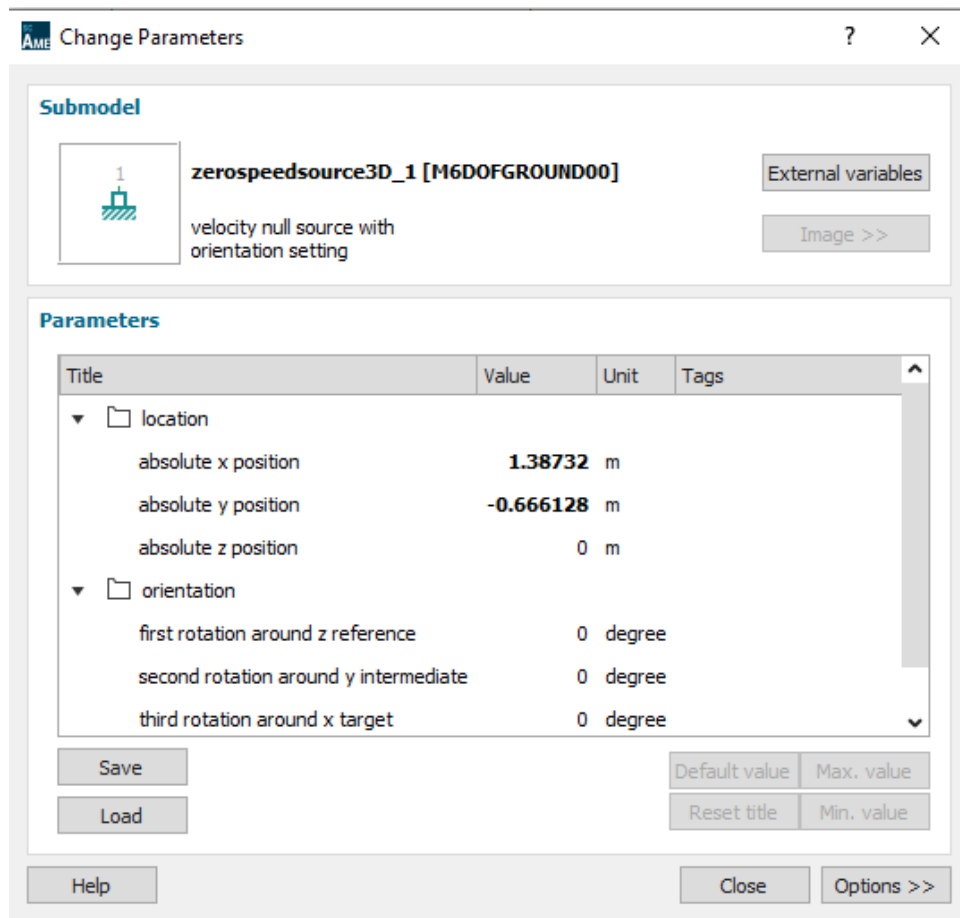


Figure 3.16: Zero speed source parameters

The m6dofpilotedpivot (1) is a sub model used to represents the turret hinge (figure 3.17). On the port 3 is connected the zero-speed source, because this port represents the part of the hinge at standstill connected to the excavator lower frame. On the port 1 is connected the rigid body that represents the turret, since it is the hinge part that rotates, but this rotation is driven by the motor that performs the turret rotation that is connected at the port 2.

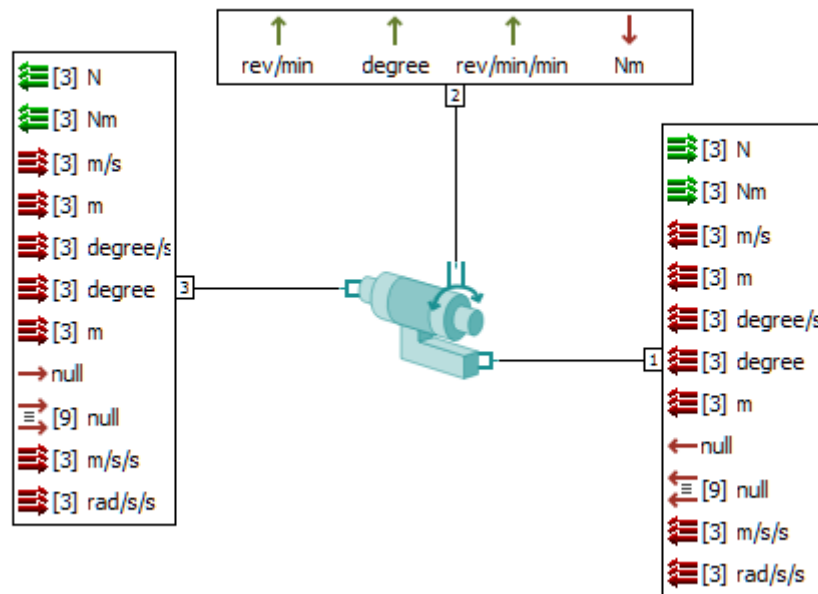


Figure 3.17: m6dofpilotedpivot inputs (red) and outputs (green) [11]

In this sub model, the parameters that can be imposed are, the orientation on the space, and the mechanical properties of the joints (figure 3.18). These parameters are the same one also for the m6dofpivot (2) and the m6dofsannularlinear (3), because they follow the mechanical approach, based on the use of spring and damper to constrain geometrically two bodies according to the joint definitions. This approach introduces several vibration modes according to the stiffness and the damping coefficients of the spring and damper, that slow down the simulation time.

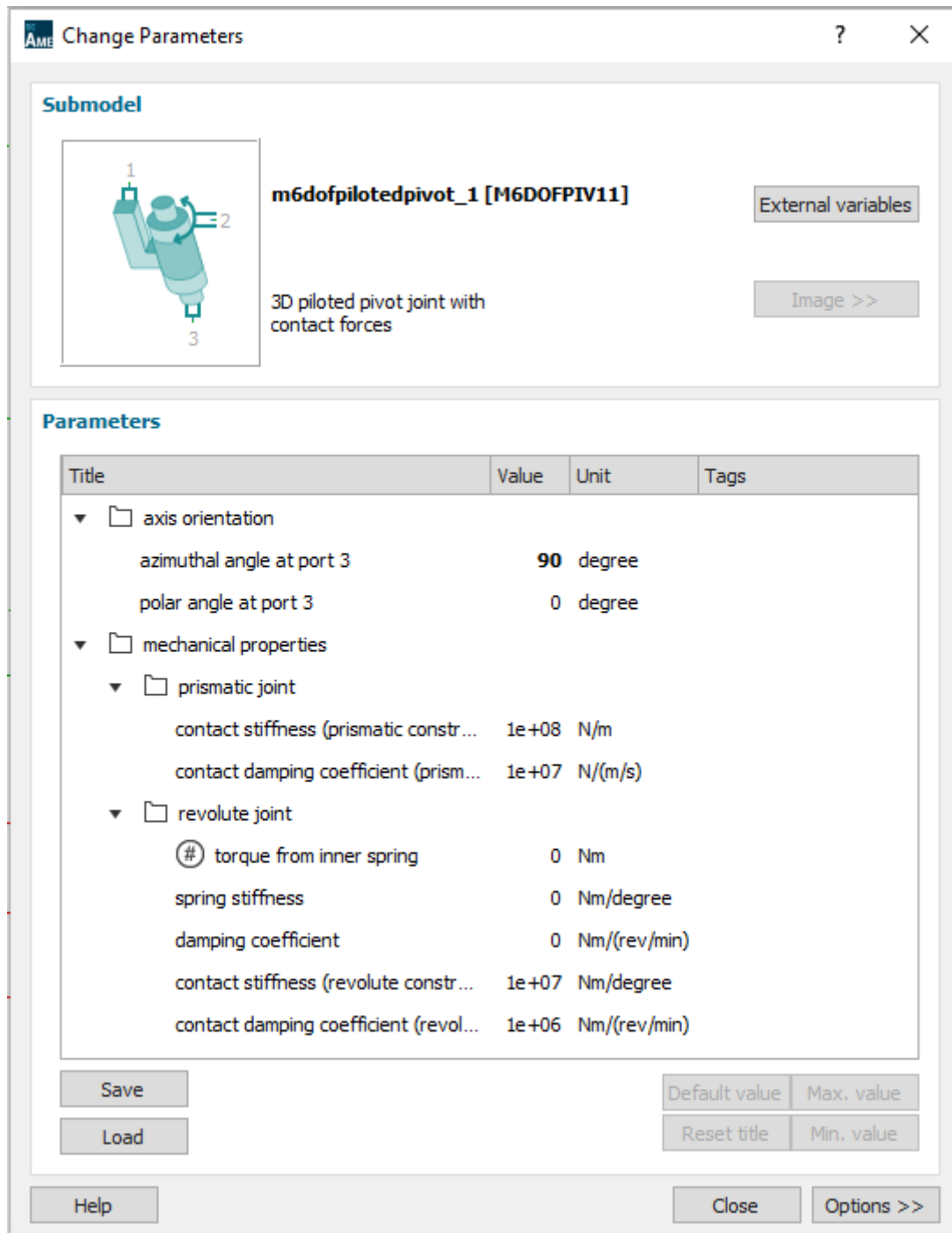


Figure 3.18: Piloted pivot parameter

Regarding, the bodies that constitutes the mechanical excavator parts that have motion, it has been used the `dynamic_3Dbody` (figure 3.19), that is equivalent of the rigid body for the 2D mechanical library but for the 3D space.

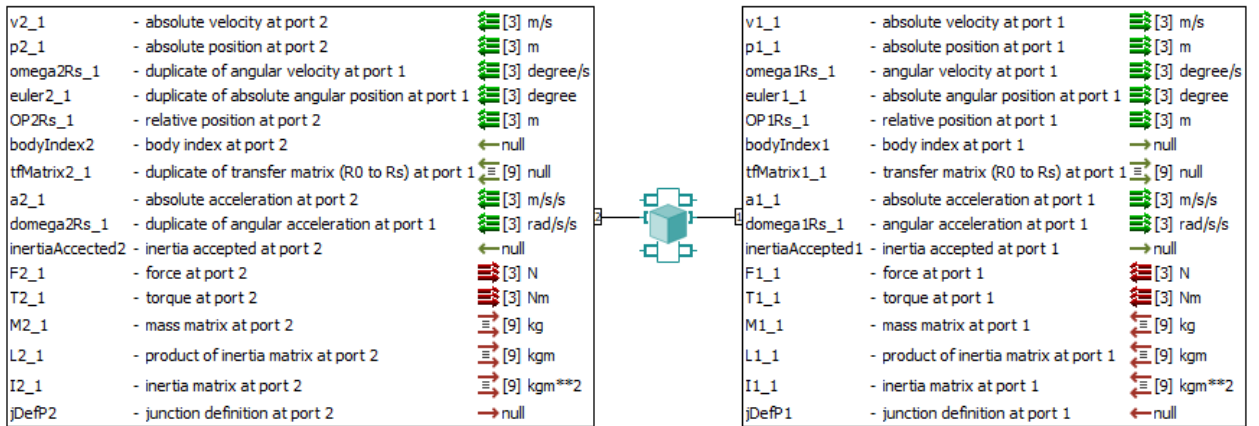


Figure 3.19: dynamic_3Dbody inputs (red) and outputs (green)

First, on this sub model, it is possible to define the number of ports, that can be connection points with other sub models or simply end points of the rigid body. Let us consider the dynamic_3Dbody that represent the turret in figure 3.20, it has been created with five ports, three for the connections with other sub models, and two as turret end points connected with the zero forces source. These three connections are: one with the turret piloted hinge, one with one port of the actuator mechanical part for the boom movement, and one with one port of the hinge that connects the turret with the boom.

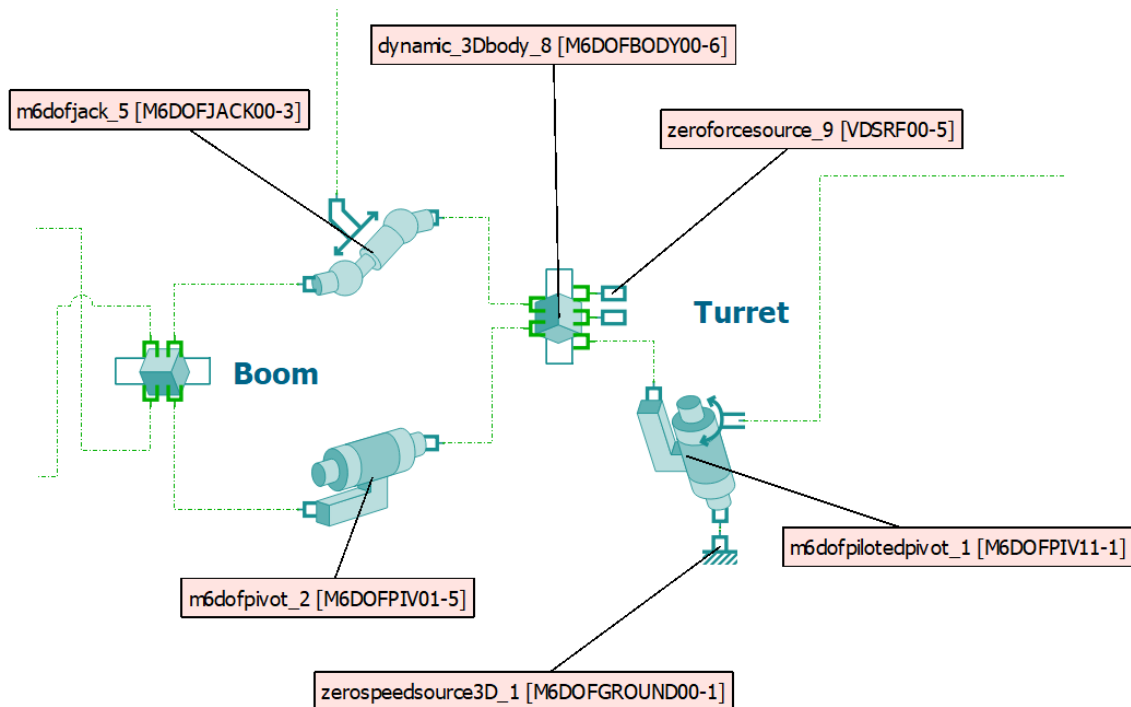


Figure 3.20: Connections of the turret sub model

Then, on the parameter mode, it is possible to impose the orientation of the rigid body under the voice solid frame orientation, the coordinates of each connection with other sub models or end points and the coordinate of the centre of gravity in items location, and the inertia property in inertia (figure 3.21). All these information coming from the CAD model, instead, the initial velocities, and advanced options are not interested.

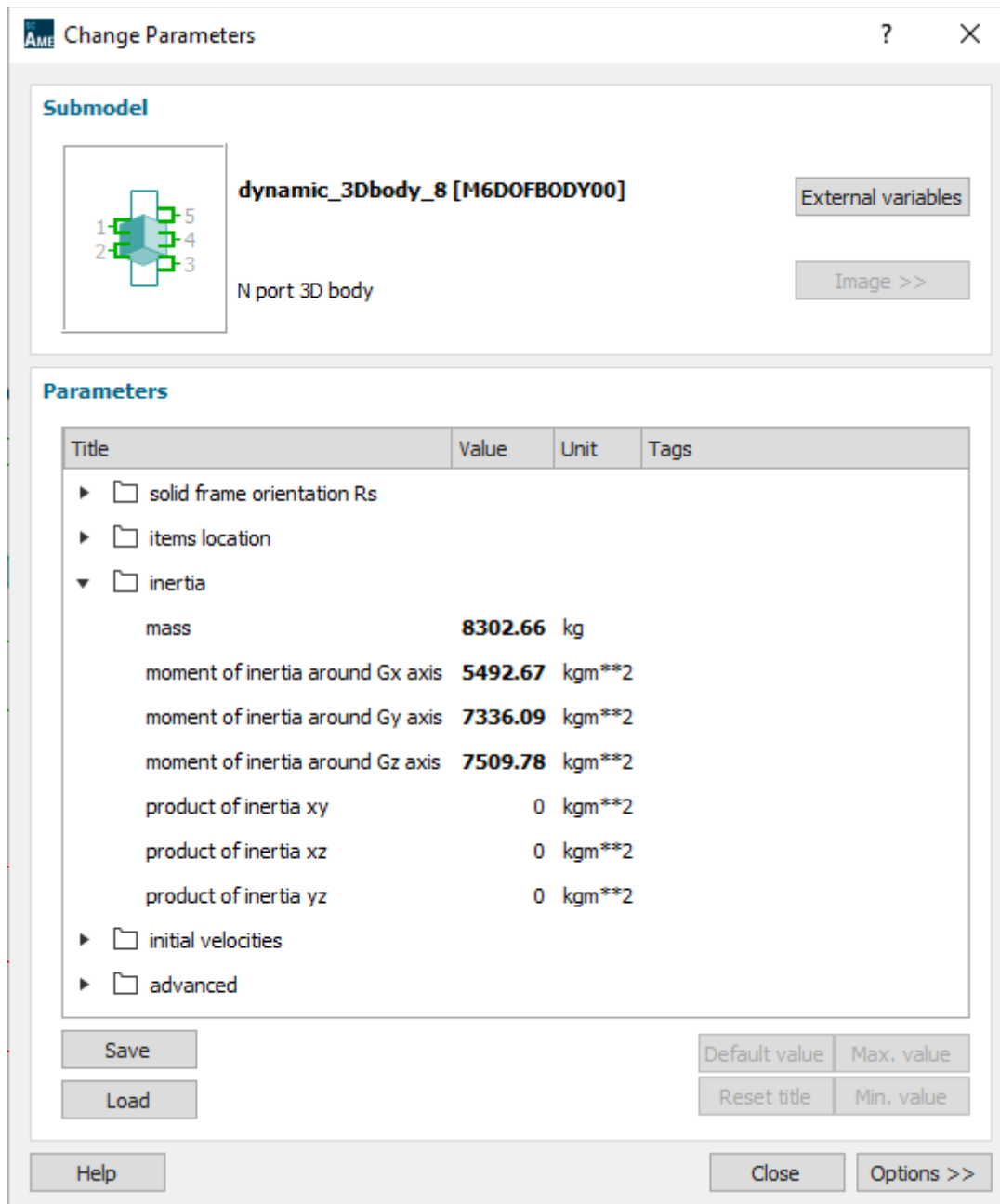


Figure 3.21: dynamic_3Dbody parameters

On the figure 3.22 is shown, how the turret rigid body with its connections and its constraints is represented on the Amesim simulation environment, after set all the parameters for this part of the mechanical system.

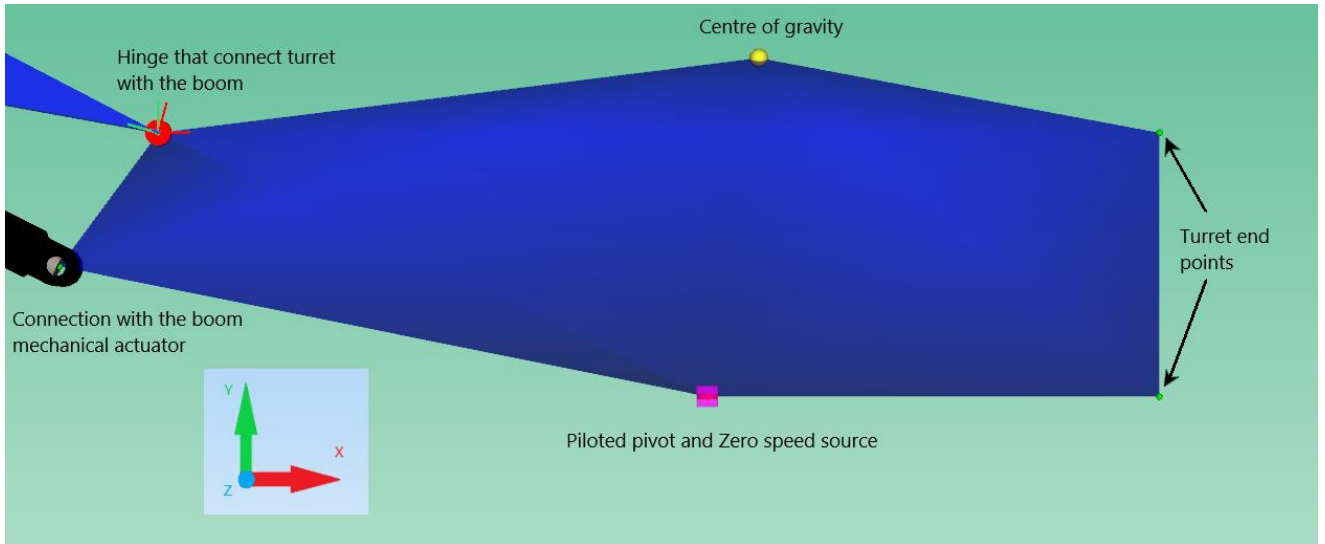


Figure 3.22: Turret rigid body sub model and its connection on the simulation environment

The m6dofjacks is the sub model that represents the mechanical part of the actuator (figure 3.23). It transmits a force along the axis described by positions of ports 1 and 3. This external driving force at port 2, comes from the hydraulic part of the linear actuator on the hydraulic circuit.

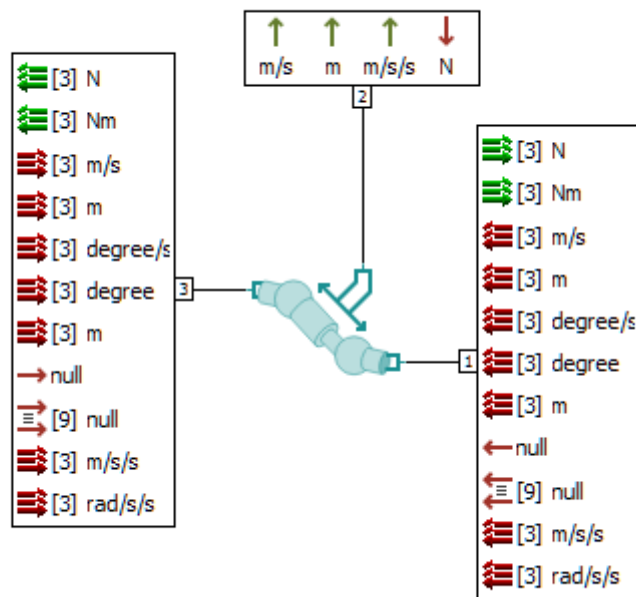


Figure 3.23: m6dofjacks inputs (red) and outputs (green) [11]

In this sub model is possible to impose the free length of the mechanical actuator, that is its total length when the actuator is completely retracted, and some mechanical properties for its non ideality (figure 3.24).

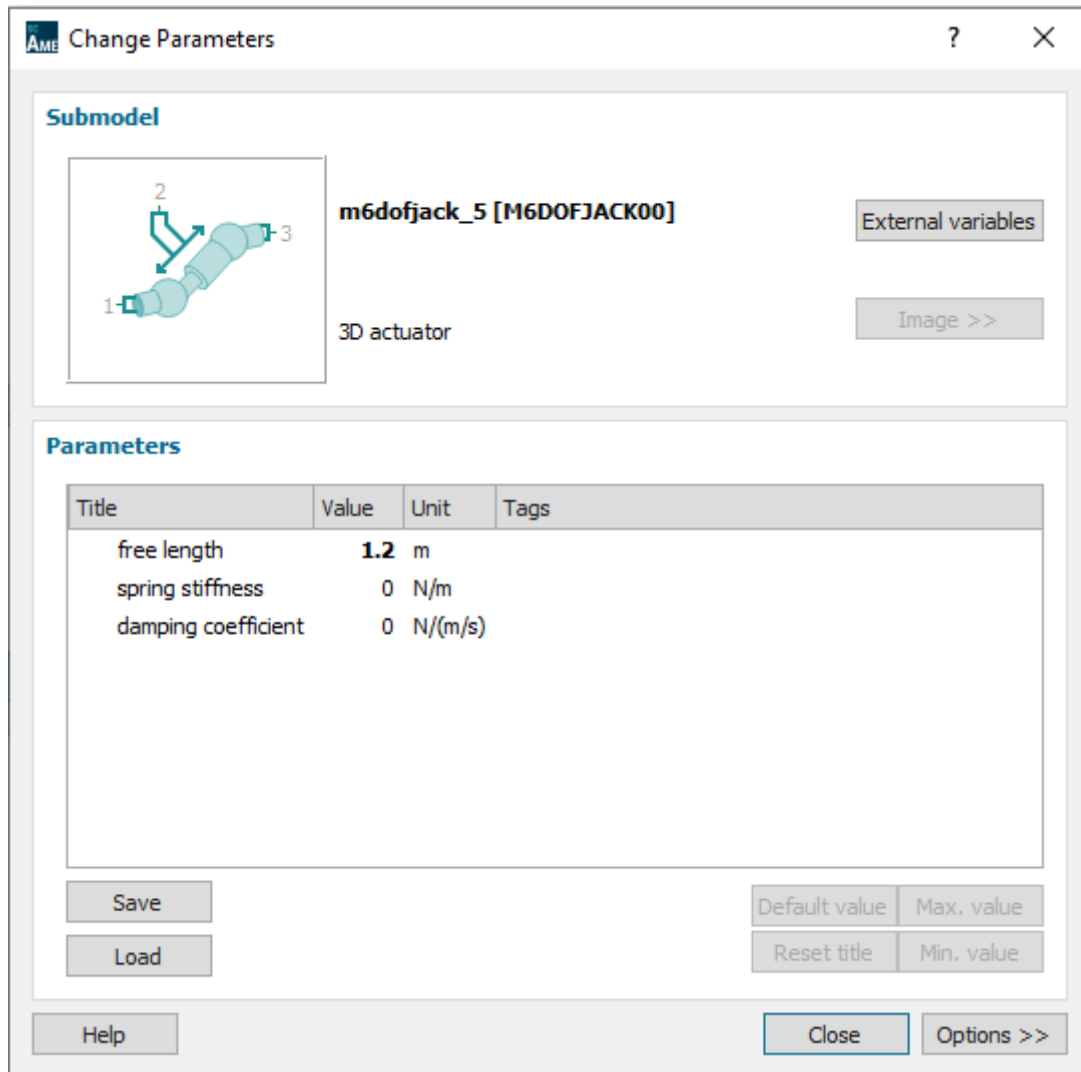


Figure 3.24: Setting parameters for m6dofjack

The m6dofpivot (2) is a sub model of a revolute joint (figure 3.25). It allows one rotational degree of freedom between the bodies connected at ports 1 and 2, so it has been used to connect the turret with boom, the boom with dipper, the dipper with bucket and bar A, and bar A with the bar B.

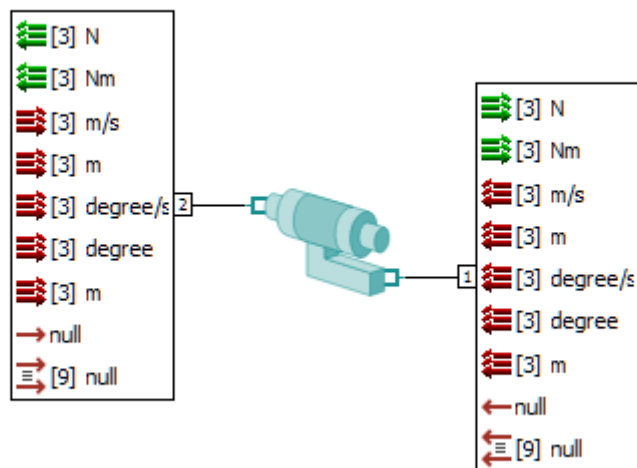


Figure 3.25: m6dofpivot inputs (red) and outputs (green) [11]

A similar approach, as explained before for the turret rigid body and its connections, have been used for the other rigid bodies presents in this model, choosing the right number of ports for each rigid body and impose the coordinates for each connection with constraints, mechanical actuators, or simply to specify end points. As soon as it has been reached the connection between bucket, and bar B, to obtain four DOFs of the system, the m6dofsannularlinear (3) must be used (figure 3.26). This sub model is an annular linear joint, it allows the full rotation of a body connected at port 1 and restricts its translation to an axis oriented by the body connected at port 2 (figure 3.27).

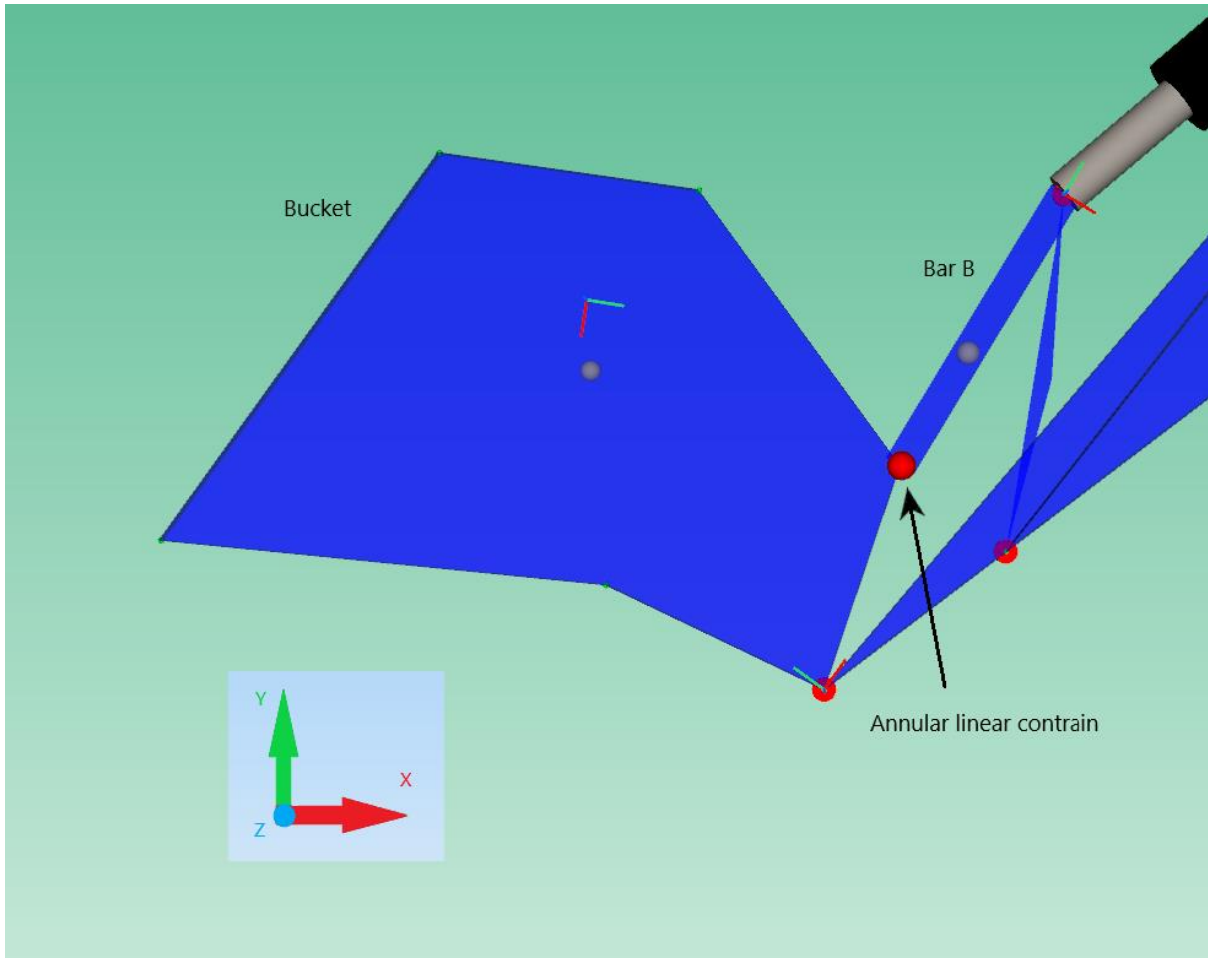


Figure 3.26: Connection point between bucket and bar B

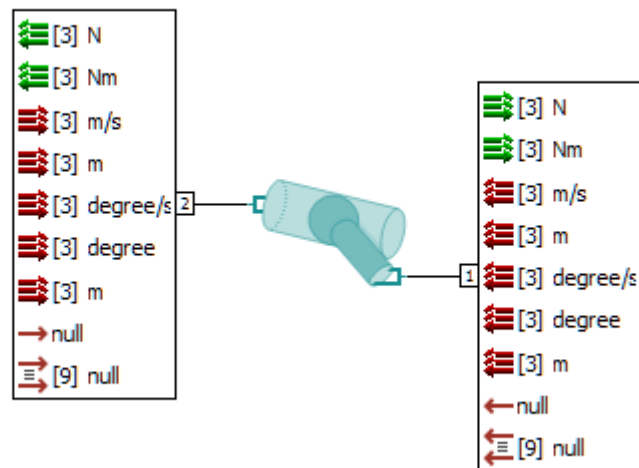


Figure 3.27: m6dofannularlinear inputs (red) and outputs (green) [11]

To apply the same forces and torques computed by the 2D in this 3D model, the 3DForceTorqueSourceRj has been used (figure 3.28). It takes as input through the dynamic_time_tables the time history of the forces and torques computed by the 2D model, that represents how the module of these vectors change in time. Through the constantId3, that is an identity matrix source, it has been imposed their direction as in figure 3.13, and the forces and torques ports not used are connected with the zero force and the zero-torque source. These forces and torques are applied to the bucket tip, so the output of this sub model is connected on the corresponded port of the rigid body that model the bucket.

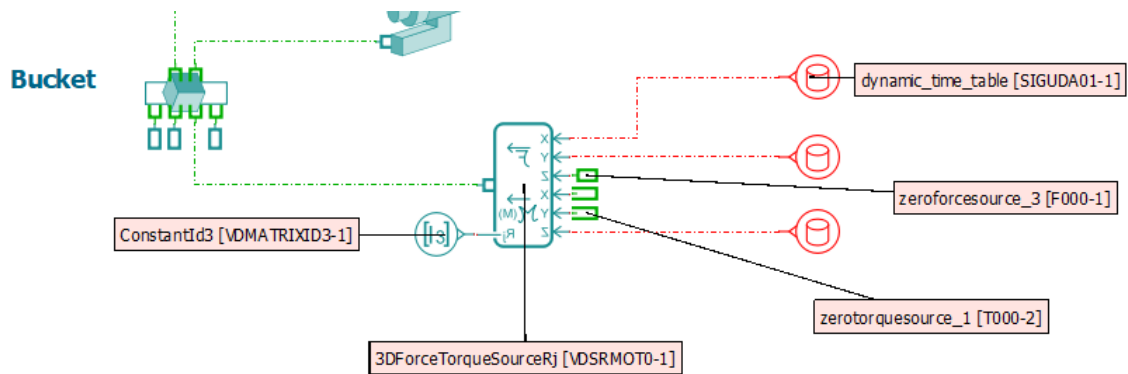


Figure 3.28: Forces and moments sub model

After connecting all the sub models, and set all parameters, it has been obtained the final system that represents all the excavator mechanical part both on the project environment (figure 3.29) and on the simulation environment (figure 3.30).

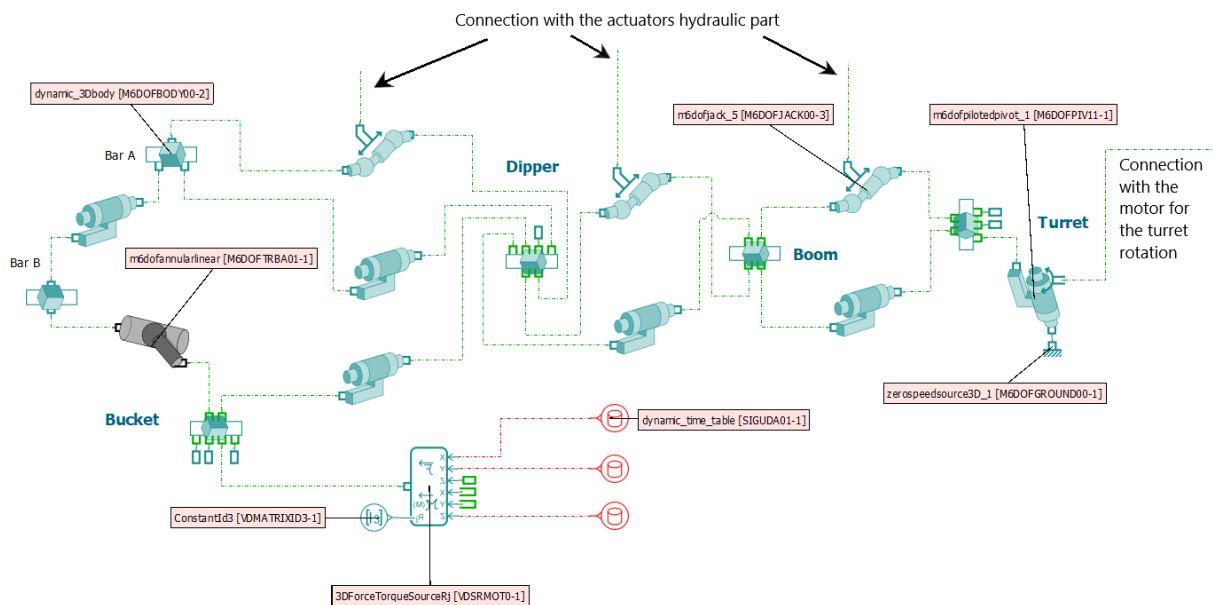


Figure 3.29: Mechanical 3D parts of the arm with rigid body on the project environment

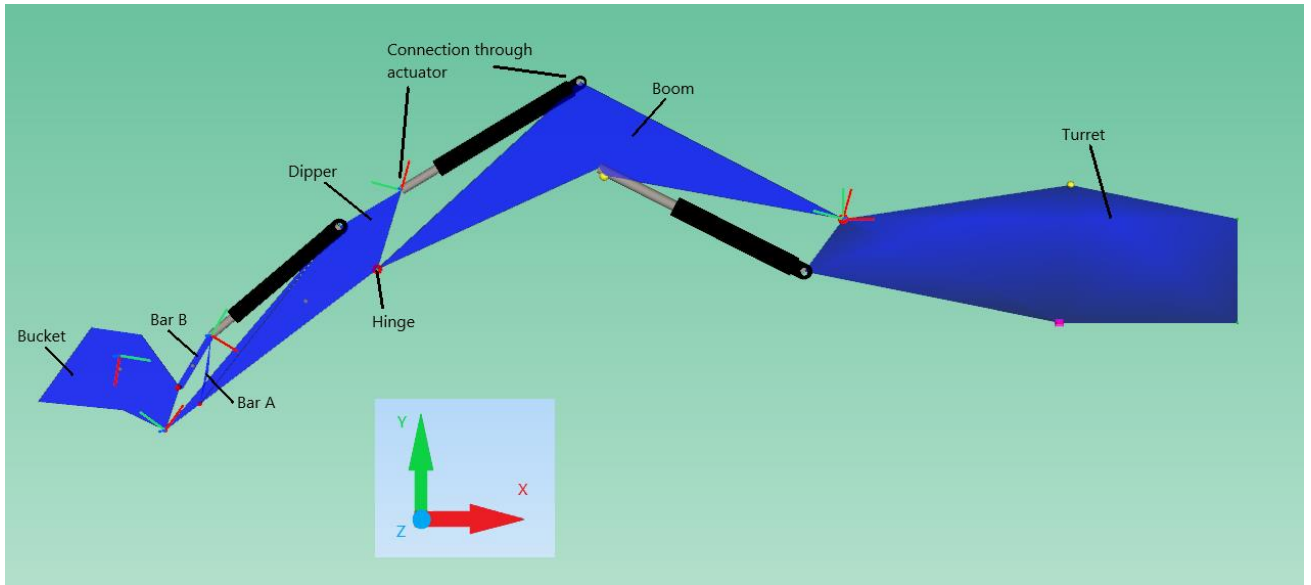


Figure 3.30: Mechanical 3D parts of the arm with rigid body on the simulation environment

Finally, have been reported into Amesim simulation environment the CAD excavator parts and attached on the corresponding rigid body sub models (figure 3.31), except the lower frame that was attached to the zero-speed source.

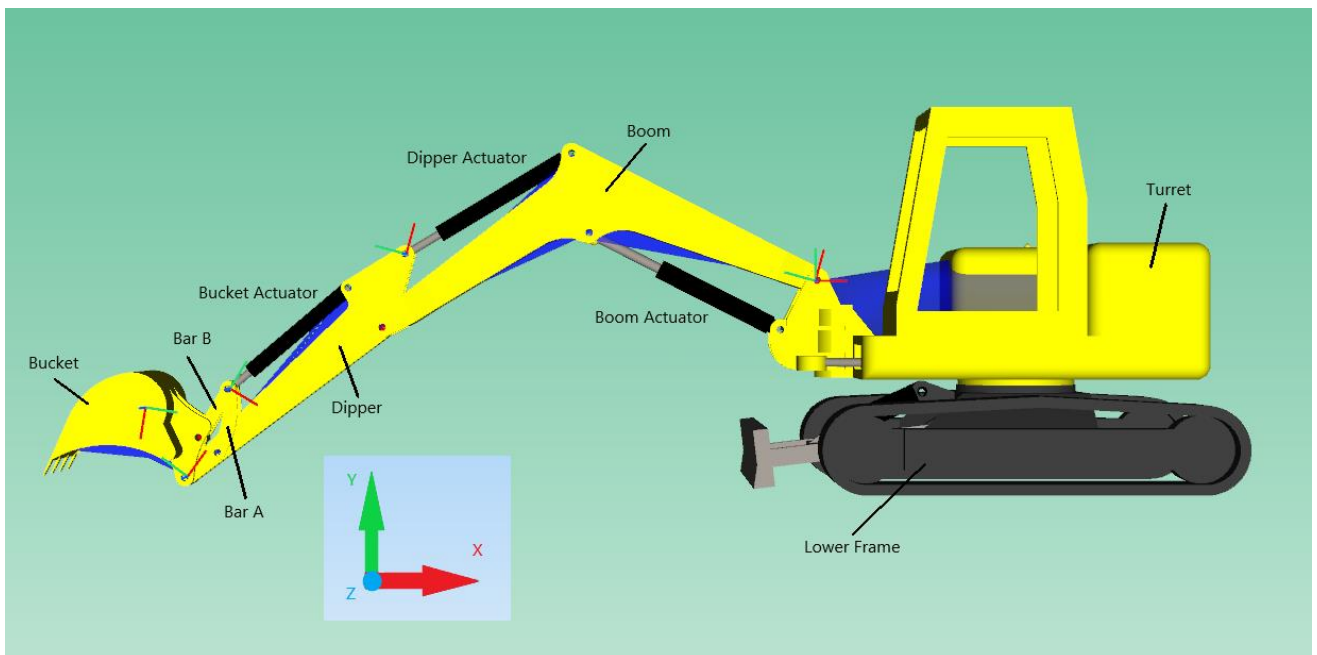


Figure 3.31: Mechanical 3D parts with rigid body on the simulation environment

3.3.2) 3D model with recursive joints

The components of the 3D mechanical library used up to now are not the only possible instruments that can be used to represent this system. There are, also other elements called recursive joints, that can give information about the inertia transferred between bodies. The recursive junctions establish link between reference and ends [11]. The reference can be a ground, or a rigid body and one end can be another recursive junction, a force source, or any other junction. Recursive junction, models perfect mechanical joints using recursive equations. These kinds of junction transfers all or part of its inertia from the end of the system to the reference. There are three kinds of recursive junctions, but in this case, have been used only two of them: the dynamic rigid junction (`dynamic_m6dofrecTjunction`) and the piloted pivot junction (`m6dofrecpilotedpivot`), they are shown in the figures 3.32 and 3.33.

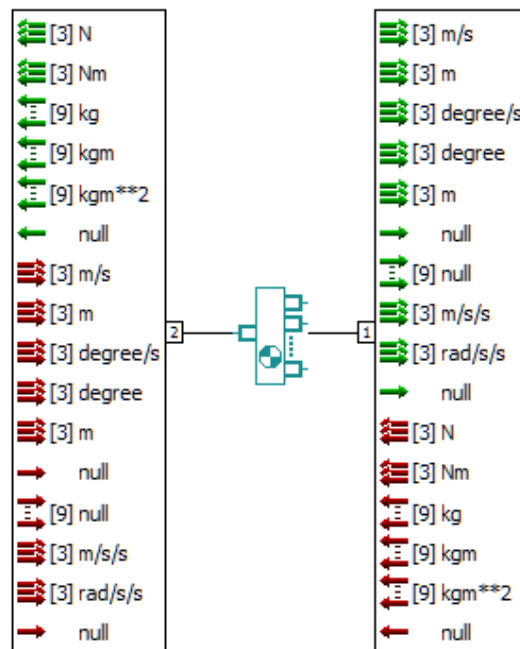


Figure 3.32: `Dynamic_m6dofTjunction` with its inputs (red) and outputs (green) [11]

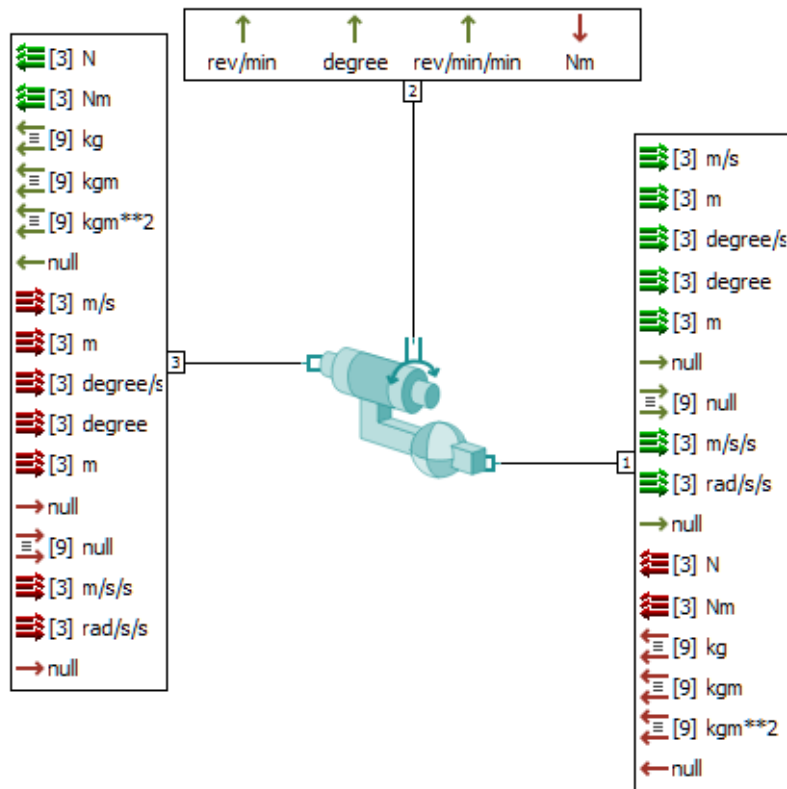
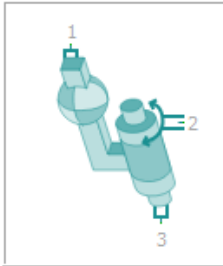


Figure 3.33: m6dofreplicatedpivot with its inputs (red) and outputs (green) [11]

Let us consider how it has been modelled the turret part and its connections with the recursive joints. A zero-speed source is used again to reproduce the non-moving parts. Connected to it there is the piloted pivot, that in this case represent both the piloted pivot and the turret model, indeed on its parameters is possible to impose not only the constrain orientation but also the inertia properties of the real excavator part, like the centre of gravity coordinates, mass and moments of inertia (figure 3.34).

AME Change Parameters ? X

Submodel



m6dofrecpilotedpivot [M6DOFRPIV00] External variables

recursive 3D piloted pivot joint Image >>

Parameters

Title	Value	Unit	Tags
inner mass	yes		
orientation			
matrix reference	from port 3		
reference axis	Y axis		
Euler decomposition	ZYX		
first rotation	0	degree	
second rotation	0	degree	
third rotation	0	degree	
items location			
coordinate reference	relative		
G : x position	0.163	m	
G : y position	0.24673	m	
G : z position	-0.521695	m	
x position at port 1	-1.38732	m	
y position at port 1	0.666128	m	
z position at port 1	0	m	
inertia			
mass	8302.66	kg	
moment of inertia around Gx axis	5492.67	kgm**2	
moment of inertia around Gy axis	7336.09	kgm**2	
moment of inertia around Gz axis	7509.78	kgm**2	
product of inertia xy	0	kgm**2	

Save Load Default value Max. value Reset title Min. value

Help Close Options >>

Figure 3.34: m6dofrecpilotedpivot parameters

After that, it has been connected the dynamic rigid junction, in which there are imposed the coordinates of the connections with other sub models and its orientation on the space (figure 3.35).

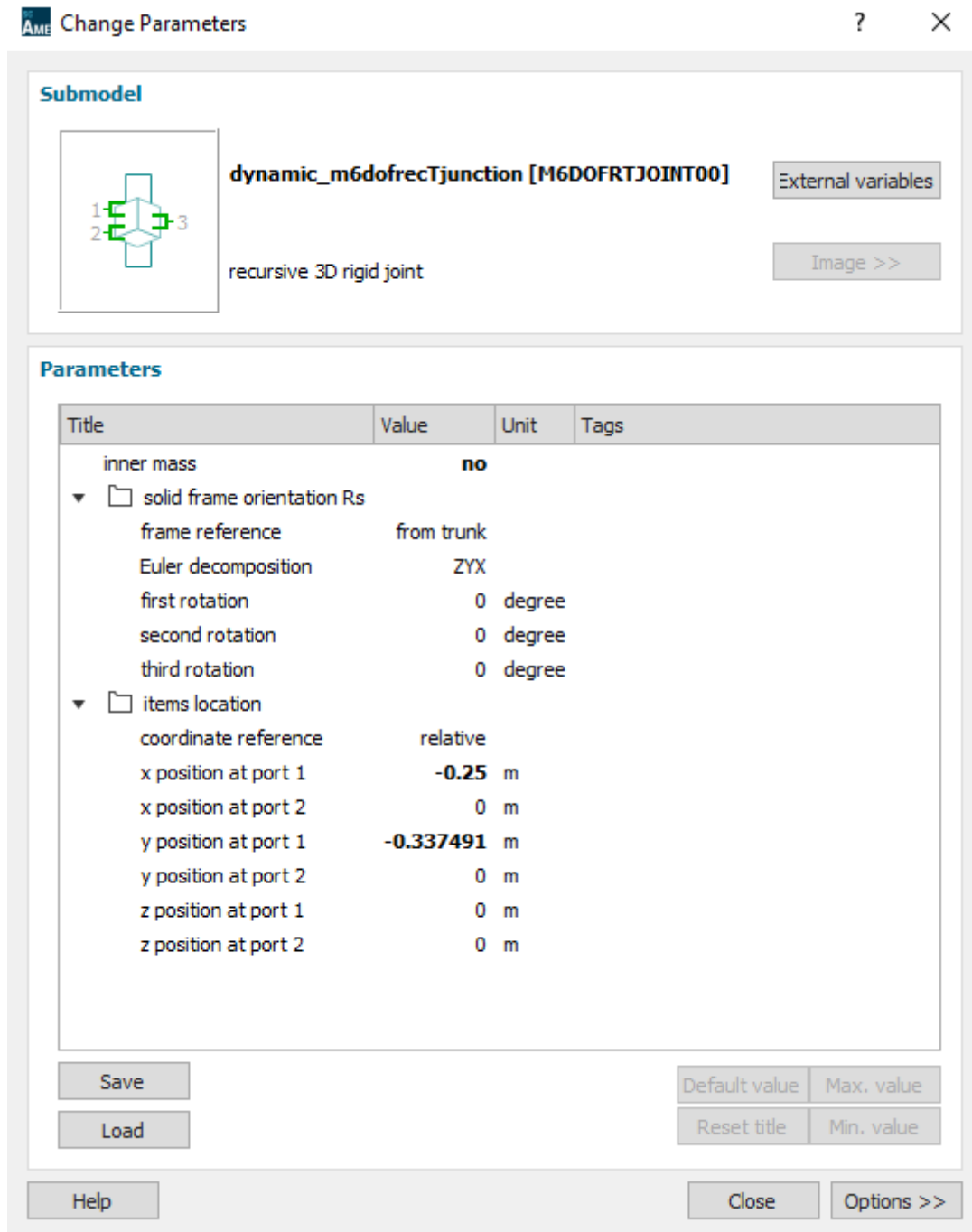


Figure 3.35: dynamic_m6dofrecTjunction parameters

It is important notice that, the port 3 on these two sub models represents their reference, so the coordinates of these two ports are dictate by the end of the previous sub model, that

means for the piloted pivot the coordinate of the port 3 is given by the zero-speed source, instead for the dynamic rigid junction by the port 1 of the piloted pivot.

The figures 3.36 and 3.37 shows how this part of the mechanical system is represented on the project and on the simulation environment of Amesim respectively.

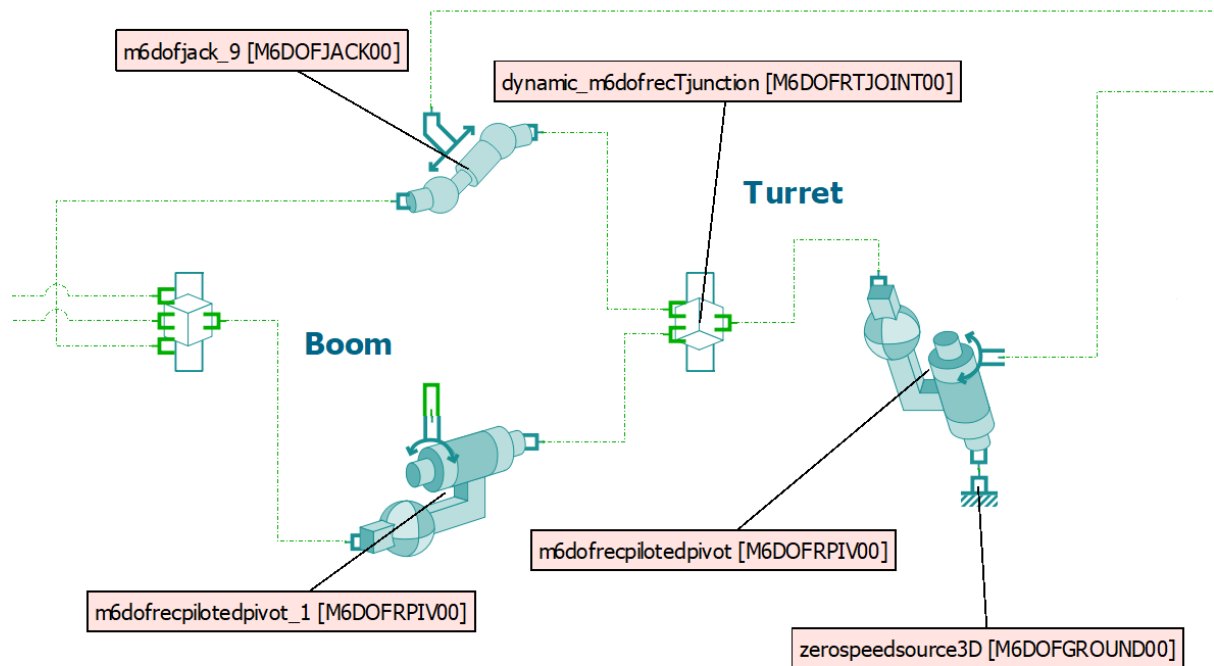


Figure 3.36: Turret sub model represented on the Amesim project environment

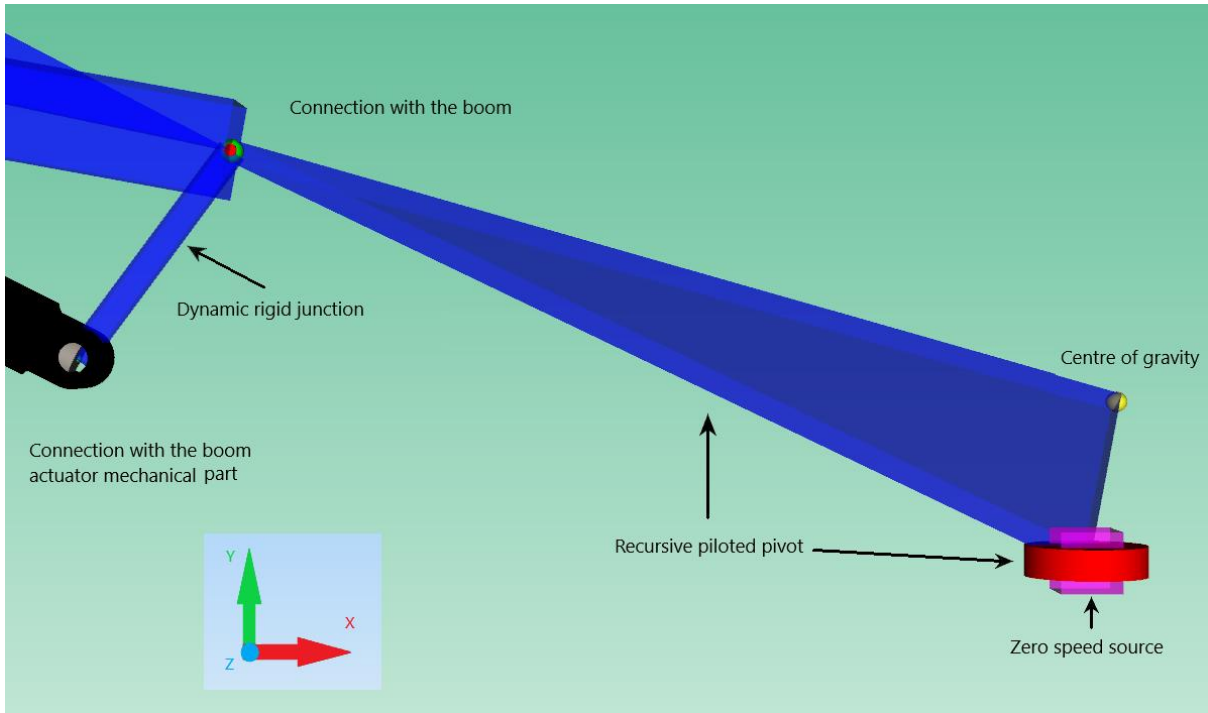


Figure 3.37: Turret model represented on the Amesim simulation environment

Following the logic explained before for the other excavator parts, it has been possible to complete the entire mechanical system with the recursive joints (figures 3.38 and 3.39), where on the piloted pivot that represents other moving parts, it has been closed the port 2 with the zero-torque source. On the bucket has been represented also its end points, closing the connection ports in its dynamic rigid junction with the zero force sources, except the port that represents the bucket tip where is connected the sub model that gives the input forces and moments.

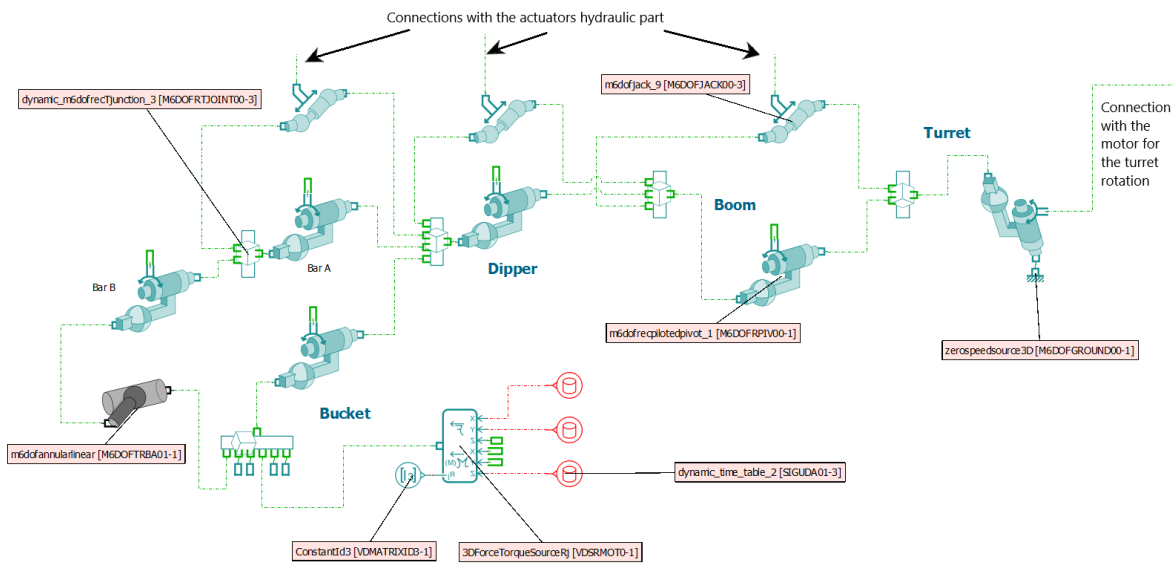


Figure 3.36: Complete 3D model in the Amesim project environment

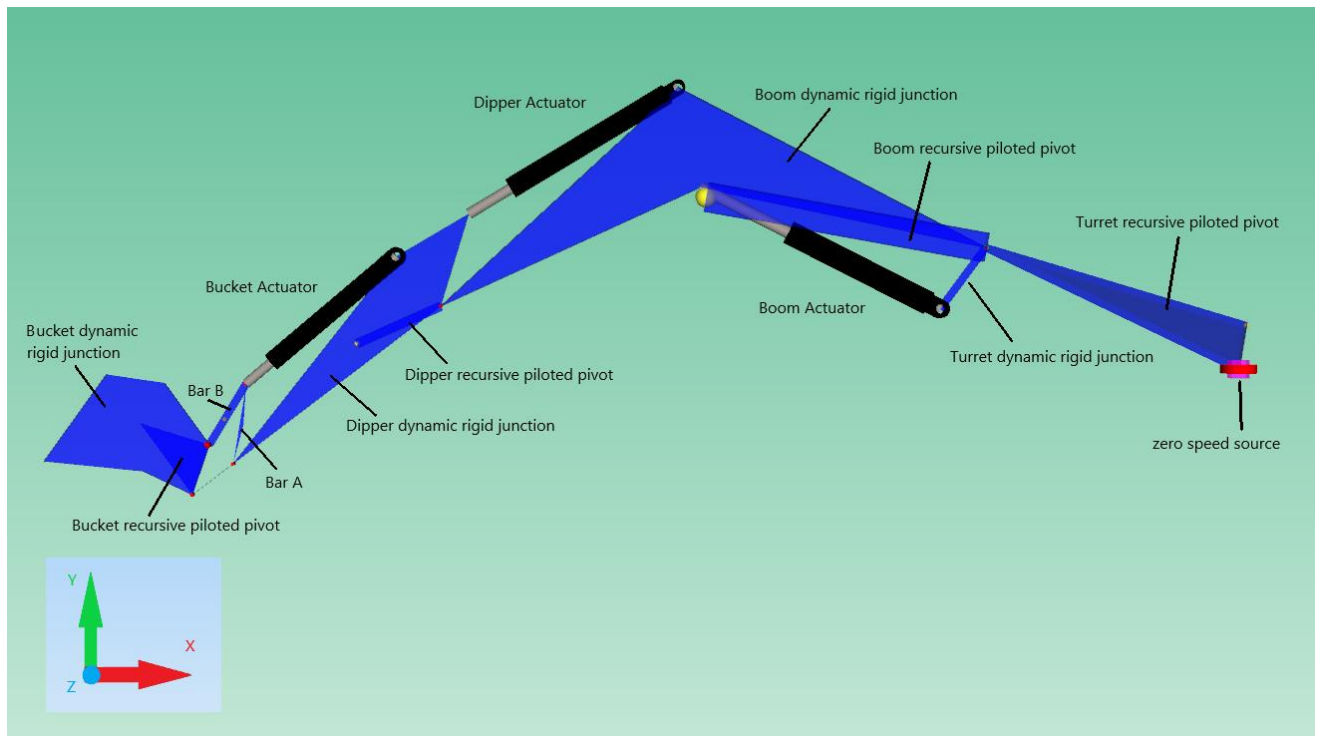


Figure 3.37: Complete 3D model in the Amesim simulation environment

Finally, it was attached for each excavator sub model, the correspondent CAD part as the rigid body model.

3.4) Hydraulic circuits

Once obtained the excavator kinetic part, it has been carried out the design of the two load sensing hydraulic circuits: pre-compensated and post-compensated hydraulic circuit.

3.4.1) LS pre-compensated hydraulic circuit

On the hydraulic circuit in figure 3.38 are presents, both parts taken from the hydraulic library and parts taken from the 1D mechanical library, as well as, from the signal and control library.

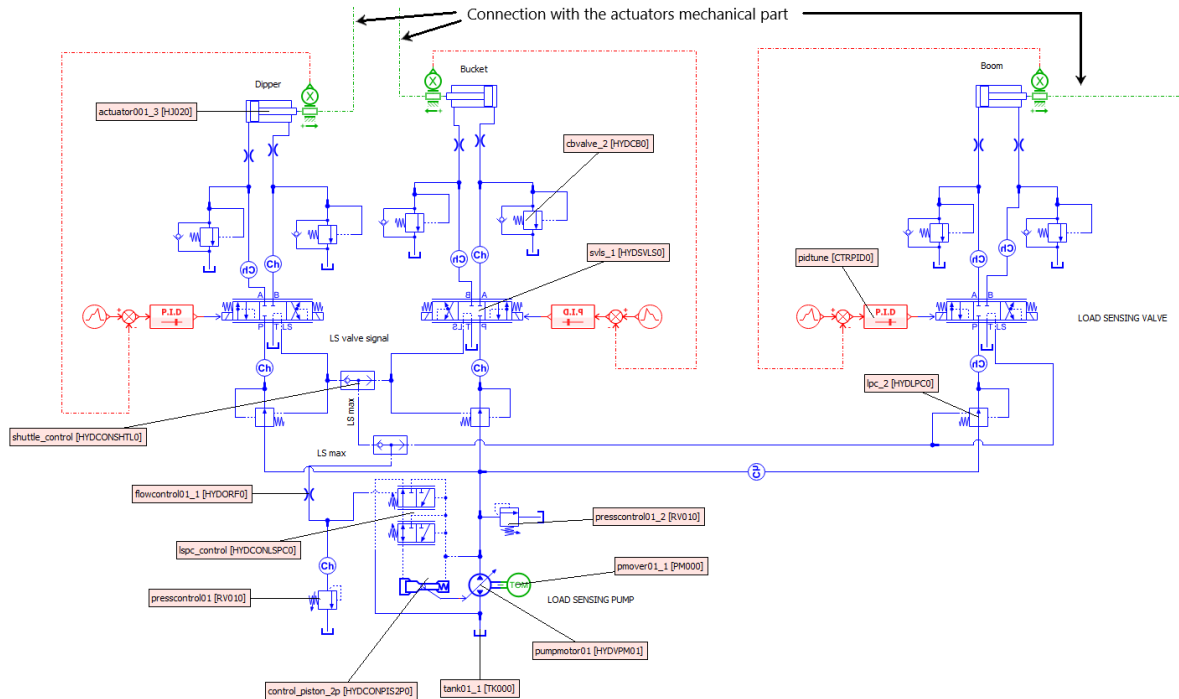


Figure 3.38: Load sensing pre-compensated hydraulic circuit

Starting from the bottom part, there is the tank where the oil is taken, and connected on it there is the variable displacement pump that is driven by a prime mover that schematises the internal combustion diesel engine. The pump regulates its displacement through the control piston that is connected to the load sensing and pressure compensator control, in which is simulated the behaviour of the absolute together with the differential pressure limiter, therefore it takes the pump delivery pressure and the global load sensing pressure and acting on the control piston adjusts the pump displacement. Following the pump delivery line, there are before the local compensator and after the distributors, because this is the pre-compensated case. The local compensators are normally open valves, where act the local load sensing pressures, instead the distributors are proportional valves with five ports and three positions, spring centred, and solenoid activated. The distributors are controlled by the PID that moves the valve main spools, trying to impose to the linear actuators the same displacements that receives in input. To select the highest load sensing pressure signal that is the global load sensing, are used two shuttle valves, one after the other, that perform this job. For safety reason, on the lines between the distributors and the actuators, there are two relief valves with non-return valves in parallel for each actuator, they have the aim to put a maximum pressure limit on the piston and on the rod chambers. Other two relief valves are placed for safety reasons, before and after the hydraulic power unit. These two valves have a pressure setting slightly higher than the absolute pressure limiter, to intervener on the pump delivery pressure only if it does not work. Finally, to the left of the hydraulic power unit, is connected a functional restrictor, that has the aim to uncouple the pressures downstream and upstream of it when one of the two safety relief valves regulate, so the hydraulic circuit is in pressure saturation condition, but this case will be discussed more in detail on the following chapter.

3.4.2) LS post-compensated hydraulic circuit

This kind of hydraulic circuit, that is shown in figure 3.39, differs from the previous one because now the local compensator is placed after the distributor, as the post-compensated must be.

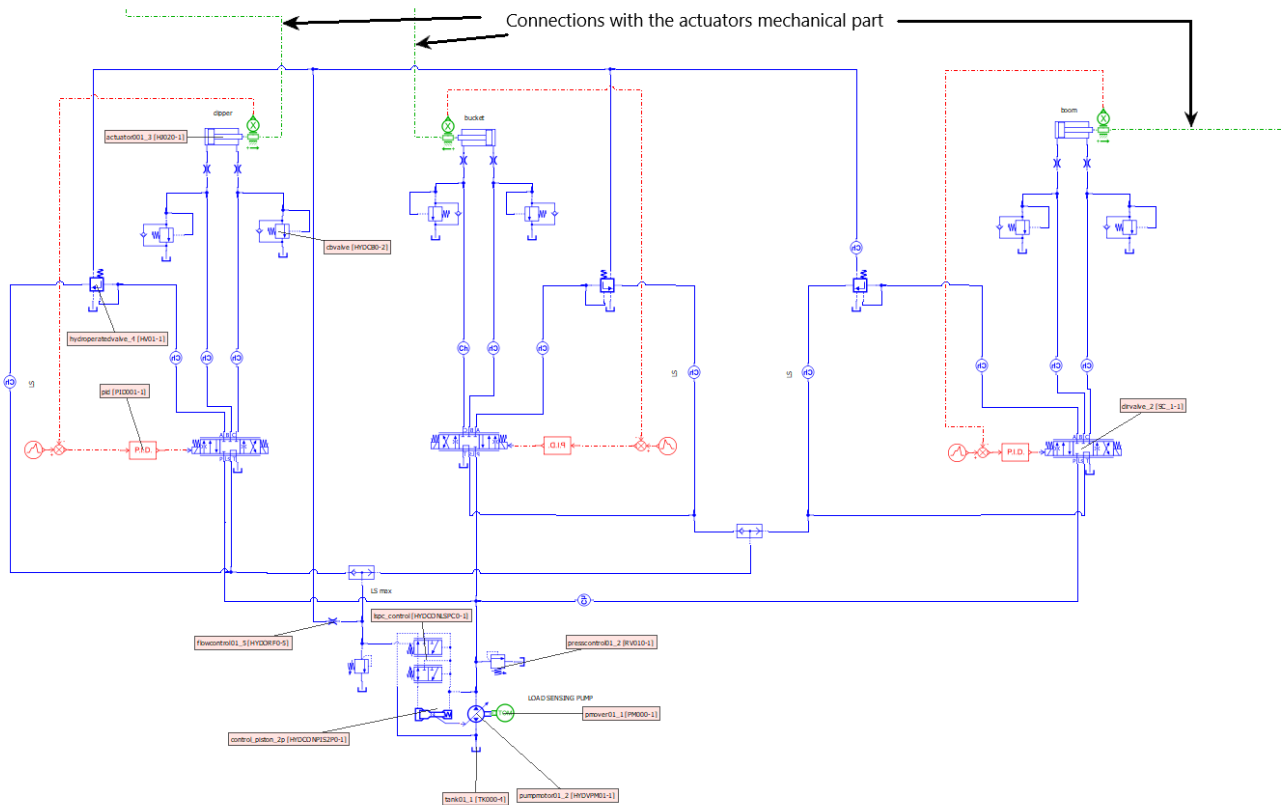


Figure 3.39: Load sensing post-compensated hydraulic circuit

The compensators in this case, is a normally closed valves, in which acts the global load sensing signal. Instead, the distributors are six ports, three position proportional valves, spring centred, and solenoid activated, that have on the extreme positions always a path that connects the port P where the fluid coming from the pump delivery port to the port A connected to the local compensator, this because between the port P and A there is a restrictor across which the pressure drop is constant. The other two ports instead, decides which chamber of the linear actuator has to powered. Since, this valve that simulates the behaviour of the real distributor is not present on the hydraulic library, so it has been created by the `valve_builder_hydr`, that is a feature on Amesim® to generate custom distributors.

3.4.3) Hydraulic circuit for the turret rotation

To understand how this system works, an ISO scheme in figure 3.40 has been reported.

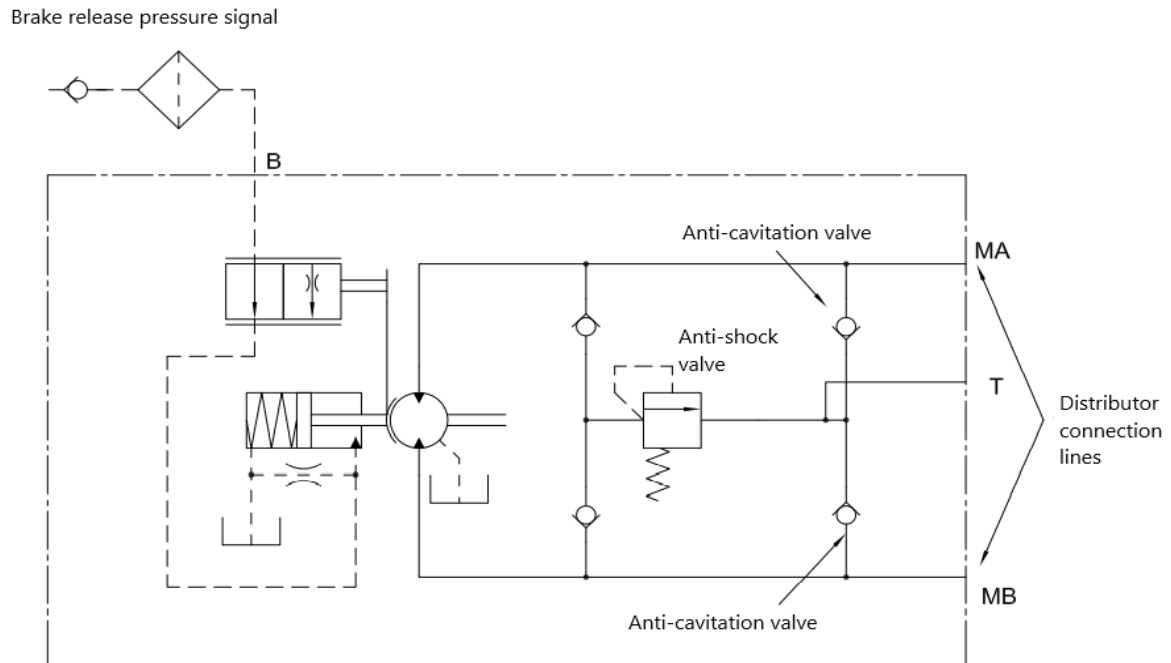


Figure 3.40: ISO scheme turret rotation hydraulic circuit [3]

The motor for the turret rotation is a fixed displacement axial piston motor, its shaft is connected to the speed reducer connected to the turret [3]. The delivered fluid coming from the distributor reaches the motor, alternatively, through the ports MA or MB, it depends on the rotation direction. On the delivery line from the distributor to the motor, there are two transversal lines that have two non-return valves. The first one is an anti-cavitation valve, the second one put in connection the anti-shock valve with the powered line of the motor to avoid, possible, pressure peaks. The anti-shock valve is connected to the tank through a direct line, that it is different with respect to the return line that pass on the distributor. This because, the discharged line of the anti-shock valve is connected to the anti-cavitation valves, so to avoid pressure drops, this discharge line must be connected to the tank as directly as possible.

Inside the motor for the turret rotation is also present a brake. To unlock the brake, a pilot pressure signal is generated by the operator. The actuator to unlock the brake is a single acting actuator, in which its outward phase is performed thanks to the presence of a spring, since the piston chamber is connected to the reservoir. Powered the rod chamber, is produced the actuator inward stroke, therefore the brake detaches from the motor rotor and stops to produce the torque needed to brakes the turret. The pilot line direct to the actuator, is intercepted by a regulation valve, where its spool is mechanically connected to the actuator rod. In the neutral position, the brake is activated, and the valve is fully open. When it is necessary to move the turret, the distributor spool moves to feed the motor and at the same

time the brake is unlocked due to the pilot signal. Powered the rod chamber of the brake actuator, when it moves inward drags the spool regulation valve, throttling the area where the fluid flows, if there is an equilibrium between the spring force and the force exerted by the pressure on the rod chamber. The restrictor that puts in connection both actuator chambers to the reservoir, allows to have a continuous flow rate, to guarantee a continuous valve regulation.

To implement this hydraulic circuit, the following components in Amesim® are adopted (figure 3.41):

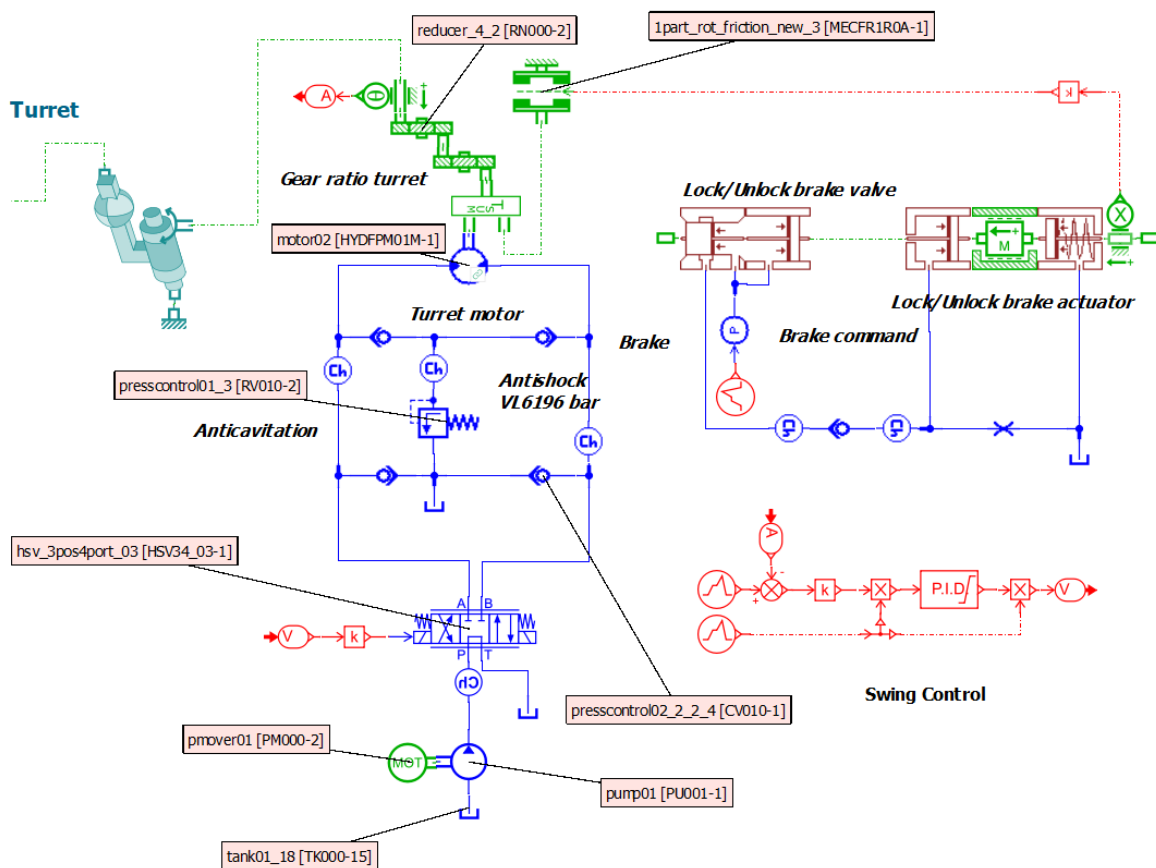


Figure 3.41: Turret rotation hydraulic circuit

A prime mover that realizes the internal combustion diesel engine drive a fixed displacement pump, that simulates the gear pump. Connected to this latter there is a 4/3 proportional control valve with an open centre in the central position, spring centred, and solenoid activated, that chooses whether the turret has to rotate clockwise or anti-clockwise. Then, there are two couples of non-return valves, the first couple performs the anti-cavitation feature, the second one puts in connection the anti-shock valve with the pump delivery line. On the upper part, there is the bi-directional motor that performs the turret rotations, connected to the speed reducer and the brake. The brake has been realised with hydraulic, hydraulic components design and 1D mechanical library, composed by the regulating valve represented by the lock-unlock brake valve, the actuator by the lock –unlock brake actuator and the rot_friction to generate the friction torque needed to stop the turret. Also in this case, the rotation is controlled by means of the PID that controls the proportional valve spool in order to performs the desired turret rotation.

3.5) Complete hydraulic circuits

Assembled all components described in the previous paragraphs, in pre and post compensated configurations, are obtained the systems with rigid body and recursive joints illustrated in the figures 3.42, 3.43, 3.44, 3.45:

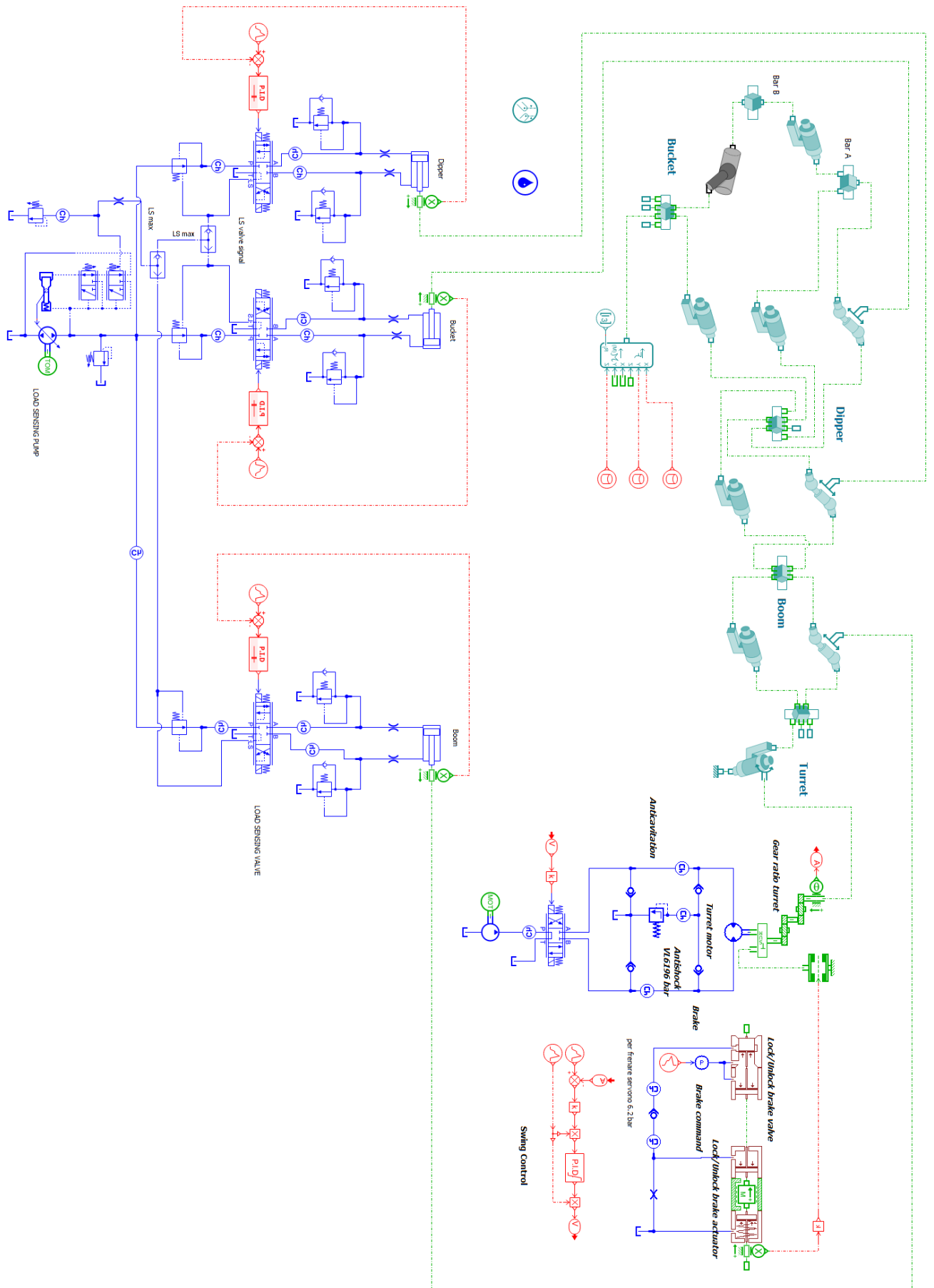


Figure 3.42: Pre-compensated with rigid body hydraulic circuit

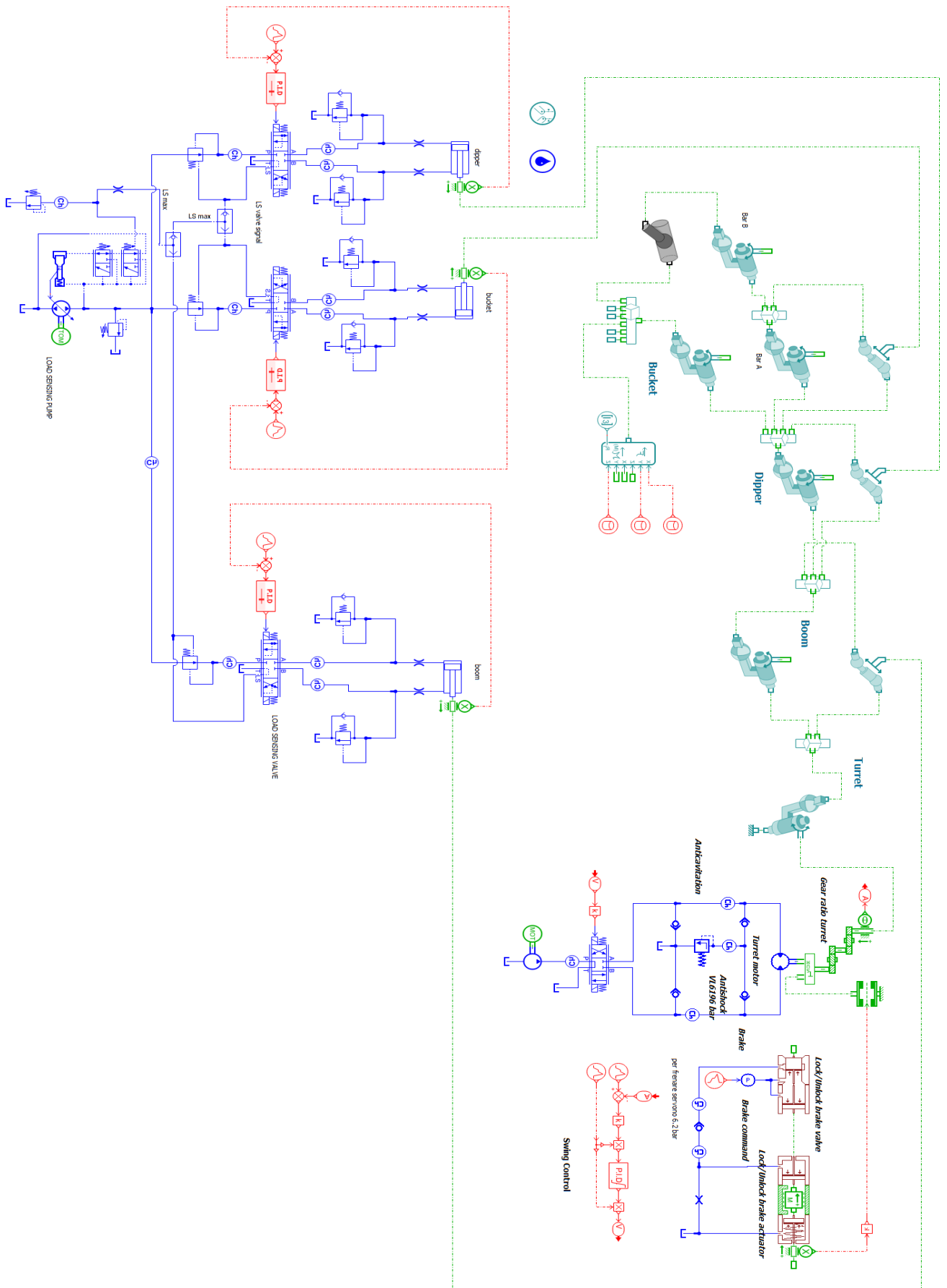


Figure 3.43: Pre-compensated with recursive joints hydraulic circuit

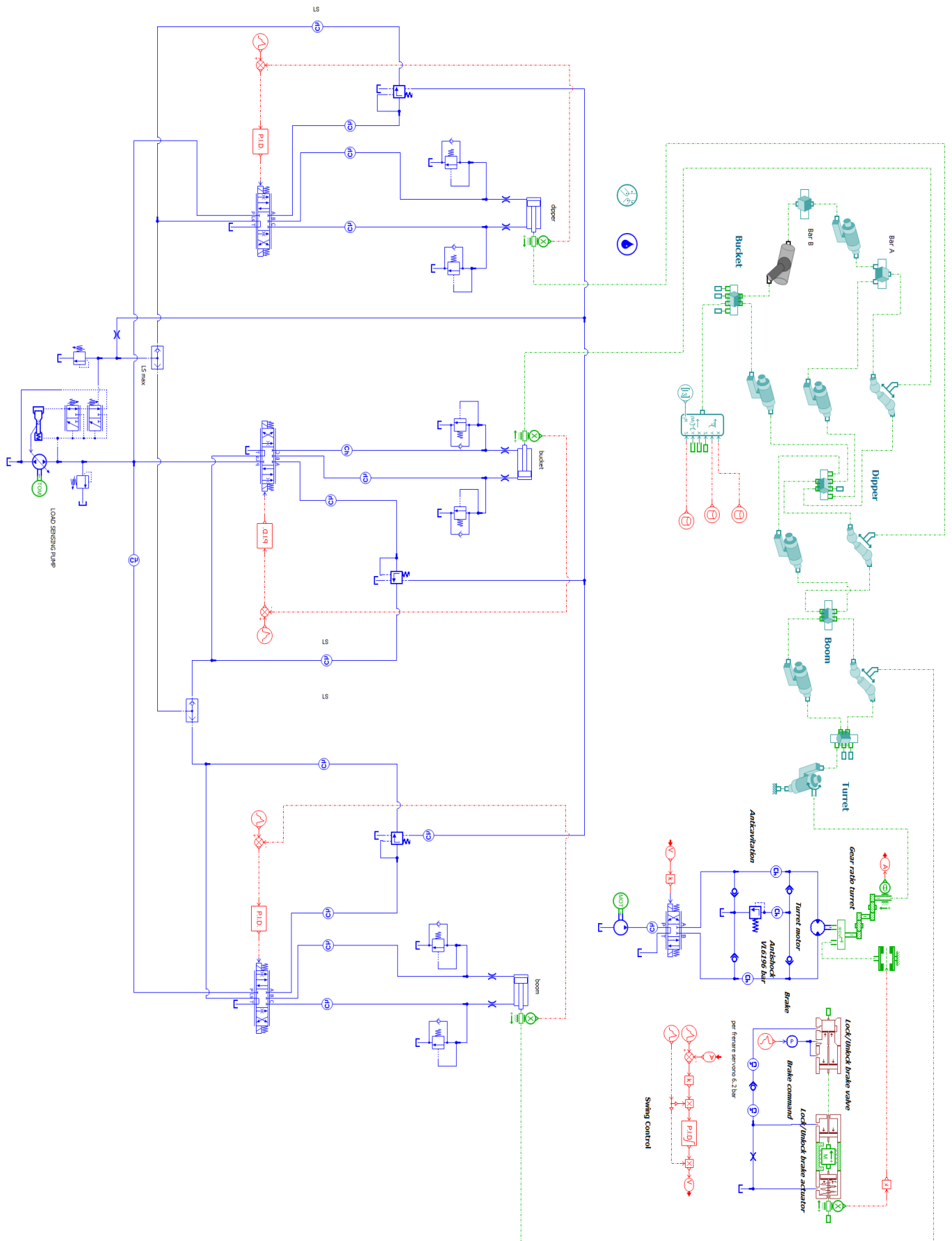


Figure 3.44: Post-compensated with rigid body hydraulic circuit

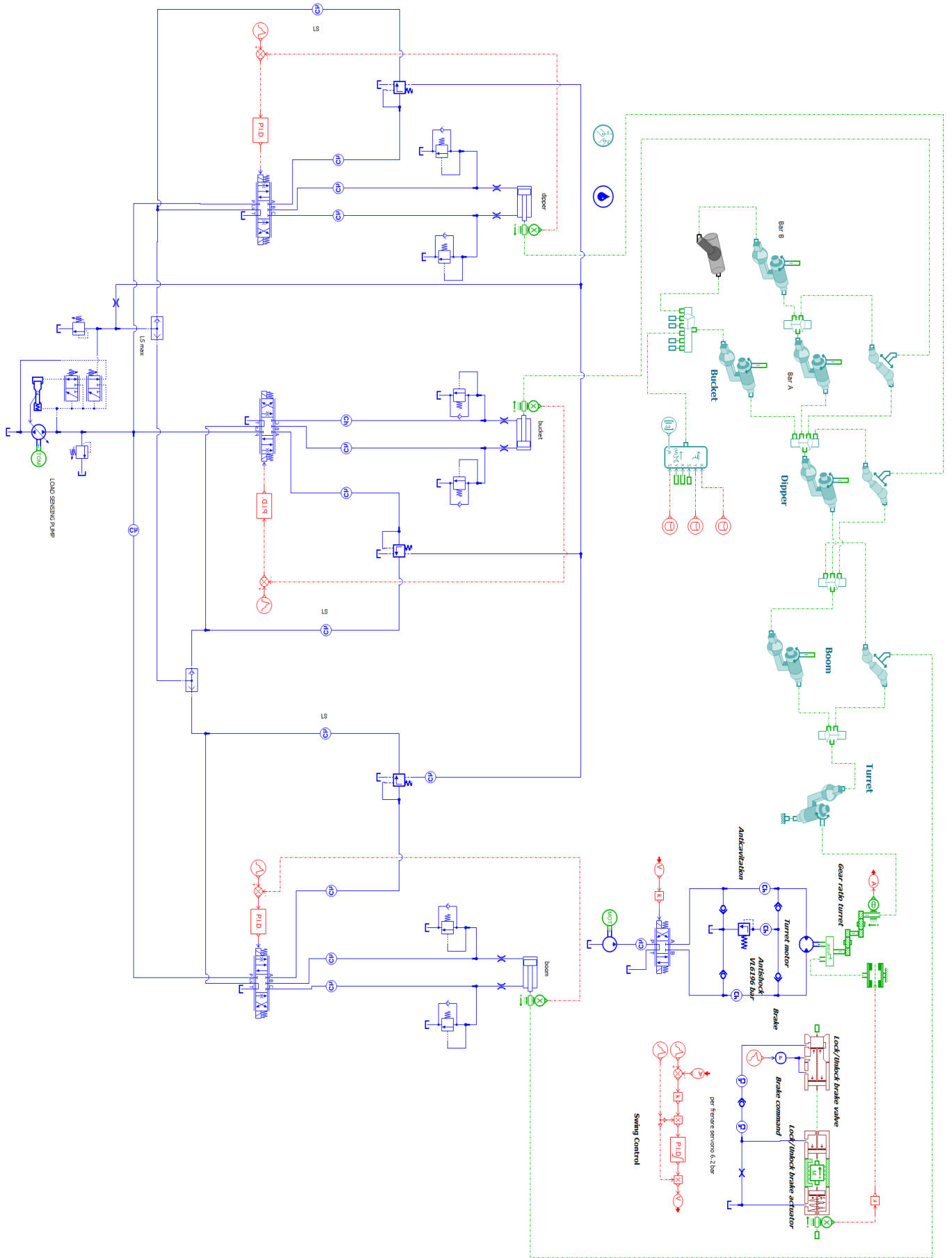


Figure 3.45: Post-compensated with recursive joints hydraulic circuit

CHAPTER 4: RESULT ANALISYS

4.1) Normal duty cycle

4.1.1) 3D system with pre-compensated hydraulic circuit and rigid bodies

Starting from the hydraulic circuit in pre-compensated configuration with rigid bodies, it has been imposed a shaft speed of the prime mover equal to 2000 rpm both in the pump that powers the actuators and, in the pump, used to power the motor for the turret rotation, because both prime movers represent the same internal combustion diesel engine that drives two different pumps. The pump that powers the actuators has a maximum displacement of 120 cc/rev, a volumetric efficiency of 0.92 and a hydraulic-mechanical efficiency of 0.96. The differential pressure limiter has a pressure setting equal to 25 bar, so increase the pump delivery pressure by this quantity, instead it has been chosen a cracking pressure of 350 bar for the absolute pressure limiter to put a limit on the delivery pump line. All the pressure setting of the relief valves used for safety reasons are imposed to 400 bar, in this way they do not interfere with the normal hydraulic circuit operation. For the local compensator point of views, it is imposed a cracking pressure equal to 10 bar, lower than the differential pressure limiter, this because it has been considered the pressure lost inside the pipes (distributed losses), moreover this value represents also the pressure drop across the distributors. The boom actuator has a piston diameter of 110 mm, a rod diameter of 70 mm and a length of stroke equal to 765 mm, the dipper actuator has a piston diameter of 95 mm, a rod diameter of 60 mm and a length of stroke of 905 mm, instead the bucket actuator has a piston diameter of 85 mm, a rod diameter of 55 mm and a length of stroke 730 mm. The fluid used has a density of 850 kg/m³, a bulk modulus of 17000 bar and an absolute viscosity of 51 cP. Regarding the hydraulic circuit for the turret rotation, it has been imposed a pump displacement of 30 cc/rev, a motor displacement of 31 cc/rev with a volumetric efficiency of 0.95 and a mechanical hydraulic efficiency equal to 0.97, and a cracking pressure for the anti-shock valve equal to 190 bar.

After that, have been imposed the inputs. Forces and moments are reproduced as already explained in the previous chapter. The figures 4.1,4.2 and 4.3 shows the inputs for the boom, dipper, and bucket valves respectively, connected to the PID controls that control the valves spool in order to impose these displacements to the actuators, and reproduce the real actuator displacements performed by the 2D.

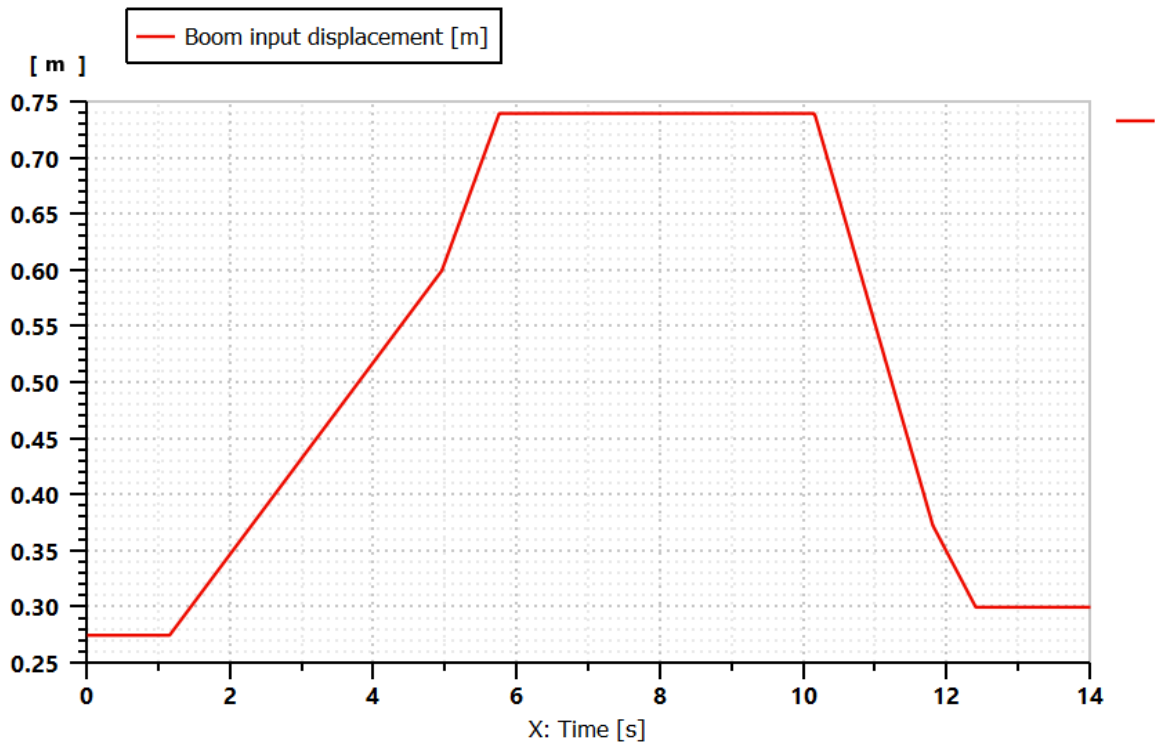


Figure 4.1: Boom input displacement

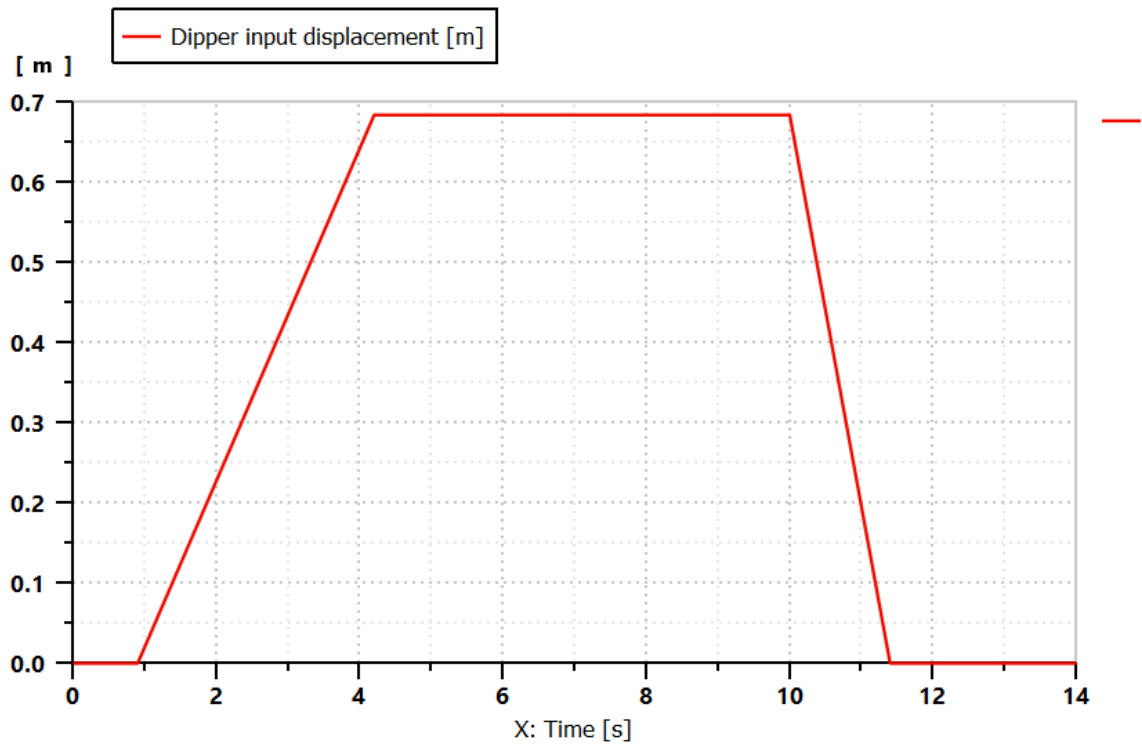


Figure 4.2: Dipper input displacement

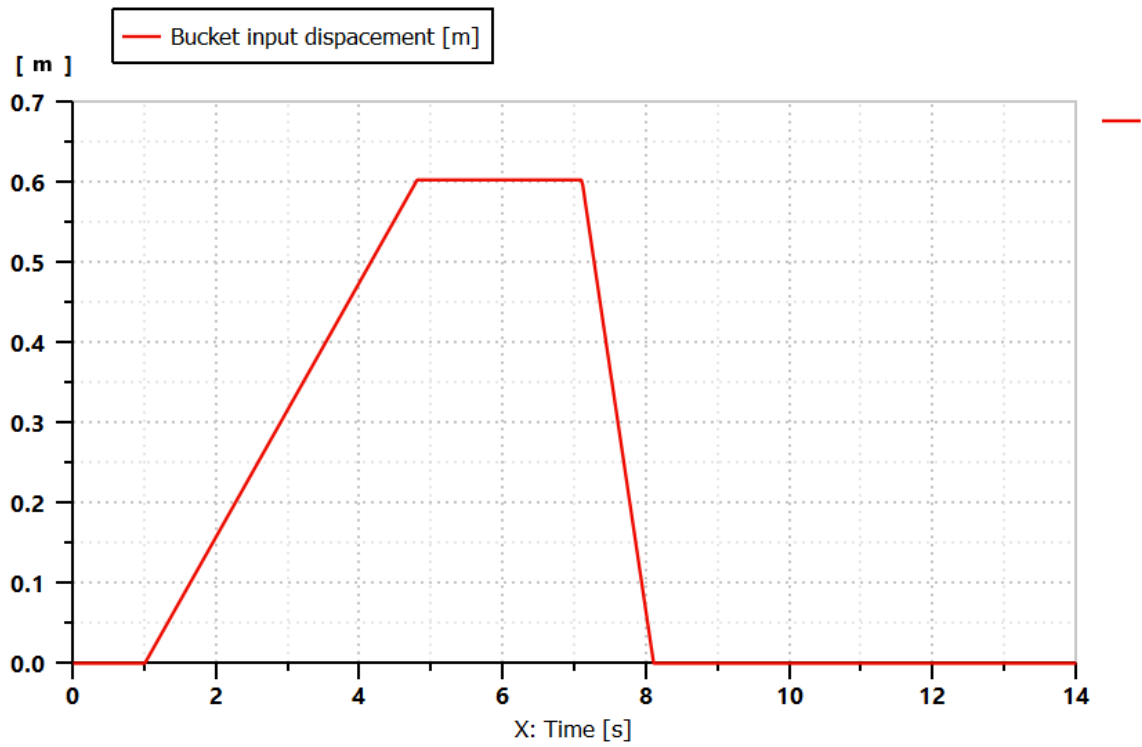


Figure 4.3: Bucket input displacement

In similar way, the input in figure 4.4 it is connected to the valve for the turret rotation through a PID controller, to controls the spool valve and performs a turret rotation from zero to ninety degree, and after discharge the material inside the bucket, another rotation of ninety degrees to come back to its original position.

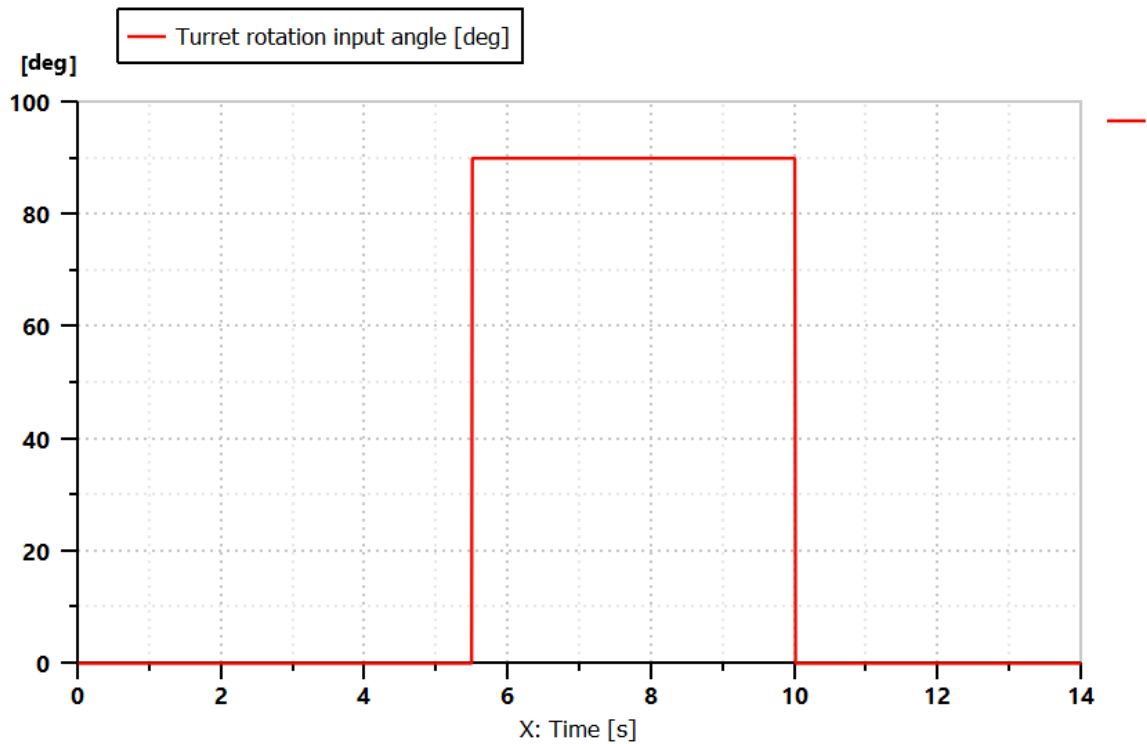


Figure 4.4: Turret rotation input angle

Together to the input of the turret rotation, a brake command signal (figure 4.5) and a valve control signal (figure 4.6) are used. On the brake command signal, 0 means brake activated, and 6.2 means brake deactivated, because 6.2 bar is the pressure needed to compress the spring and deactivated the brake. Instead, regarding the valve control signal, 0 means that the PID does not control the valve, so the valve is in its central position when the brake is activated to maintain the turret on its original position or when the turret must reach the desired position, and on the opposite way 1 means that the PID controls the valve to perform the rotation.

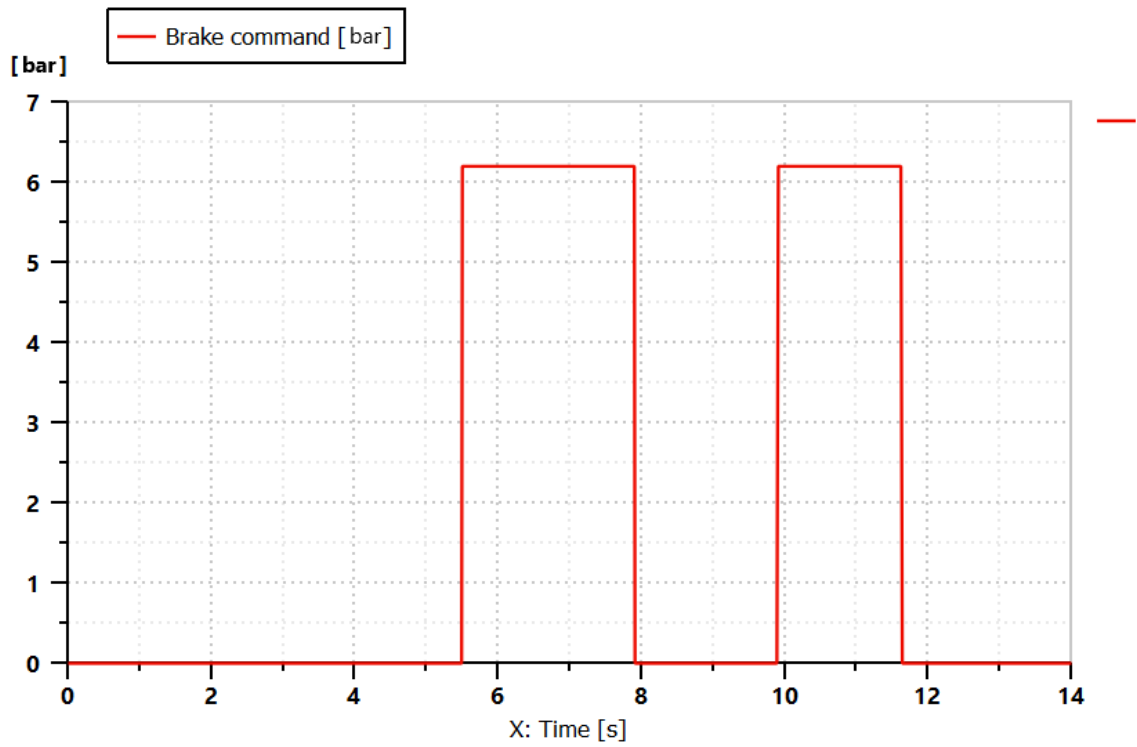


Figure 4.5: Brake command signal

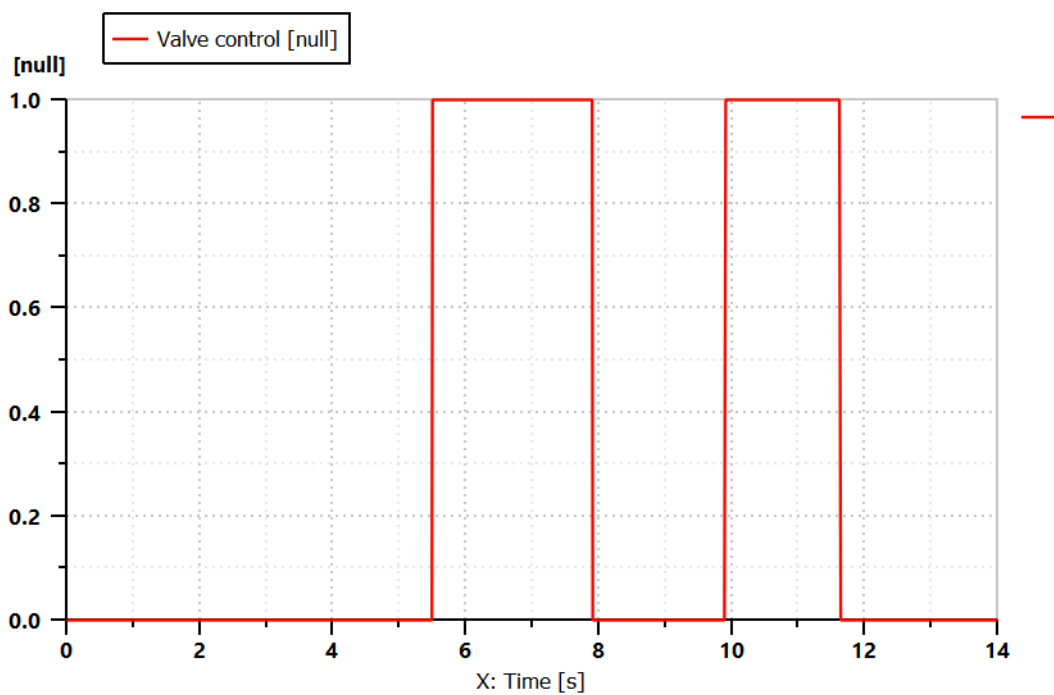


Figure 4.6: Valve control signal

After set all the parameters and inputs, the simulation is performed and once got the results they have been analysed. At the time t equal to 0 s the excavator is in its rest position as the figure 4.7 illustrates.

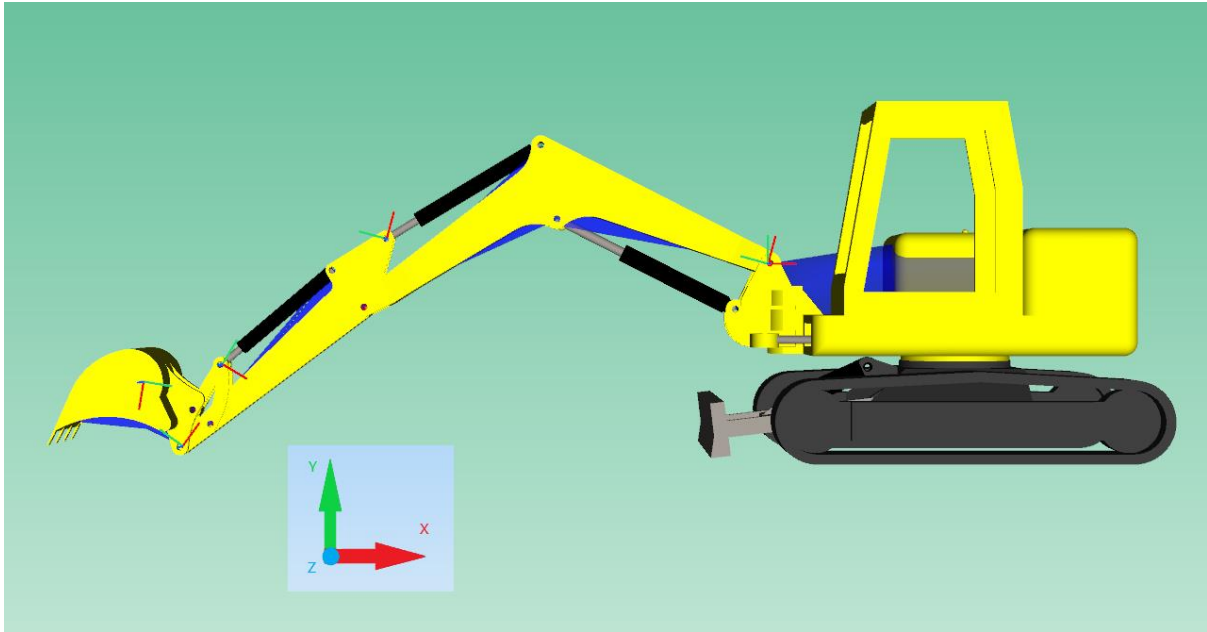


Figure 4.7: Excavator position at time t equal to 0 s

The figures 4.8, 4.9 and 4.10 shows as the boom, dipper and bucket displacements obtained, approximates the real displacements of these actuators coming from the 2D model, since on the valves of this new model is not possible directly impose the precise positions of the valves main spool.

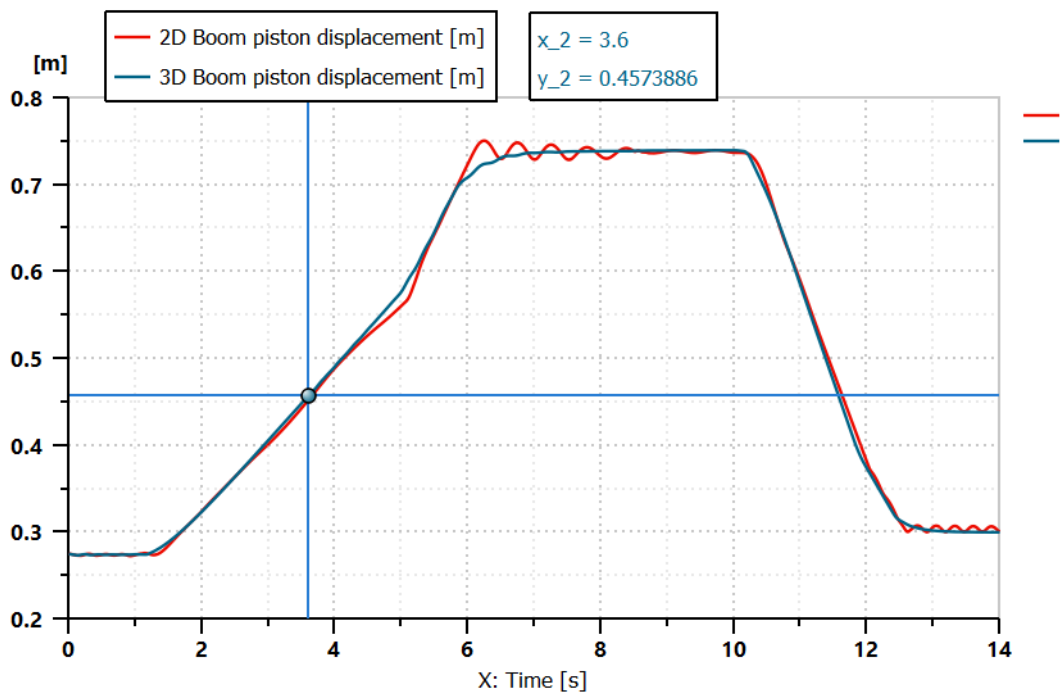


Figure 4.8: 2D and 3D Boom piston displacements

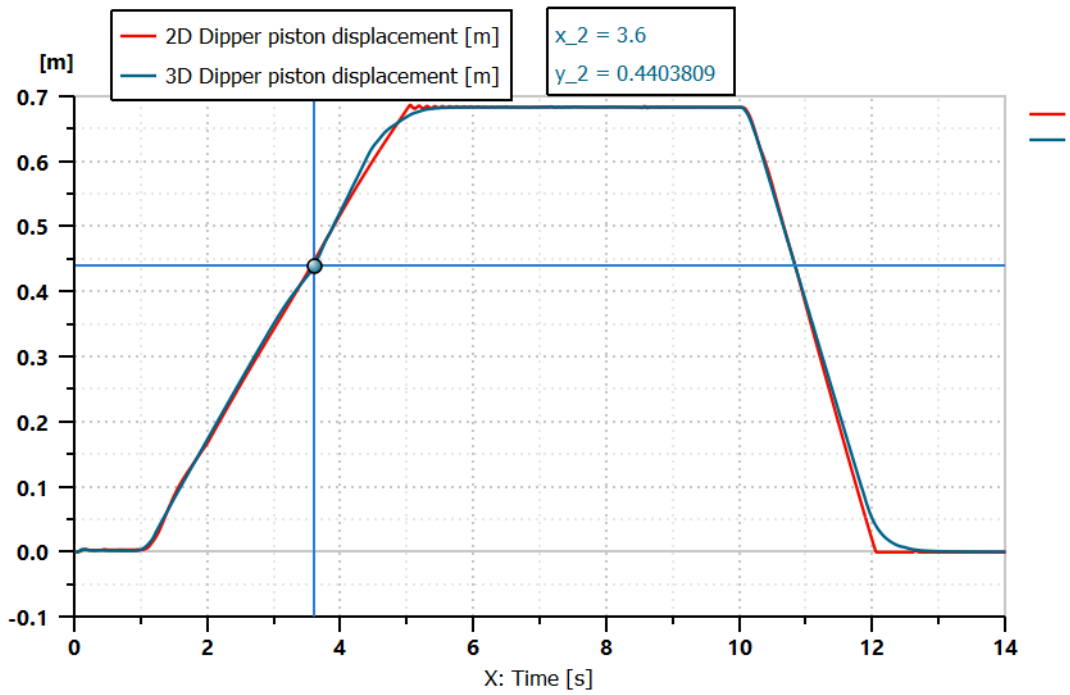


Figure 4.9: 2D and 3D Dipper piston displacements

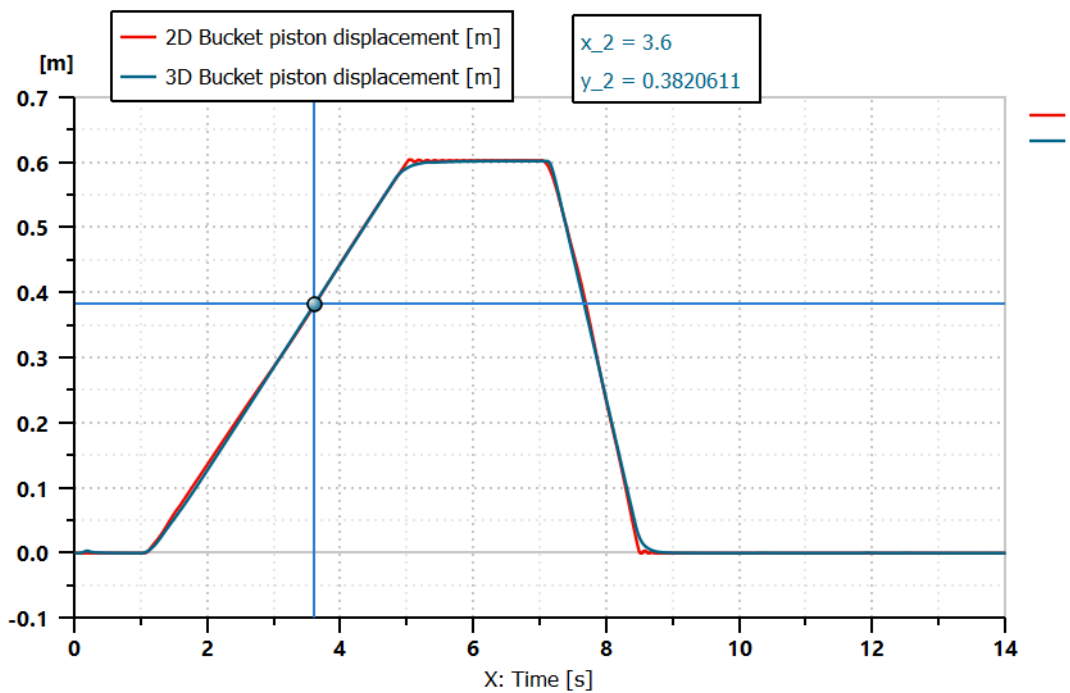


Figure 4.10: 2D and 3D Boom piston displacements

At the time t equal to 3.6 s the excavator performs the digging activity, and it is on the configuration shows in figure 4.11.

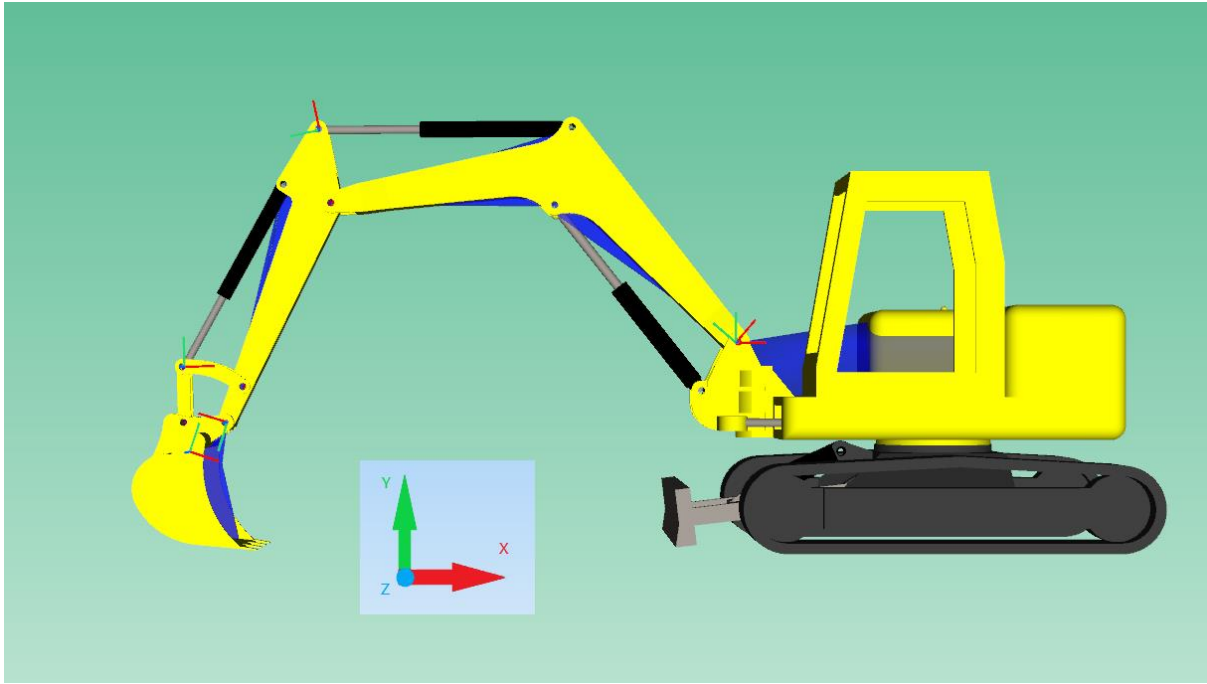


Figure 4.11: Excavator position at time t equal to 3.6 s

On the figure 4.12 is possible to appreciate, as the excavator turret performs its rotation and as the brake works properly.

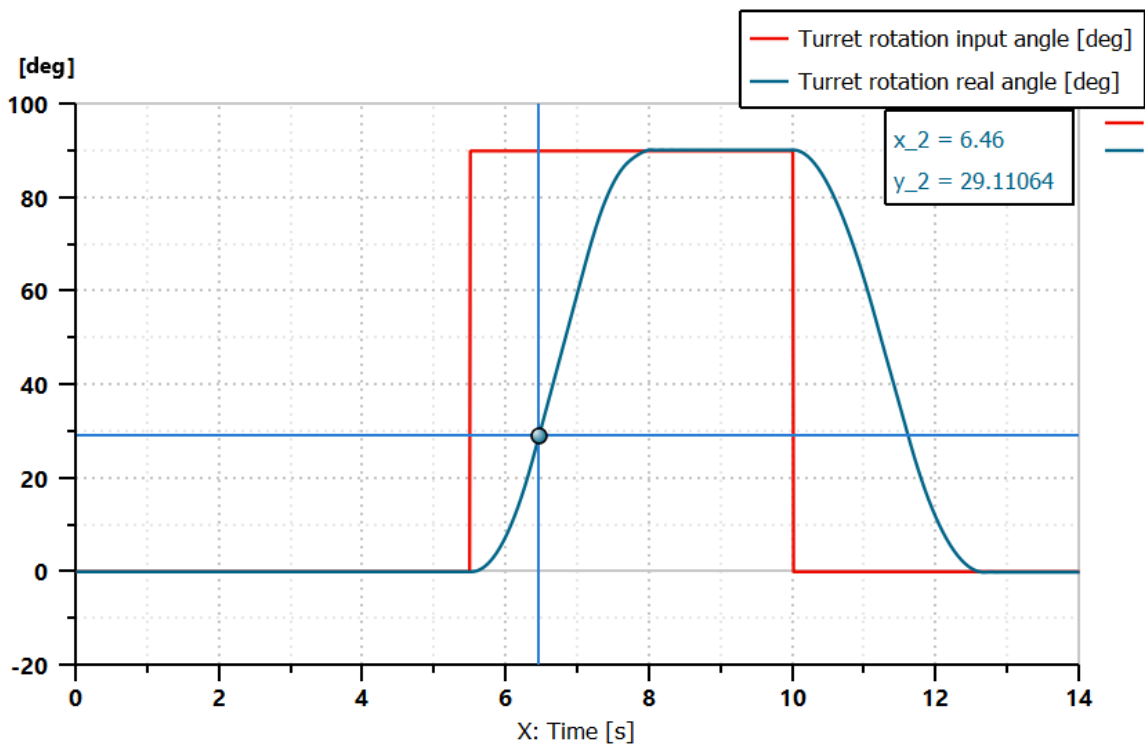


Figure 4.12: Turret rotation input and real angle

At the time t equal to 6.46 s the excavator turret is rotating (figure 4.13) to reaches the configuration in which discharges the material inside the bucket.



Figure 4.13: Excavator position at time t equal to 6.46 s

Analysing the hydraulic circuit in pre-compensated configuration, it is possible notice that the pump does not work with its maximum displacement, because the pump displacement modulation factor is lower the one (figure 4.14), so it means that the hydraulic circuit is not in the flow saturation condition.

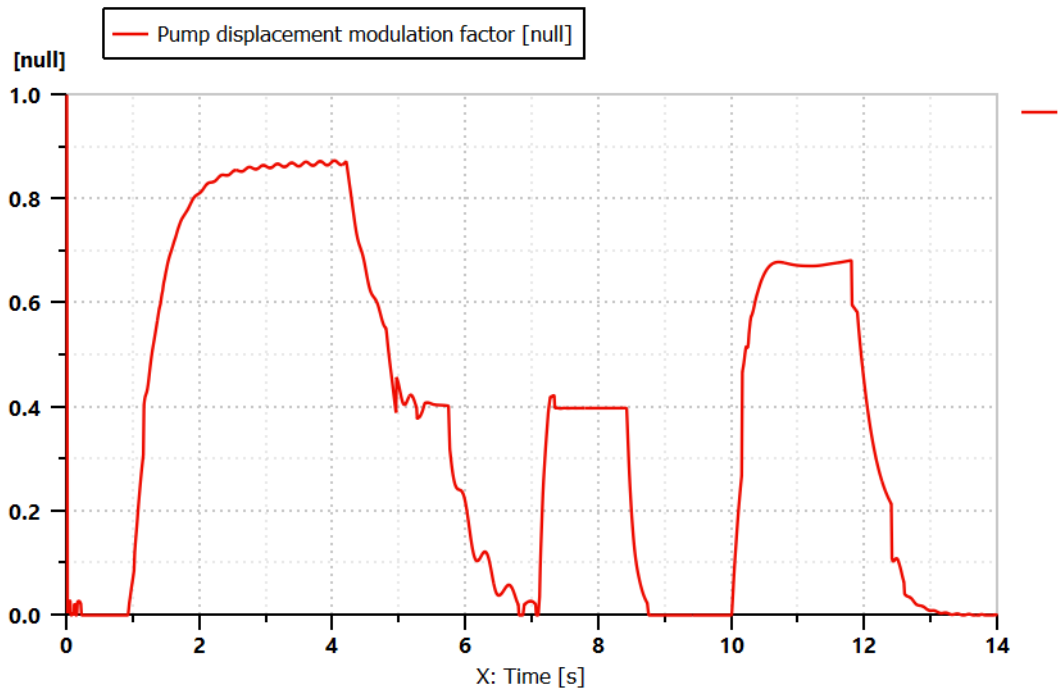


Figure 4.14: Pump displacement modulation factor

In the figure 4.15 is clear that the pump has a pressure along its delivery line higher than the global load sensing pressure signal to about 25 bar, that is the pressure setting of the differential pressure limiter. This difference is not precise because in these systems are consider the non ideality of the components that represents the hydraulic circuit.

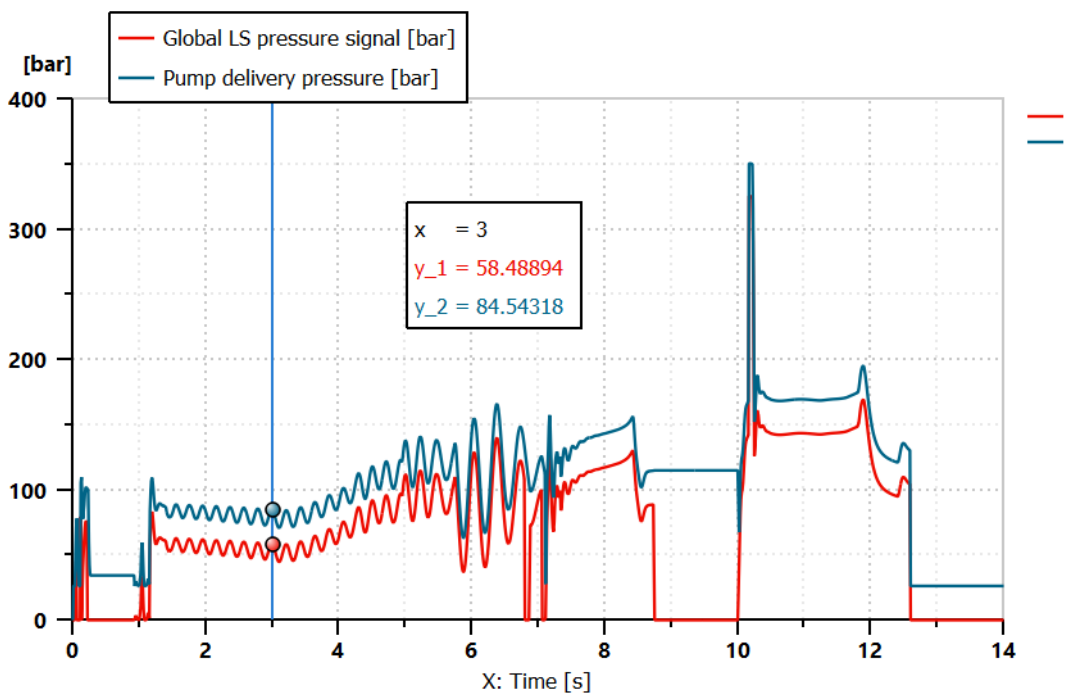


Figure 4.15: Global LS pressure compared with the pump delivery pressure

Instead, the figures 4.16, 4.17 and 4.18 shows that on the boom, dipper, and bucket distributors there is a pressure drop roughly 10 bar, that is equal to pressure setting of the local compensator as expected. The port P in these figures represents the distributor port connected to the pump, instead the port A represent the distributor port connected to the actuator piston side to accomplish the actuators outward stroke.

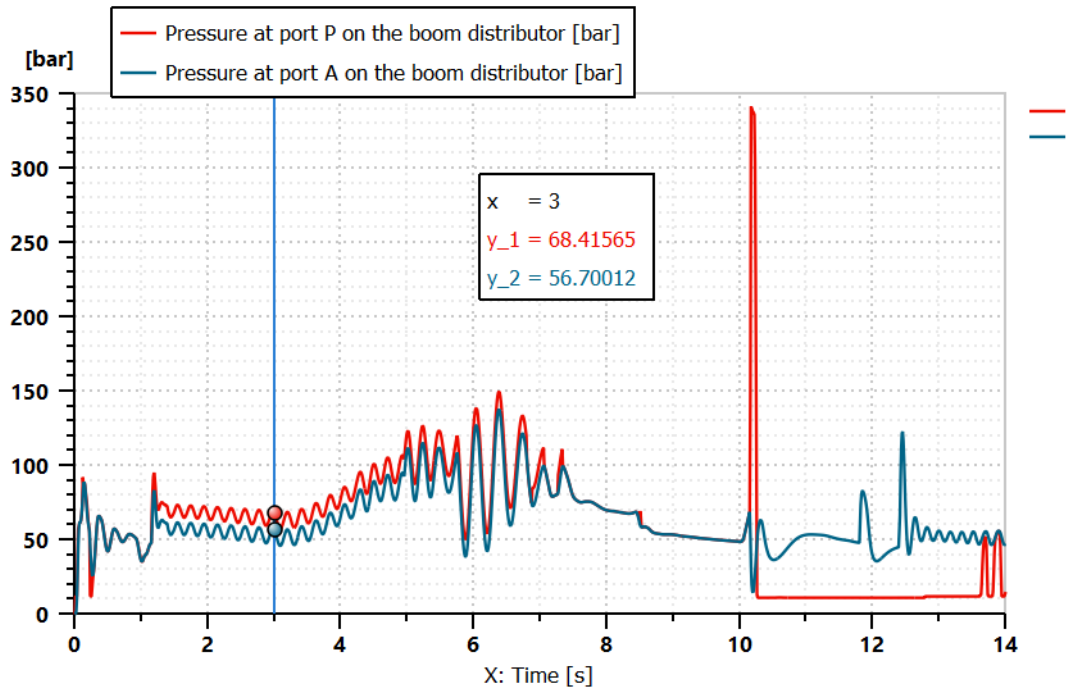


Figure 4.16: Pressure at port P compared with the pressure at port A on the boom distributor

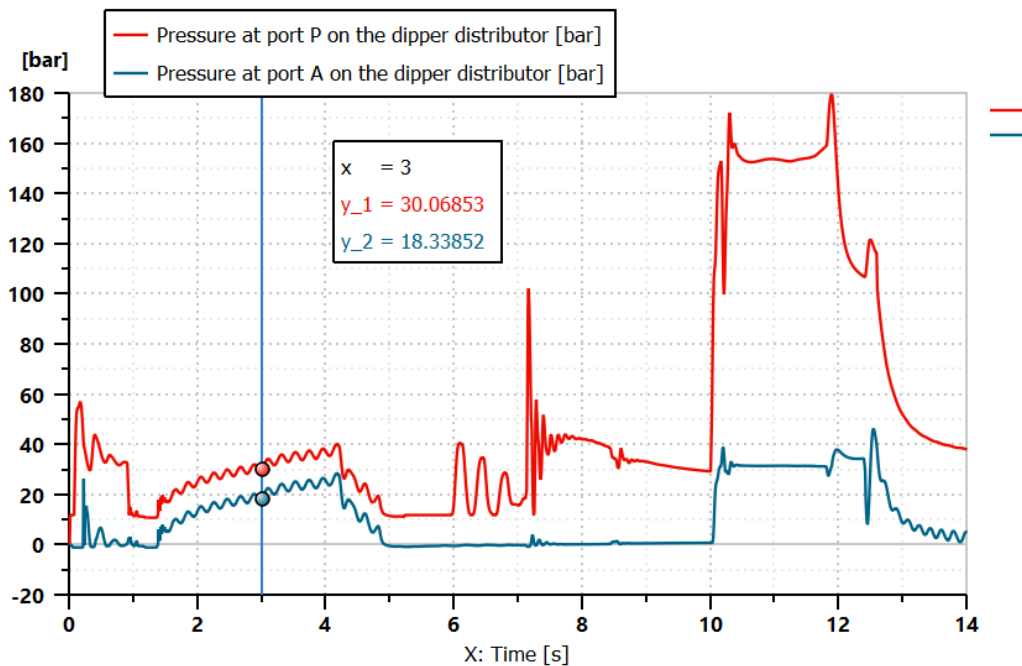


Figure 4.17: Pressure at port P compared with the pressure at port A on the dipper distributor

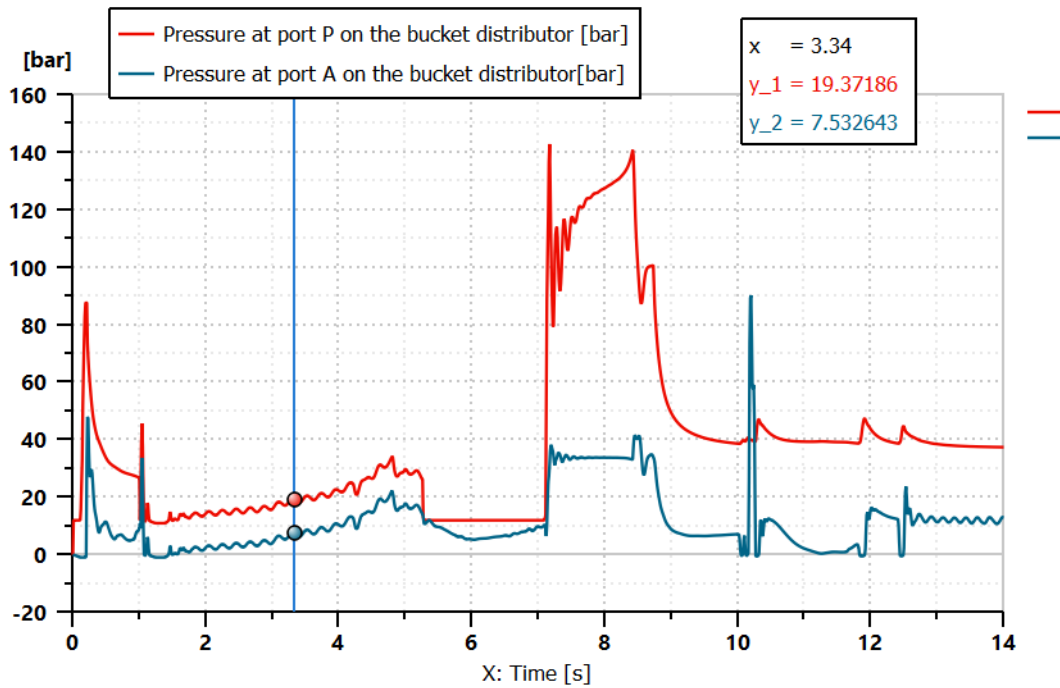


Figure 4.18: Pressure at port P compared with the pressure at port A on the bucket distributor

4.1.2) 3D system with post-compensated hydraulic circuit and rigid bodies

On the post-compensated hydraulic circuit has been imposed the same parameters and inputs of the previous case for all the components that represents this hydraulic circuit, except for the local compensator that now it has a pressure setting s_c equal to 2 bar, lower than the pre-compensated case, because it is a valve normally close so it must always regulate and also because its pressure setting affect the maximum flow rate discharged by the valves as already explained in the chapter 1.

After running the simulation, the results have been obtained. On the figure 4.19,4.20 and 4.21, are illustrated as the actuator's displacements recreate the real actuators displacements with this model.

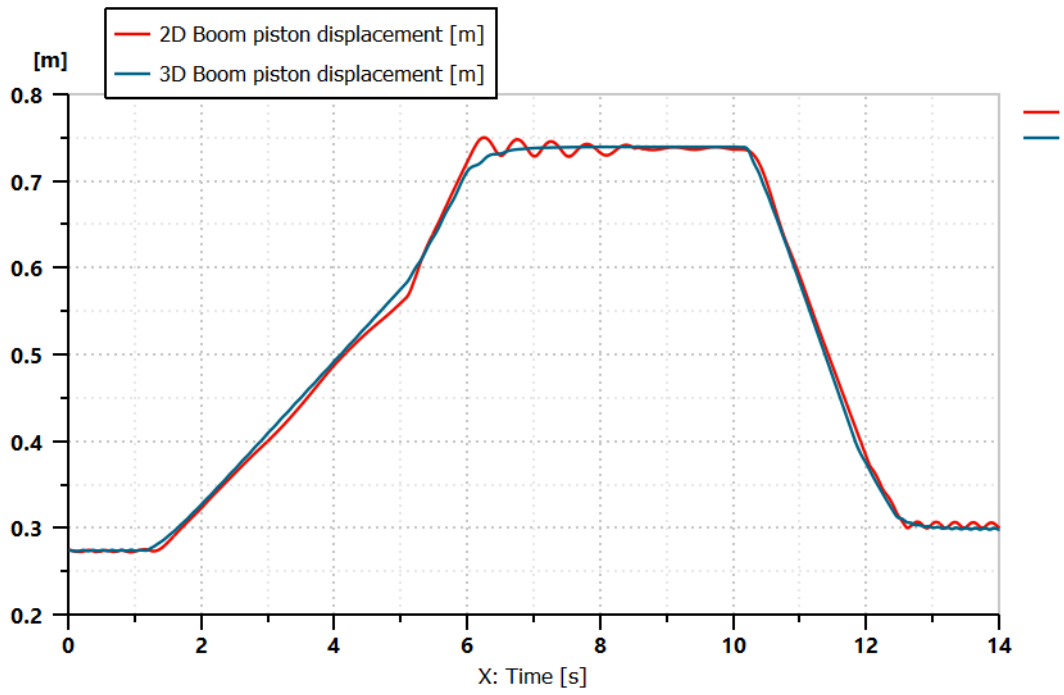


Figure 4.19: 2D and 3D Boom piston displacements

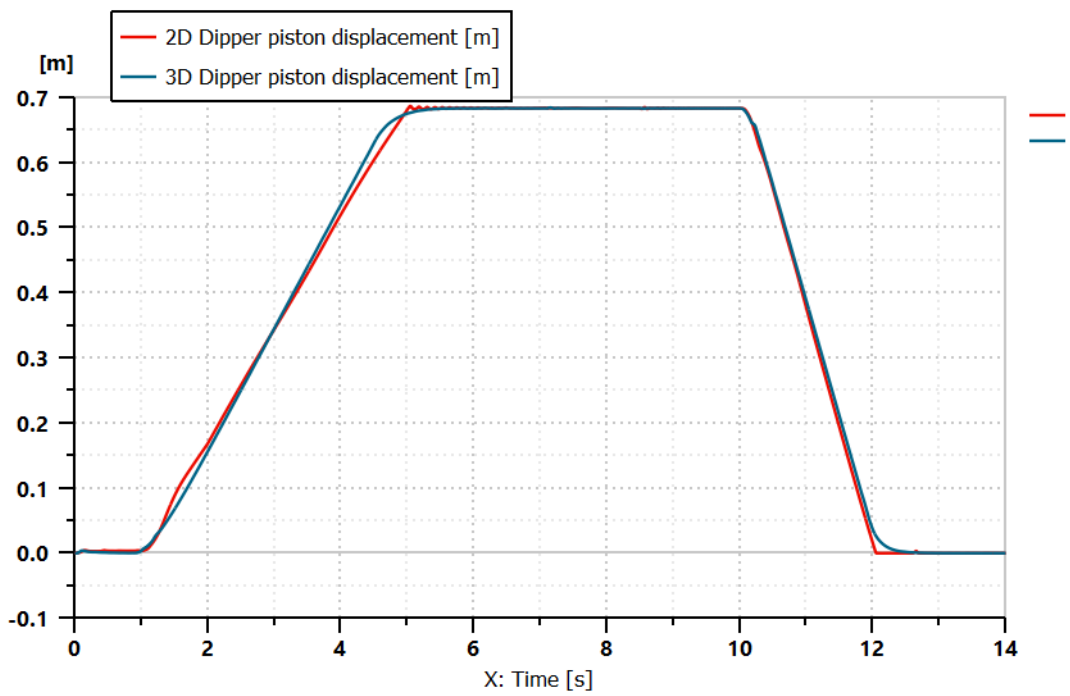


Figure 4.20: 2D and 3D Dipper piston displacements

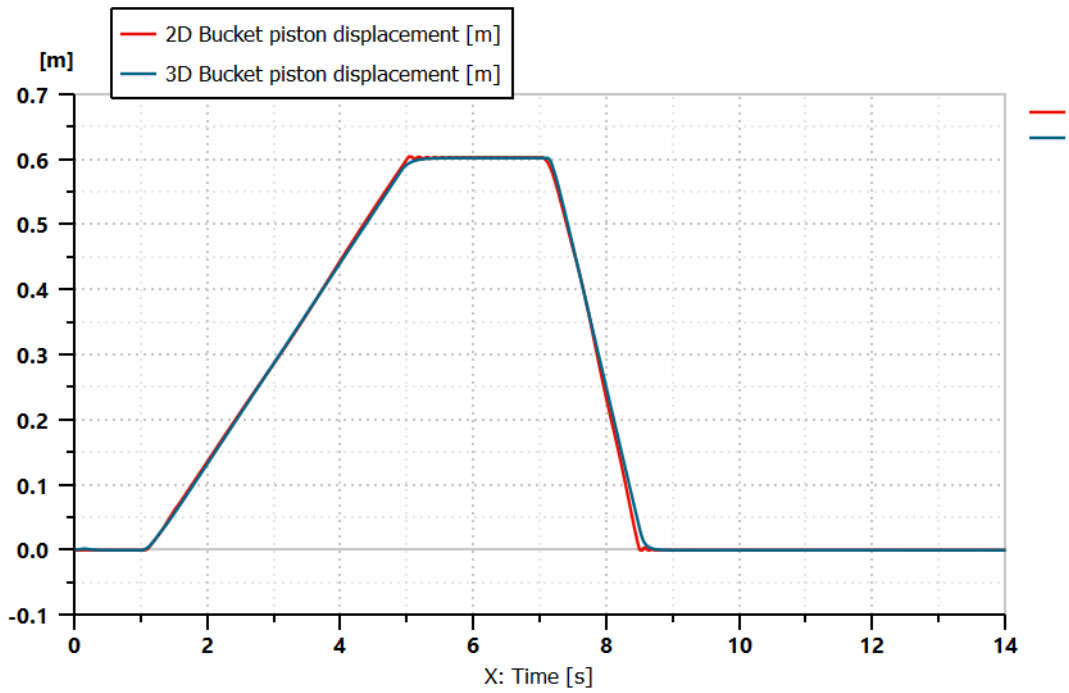


Figure 4.21: 2D and 3D Bucket piston displacements

Looking to the turret rotation in figure 4.22 it is evident that the turret performs the same rotation as the previous case, this because the hydraulic circuit that has the aim to rotate the turret is independent with respect to the configuration of the hydraulic circuit that powers the actuators.

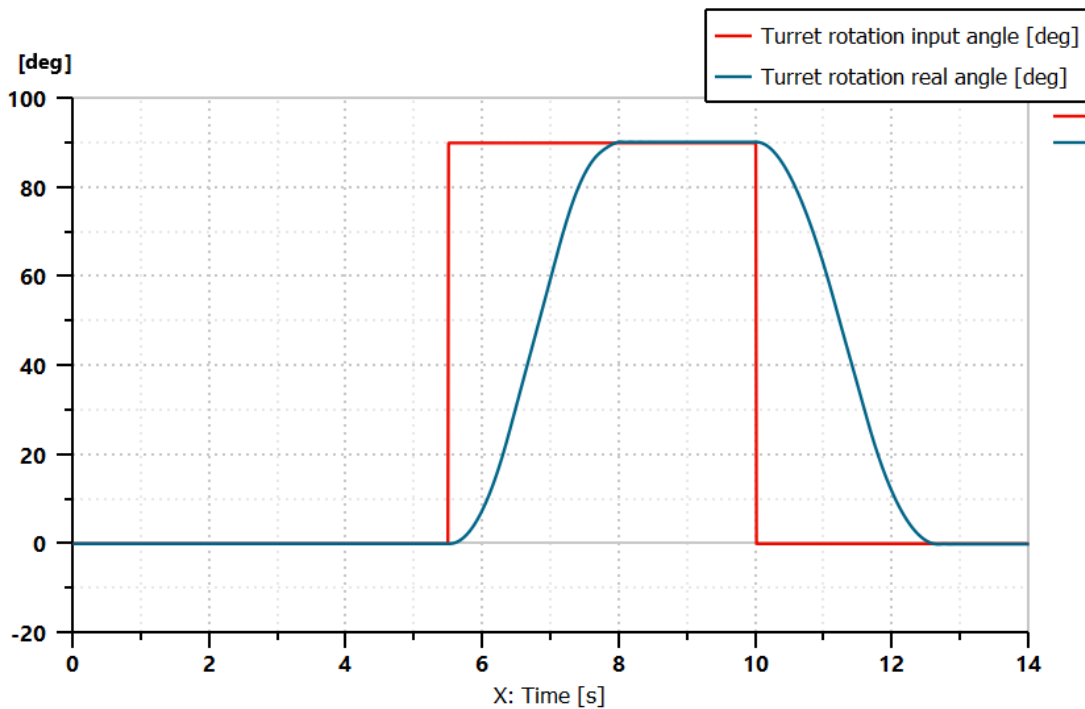


Figure 4.22: Turret rotation input and real angle

Also in the hydraulic circuit in post-compensated configuration the pump displacement modulation factor is less than 1 (figure 4.23), so the system does not work in flow saturation.

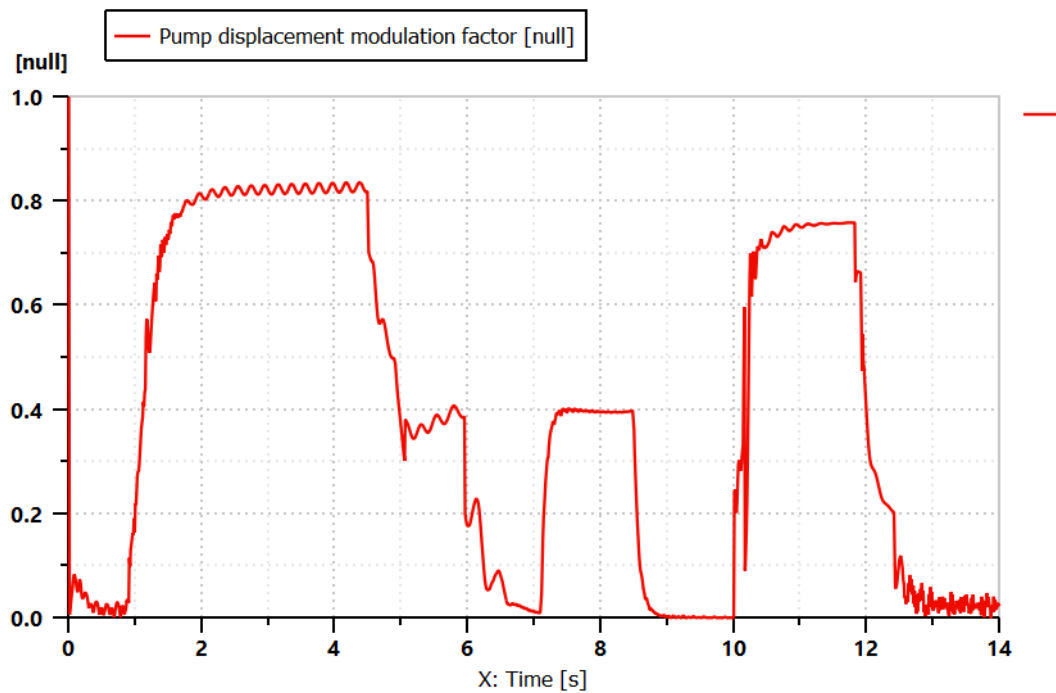


Figure 4.23: Pump displacement modulation factor

In the figure 4.24, it can be notice that the pump delivery pressure is higher than the global load sensing to about 25 bar that is the pressure setting of the differential pressure limiter, so even in this case the hydraulic power unit works properly. In this case the pressures to manage are higher than the previous case, because to power the actuators the oil must go through the distributors twice, therefore there are more pressure losses to overcome due to the non ideality of the valve.

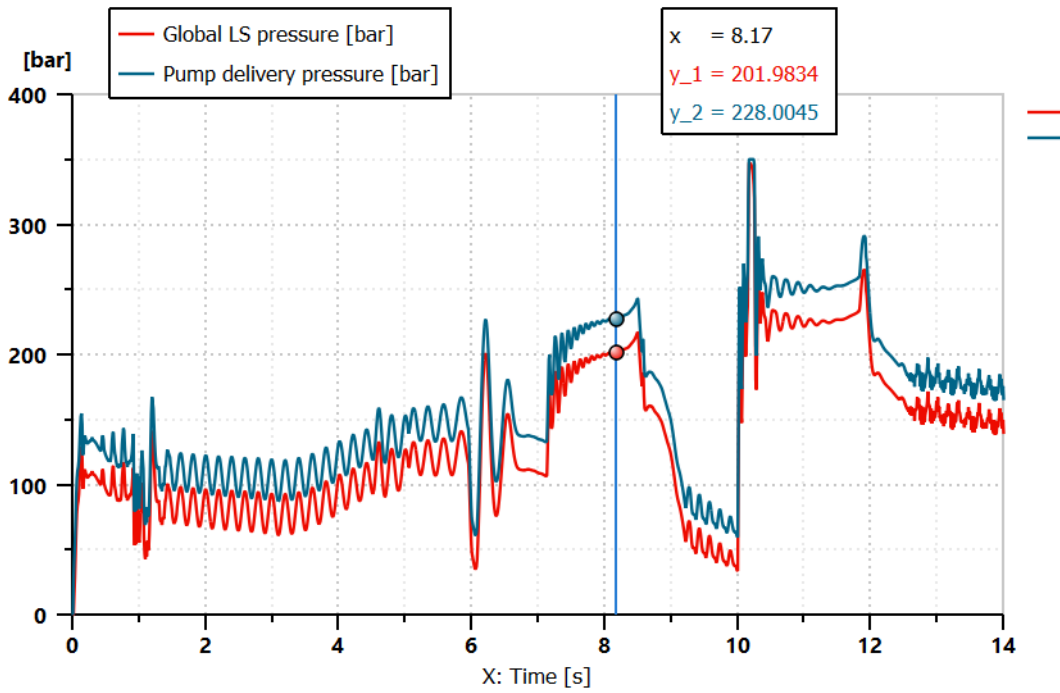


Figure 4.24: Global LS pressure compared with the pump delivery pressure

Instead, the figures 4.25, 4.26 and 4.27 shows the pressure drop across the distributors equal in this case to the difference between the differential pressure limiter setting s and the local compensator pressure setting s_c , that is about 23 bar. The port P represents again the valve port connected to the pump delivery line and the port A represents the valve port connected to the local compensator.

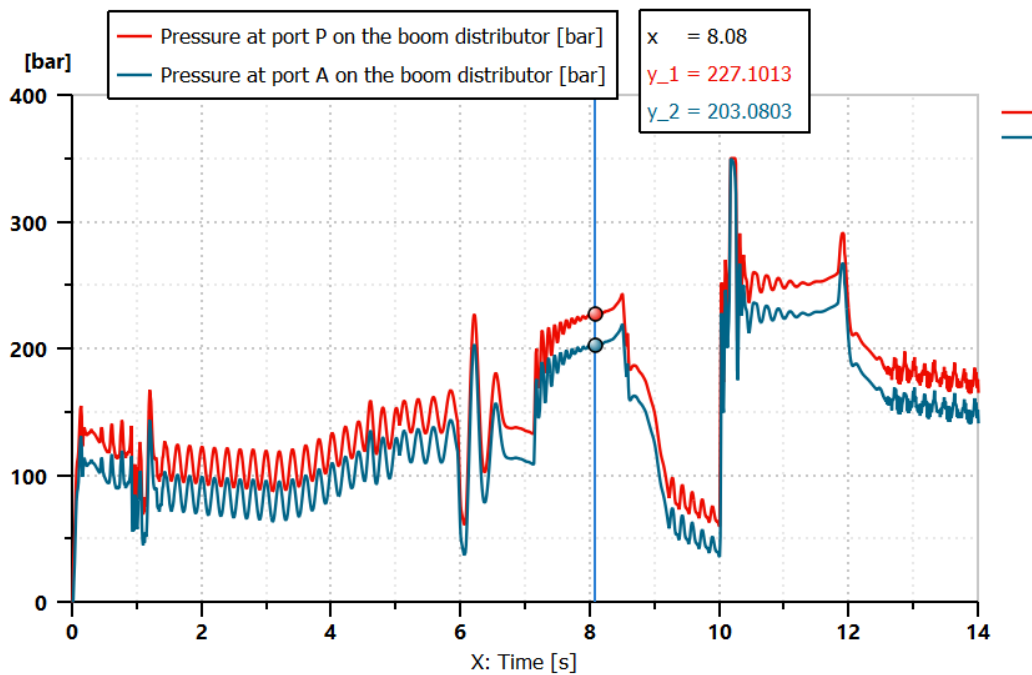


Figure 4.25: Pressure at port P compared with the pressure at port A on the boom distributor

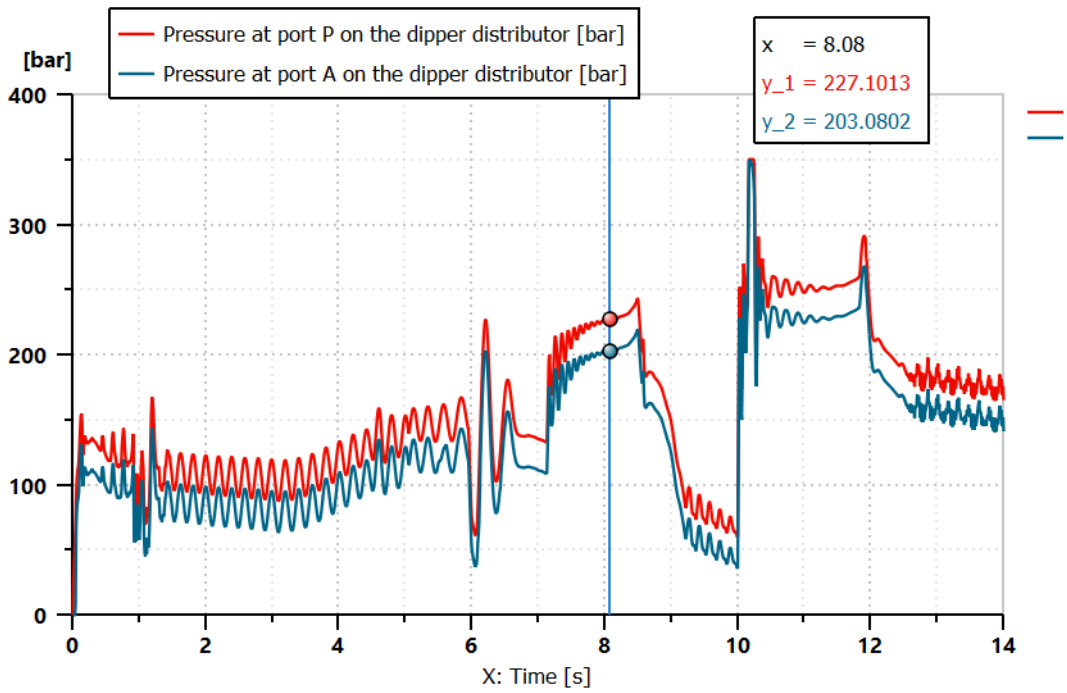


Figure 4.26: Pressure at port P compared with the pressure at port A on the dipper distributor

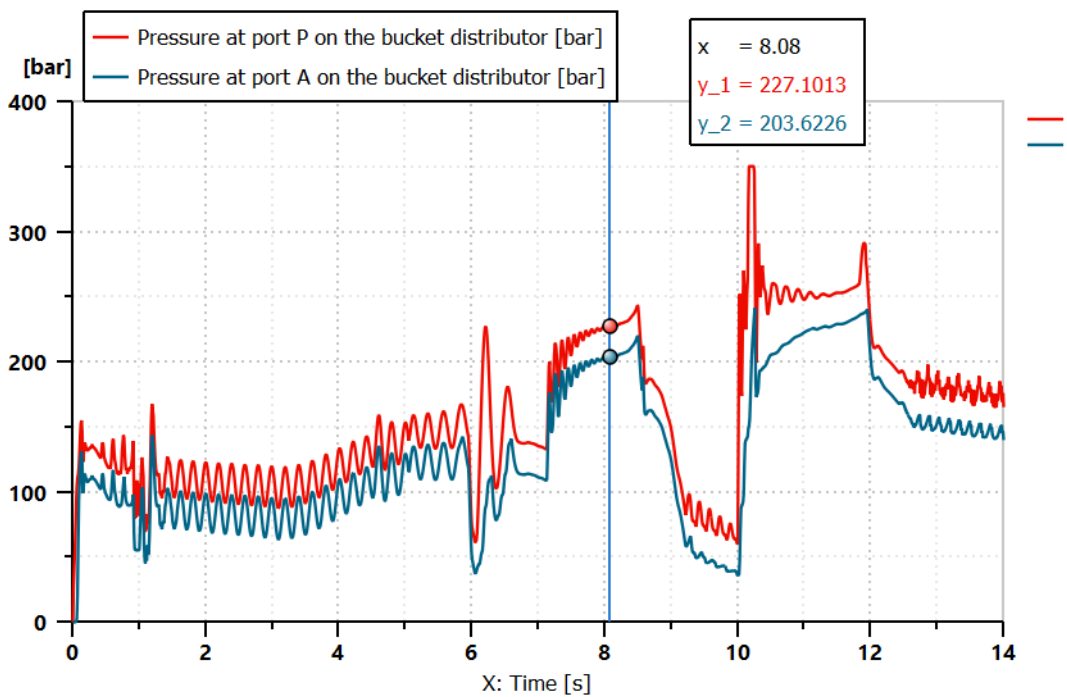


Figure 4.27: Pressure at port P compared with the pressure at port A on the boom distributor

4.1.3) 3D systems with recursive joints

The advantage to use the recursive joints is that it is possible to extract information, regarding the inertia changes during the excavator activity, with respect to the rigid bodies of the 3D mechanical library, that does not have this feature, as discussed in the previous chapter. For example, the figures 4.28, 4.29, 4.30 represents as the mass changes in time along x, along y, and along z direction respectively, on the recursive joint that models the boom at the port 3, that is the reference port of this joint.

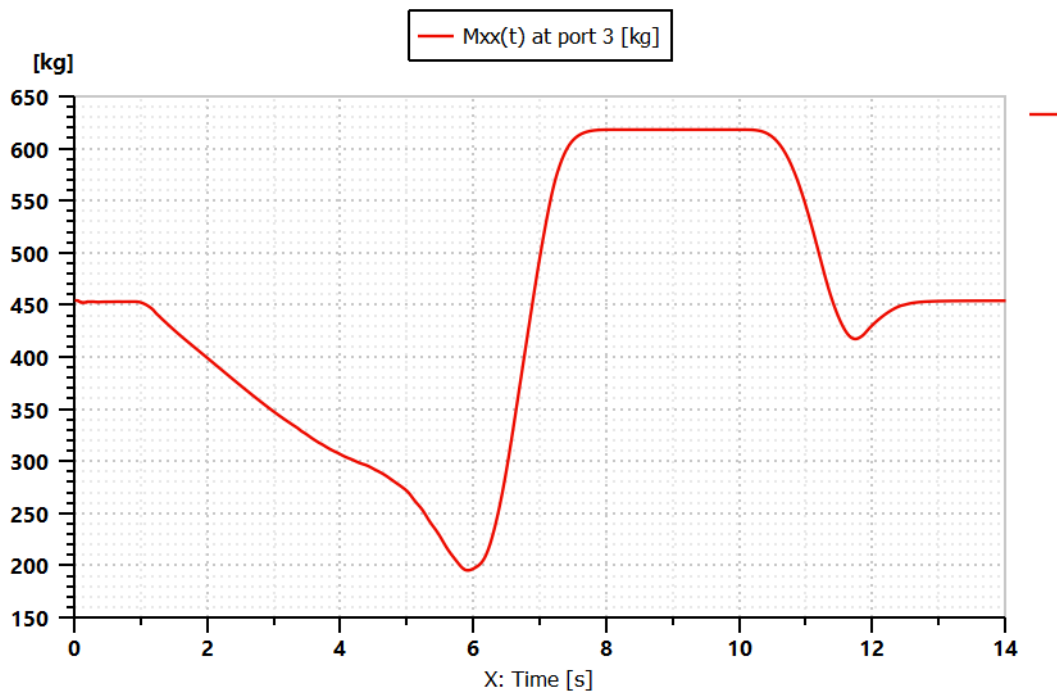


Figure 4.26: Change of the mass along x at the boom reference port

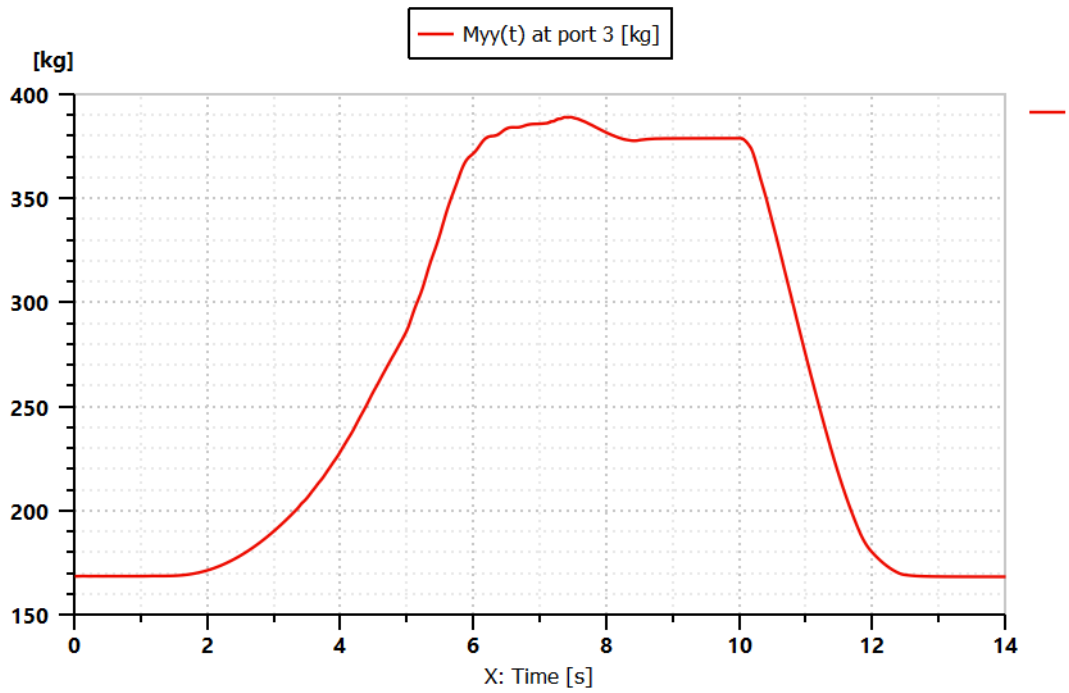


Figure 4.27: Change of the mass along y at the boom reference port

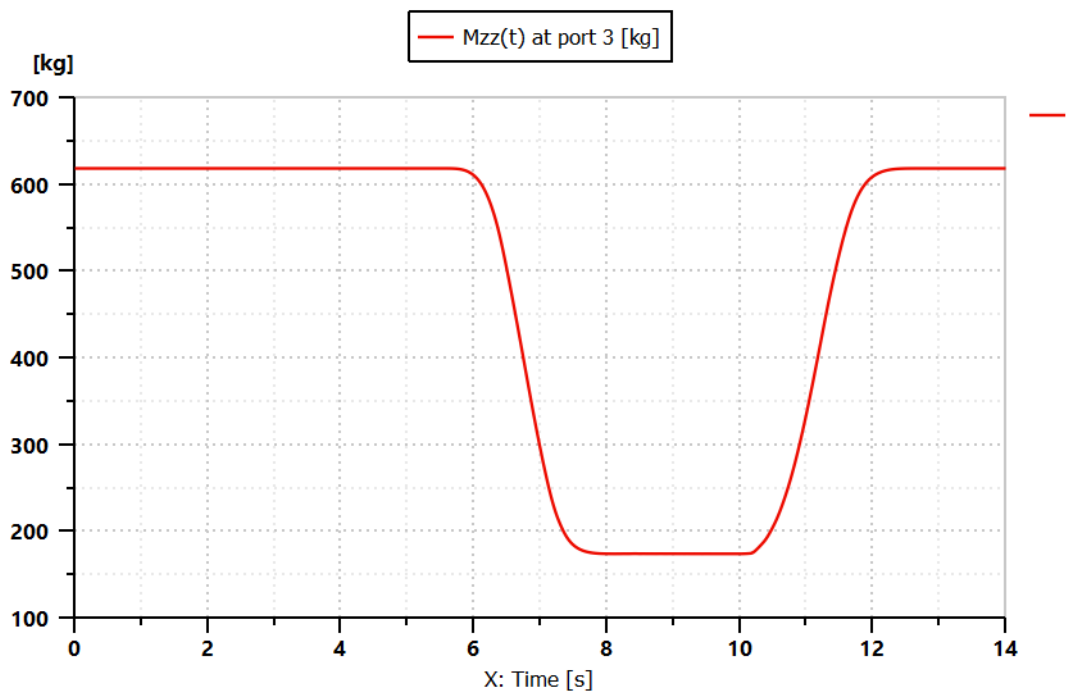


Figure 4.28: Change of the mass along z at the boom reference port

As well as figures 4.29, 4.30, 4.31 shows how the moment of inertia changes in time along the x , y , z direction respectively.

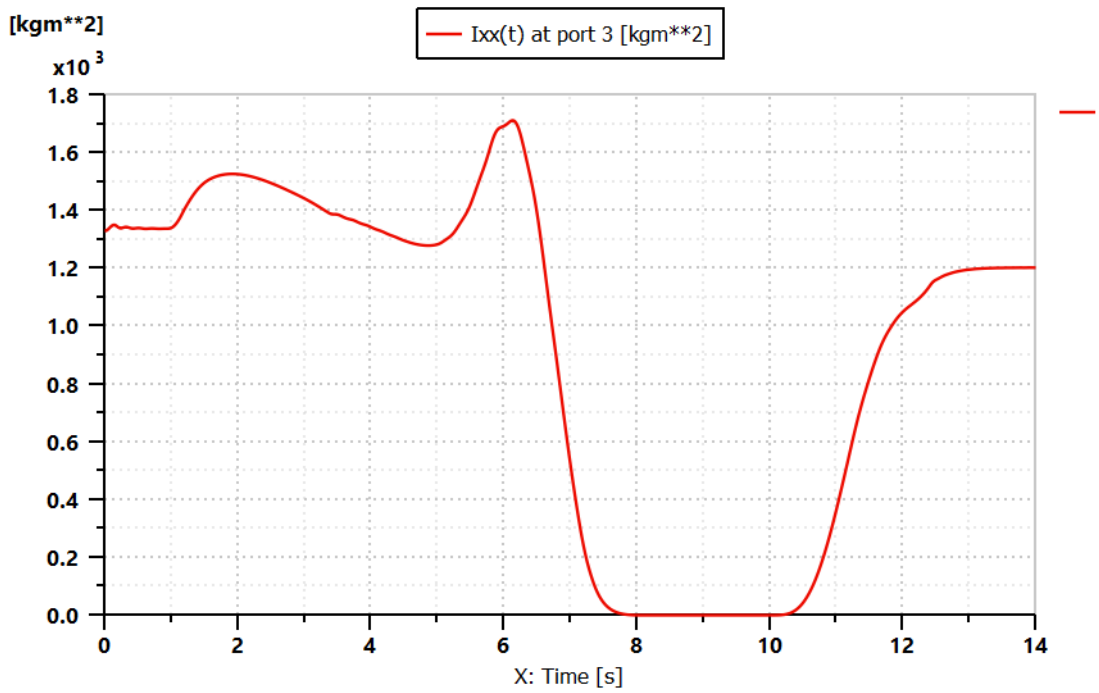


Figure 4.29: Change of the mass moment of inertia along x at the boom reference port

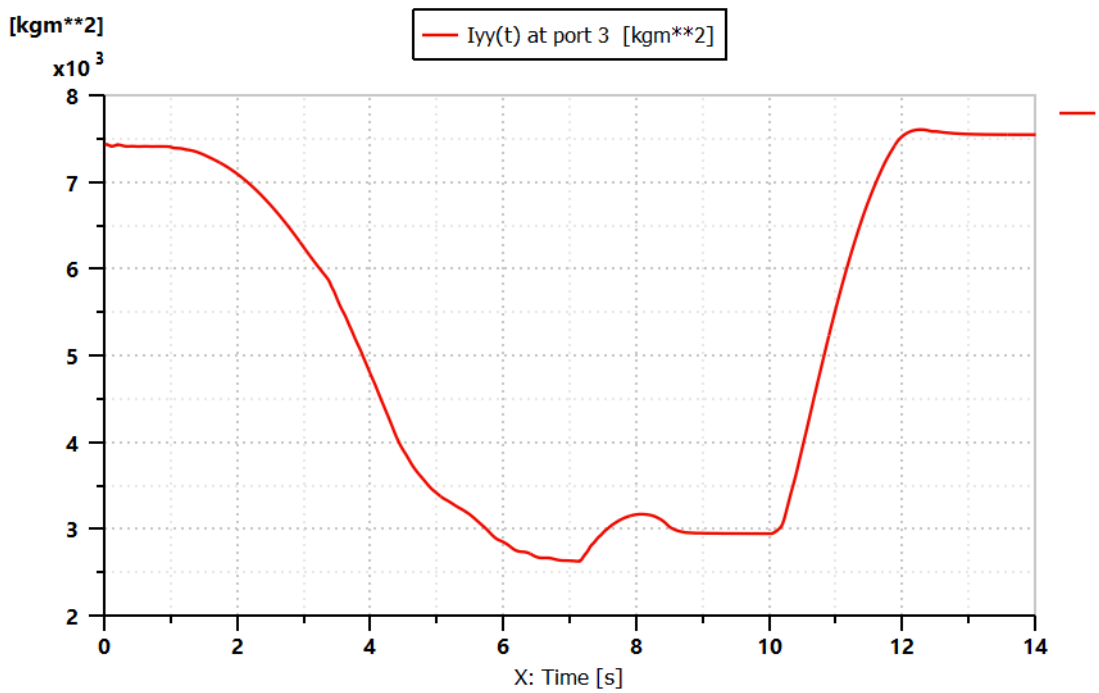


Figure 4.30: Change of the mass moment of inertia along y at the boom reference port

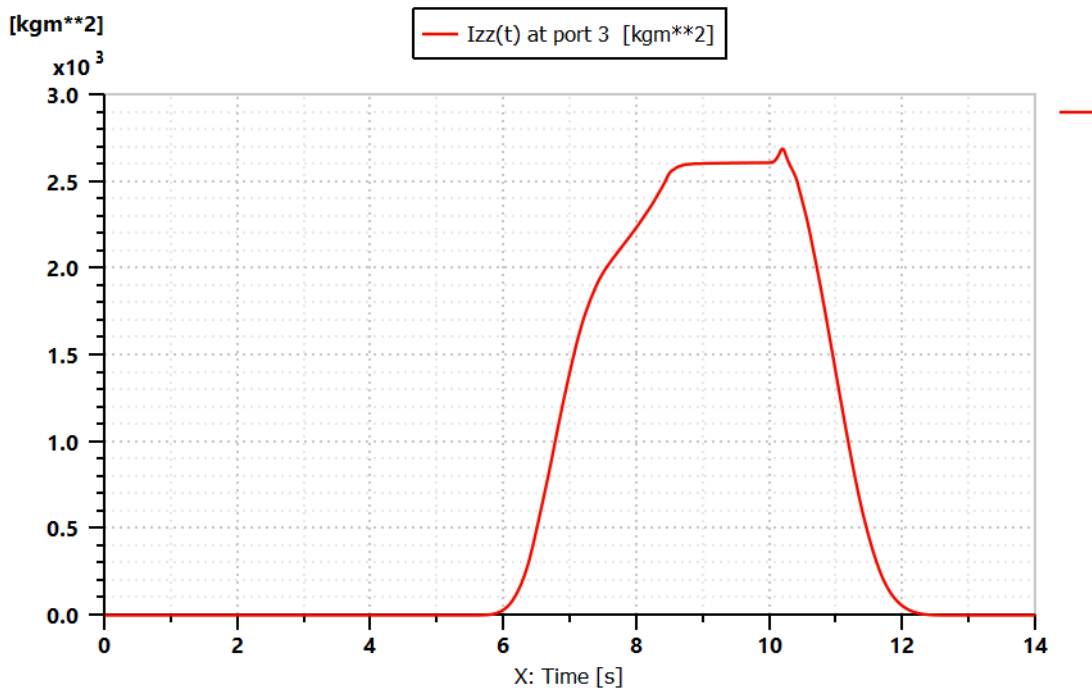


Figure 4.31: Change of the mass moment of inertia along z at the boom reference port

These evolutions in time of the mass changing coming from each element that composed the arm, that transfers all or part of its inertia form one element to the next one through its recursive joint. As effect of this, can be notice some differences on the forces exerts by the actuators between rigid bodies and recursive joints model (figure 4.32,4.33,4.34) in terms of evolution in time and module.

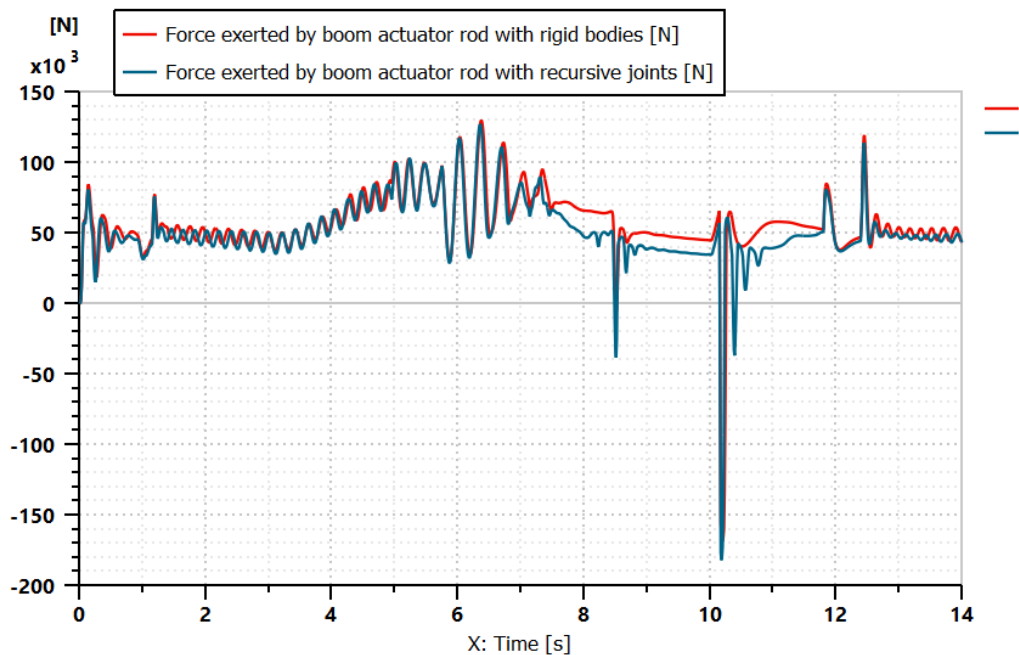


Figure 4.32: Comparison of the boom actuator forces with rigid bodies and recursive joints

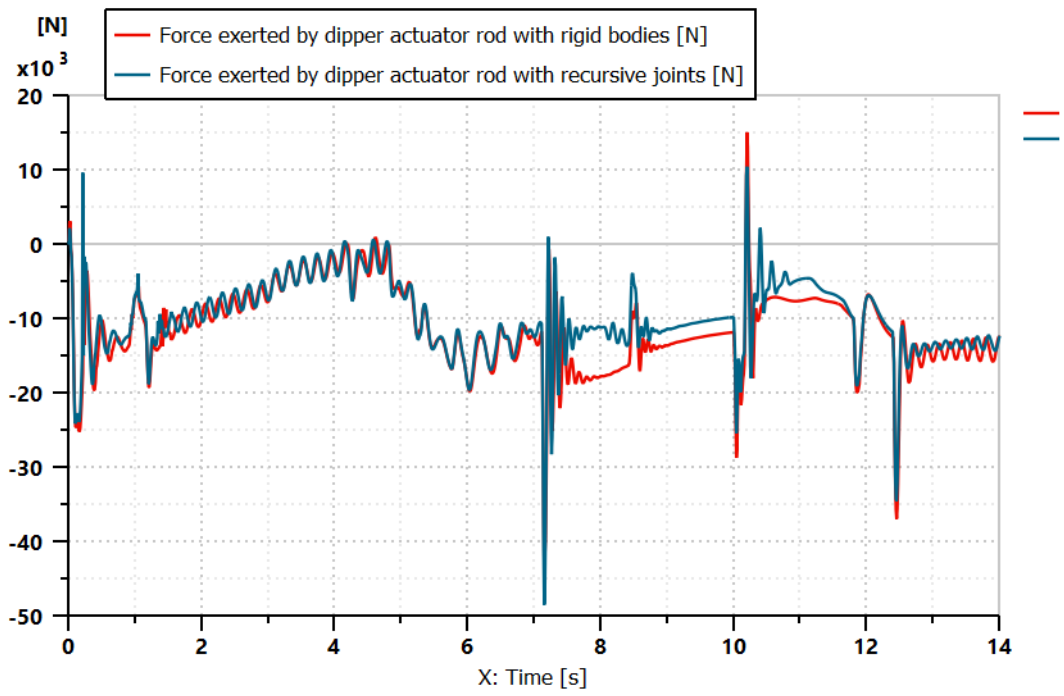


Figure 4.33: Comparison of the dipper actuator forces with rigid bodies and recursive joints

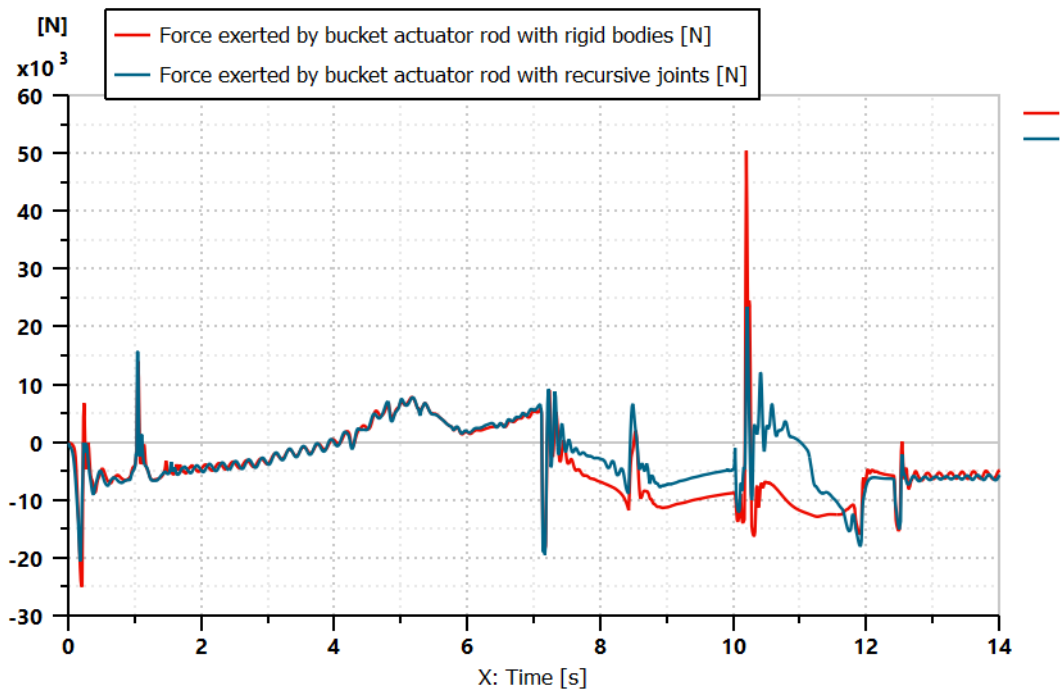


Figure 4.34: Comparison of the boom actuator forces with rigid bodies and recursive joints

To reach the pressure saturation condition of this hydraulic circuit, it has been increased on the actuator hydraulic part of the boom the viscous friction coefficient (figure 4.36) by two orders of magnitude from $2.8 \cdot 10^4$ N/(m/s) to $2.8 \cdot 10^6$ N/(m/s), in order to have a resistive load that simulates a difficult digging activity.

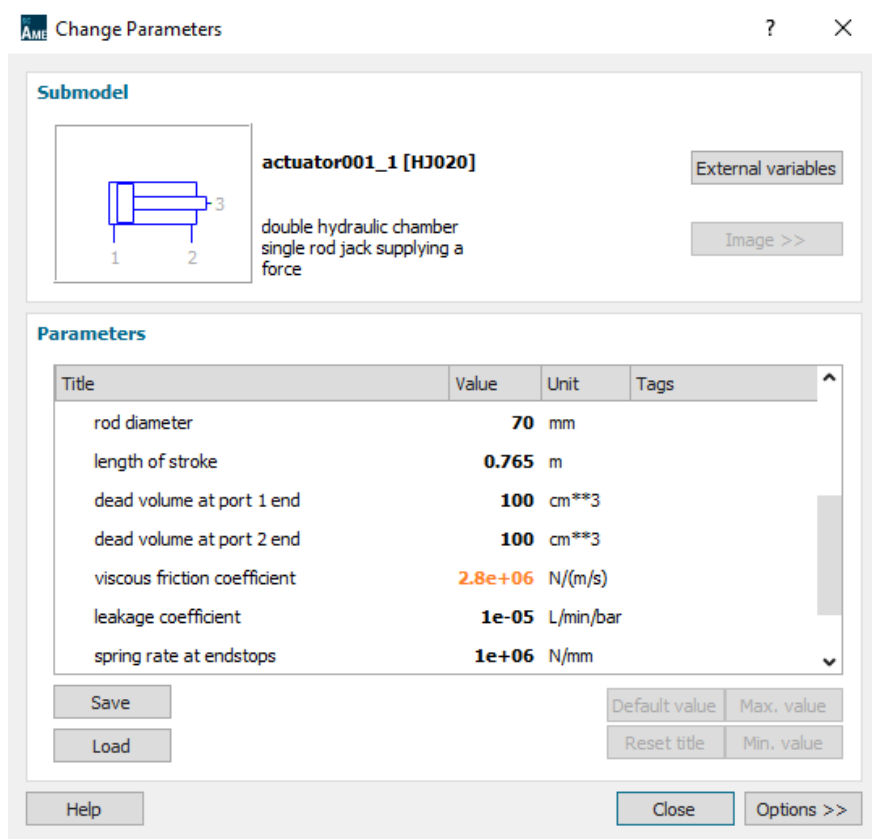


Figure 4.36: Increasing of the viscous friction coefficient on the boom actuator parameters

To verify that the boom actuator reaches a pressure higher than $p^* - s$, it has been plotted the load sensing pressure signals related to the boom, dipper, and bucket of each distributor respectively (figure 4.37).

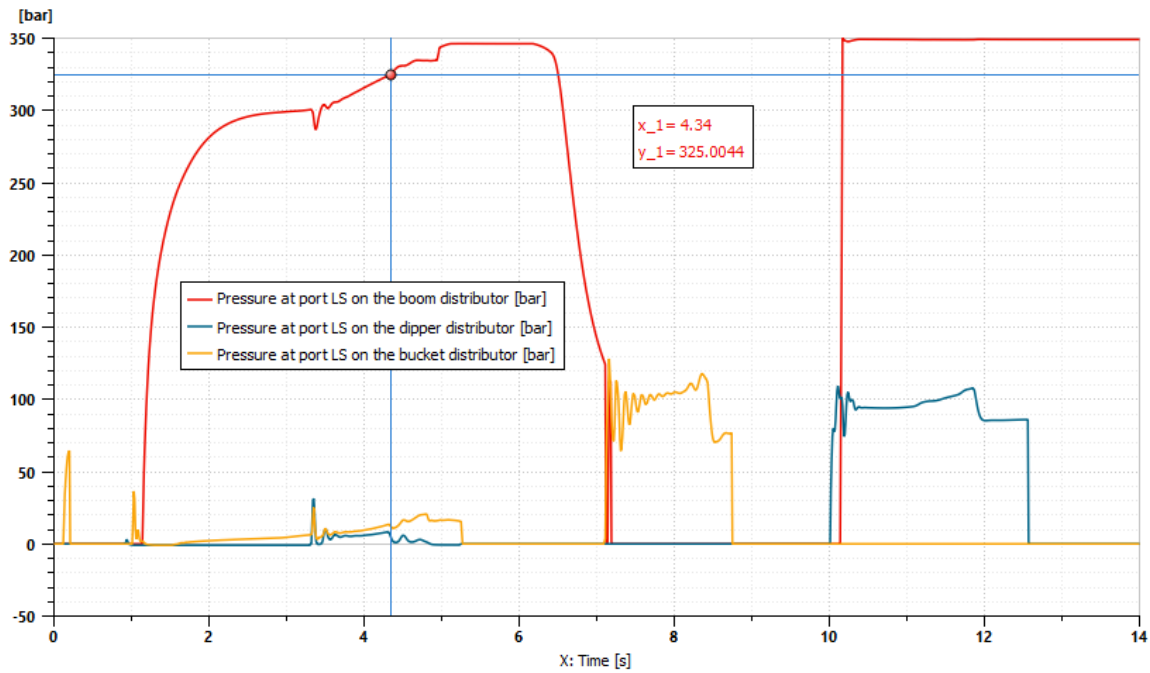


Figure 4.37: Load sensing pressure signals in pressure saturations

It is evident from the figure 4.37, that the boom actuator achieves this critical condition under study in between 4.35 s and 6.5 s and from 10 s to 14 s, because it has been imposed $p^* = 350$ bar on the absolute pressure limiter, and $s = 25$ bar to the differential one. Therefore, the pressure to overcome to have a pressure saturation condition is $p^* - s = 325$ bar.

Looking at the figure 4.38, on the time intervals when the pressure saturation occurs, there is the lost of controllability, because the pressure drop across the distributor decreases, so the flowrate decreases, and the actuator is not able to follow the command imposed.

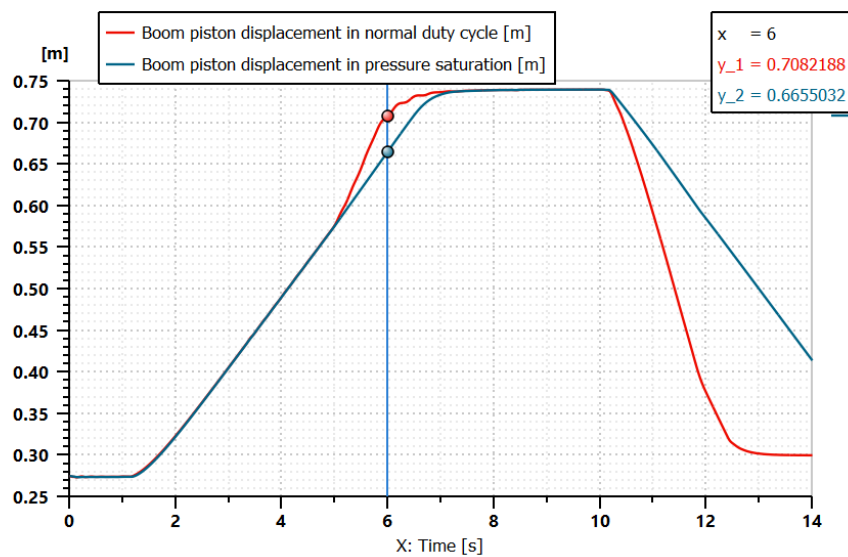


Figure 4.38: Boom behaviour in pressure saturation

Regarding the dipper and the bucket (figure 4.39 and 4.40), it is not present any perturbation of the actuator behaviour due to the pressure saturation, because the pressure information coming from the load is lower than p^* .

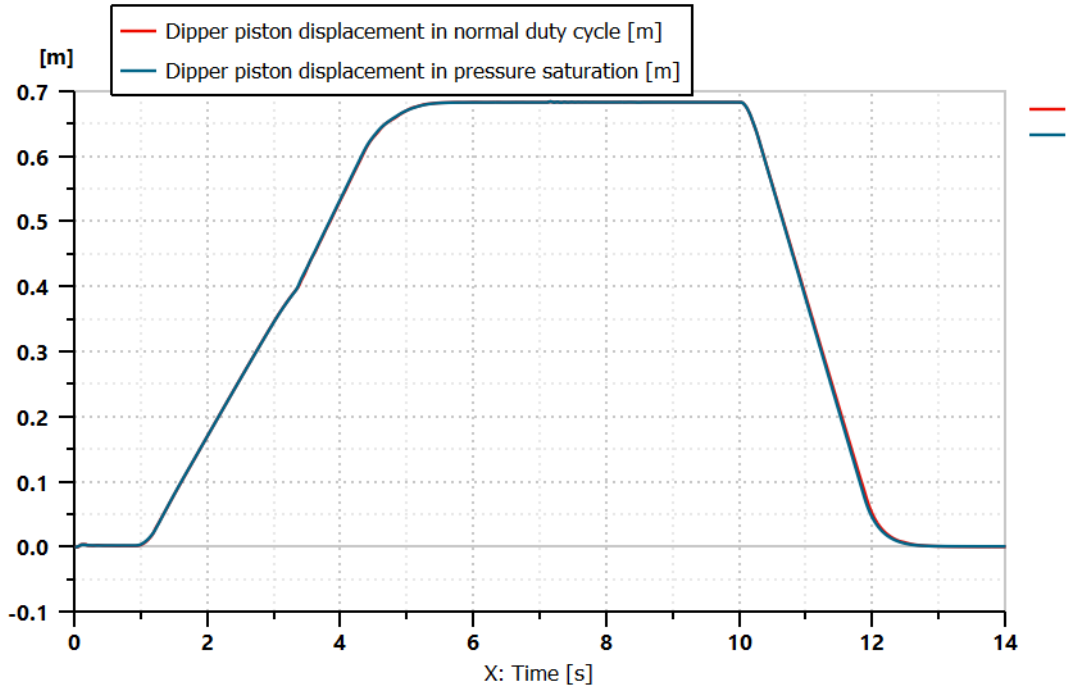


Figure 4.39: Dipper behaviour in pressure saturation

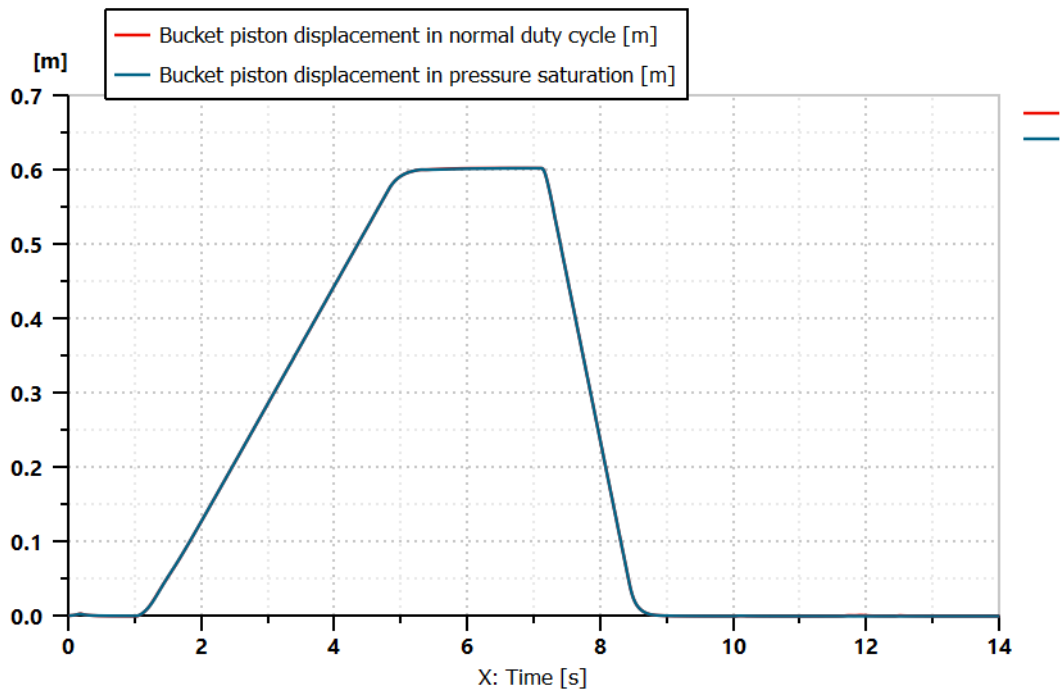


Figure 4.40: Bucket behaviour in pressure saturation

4.2.2) Flow saturation in pre-compensated hydraulic circuit

The flow saturation condition has been achieved, reducing the pump maximum displacement from 120 cc/rev to 90 cc/rev, to simulate a condition where the sum of the user flow rates is higher than the maximum flow rate generated by the pump. In fact, in this case, the pump works with its maximum displacement, as shown in figure 4.41, because the pump displacement modulation factor, is equal to 1 in the time frame between 1.9 s and 4.8 s.

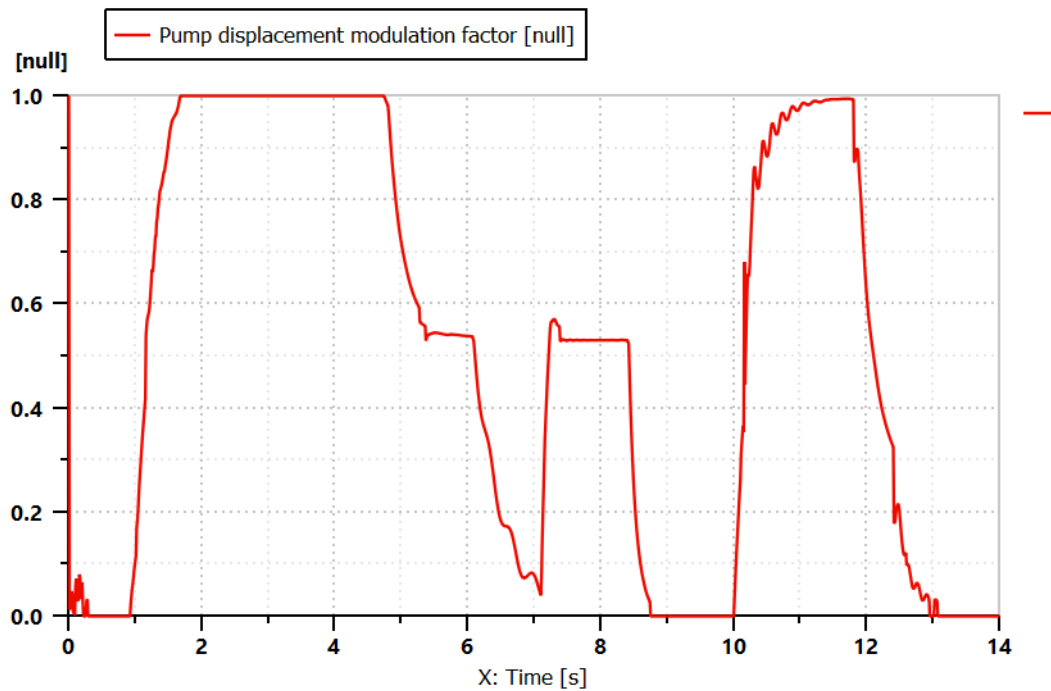


Figure 4.41: Pump displacement modulation factor

In flow saturation with pre-compensated hydraulic circuit, the problem that the user with the highest load gets the remaining flow rate arises, because the pump is not able to satisfy the sum of the flow rates that the users need. Therefore, the most loaded user has a lower pressure drop across its distributor, that depends also by the other commands, with a loss of its controllability as already explained in chapter 2, when the local compensators are introduced. In figure 4.42 are represented, again, the load sensing pressure signals coming from the distributors, to understand which actuator is the most loaded when happen this condition.

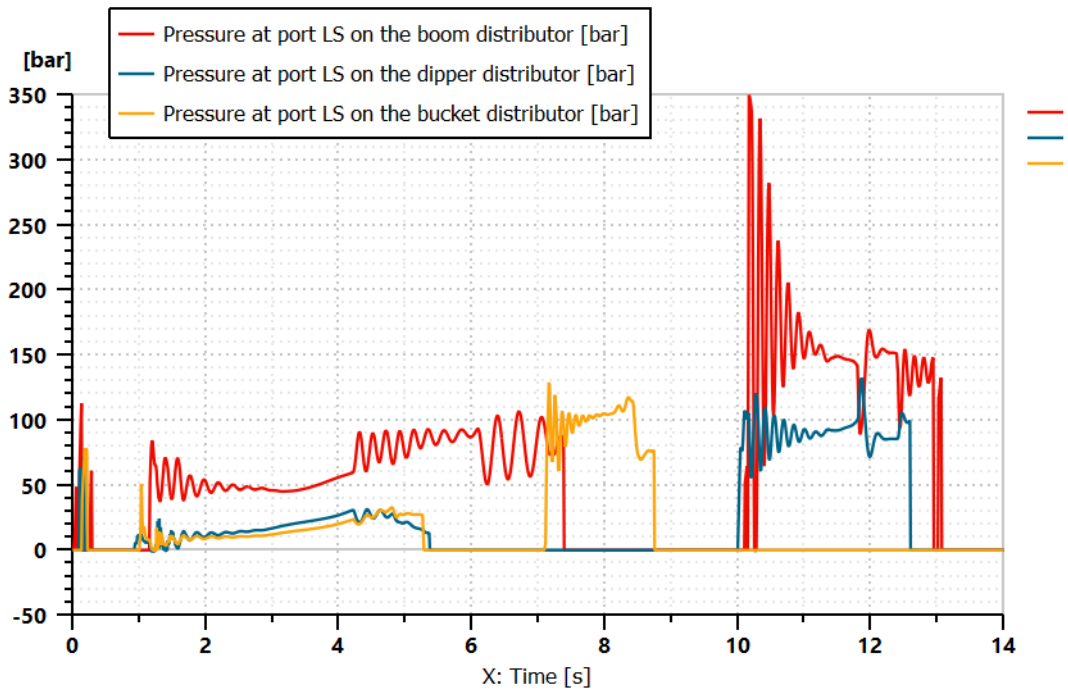


Figure 4.42: Load sensing pressure signals in flow saturation

It can be noticed that the boom is the most loaded on the time frame where the flow saturation occurs, indeed looking the figure 4.43, the control of its actuator is lost.

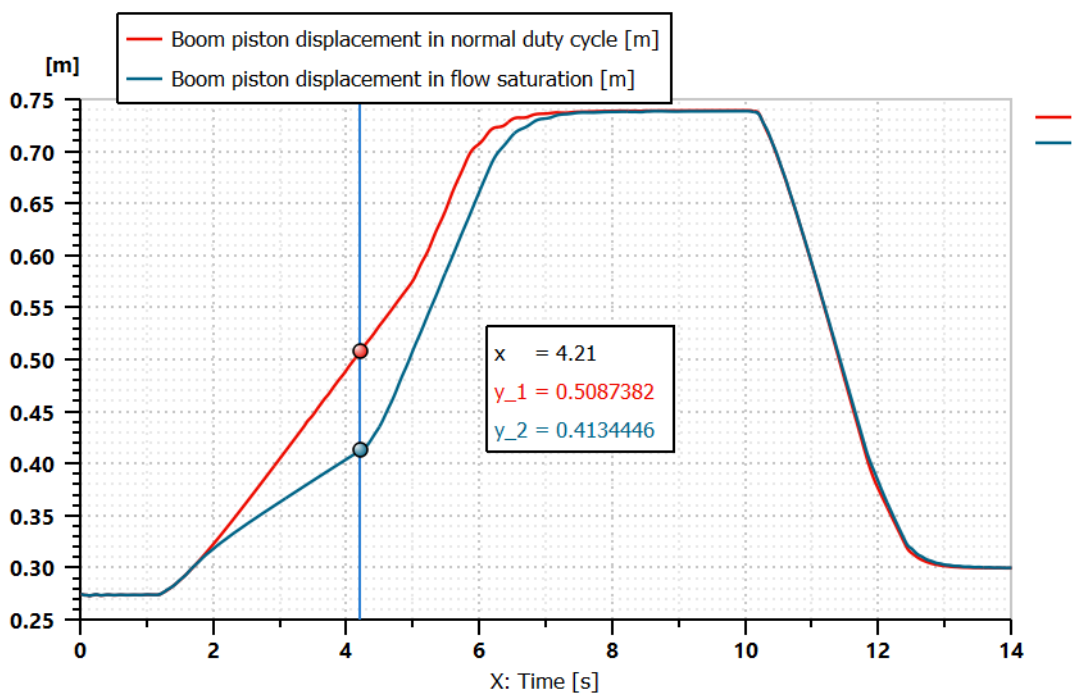


Figure 4.43: Boom behaviour in flow saturation

From the dipper (figure 4.44) and the bucket (Figure 4.45) point of view, the pressures inside their actuators are lower than the boom one in this time frame, so these actuators normally accomplish their task.

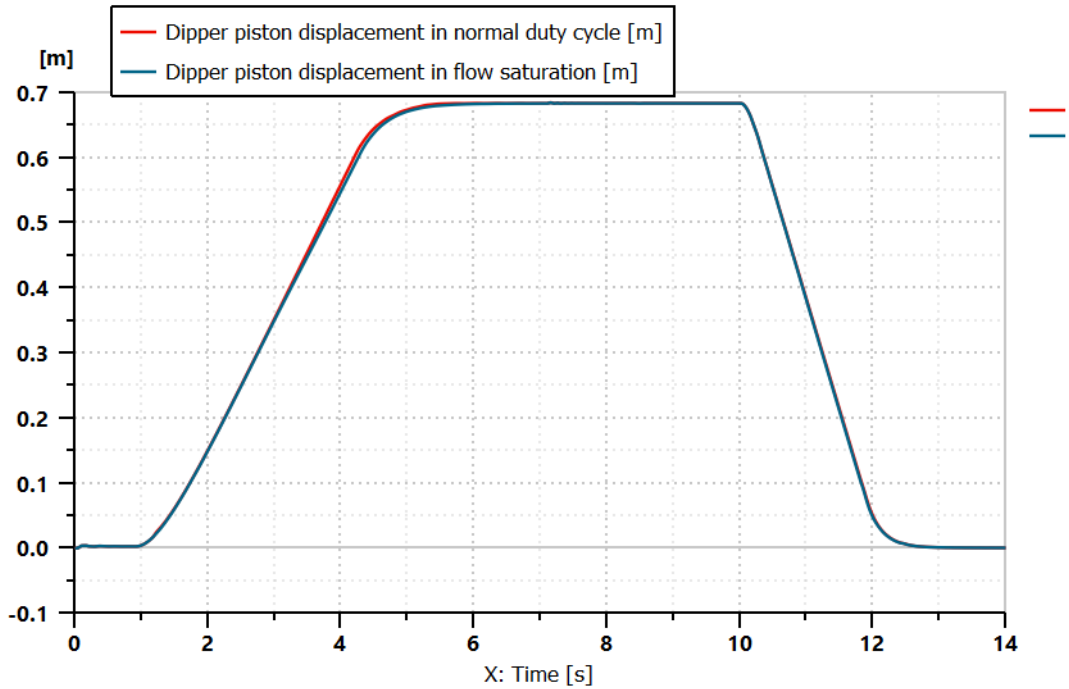


Figure 4.44: Dipper behaviour in flow saturation

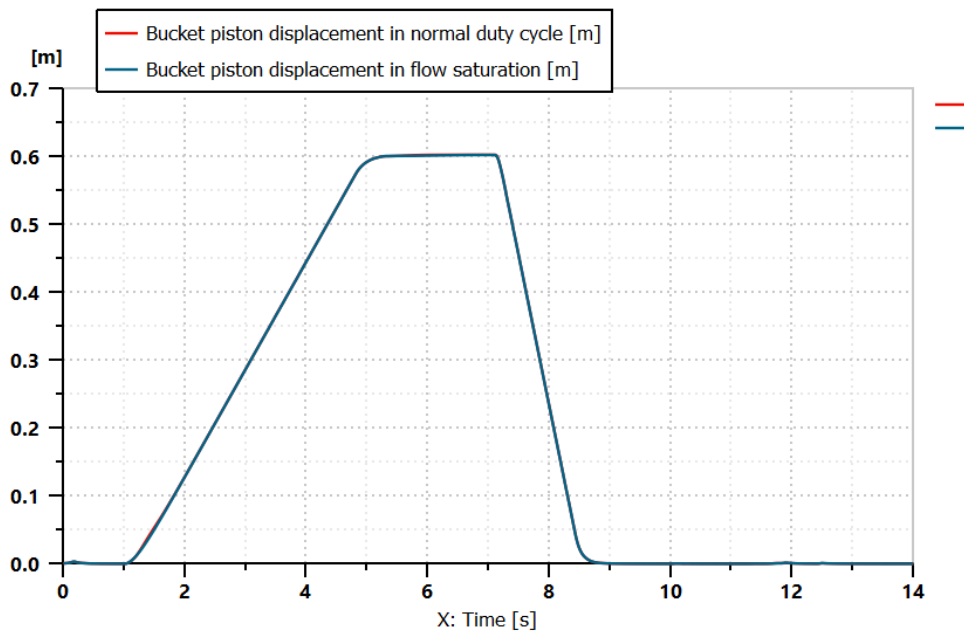


Figure 4.45: Bucket behaviour in flow saturation

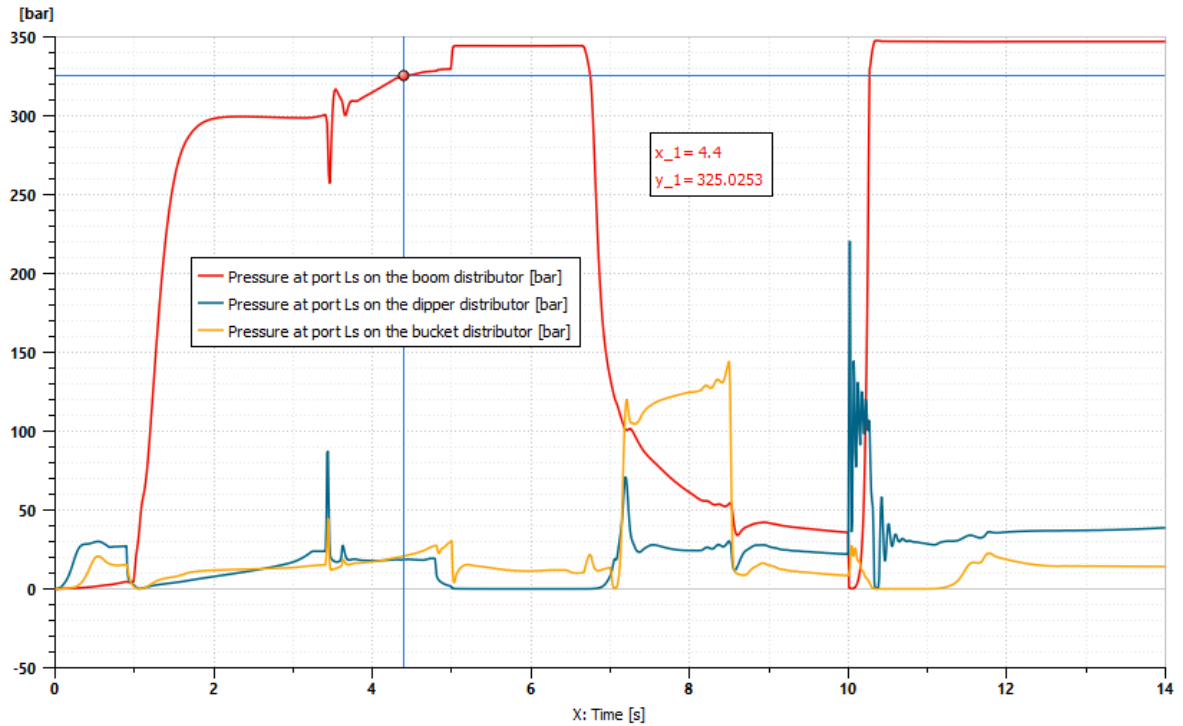


Figure 4.47: Load sensing pressure signals in pressure saturation

Looking at the figures 4.48, it can be noticed the lost of controllability for the boom in these two-time intervals.

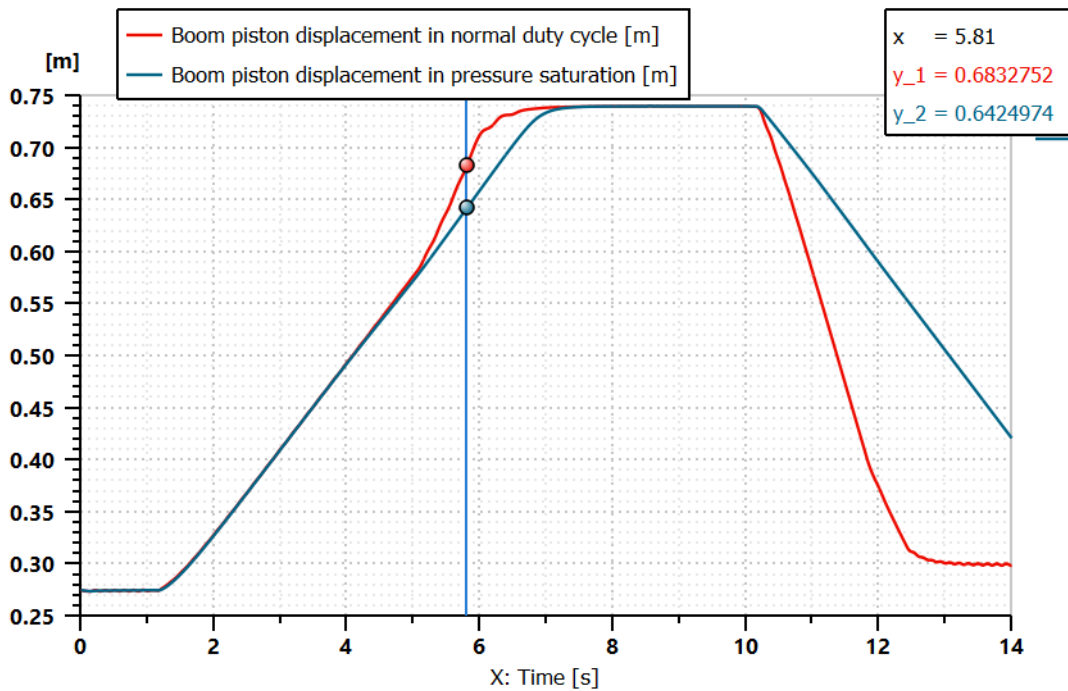


Figure 4.48: Boom behaviour in pressure saturation

Instead regarding the dipper (figure 4.49), the lost of controllability is more evident on the second time interval, because on the first one its distributor regulates a bit since the actuator is almost arrived in its final position.

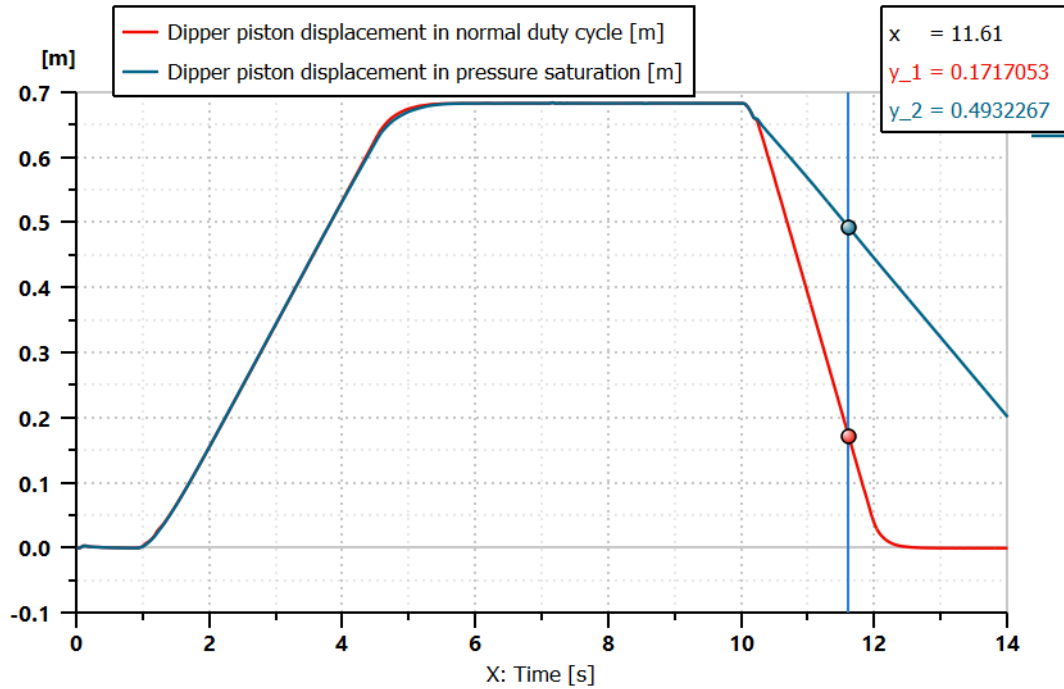


Figure 4.49: Dipper behaviour in pressure saturation

For the bucket (figure 4.50) the lost of controllability is not evident, because in this two time intervals its distributor does not regulate.

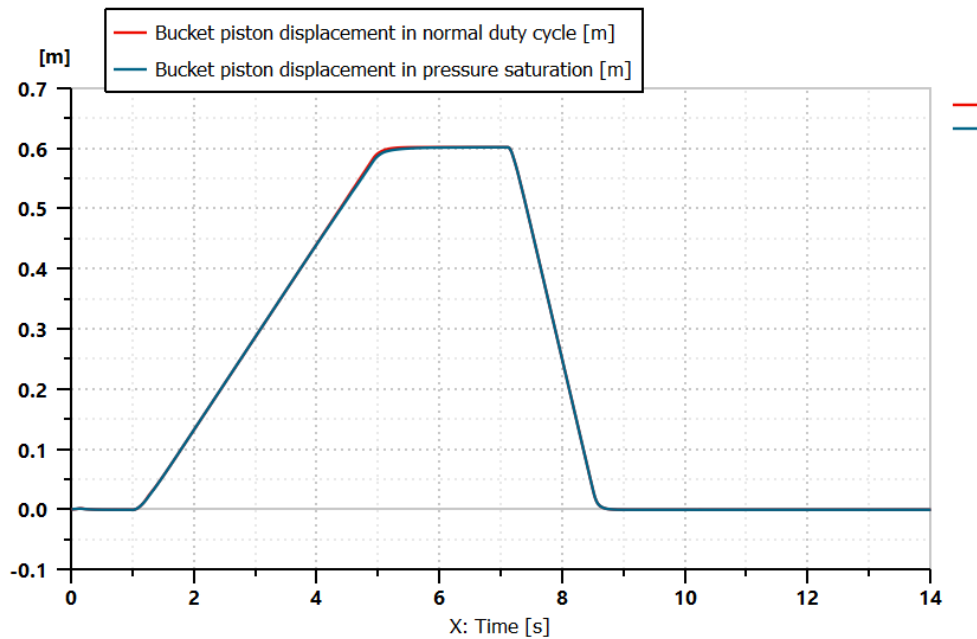


Figure 4.50: Bucket behaviour in pressure saturation

4.2.4) Flow saturation in post-compensated hydraulic circuit

Once again, it has been reduced the maximum pump displacement, but in this case from 120 cc/rev to 70 cc/rev, because in this way the system is in flow saturation with the pump displacement modulation factor equal to 1 (figure 4.51), and has all three distributors completely open, so their fractional spool positions are equal to 1 from 3.7 s to 4.8 s (figure 4.52).

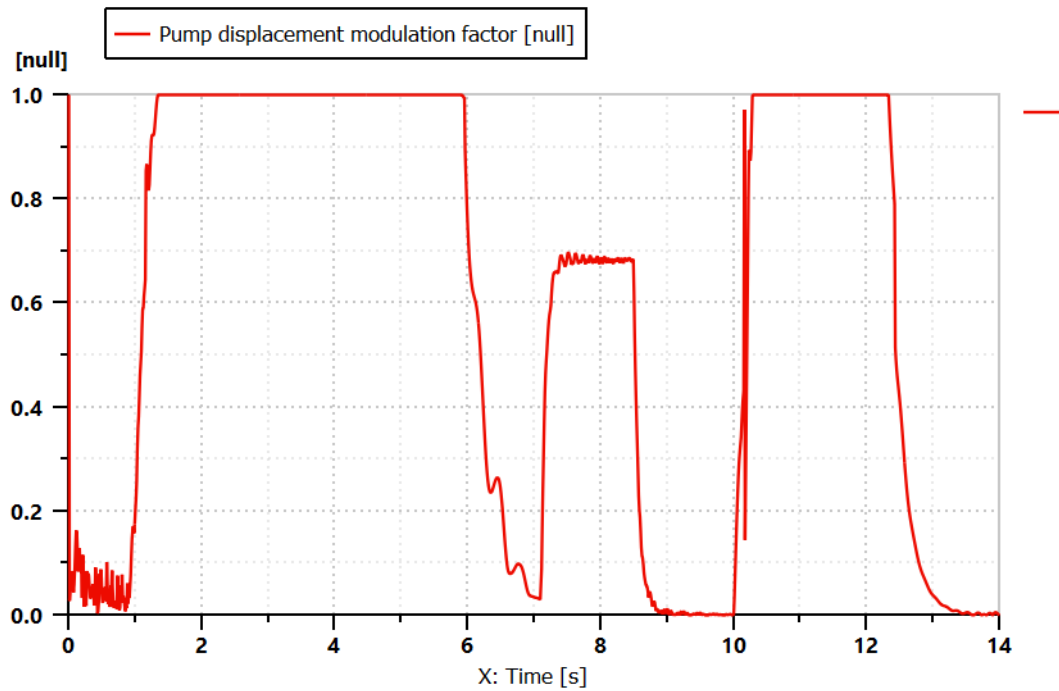


Figure 4.51: Pump displacement modulation factor

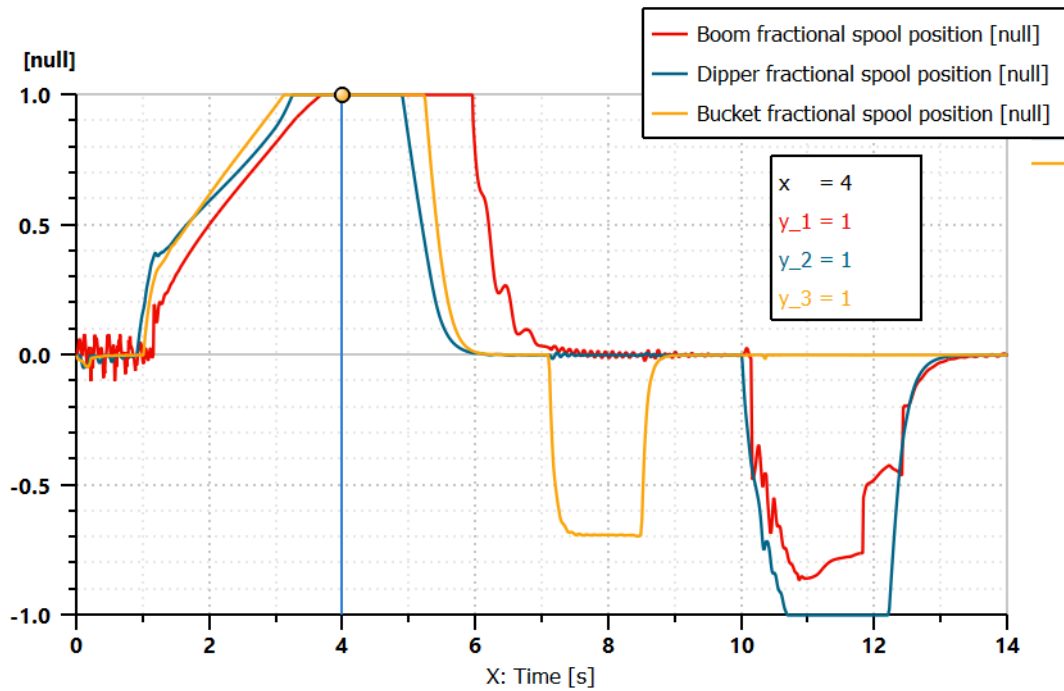


Figure 4.52: Distributors fractional spool position

Now, the pump delivery pressure is lower than $p_{LS} + s$, therefore there is a new Δp across the distributors lower than the normal working condition, that was equal to the difference between the cracking pressure of the differential pressure limiter and the cracking pressure of the local compensator ($s - s_c'$), but equal to all distributors as show on the figures 4.53,4.54,4.55.

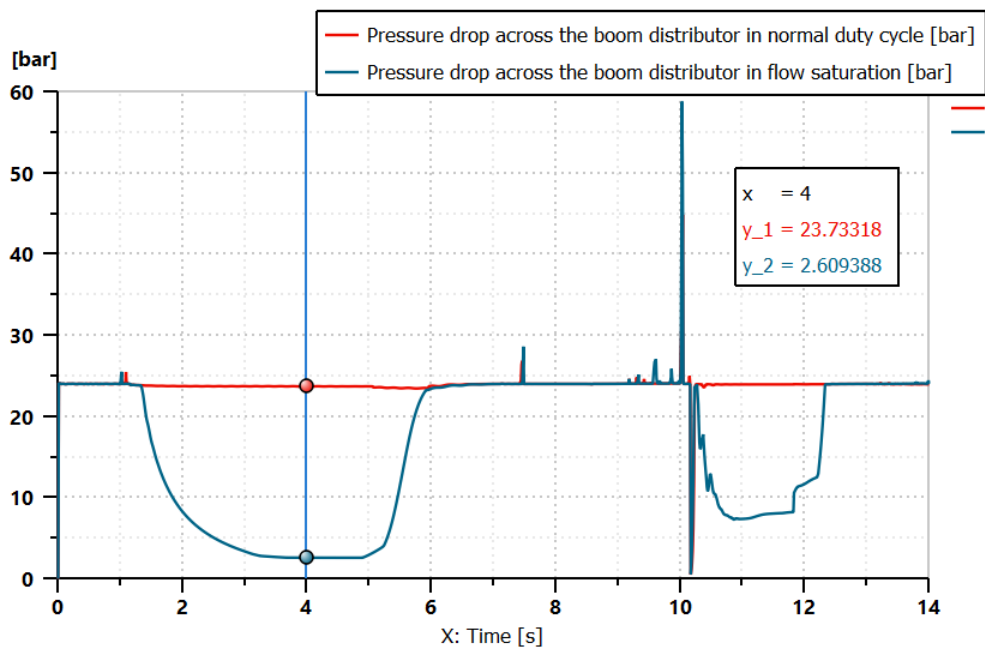


Figure 4.53: Pressure drop across the boom distributor in normal condition and in flow saturation

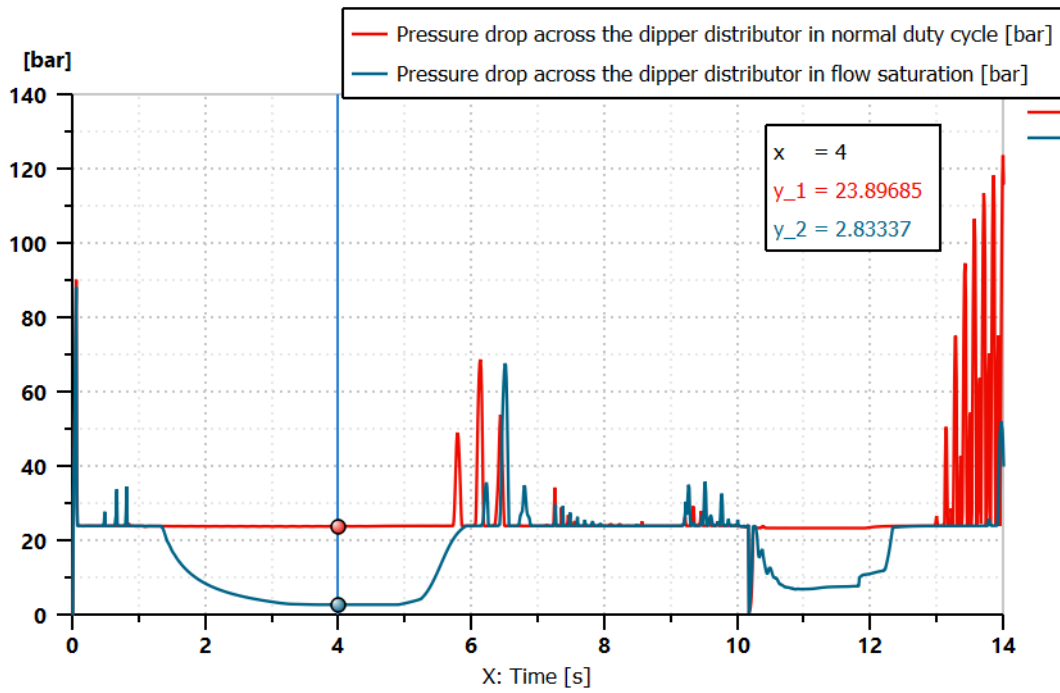


Figure 4.54: Pressure drop across the dipper distributor in normal condition and in flow saturation

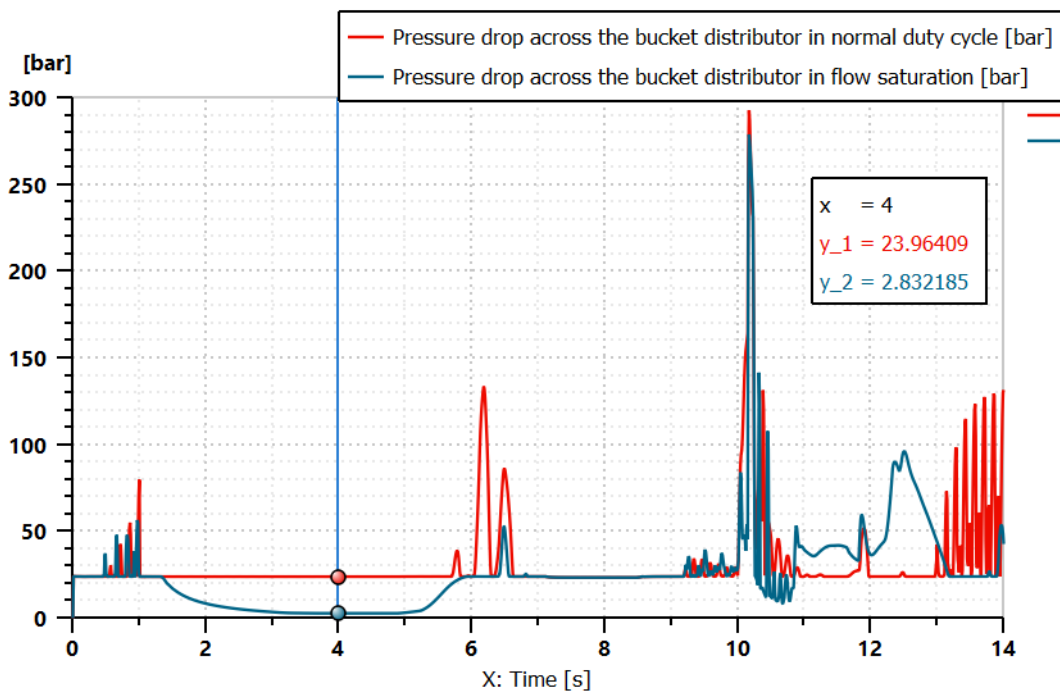


Figure 4.55: Pressure drop across the bucket distributor in normal condition and in flow saturation

This means that the maximum flow rate generated by the pump is shared between the users, because they have the same pressure difference across the valves and the same throttling area

that power each actuator, moreover these flow rates are lower than the flow rates in normal condition as illustrated on the figures 4.56, 4.57, 4.58.

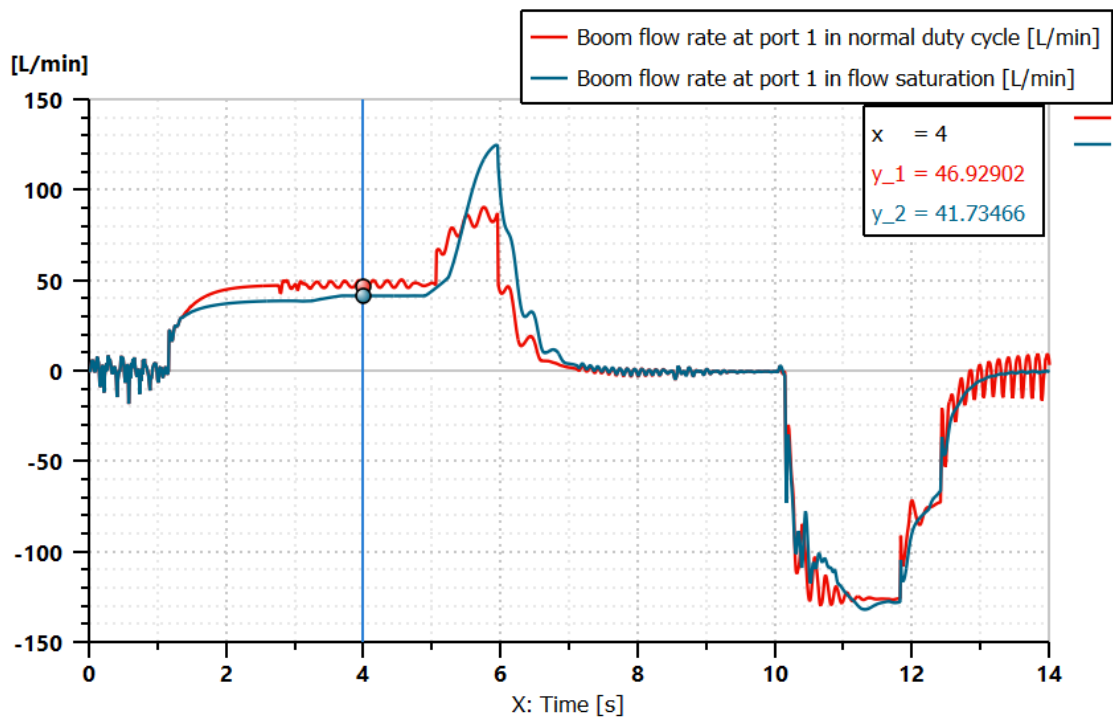


Figure 4.56: Boom flow rate in normal condition and in flow saturation

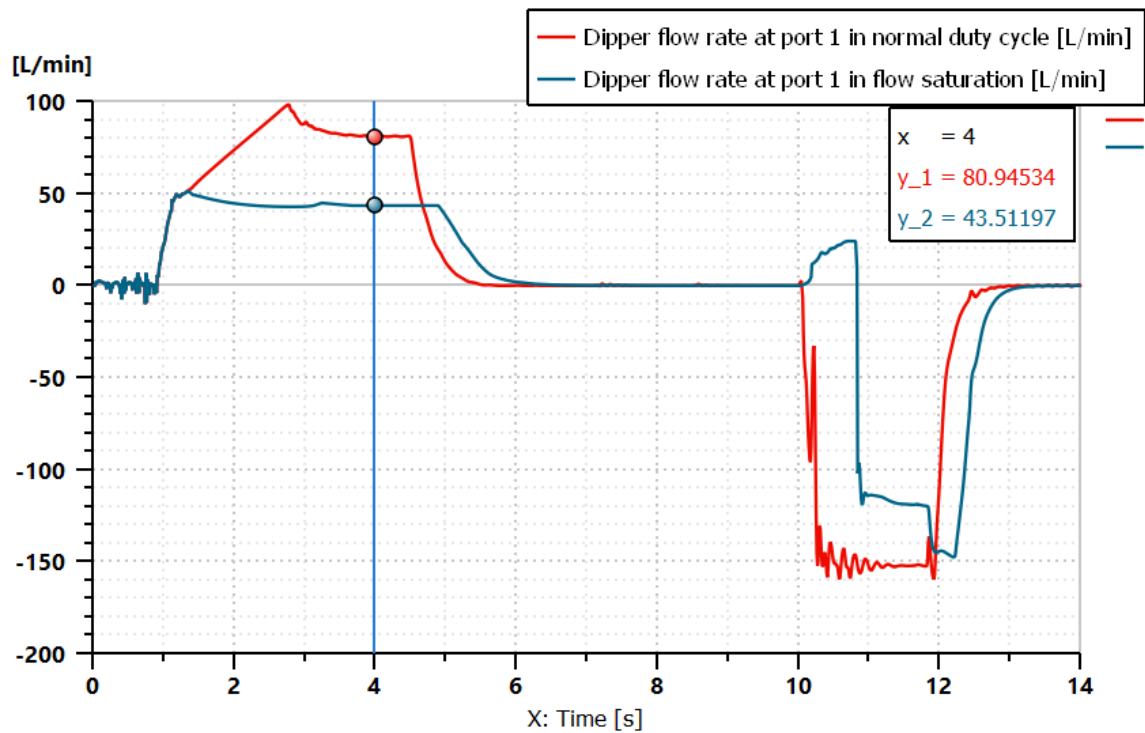


Figure 4.57: Dipper flow rate in normal condition and in flow saturation

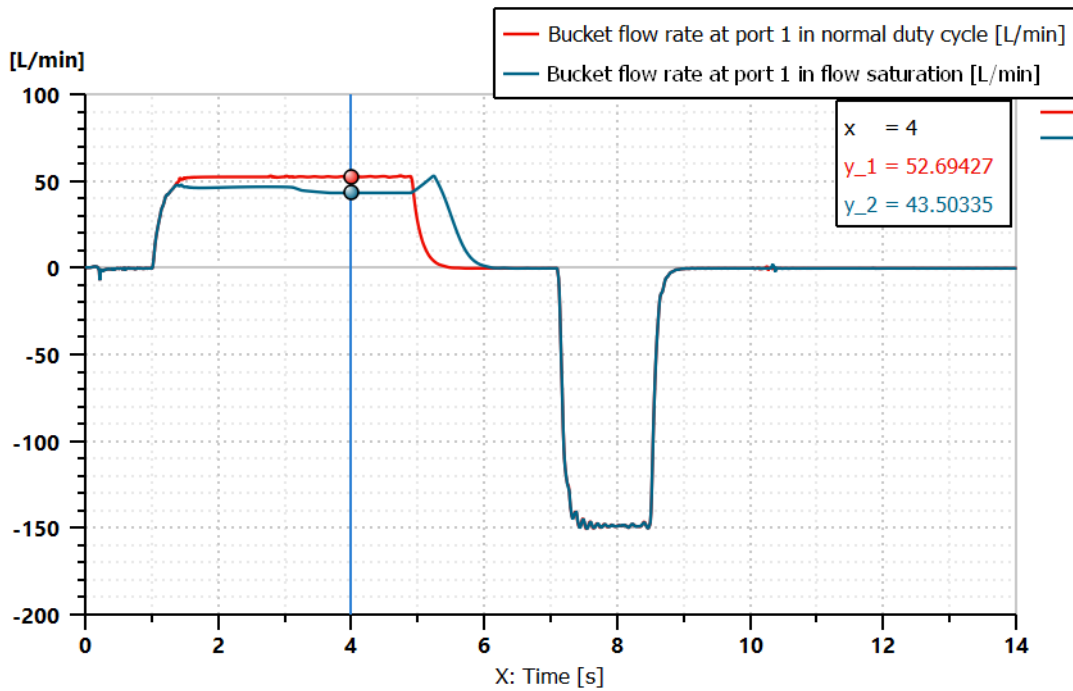


Figure 4.58: Bucket flow rate in normal condition and in flow saturation

As a consequence of the flow sharing the actuators follow the same path of the normal duty cycle but they move slowly (figures 4.59, 4.60, 4.61), because reducing the flow rates imply to reduce the velocities. On the boom and dipper can be notice a reduction of the velocity also in its actuator inward stroke, but the flow rates depend on both the reductions of the pressure drop and the valve throttling area, therefore the lost of the controllability occurs as in pressure saturation condition but with a different cause.

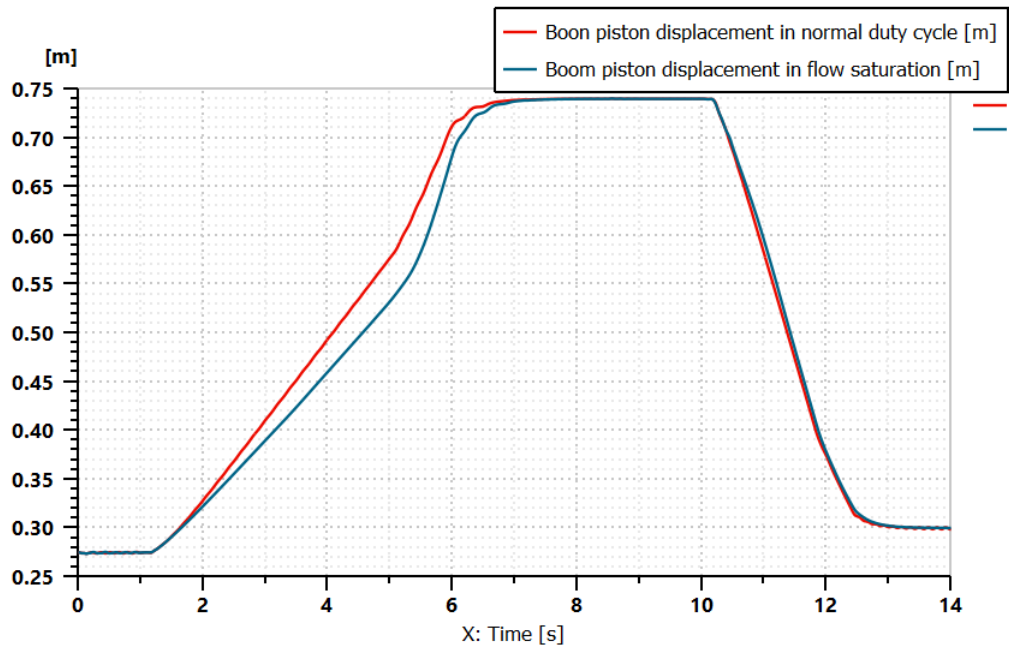


Figure 4.59: Boom behaviour in flow saturation

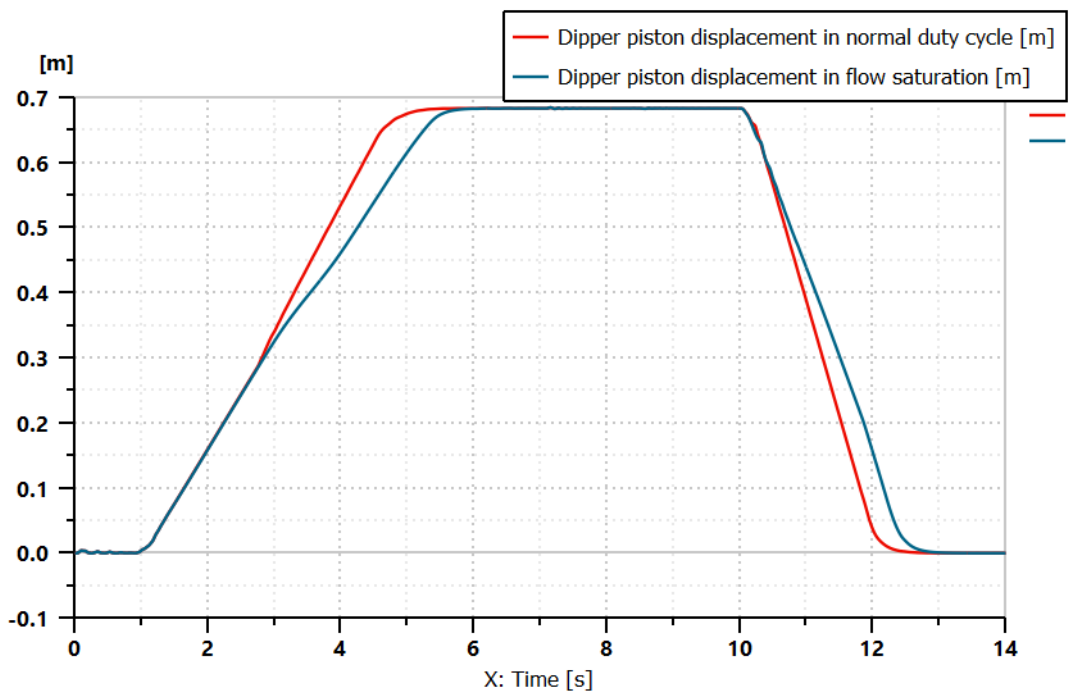


Figure 4.60: Dipper behaviour in flow saturation

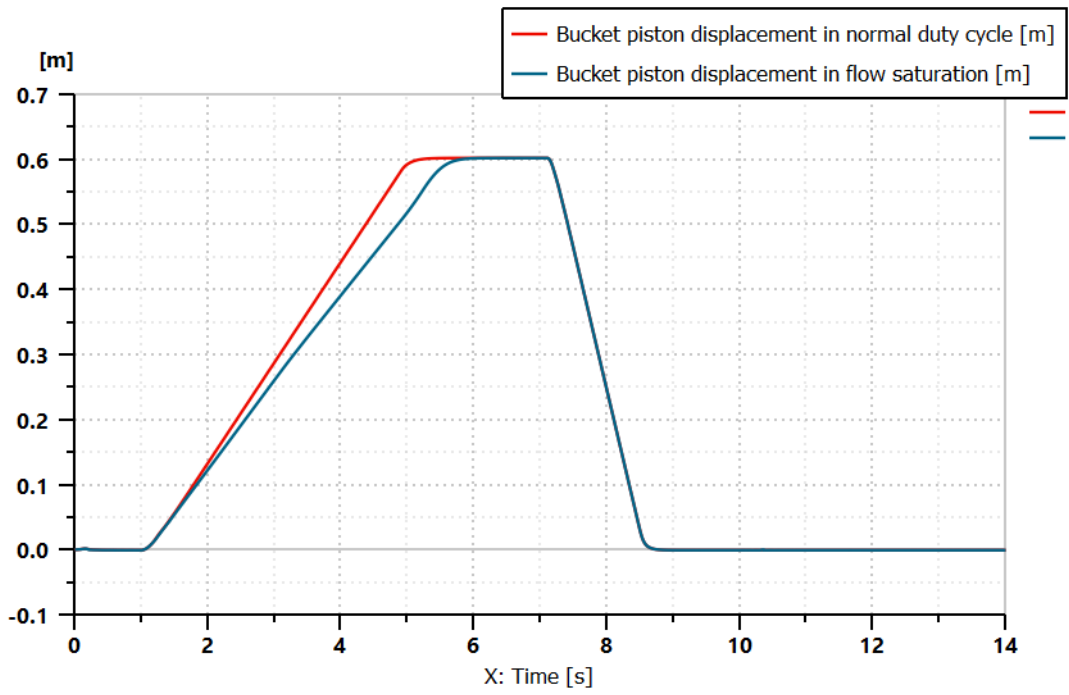


Figure 4.61: Bucket behaviour in flow saturation

CONCLUSIONS

In conclusion, all the result obtained confirmed that the systems behave has expected, even if is not possible decide which architecture is better because, most of the time the right choice is related to the application and to the other environmental factors related to the application field [2]. These two hydraulic circuits have been compered in terms of critical conditions, but some words can be spent also for the control accuracy point of view. Accurately delivery of flow to the users independently of their load is one of the main features of LS valves. This feature is a key the success of LS systems in many applications. In pre compensated valves, the setting of the compensator spring s_c defines the flow to the actuator in conjunction with the metering orifice, that is the main spool of the valve when regulates. This concept makes the valve extremely accurate independent from external conditions (i.e oil temperature). However, in post compensated valves, both the settings of the differential pressure limiter s and of the compensator spring s_c' define the flow to the user, in conjunction with the metering orifice. First, the value of $(s - s_c')$ across the metering orifice can be affected by environmental conditions. In fact, the pump is usually located at a certain distance from the valve, connected by hoses or pipes and fittings. These elements cause major and minor pressure losses that follows well know relations of pipe flows. Therefore, the actual pressure differential at the metering orifices is always lower than the ideal: $(s - s_c' - \epsilon)$. The value of ϵ is representative of these losses, and it varies with the flow rate as well as the temperature, which affects the fluid viscosity. In other words, the accuracy of a post compensated valve section is affected by the oil temperature and by the amount of flow demanded by other users. Second, in a post compensated system the setting of the pump margin contributes to the pressure drop across the metering orifices. This makes the system highly sensitive to maintenance or to replace the main pump, while this is not the case for the pre compensate LS solution. The European parliament declared that by 2035, is not possible produce operating machines that use diesel engines, so the producers of them try to develop machines that used other type of fuels, for instance hydrogen, or adopt electric motors with lithium battery. These can be more efficient running the machine only when needed, can be reduced noise and vibration feel by the operation and other people that are around the machine during its working activity and reduce the emission of CO₂ and NO_x dangerous for the people and the environment, but thanks to its high power to weight ratio, its versatile layout flexibility and easily actuator control, the hydraulic circuit is difficult to replace with other technology, even if it has an inevitable presence of energy losses.

APPENDIX A: Computation of the Resistive Forces

A1: Description and usage

In the figure A1.1 there is a soil sub model used to compute the soil resistive force when digging. The theory behind this sub model has been defined by Edward McKyes in "Soil cutting and Tillage" 1985, and extended to excavator digging by Howard N. Cannon in "Extended Earthmoving with an Autonomous Excavator" 1999 [10].

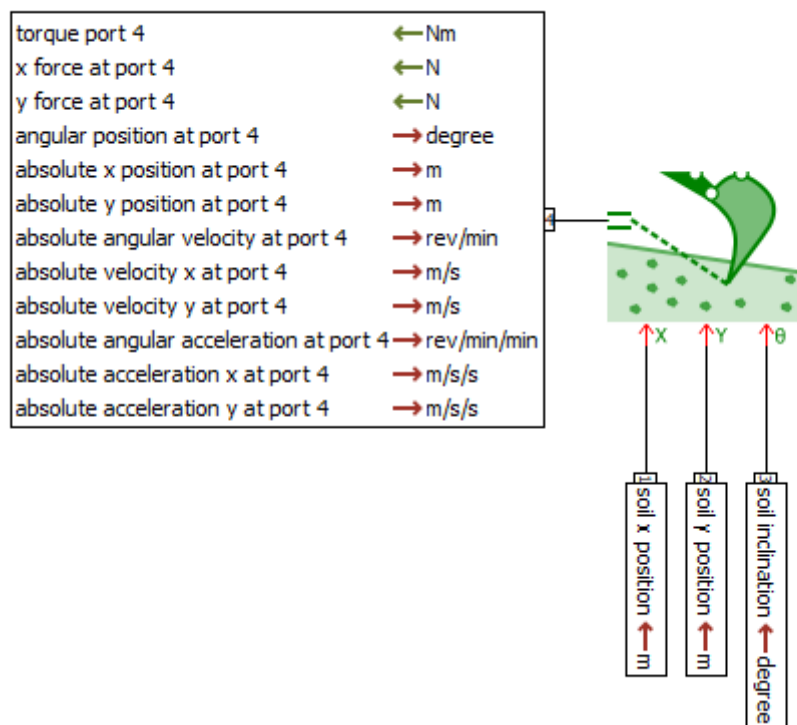


Figure A1.1: Soil sub model [10]

The three signal ports 1, 2 and 3 respectively represent the X, Y and inclination of the soil. The fourth one is a standard 2D port representing the tip of the tool blade. Note that the tool position, velocity and acceleration are not computed in this sub model. Therefore, this sub model needs to be connected to a 2D body representing the tool position, mass and inertia. This sub model can be used to compute the digging force of any blade or bucket entering an earthy ground. It will also compute the digged soil volume and its weight applied to the tool. This sub model should be connected to a 2D body

A2: Parameter settings

Sets the direction in which you want to dig along the X axis, either **positive along x axis** or **negative along x axis** (figure A2.1) [10].

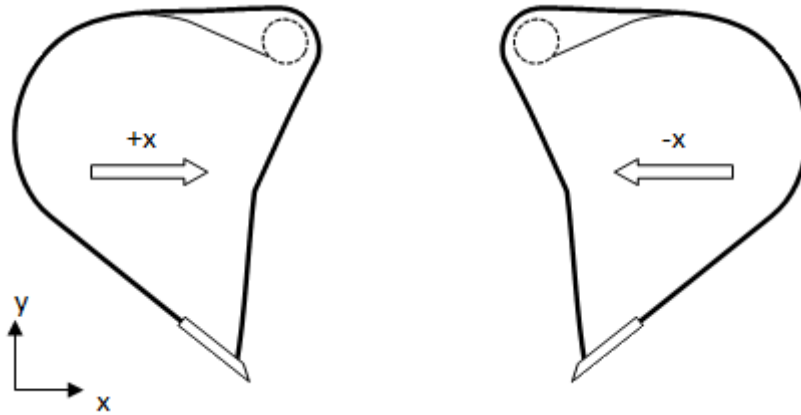


Figure A2.1: positive and negative bucket dig [10]

The tool geometry used in this sub model is a simplified representation of an excavator or any other earthmoving machinery. The geometry parameters are the following:

- tool blade length (Lblade) is the length of flat part of the bucket blade starting from its tip;
- tool back plate length (LBBladeY) is the length of a virtual blade representing the back of the bucket. It is perpendicular to the bucket blade and starts at the bucket blade end;
- tool top corner x position (LBBladeX) is the distance between the tip of the blade and the tool top corner along the blade direction.

Represented in figure A2.2

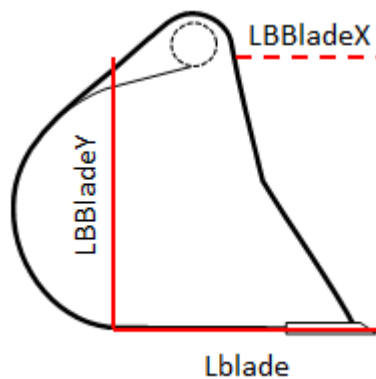


Figure A2.2: Bucket parameters [10]

- tool width (toolW) is simply the width of the tool
- tool maximum capacity (volMax) is maximum volume of soil the bucket can carry, note that this value takes into account the extra carried volume due to the repose angle
- volume in tool (Vs) is the initial volume carried by the bucket at the start of the simulation

The average position of the center of gravity of the digged earth inside the tool can be defined with the two following parameters:

- soil in tool center of gravity relative x position (Gx)
- soil in tool center of gravity relative y position (Gy)

These positions are relative to the port 4 which is the tip of the bucket blade and relative to the bucket frame, as shown in figure A2.3, this means that there is no need to change the Gx sign when changing the digging way option.

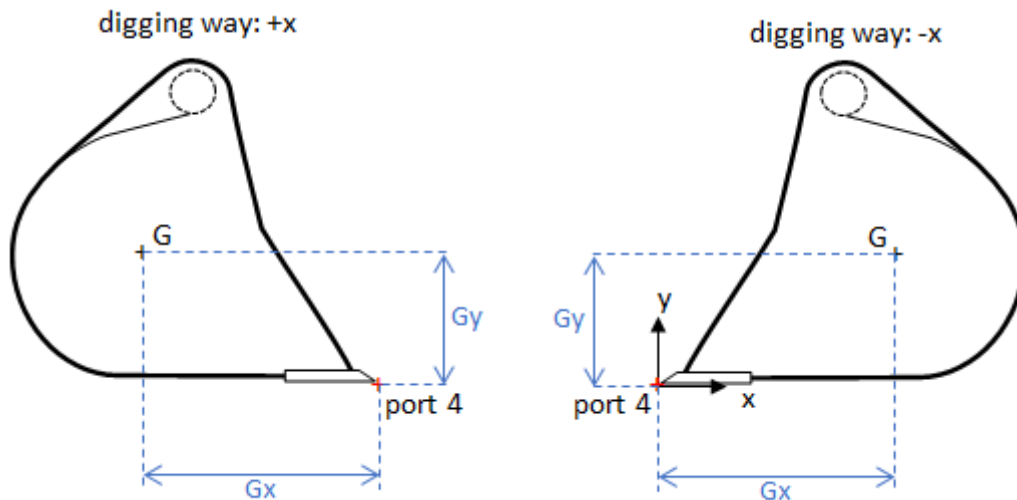


Figure A2.3: centre of gravity of the digged earth [10]

The soil density (*gamma*) refers to the soil or material bulk density. It corresponds to the mass per unit of volume of soil. It depends on the natural density, compacting and humidity content. The relationship between the dry and humid density is usually expressed as

$$\text{Gamma} = (1 + w) * \text{gammad}$$

where

- *gamma* is the effective density [kg/m**3]
- *gammad* is the dry bulk density [kg/m**3]
- *w* is the soil water content (fraction. use *w*/100 if *w* is expressed as percentage)

The repose angle (*repAngle*) is the steepest angle of descent or dip relative to the horizontal plane to which a material can be piled without slumping (figure A2.4). This angle will be used to define the maximum angle the pile of material inside the bucket can have before flowing.

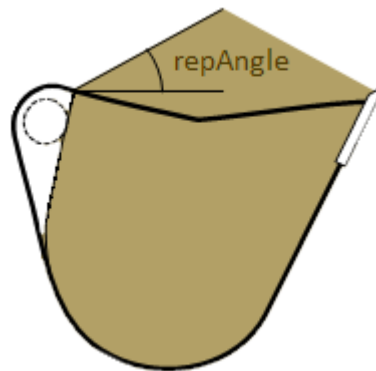


Figure A2.4: Repose angle [10]

The failure surface, which is the boundary between the soil that is static and the soil that is moving due to the motion of the tool, is assumed to be a plane. The angle that makes this plane with the soil surface is called the *soil surface failure angle (beta)* in figure A2.5. The smaller the value is, the bigger is the wedge of soil pushed by the tool. This angle is typically a function of the rake and frictions angles but difficult to determine. It is normally based on test data.

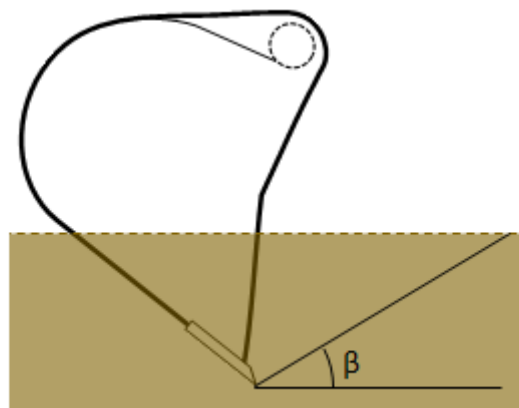


Figure A2.5: Soil surface failure angle beta (β) [10]

The emptying time constant (*empTau*) defines the rate at which the tool will empty the material when outside the soil. The higher the constant, the slower rate the bucket is emptied.

The soil position is defined in the absolute frame with x_{Soil} , y_{Soil} and θ_{Soil} input variables representing respectively the soil frame position and inclination (figure A2.6).

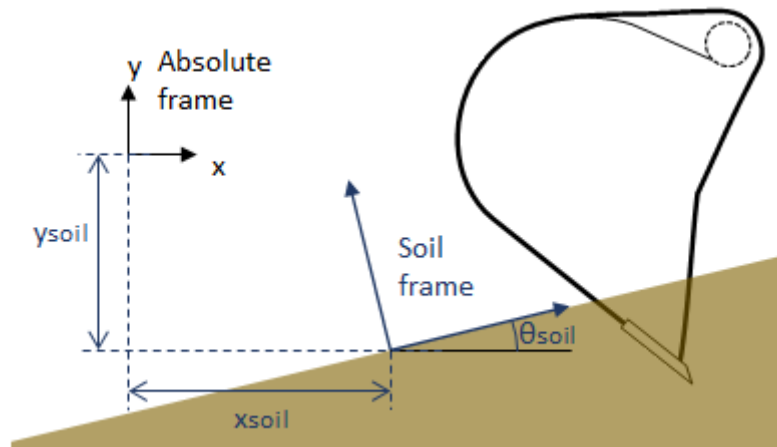


Figure A2.6: Soil position in absolute frame reference [10]

Note that in the above illustration θ and x_{soil} are positive contrary to y_{soil} which is negative. The reason why these quantities are not fixed parameters, but variables is that the current sub model does not keep any history of previous digging cycles. Thus after one digging cycle, the soil surface remains the same, and no "hole" is considered. To represent a more realistic series of digging cycles, it is then possible to decrease the altitude (y_{Soil}) of the soil after each cycle.

When digging two friction phenomenon take place:

- soil-soil, it represents the cohesion of the earth, it acts along soil failure direction
- soil-tool, it represents the adhesion of the earth to the tool, it acts along the tool blade

Both of these friction phenomenon are setup the same way with three parameters.

For the soil-soil cohesion:

- soil-soil cohesion factor (f_{cs}) in $[N/m^{**2}]$
- soil-soil friction angle (ϕ)
- soil-soil stick velocity threshold ($v_{relSoil}$)

For the soil-tool adhesion:

- soil-tool adhesion factor (f_{ct}) in $[N/m^{**2}]$
- soil-tool friction angle (δ)
- soil-tool stick velocity threshold ($v_{relTool}$)

On the figure A2.7 there are represented the forces exchanged between soil and bucket and soil with soil.

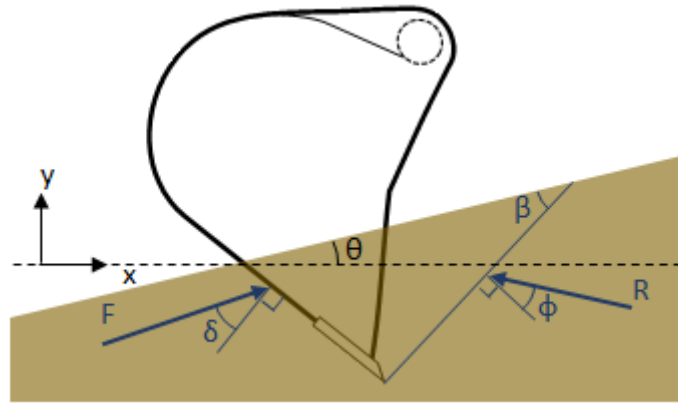


Figure A2.7: Friction forces when the bucket dig [10]

With :

- θ the soil orientation angle
- β the soil failure angle
- F the force exerted by the tool on the soil
- R the resisting force of the soil

The dry friction numerical model implemented in this sub model uses a hyperbolic tangent function to have a smooth transition between movement and stop or when the velocity sign changes. The *stick velocity threshold* parameter defines the transition rate of the friction model, the smaller it is, the faster is the transition, as illustrate the figure A2.8.

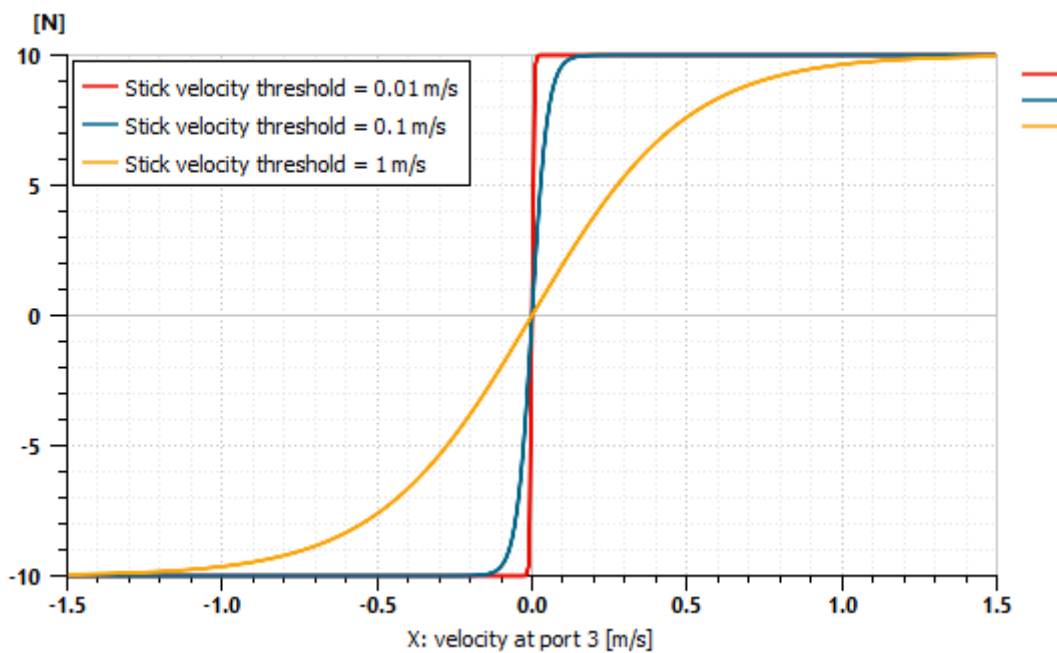


Figure A2.8: Friction force as a function of sliding velocity [10]

The absolute coordinates of the three points defining the tool are saved as internal variable and can be plotted.

These three points are:

- the tip of the blade ($tipX$, $tipY$)
- the end of the blade, intersection points between the blade and the back plate ($endX$, $endY$)
- the tool top point ($topX$, $topY$)

Displaying these three points in a 2D animation can help to set up this sub model, especially for the tool orientation (Figure A2.9):

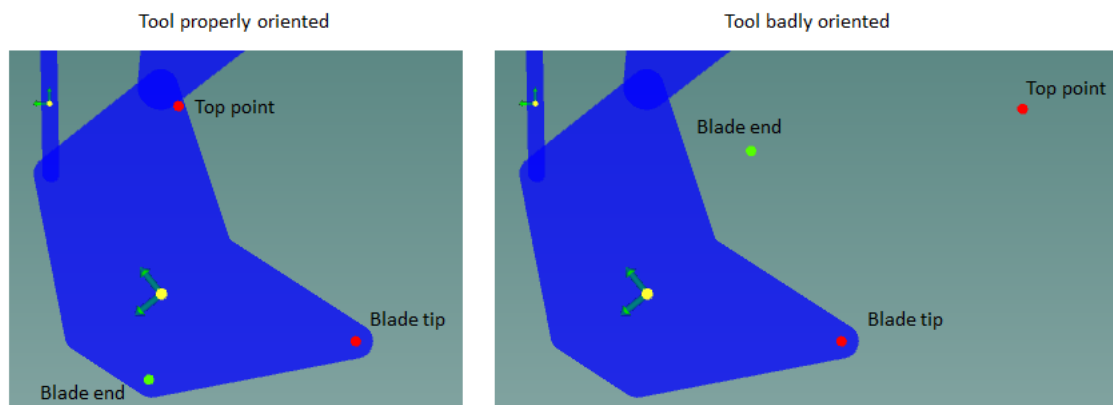


Figure A2.9: Positioning of the three points defining the tool [10]

Note that the orientation of the tool need to be set up in the connected 2D body with the help of the "joint relative angular position at port X" parameter. The port number is the one connected to the digging force sub model.

A3: Theory and equations

The theory mentioned in A1 section, is limited to a digging tool represented by a sole blade, in order to extend it to a more complex tool like a bucket, a back plate has been introduced [10]. Thanks to this addition it is possible to dig at a greater depth where the tool blade is fully under the soil. But as the earthmoving equations are valid for one blade, the concept of a fictive blade was also introduced. It means when the blade is fully under the soil, we will not consider it as the cutting blade, but we will use a fictive blade that connect the tip of the real plate to the intersection of the back plate and the soil surface (figure A3.1).

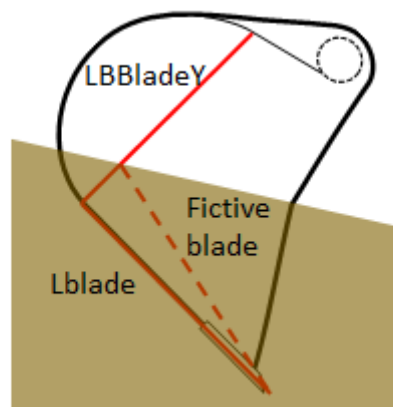


Figure A3.1: Fictive blade concept [10]

Note that the fictive blade will affect the length of the cutting blade in the soil (L_{insoil} variable) and the rake angle ρ .

The digging depth (d_{gd}) correspond to the distance from the soil surface to the tip of the blade on the Y axis. The rake angle (ρ) is the angle between the tool blade and the soil (figure A3.2).

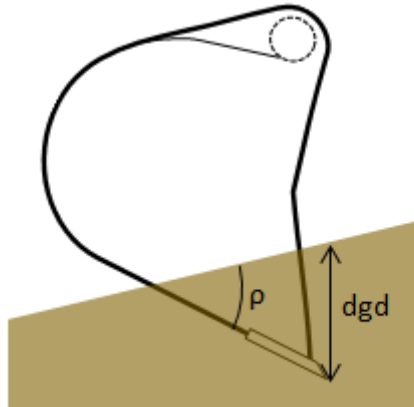


Figure A3.2: digging depth [10]

The equation to calculate the digging depth is:

$$Dgd = \tan(\theta_{soil}) * (x4 - x_{soil}) + y4 - y_{soil}$$

With:

- θ_{soil} : soil orientation angle
- $x4$: x position at port 4 (tip of the blade)
- $y4$: y position at port 4 (tip of the blade)
- x_{soil} : soil absolute x position
- y_{soil} : soil absolute y position

For the rake angle:

if there is no fictive blade

$$\rho = \theta4 - \theta_{soil}$$

With:

- $\theta4$: cutting blade orientation

As with the fictive blade:

$$\rho = \theta_{soil} - \theta4 + \arctan \left[\frac{(dgd * \cos(\theta_{soil}) \sin(\rho_{ini}) - L_{blade}) * \tan(\rho_{ini})}{L_{blade}} \right]$$

With:

- ρ_{ini} : rake angle without the fictive blade
- L_{blade} : length of the tool cutting blade

Filling: the volume inside the bucket is calculating by continually integrating the volume of material that passes over the blade tip during digging:

$$V_s = \int (v_{x4} * dgd * toolW) dt$$

With:

- $vx4$: tool velocity on the X axis at port 4
- $toolW$: tool width

Emptying: when the maximum bucket capacity becomes lower than the volume inside the bucket and the bucket is outside of the soil.

The emptying equation uses a first order model:

$$V_s = \int (volMax - V_{sempTau}) dt$$

With:

- $volMax$: tool maximum capacity
- $empTau$: emptying time constant

To calculate the digging force, we use the fundamental earthmoving equation and the theory explained on the theory mentioned in section A1.

Three forces are computed and summed in the earthmoving equation:

$$FEE = F_w + F_c + F_q$$

With:

- FEE : Force of the earthmoving equation
- F_w : force due to the weight of the material
- F_c : force due to the cohesion of the soil
- F_q : force due to the surcharge pressure

Visualized in figure A3.3

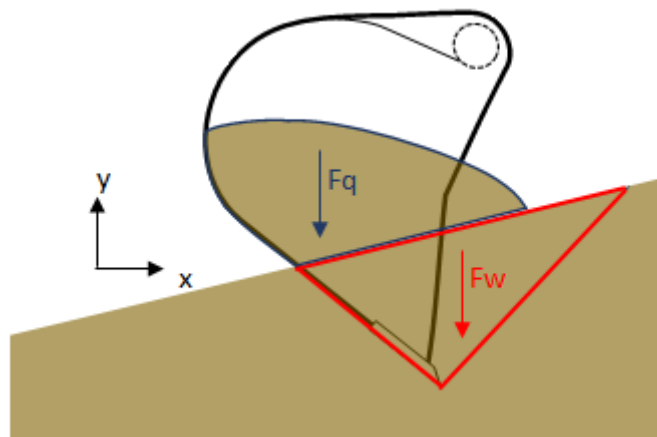


Figure A3.3: Forces of the earth moving equation [10]

The force due to the adhesion of the soil to the tool F_a is also calculated and directly taken into account when computing the forces at the 2D port.

The force and torque at port 4 are computed as follow:

$$F_{x4} = FEE * (\cos(\delta)\sin(\rho - \theta_{soil}) - \sin(\delta)\cos(\rho - \theta_{soil})) + Fa.\cos(\theta_4)$$

$$F_{y4} = -FEE * (\cos(\delta)\cos(\rho - \theta_{soil}) + \sin(\delta)\sin(\rho - \theta_{soil})) - Fa * \sin(\theta_4) - Q * \gamma * g$$

$$T_4 = Vs * g * \gamma * \sqrt{Gx^2 + Gy^2} * \cos(\theta_4 - \arctan\frac{Gy}{Gx})$$

This sub model has several limitations on the digging force computation:

- The sum of the soil angular orientation and the soil failure angle must be less than 90°. The simulation will stop if this criteria is not met.
- The bucket cannot fully go under the soil surface (top point). This will stop the simulation
- The sum of the rake, failure, soil-soil friction and soil-tool friction angles must be below 180°: $\rho + \phi + \beta + \delta < 180^\circ$. This will stop the simulation.
- If the rake angle is greater than the sum of the soil orientation angle plus 90 degrees, the rake angle will be saturated to that sum. This will raise a warning but the simulation will continue.
- If the digging tool has a movement that press the soil under itself, the earthmoving equation results may not be correct. This will raise a warning but the simulation will continue.
- This sub model is not yet compatible with the 2D mechanical assistant, consequently nothing will be displayed in the planar automatic animation.

BIBLIOGRAPHY

Books

- [1] Nervegna, N.; Rundo, M.: “*Passi nell’Oleodinamica*”, Politeko, Torino 2018.
- [2] Vacca, A.; Franzoni, G.: “*Hydraulic Fluid Power fundamentals, applications and circuit design*”, Wiley, Hoboken, NJ 2021.

Theses

- [3] Lovuolo, F.: “*Studio e modellazione dell’impianto idraulico di un escavatore*”, Politecnico di Torino, December 2009.
- [4] Fresia, P.: “*Modellazione e analisi sperimentale su limitatore di pressione per pompe oleodinamiche a cilindrata variabile*”, Politecnico di Torino, December 2019.
- [5] Padovani, D.: “*Analisi e sviluppo di componenti per impianti load sensing*”, Politecnico di Torino, April 2011.

Publications

- [6] Padovani, D.; Rundo, M.; Altare, G.: “*The Working Hydraulics of Valve-Controlled Mobile Machines: Classification and Review*”, Journal of Dynamic Systems, Measurement, and Control, July 2020.

Web Sites

- [7] www.google.it/images/excavator
- [8] www.linde-hydraulics.com/downloads/Brochure-VW22/18M5-03/
- [9] www.gregorypoole.com/guide-to-the-different-types-and-sizes-of-excavators/

Software Library

- [10] Simcentre Amesim 2021.2: “*PLMDIGF00 - computes the digging force on earthy ground*”.
- [11] Simcentre Amesim 2021.2: “*3D mechanical library*”.